

Virginie Algay, M.Sc.

**Isoxazole Linked siRNA
Cholesterol Conjugates
by Catalyst Free Nitrile Oxide/Alkyne
Cycloadditions**

Thesis presented for the Ph.D. degree
submitted to



NUI MAYNOOTH

Ollscoil na hÉireann Má Nuad

Department of Chemistry
National University of Ireland, Maynooth

February 2012

Head of Department : Professor John Lowry

Supervisor: Dr. Frances Heaney

TABLE OF CONTENTS

Acknowledgments	3
Abstract	6
List of abbreviations	8

CHAPTER 1: The Biology of RNA and Synthetic Value of Cycloaddition Chemistry with Nitrones and Nitrile oxides as Route to Chemically Modified Biomolecules

9

I. DNA AND RNA	10
I.1. History of DNA	10
I.2. Structure of DNA and RNA	10
I.3. Gene expression	11
II. CONTROL OF GENE EXPRESSION	12
II.1. Antisense approach	13
II.2. The triplex approach	19
II.3. The DNA quadruplex	22
II.4. RNA interference (RNAi)	24
II.5. Other potential therapeutic nucleic acid analogues	27
III. DELIVERY OF NUCLEIC ACID THERAPEUTICS	30
IV. CLICK CHEMISTRY	32
IV.1. 1,3-Dipolar cycloaddition reactions	33
IV.2. Azide/alkyne cycloaddition reaction	37
III. NITRONE CHEMISTRY	41
III.1. Generation of nitrones	42
III.2. 1,3-Dipolar cycloaddition of nitrones	42
IV. NITRILE OXIDE CHEMISTRY	43
VI.1. Generation of nitrile oxides with CAT	44
VI.2. Reactions of nitrile oxides	46
VII. OBJECTIVES OF THIS THESIS	49

CHAPTER 2: Optimization of Cycloaddition Between Maleimides and Nitron or Nitrile Oxide 1,3-Dipoles. Synthesis and Cycloaddition of Maleimido-Sugar Click Partners

50

I. INTRODUCTION	51
II. REACTIONS WITH NITRONE	54
II.1. Nitron preparation	54
II.2. 1,3-Dipolar cycloaddition	55
III. REACTIONS WITH NITRILE OXIDES	62
III.1. Oxime preparation	63
III.2. 1,3-Dipolar cycloaddition	63
III. 3. Preformed nitrile oxides	65
IV. APPLICATION TO SUGAR MOIETY	66
IV.1. Synthesis of target maleimido-sugar	67
IV.2. 1,3-Dipolar cycloaddition	72

V. STABILITY TESTS	77
V.1. Stability towards Methylamine	78
V.2. Stability towards potassium carbonate	79
VI. CONCLUSION	82
CHAPTER 3: Synthesis of Thymidine Alkynes and their Cycloaddition to Nitrile Oxides -----	83
I. INTRODUCTION	84
II. SYNTHESIS AND CYCLOADDITION OF C3'-O-PROPARGYL THYMIDINE	84
III. SYNTHESIS AND CYCLOADDITION OF C3'-O-N3-BISPROPARGYL THYMIDINE ..	87
IV. SYNTHESIS AND CYCLOADDITION OF PHOSPHODIESTER THYMIDINE	89
V. CONCLUSION	91
CHAPTER 4: Synthesis and Cycloaddition of Click Partners Bearing a Cholesterol Core ----	92
I. INTRODUCTION	93
II. CHOLESTEROL DERIVATIVES AS CLICK REACTION PARTNERS	93
II.1. Structure of cholesterol	93
II.2. Synthesis and cycloaddition of cholesterol alkyne derivatives	94
II.3. Synthesis and cycloaddition of amido-carbamate linked cholesterol oximes	99
II.4. Synthesis and cycloaddition of ether linked cholesterol oximes	103
III. CONCLUSION	108
CHAPTER 5: Application of the Nitrile Oxide/Alkyne Cycloaddition to Oligonucleotides -----	110
I. INTRODUCTION.....	111
II. AUTOMATED OLIGONUCLEOTIDE SYNTHESIS	111
II.1. Building blocks	113
II.2. Deblocking (Step 1)	113
II.3. Coupling (Step 2)	114
II.4. Capping (Step 3)	115
II.5. Oxidation (Step 4)	115
II.6. Cleavage/deprotection and purification	116
III. CONJUGATION TO DNA	116
III.1. Conjugation of "small" ligands to [T]-(CPG)	116
III.2. Conjugation of "small" ligands to [DNA]-(CPG)	119
III.3. Conjugation to steroidal oximes	129
IV. CONJUGATION TO RNA	132
IV.1. Conjugation at the 2'-position of the 3'-terminus	132
IV.2. Conjugation at the 2'-position of the 5'-terminus or at an internal position ...	136
IV.3. Conjugation at the 3'-position of the 3'-terminus	137
V. ASSAYS FOR RNA INTERFERENCE EVALUATION	141
V.1. siRNA transfection into Cho-K1 cells for eGFP gene knockdown	141
V.2. Luciferase reporter assay	145
VI. CONCLUSION	151
EXPERIMENTAL -----	153
APPENDIX -----	201
REFERENCES -----	214

Acknowledgments / Remerciements / Buíochas Mór

First, I would like to express my deepest gratitude to my supervisor, Dr. Frances Heaney who gave me the opportunity to do that thesis. For her stimulating suggestions, her help, her encouragement, and for her HUGE patience (especially with my English ;-)) I am forever in debt to her.

Thank you to NUI Maynooth and the SFI scholarship which have both supported me during this project.

I would like to thank all the other academic staff members from the Chemistry Department of NUI Maynooth for their help and support for the last five years. Ria, Ann, Barbara, Ollie, Niamh, Ken (I am sorry, I never found that coin!), Noel (for fixing absolutely everything, from my computer to... Everything!) Thanks to the other lecturers, and especially Dr. Jennifer MacManus and her girly lab, Ruth and Susan, for their help to run the PAGE experiments. Thanks to Dr. Ishwar Sing for his support and his help to set up this project. Thanks to all my colleagues post-grades, I love them all but they are too many names for me to write them... OK, I try... Trish, Alanna, Niall, Joey (what's up!), Conor, Lynn, Haowee (thank you for my first tiny nuclear mushroom cloud ;-), Haixen (for making us discover the "surprising" Chinese goodies), Ursula, Ciaran, Dean, Wayne, Rob, Niamh, Carol, Lorna, Roisin, Gama, Adelaide, and the eldest... Sinead, Enrico, Valeria, Richard, Declan, Denis, Rob C, John W, Gillian, Clair, Foxy, Ciaran, Ken, Theresa, Eimear, Martin, Paddy, Paul... and more. Everyone has been beautifully nice with me from day one, making me feel so welcome. Thanks for making every day enjoyable, it would not have been the same without them.

Thanks to the Dr. Sean Doyle laboratory (NUIM), Dr. Luke O'Shaughnessy and to the Dr. Paul Moynagh group (NUIM), especially and Dr. Paola Atzei and Dr. Mark Mellet, for running the biological assays.

A special THANKS to my lab sister, Dr. Linda Doyle, she made me feel so welcome when I arrived. She was the best help I could get, always there for me, always smiling and in a great mood. I wish her the very best for the future ☺

Thanks to my lab brother "Coli", (future) Dr. Colin Freeman, we finished this adventure together, best of luck LITTLE PIG!

Thanks to my lab buddy "Murph", (future) Dr. John Murphy for the frequent rides to the train station, the chicken wings!!! The "young ones" and anything that could go before...
BAAAAAAAABY!!!!

Merci à mes amis de Master: Gege, Tahis, Seb, Yann et Yan, Fred, Thibault, Guillaume, Max, Chafik, "mon ex (but best) colloc" Damien, je serais toujours là pour vous. Et évidemment toutes mes pensées vont à Jérôme, merci de m'avoir rappelé ce qui est important. REPOSE EN PAIX MON COPAIN <3

A SUPER THANKS to all my wonderful friends outside the lab who keep me sane along the years... or insane should I say! Few names, starting with my Handsome BROTHERS from other mothers: Michael Valette (toujours à mes cotés apres toutes ces années et j espère pour encore un million d'autres) and Florent Duffros (Montpellier, Marrakesh, Ibiza... le tout épicé de Jungle Juice... que de beaux souvenirs), mon Benjamin (qui m'aura fait le plus inoubliable des cadeaux, on aura tous laissé une partie de nous dans la Micra), mon Waga (aka Sire Lupus ! mon chevalier sans peur et sans reproche, qui aura toujours une place speciale dans mon cœur), ma Jess (à nos folles années, de Castres à Toulouse, qui aurait cru à nos superbes carrières), ma p'tite Lulu (for those magic nights as "Chargées de Com" chasing the "Jeunes Cadres Dynamics"), mon Coupain Sadry (du PoP aRT a Montpel jusqu'à Pygmalion Dublin, on en a fait du chemin!), Mika (t'entendre râler me manque), Abbey and Patrice (I will never forget the great times in Berlin! How could I?!), Constance (my partner in so many crimes... You are beautiful!), Greg (my Besty!), Barbara (Monday Millions! Tuesday Billions!! And Steak Wednesday! Many more to come now ☺), Nick (the best host on planet earth!), Jefferson (my Diva!), Gary!! (for giving me the best advices, always! X FACTOR BABY!), Aurelien (pour ses bon petits plats), Dave (plenty of cranberry juice to come!), Mike (LA, here I come!!!), Manu (mon parisien prefere), Guido (I would think about you each time I see a knife or a key), Stephen (you are, still, like a brother to me), Miren (if only those walls could talk)... New friends, old friends I have shared extraordinary moments with all of you, and I will never forget them. To my friends from Castres, Helsinki, Montpellier, Pavia, Dublin and all the other marvelous cities I have been. THANKS to everyone involved in my baby ELEKTROSHOCK. And obviously, A VERY BIG THANKS to all the stupefying "BAMBOULINETS"... So many stories to tell (or not) to the grandkids ☺

I am very grateful for my lucky star I had the most "fantabulous" amazing 29 years so far. I have an angel, always levitating around me, I am sure I do ☺
I cannot tell where I will be in another 29 years but the future looks SHINNY BRIGHT!!!

Merci à mon P'tit LOUIES, aka MON LOULOUIIIIIII, le plus fidèle des compagnons.

The last but far to be the least, le meilleur pour la fin... MERCI A MA FAMILLE, ma grand-mère, Yamina, mes oncles et tantes, mes cousins et cousines, à la mémoire de mon grand-père Achour, et surtout à MES PARENTS BAYA ET JEAN-LOUIS ALGAY. Les deux plus belles personnes sur cette planète. Merci pour votre soutien, votre compréhension, pour vos encouragements et votre amour. Même si je suis toujours en vadrouille, vous êtes toujours dans mon cœur et je vous aime plus que tout au monde <3

... BANANAAAAAAAAAAAAAAS !!!

DECLARATION

I hereby certify that this thesis has not been submitted before, in whole or in part, to this or any other university for any degree and is except where otherwise stated, the original work of the author.

Signed: _____

Date: _____

Virginie ALGAY

ABSTRACT

The ultimate goal of the novel work discussed in this Ph.D. thesis was the syntheses of a range of chemically modified siRNAs by catalyst free **Click Cycloaddition Chemistry**.

The first chapter overviews the structure and biological function of RNA, before turning to a discussion on the synthetic value of dipolar cycloaddition chemistry of nitrones and nitrile oxides with alkene and alkyne dipolarophiles Chapter 2 presents the somewhat disappointing findings on the cycloaddition reactions of maleimides. Reactions with “simple” maleimides suffered from poor yield and/or poor diastereoselectivity, and synthetic access to the desired sugar maleimides was plagued by poor chemoselectivity. Following a protection/deprotection strategy a glucofuranoside with a pendant maleimide was formed, and its cycloaddition potential explored with nitrones and nitrile oxides. Unfortunately the pyrrolo-isoxazole skeleton resulting from cycloaddition to the maleimides was unstable to the standard conditions of oligonucleotide cleavage and thus Chapter 2 concludes that the plan to prepare chemically modified oligonucleotides by cycloaddition to maleimides should be abandoned.

The third chapter reports on the successes of solution phase cycloaddition between thymidine-alkynes, as model oligonucleotide substrates, and nitrile oxide dipoles using a chloramine-T protocol. The fourth chapter presents the synthesis of isoxazole linked cholesterol conjugates by nitrile oxide/alkyne cycloadditions. Novel alkyne and oxime modified cholesterol derivatives were prepared and demonstrated to be efficient dipolarophiles and dipole precursors.

Chapter 5 embraces the synthetic success discussed in chapters 3 and 4 and applies them to oligonucleotide conjugation on the solid phase. Isoxazole linked aryl and cholesterol conjugates were formed by a convenient and fast protocol. Two distinct formations of siRNAs duplexes have been synthesized, siRNAs with 3'-overhang where strands were modified by addition of an extra U(2'-Chol) or

U(3'-Chol) at the 3'- or 5'-terminus, and bluntmers with no overhang. The goal was to evaluate the biological consequences of the chemical modifications introduced. Unfortunately, the Luciferase assay did not show any evidence of activity. However, a real gene knockdown resulted from the siRNA transfection into CHO-K1 cells for eGFP gene.

The sixth chapter details the experimental procedures together with full characterization of all the new compounds described in this thesis., It is followed by an appendix which carries a detailed description of structural determination of the protected maleimido-sugar, as representative example, a listing of the presentations delivered by the author and a copy of the first peer reviewed paper arising from this authors work. Finally, a complete bibliography of articles referred to in this thesis is included.

LIST OF ABBREVIATIONS

°C degree Celsius	MALDI matrix-assisted laser
Δ reflux	desorption/ionization
Ac acetyl	max maximum
Ago Argonaute	<i>m</i> -CPBA <i>meta</i> -chloroperbenzoic acid
Ar argon or aryl	mg milligram
BMT 5-(benzylmercapto)-1H-tetrazole	Me methyl
b.p. boiling point	MK-10 Montmorillonite K-10
bp base pair	min minute
br broad	Mp melting point
Bz benzyl	MPPS macroporous polystyrene
<i>C. elegans</i> <i>Caenorhabditis elegans</i>	mol mole
Cne 2-cyanoethyl group	MS mass spectrometry
COSY correlation spectroscopy	MW microwave
Cp cyclopentadienyl	<i>n</i> ° number
Cp* pentamethylcyclopentadienyl	N nitrogen
CPG controlled pore glass	NBM <i>N</i> -bromo propyl maleimide
CuAAC Cu catalyzed azide-alkyne cycloaddition	NCS <i>N</i> -chlorosuccinimide
d doublet	NMM <i>N</i> -methyl maleimide
DCA dichloroacetic acid	NPM <i>N</i> -phenyl maleimide
DCC <i>N,N</i> -dicyclohexylcarbodiimide	NMR nuclear magnetic resonance
DCM dichloromethane	nt nucleotide
dd doublet of doublets	p page
DFT density functional theory	PAZ piwi argonaut and zwillie
DIPEA <i>N,N</i> -diisopropylethylamine	PEG polyethylene glycol
DNA deoxyribonucleic acid	Ph. D. Doctor of Philosophy
DMAP 4-dimethylaminopyridine	pKa acid dissociation constant
DMF dimethylformamide	Ph phenyl
DMSO dimethylsulfoxide	PNA peptide nucleic acid
DMT 4,4'-dimethoxytrityl group	ppm parts per million
DEPC diethylpyrocarbonate	RISC RNA induced silencing complex
ds double strand	RNA ribonucleic acid
eq equivalent	RNAi RNA interference
EWG electron-withdrawing groups	mRNA messenger RNA
FAB fast atom bombardment	siRNA short interfering RNA
FMO frontier molecular orbital	RuAAC Ru catalyzed azide-alkyne cycloaddition
g gram	rt room temperature
h hour	s singlet
H hydrogen	t triplet
HDGS homology dependent gene silencing	T temperature
HIV human immunodeficiency virus	<i>t</i> -Bu <i>tert</i> -butyl
HOMO highest occupied molecular orbital	TCA trichloroacetic acid
HPLC high performance liquid chromatography	THF tetrahydrofuran
Hz hertz	TMS trimethylsilyl
J coupling constant	TOF time-of-flight
L litter	UV ultra-violet
LUMO lowest unoccupied molecular orbital	vis. visible
m multiplet	W watt
M mol.L ⁻¹	

CHAPTER 1:

The Biology of RNA and
Synthetic Value of Cycloaddition
Chemistry with Nitrones and Nitrile Oxides
as Routes to Chemically
Modified Biomolecules.

I. DNA and RNA

All modern life on Earth uses three classes of biological macromolecules each with a critical role. **Proteins**, the core element of all living systems, are involved in virtually all cell functions whilst the nucleic acids, **deoxyribonucleic acid (DNA)** and **ribonucleic acid (RNA)**, carry genetic information that can be inherited from one generation to the next.

I.1. History of DNA

DNA, first isolated from white blood cells by the Swiss physician **Friedrich Miescher** in **1869**, is the major component of pus from infections and was originally called “nuclein”. Miescher determined that the molecule was made up of hydrogen (H), oxygen (O), nitrogen (N) and phosphorus (P). Meanwhile, other scientists continued to investigate its structure. One of these, the Russian **Phoebus Levene**, a physician turned chemist, discovered the order of the three major components of a single nucleotide (phosphate-sugar-base); he identified the carbohydrate components of RNA (ribose) and of DNA (deoxyribose) and correctly established the way RNA and DNA molecules are assembled. In **1943**, the American **Oswald Avery** proved that DNA carries genetic information and in **1952 Alfred Hershey** and **Martha Chase** confirmed the role of DNA in heredity. In **1953 James Watson** and **Francis Crick** presented the double helix model that is still in vogue (Figure 1.1).

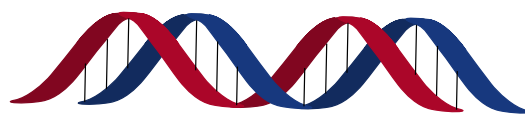


Figure 1.1: DNA model.

I.2. Structure of DNA and RNA

DNA consists of two long polymers of simple units called nucleotides, with backbones made of sugars linked by phosphate triesters groups (Figure 1.2). The polymeric strands run in opposite directions and are therefore anti-parallel. Attached to each sugar is one of four types of nucleobase: adenine (A), guanine (G), thymine (T), and cytosine (C). It is the sequence of these four nucleobases along the

backbone that encodes information. This information is read using the genetic code. In double-stranded DNA, one strand codes for the RNA that is translated into protein; it is referred to as the antisense strand. It carries the information necessary to make proteins by binding to a corresponding messenger RNA. The strand that does not code for RNA is called the sense strand.

The chemical structure of RNA is very similar to that of DNA, with two differences: RNA has a ribose sugar, while DNA has a deoxyribose sugar which lacks an oxygen atom at the 2'-position. RNA has the nucleobase uracil (U) in place of DNA's thymine (T). Uracil and thymine have similar base-pairing properties.

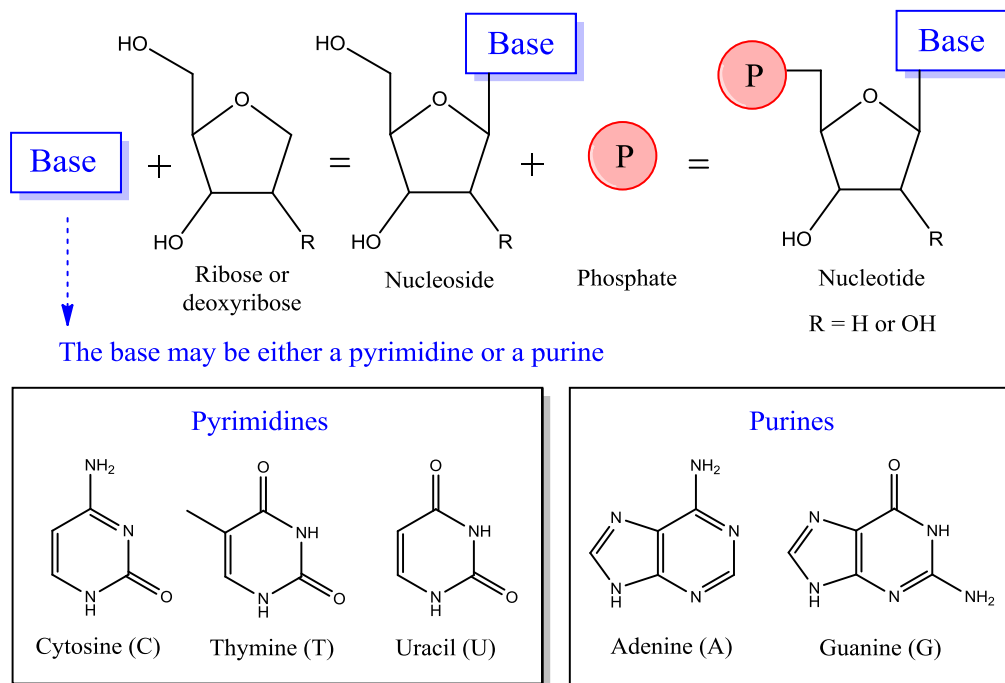


Figure 1.2: The three components of nucleotides.

1.3. Gene expression

The story of the genetic code does not end with the solving of the 3D structure of DNA. The concept of gene expression emerged during the late 1950s, and is associated with Crick's description of his "*Central Dogma of Molecular Biology*".¹ This doctrine asserted that a gene, which is a sequence of DNA, led to the formation of RNA, which in turn led to the synthesis of proteins. This process can be divided in two parts as shown in figure 1.3.² One strand of the DNA double helix is used as a

template by an RNA polymerase to synthesize a messenger RNA (mRNA) by a process called **Transcription**. This mRNA goes through different types of maturation and migrates from the nucleus to the cytoplasm. The next step is **Translation** where the mRNA is decoded by the ribosome to produce a specific amino acid chain, or polypeptide, that will fold into an active protein. **Proteins** are the core element of all living systems and are involved in diverse cell functions including structural support, bodily movement, and defence.

DNA is the same in all cells, but the range of gene products differs. The diversity of cell types and tissues in complex organisms, like humans, results from differential gene activity. Gene activity/expression is a highly regulated process by which a cell can answer to external signals and adapt to changes in the environment. Control of gene expression evolved in the most primitive single-celled organisms to protect them from viruses a long time before plants and animals existed on the planet. In the past few years scientists have discovered that control of gene expression, still exists today in humans and that if it was possible to harness it, the potential may exist to change forever the way that doctors fight disease.

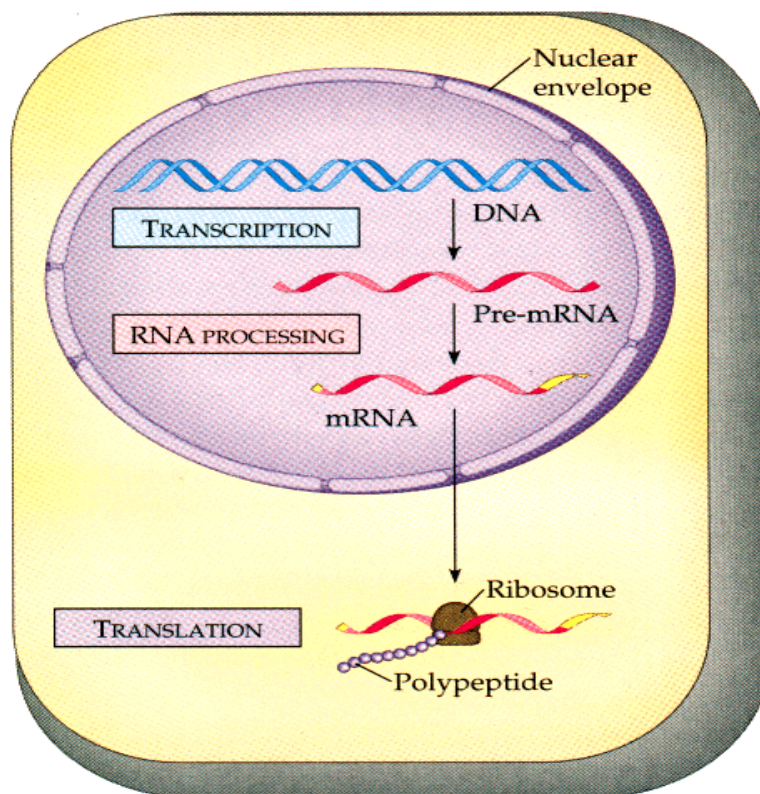


Figure 1.3: Biological mechanism of protein synthesis.

II. CONTROL OF GENE EXPRESSION

Many pharmacological advances involve creating small molecules that upon binding to proteins interfere with their function. Typical of such compounds are propranolol, which blocks the β -adrenergic receptor; cimetidine, which blocks the H₂ receptors, and the calcium-channel blockers; angiotensin-converting-enzyme inhibitor; and inhibitors of the H⁺/K⁺-ATPase pump. Another way to block protein function is to prevent either the transcription of the DNA into mRNA or the translation of mRNA into protein.^{3,4}

Traditional small-molecule antiviral agents inhibit enzymes that are important to viral replication or reverse transcription. The synthesis and design of nucleoside-based antiviral agents is well-established and many clinically important drugs have been developed (e.g. acyclovir and AZT).⁵ However, it has proved difficult to develop compounds with the ability to eliminate viruses entirely or to prevent their integration into the host genome. For this reason a number of oligonucleotide-based approaches are now being developed.

It has been more than three decades since it was shown that antisense oligodeoxynucleotides could selectively block the expression of targeted genes.^{3,6} Much has happened to the field of oligonucleotide chemistry and applications over this time. New chemistries have developed an expanding repertory of novel methods and oligonucleotide agents.

II.1. Antisense approaches

II.1.a. The mechanism

Viruses and bacteria have unique proteins that are essential for their survival. The mRNA sequences that encode these proteins are absent in the human genome, so any method to eliminate foreign mRNA molecules without interfering with the mRNA of the host is potentially of great therapeutic value. Moreover, advances in

DNA sequencing technology have made the information required to target pathogens readily obtainable. If the nucleic acid sequence encoding a disease or foreign protein is known, an antisense oligonucleotides designed to hybridize highly specifically to the corresponding mRNA can be synthesized. The newly formed duplex can be degraded by enzymes potentially arresting/stalling the disease condition. By this mechanism antisense oligonucleotides can, for example, inhibit the expression of particular proteins encoded by our own genome for the uncontrolled growth of cancer cells, or the genomes of viruses and other infectious agents (Figure 1.4).⁶⁻⁸

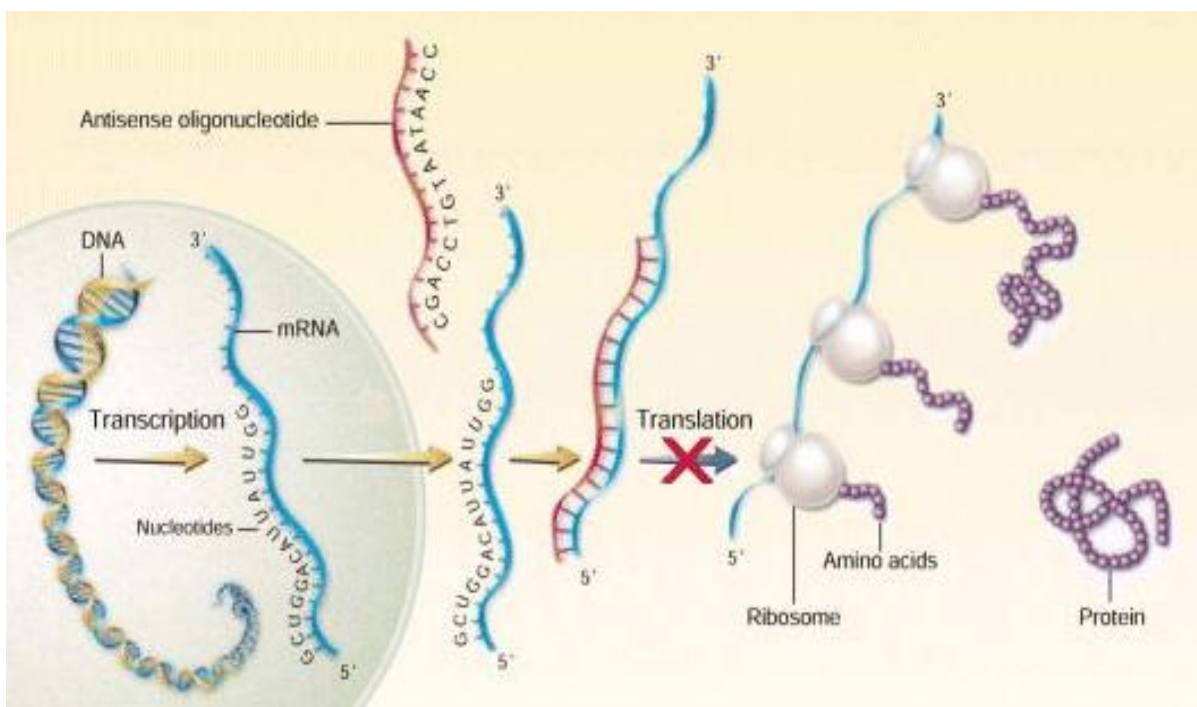


Figure 1.4: Blockage of translation by antisense therapy.⁹

II.1.b. DNase-resistant antisense oligonucleotides

Unfortunately, simply adding chemically unmodified antisense oligonucleotides to cells in culture or to organisms in vivo does not normally result in a significant antisense effect. This is because unmodified oligonucleotides are unstable in biological media and are degraded by endogenous DNase enzymes. It is therefore necessary to chemically modify antisense oligonucleotides to make them stable in cells. There are different types of DNase enzymes: those with

5'-exonuclease activity digest the oligonucleotide from the 5'-end; 3'-exonucleases digest from the 3'-end; and endonucleases digest from within the DNA chain.¹⁰ Whatever the nature of the DNase enzyme, any modification of the phosphodiester backbone is likely to inhibit its action and a selection of phosphodiester backbone analogues, developed with this goal in mind are shown in figure 1.5.^{11,12}

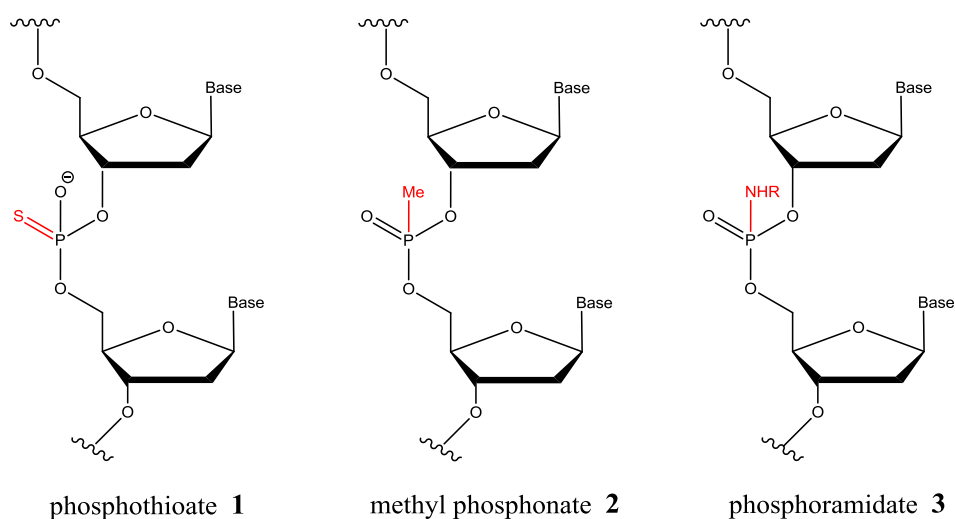


Figure 1.5: Structures of common modifications to the phosphodiester backbone found in antisense oligonucleotides.

Some modifications to the phosphodiester backbone, such as methyl phosphonates **2**, are less desirable because they prevent the mRNA of the DNA/mRNA hybrid from being a substrate for RNase H. They also have a negative effect on the aqueous solubility of the antisense oligonucleotides because the backbone is uncharged. Further, the phosphorus atoms in the backbone of phosphorothioate **1** and methyl phosphonates **2** are chiral and stereospecific methods for their synthesis are not routinely available and the use of diastereomeric oligonucleotides is not pharmaceutically attractive. Another synthetic difficulty, with the methyl phosphonate modification by the phosphoramidite method, is the instability to aqueous base, which requires that the protecting groups on the heterocyclic bases be cleavable under mild conditions.

It is also a drawback that the duplexes formed between backbone-modified antisense oligonucleotides and target mRNAs are generally thermodynamically less

stable than normal DNA/RNA hybrids. In the case of phosphorothioates **1** this is due to the steric bulk of the sulfur atoms.

In the antisense field more work has been carried out on phosphorothioate oligonucleotides (SODNS) than on any other modification.^{13,14} This is because they are relatively easy to synthesize; they have good resistance to undesirable DNase degradation; they do not inhibit the beneficial RNase H digestion of mRNA in SODN/mRNA hybrids. Because clinical studies required large quantities, solid-phase methods have been developed to synthesize SODNS in multi-kilogram amounts. Synthesis involves a solid-phase phosphoramidite method using tetraethylthiuram disulfide (disulfiram) to introduce the sulfur atom instead of the traditional iodine oxidation step (Figure 1.6).¹⁵⁻¹⁸

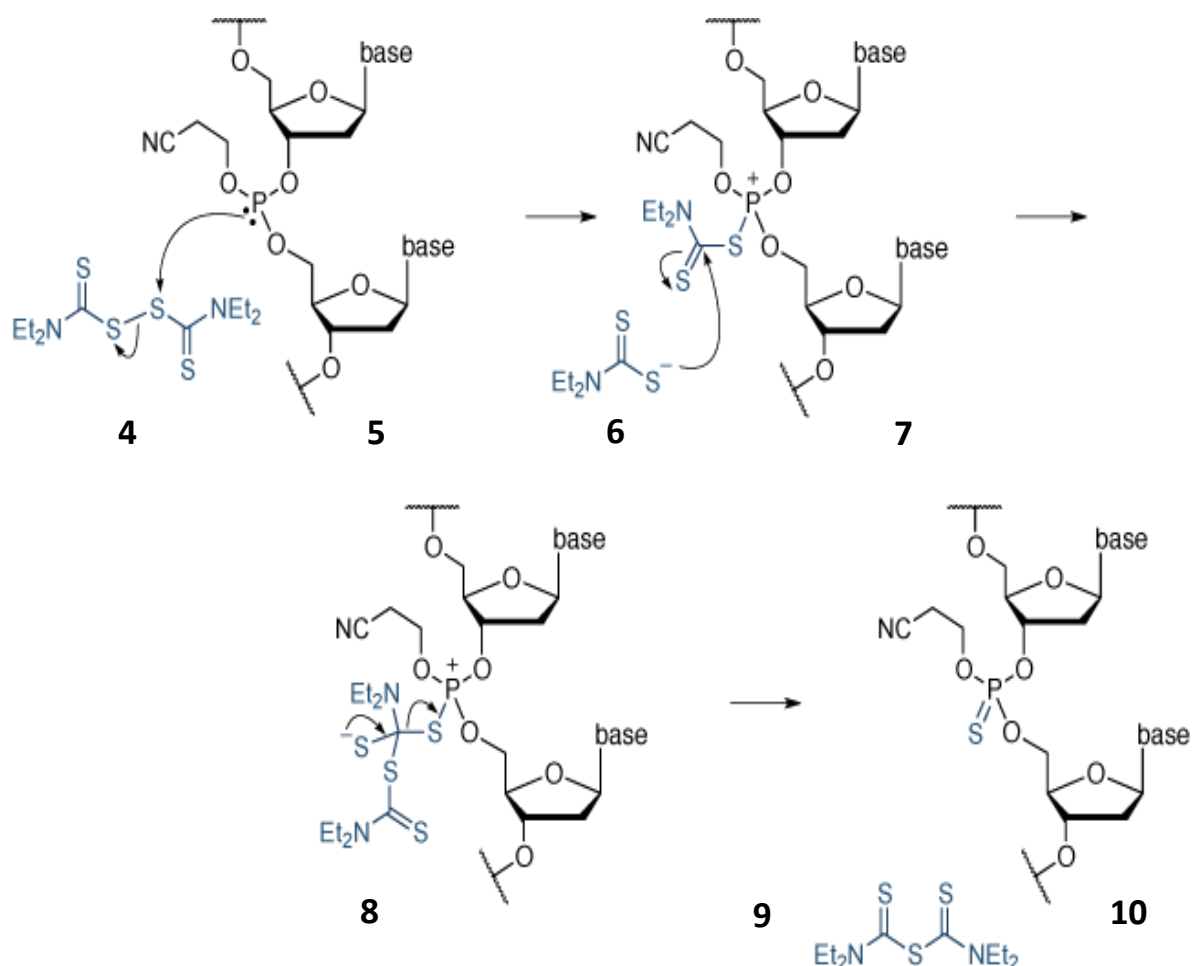


Figure 1.6: Sulfurization of the DNA backbone at the end of a cycle in solid-phase phosphoramidite oligonucleotide synthesis of SODNS.

It is possible to combine more than one modification in a single oligonucleotide: one common strategy is to alternate sections of modified backbone with lengths of normal (phosphodiester) DNA backbone. For example oligonucleotides with phosphorothioate or methyl phosphonate groups at the 5'- and 3'-ends tend to have reasonably good stability in vivo, presumably because DNA exonucleases are more prevalent in cells than endonucleases.

Selected modifications to the sugar moiety of antisense oligonucleotides, also known to prevent DNase degradation, are summarized in figure 1.7.¹⁹

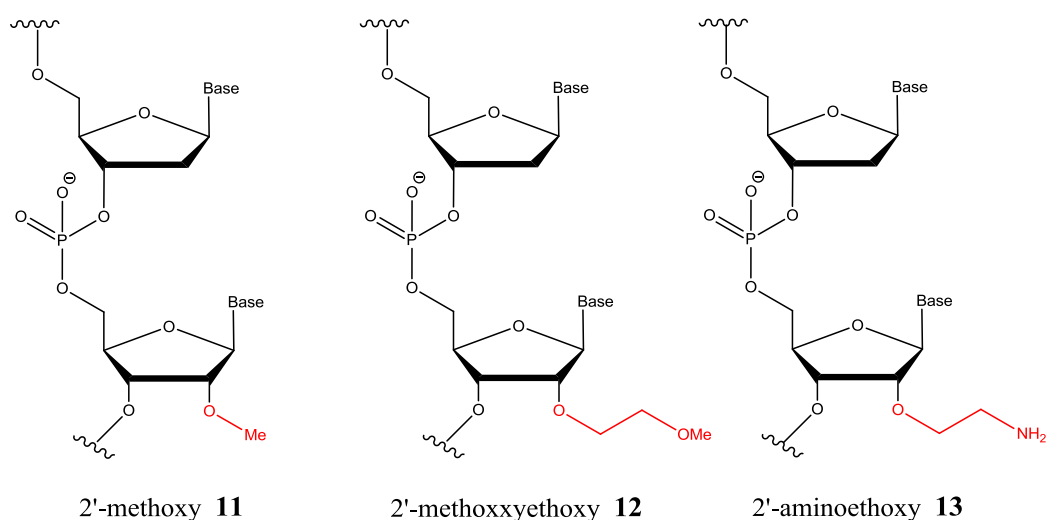


Figure 1.7: Structures of common modifications to the deoxyribose sugar found in antisense oligonucleotides.

II.1.c. Applications of antisense activity

Antisense drugs are being developed to treat cancers (including lung cancer, colorectal carcinoma, pancreatic carcinoma, malignant glioma and malignant melanoma), diabetes, amyotrophic lateral sclerosis (ALS), Duchenne muscular dystrophy and diseases such as asthma and arthritis with an inflammatory component. Some examples are summarized in table 1.1.¹⁹⁻²⁴ Most potential therapies have not yet produced significant clinical results, though one antisense drug, fomivirsen (marketed as Vitravene), has been approved by the U.S. Food and Drug Administration (FDA) as a treatment for cytomegalovirus retinitis.

Table 1.1: Example antisense therapies

Diseases	Drugs	Successes	Structures
Cytomegalovirus retinitis	Fomivirsen (marketed as Vitravene)	Approved by the U.S. FDA in Aug 1998 as a treatment.	A phosphorothioate antisense oligodeoxynucleotide, 21 nt: 5'-GGG TTT GCT CTT CTT CTT GCG-3'
Hemorrhagic fever viruses Marburg and Ebola	AVI-6002 and AVI-6003	The usual mortality rate for monkeys infected with Ebola virus is 100%. In late 2008, preclinical results of AVI-6002 and AVI-6003 (developed by AVI BioPharma, a U.S. biotechnology firm) demonstrated reproducible and high rates of survival in non-human primates challenged with a lethal infection of the Ebola and Marburg viruses, respectively.	Anti-viral potency is enhanced by the addition of positively-charged components to the morpholino oligomer chain
Cancer	AP 12009	In 2006, German physicians reported on a dose-escalation study for the compound in patients with high grade gliomas. At the time of the report, the median overall survival had not been obtained and the authors hinted at a potential cure.	A phosphorothioate antisense oligodeoxynucleotide specific for the mRNA of human transforming growth factor TGF-beta2
HIV/AIDS	/	Starting in 2004, researchers in the US have been conducting research on using antisense technology to combat HIV.[6] In February 2010 researchers reported success in reducing HIV viral load using patient T-cells which had been harvested, modified with an RNA antisense strand to the HIV viral envelope protein, and re-infused into the patient during a planned lapse in retroviral drug therapy.	Autologous transfer of CD4+ T lymphocytes genetically modified with VRX496TM, a HIV-based lentiviral vector encoding for a RNA antisense targeting HIV
High cholesterol	Mipomersen	In 2010, it successfully completed phase 3 trials for some types of high cholesterol.	A phosphorothioate antisense oligodeoxynucleotide, 20 nt: 3'-G ⁺ C ⁺ U ⁺ C ⁺ dAdGdTdCdTdTdGdmC dTdTdmCG ⁺ C ⁺ A ⁺ C ⁺ C ⁺ -5' [* = 2'-O-(2-methoxyethyl)]

II.2. The triplex approach

II.2.a. The mechanism

The antisense approach is elegant, but suffers from one major potential disadvantage: there are often very large numbers of mRNA molecules in a cell, and it is therefore difficult to achieve complete inhibition of a specific mRNA. Moreover, response mechanisms exist that can lead to increased mRNA production in response to destruction of mRNA in antisense therapy.⁴ In theory a much more attractive approach to block the synthesis of specific proteins is direct inhibition of genomic DNA. Switching off genes directly by an external agent is an extremely attractive proposition and in principle it could be achieved by sterically blocking the double helix so that the proteins interacting with DNA can no longer bind. This would directly prevent replication and transcription. It would also offer the possibility of interfering with regions of DNA involved in the regulation of gene expression. The challenge is to develop a chemical agent that can bind tightly to a specific region of duplex DNA in the presence of the entire human genome. This is a major task but it is not insurmountable. If such an agent could be developed it would have profound implications in molecular biology and in medicine. Nature offers us clues to solve the problem. It has been known for some time that, for certain sequences, a third strand of natural DNA can fit into the major groove of the DNA duplex and interact with the base pairs to form a triple helix (Figure 1.8).^{4,25}

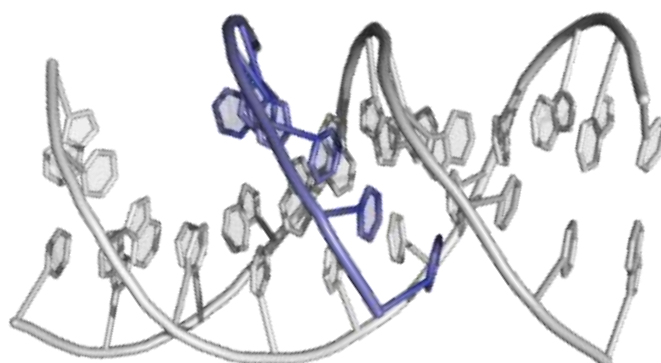


Figure 1.8: 3D representation of a DNA triplex. The strands of the DNA duplex are shown in white; the third (triplex-forming) strand is shown in blue.⁴

Triple helices were first observed by Felsenfeld, Davies and Rich in 1957. However, using natural DNA or synthetic oligonucleotides containing natural bases it was only possible to create triplexes if one of the strands of the duplex was purine-rich. Triple helices are able to form because the purine bases of DNA have hydrogen bonding donors and acceptors that are capable of forming two additional hydrogen bonds within the major groove. These bonds are called *Hoogsteen bonds*. Duplexes capable of forming triple helices contain purine bases in one strand and pyrimidines in the complementary strand, so a pre-requisite for triplex formation is a homopyrimidine/homopurine region of DNA. Triplex forming oligonucleotides (TFOs) can be oriented antiparallel or parallel to the purine strand of the duplex (Figure 1.9).²⁵

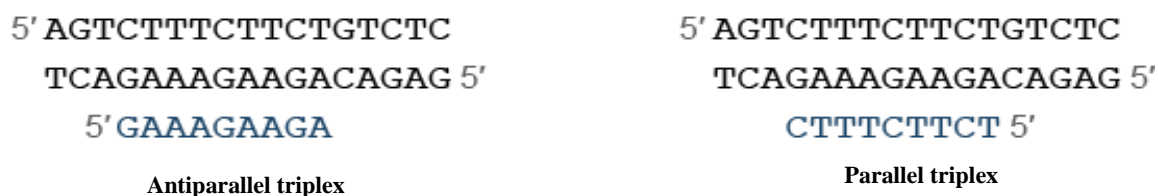


Figure 1.9: Triplex orientations of a DNA triplex. Triplex-forming oligonucleotides (TFO in blue) can be oriented either antiparallel or parallel to the purine-rich of the DNA duplex.

Antiparallel triplexes are unstable at all pH values. The TFO, as shown in figure 1.10, is composed mostly of G and A bases.

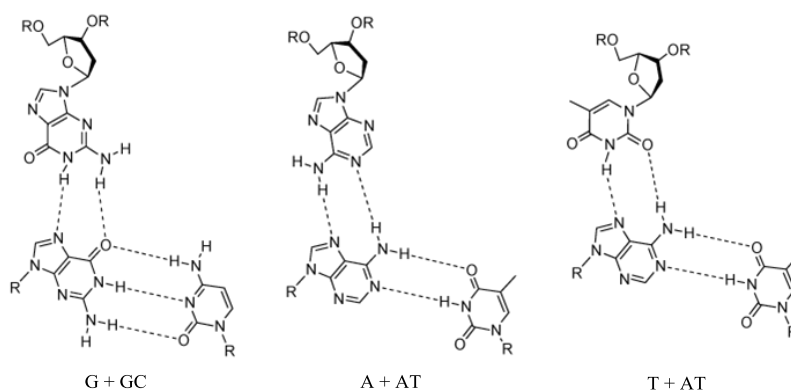


Figure 1.10: Structures of a segment of antiparallel DNA triplexes indicating A and T triplets with AT base pairs and a G triplet with a GC base pair.

- the anilinothiazole S - specifically H-bonds to TA base pairs;
- the methyl pyrimidone base PO - stabilizes triplexes containing CG base pairs by the formation of an N-H...N hydrogen bond and a weak C-H...O hydrogen bond;
- the pyrimidine analogue MP (3-methyl-2-aminopyridine) - specifically recognizes G-C. It has a $pK_a > 6$, and unlike cytosine it is partially protonated at physiological pH;
- the 5-aminopropargyl-2'-aminoethoxythymidine nucleoside Ba - it has two primary amine groups that are protonated at pH 7, and which interact with the anionic phosphate groups in the neighboring duplex. The triple bond stabilizes the correct helical conformation in the third strand through π stacking interactions with the surrounding bases. It is important that the TFO is able to adopt a stable conformation that is compatible with the shape of the major groove of the duplex.

These chemical modifications go some way towards solving the "triplex stability problem" and it is likely that further advances will be made in the near future.

II.3. The DNA quadruplex

II.2.a. The mechanism

The ends of chromosomes, known as telomeres consist of G-rich sequences, in humans the sequence is $(GGGTTA)_n$ where n is several hundred. These sequences cannot be fully copied as it is not possible for replication to extend right to the end of a DNA duplex, so the telomeres get progressively shorter through multiple cycles of cell division. Eventually the number of $(GGGTTA)_n$ repeats falls below a critical level and the cell dies. This is probably a process that has evolved to define the useful lifetime of a cell. However, in stem cells and in most cancer cells, $(GGGTTA)_n$ repeats are added to the ends of chromosomes by a specific enzyme called telomerase, which is not present in most normal differentiated cells and the cells become immortal. This means that telomerase may be a good target for novel antitumor agents. Telomerase incorporates a single strand of RNA containing the sequence rUUACCC which acts as a template for the synthesis of the dGGGTTA repeats.²⁹⁻³¹

It is known that G-rich sequences such as telomeres can fold into quadruplexes (Figure 1.12). These structures form slowly, but are extremely stable, with high melting temperatures.

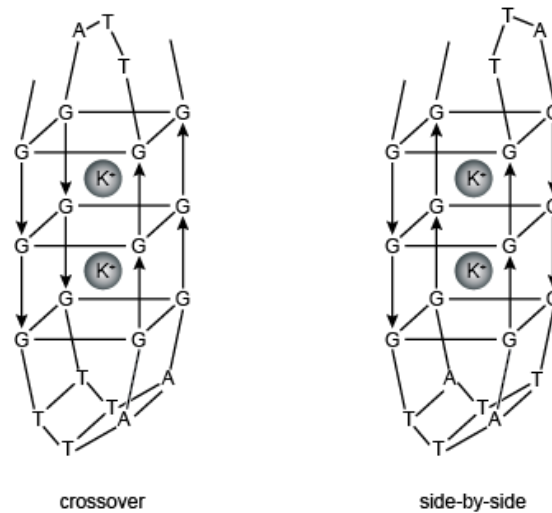


Figure 1.12: Schematic representations and three-dimensional structure of G-quadruplexes.²⁹

Quadruplexes consist of stacks of G-quartets, formed by the association of four G-rich DNA strands and stabilized by hydrogen-bonding between bases and by metal ions (commonly potassium, but occasionally sodium; Figure 1.13).³² These "four strands" can actually be part of the same single strand of DNA: in this case the quadruplex is intramolecular. It has not been proved that telomeres exist as quadruplexes in vivo but it is possible that these structures have some biological role. Quadruplexes are interesting from a structural point of view as different arrangements of the strands can give rise to alternative quadruplex structures.

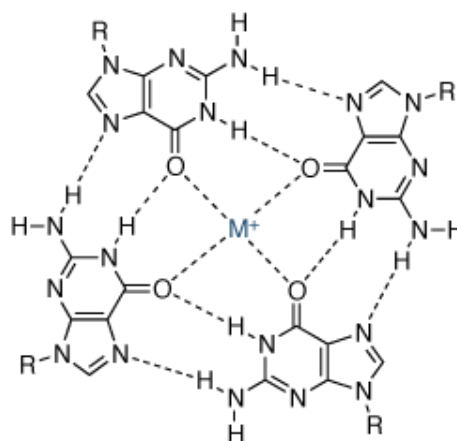


Figure 1.13: Bonding in the G-quartet.

There has been substantial recent work on developing drugs that bind to DNA quadruplexes. Molecules that can either facilitate quadruplex formation or stabilize quadruplexes have the potential to interfere with replication, inhibit telomerase activity and arrest cancer cell growth.

II.4. RNA interference (RNAi)

In 2002, the journal *Science* proclaimed **RNA interference (RNAi)** the "breakthrough of the year". Here was a part of the body's natural immune system that might be enlisted to fight almost every diseases imaginable, brain disorders like Huntington's and Alzheimer's, deadly viral infections like HIV, cancers... EVERY condition in which "silencing" rogue genes might stop disease onset or progression. The molecules of interest in this process are "**short interfering RNAs**" (**siRNAs**) which include several classes of regulatory 20-25 nucleotides-long double-stranded RNAs (ribonucleic acids). Once the biomedical field became aware of their potential as therapeutics, the challenge for the chemist was to provide those new molecular research tools by using easy and reproducible chemistry.

II.4.a. Discovery of RNAi

The phenomenon of double-stranded RNA (dsRNA) to induce gene silencing, now known as RNAi,³³ emerged from studies dating back to the 1980s. It was initially observed in plants, that the introduction of exogenous "transgenes" having some amount of sequence homology with endogenous genes, resulted in alteration of the levels of expression. The phenomenon was termed "homology dependent gene silencing" (HDGS).³⁴ Further work suggested that HDGS operates in a wide variety of organisms,^{35,36} and that it could be correlated to covalent modification of genomic DNA. It was not until later investigations in worms (*C. elegans*) in the 1990s that RNA was shown to trigger gene silencing in an inheritable manner. Both sense and antisense RNAs, when injected separately, were equally effective at silencing homologous target genes.³⁷ Following this, a seminal discovery by Fire and Mello demonstrated that the combination of sense and antisense RNAs,

essentially dsRNA, effected down-regulation by more than one order of magnitude than either RNA strand alone.³⁸ This finding led to the realization that RNA was responsible for the HDGS phenomena observed a decade earlier and sparked the cascade of research on RNAi in mammalian cells that continues to grow.³⁶ Initial *in vitro* investigations of RNAi showed that RNAi-induced silencing was realized *via* degradation of mRNA.³⁹ An assembly of the dsRNA with a nuclease to form a “RNA-induced silencing complex” (RISC) was observed. The cells involved in the process were shown to possess discrete ~25 nucleotide b.p. RNA molecules homologous to the target gene. It was discovered shortly thereafter that these RNAs co-fractionated with the RISC.^{40,41} A critical extension by Zamore and co-workers, determined that cell-free extracts retained the ability to process dsRNA into siRNAs.⁴² Quickly, more became known about both the protein and nucleic acid components of RISC. Having a total size of ~500 kDa, the RISC was shown to contain the Argonaute-2 (Ago-2) protein and a family of RNAase III proteins called Dicer.⁴³ Dicer contains dual RNAase III domains and dsRNA-binding motifs. It processes dsRNA into siRNAs and is recruited into the RISC by association between the Piwi Argonaut and Zwillie (PAZ) domains found on both Dicer and Ago-2.

II.4.b. RNAi Mechanism

The RNAi mechanism, which involves disruption of gene expression by a dsRNA, one strand of which is complementary to a section of the mRNA, is described in detail in several recent reviews.^{44,45} An overview of the RNAi pathway is shown in figure 1.14.⁴⁶ It is known from the RNAi assay, that dsRNAs introduced into the cell are processed in the cytoplasm by an enzyme of the Dicer family leading to small interfering RNAs (siRNAs). Next, the siRNA is assembled into an RNA-induced silencing complex (RISC). In fruit flies and mammals, the antisense strand is directly incorporated into RISC and activates it. In worms and plants the antisense strand might first be involved in an amplification process, during which new long dsRNAs are synthesized, which are again cleaved by Dicer. Finally, antisense siRNA strands guide the RISCs to complementary mRNA molecules, where they cleave and destroy the cognate mRNA. This process leaves the genomic DNA intact but suppresses gene expression by mRNA degradation.

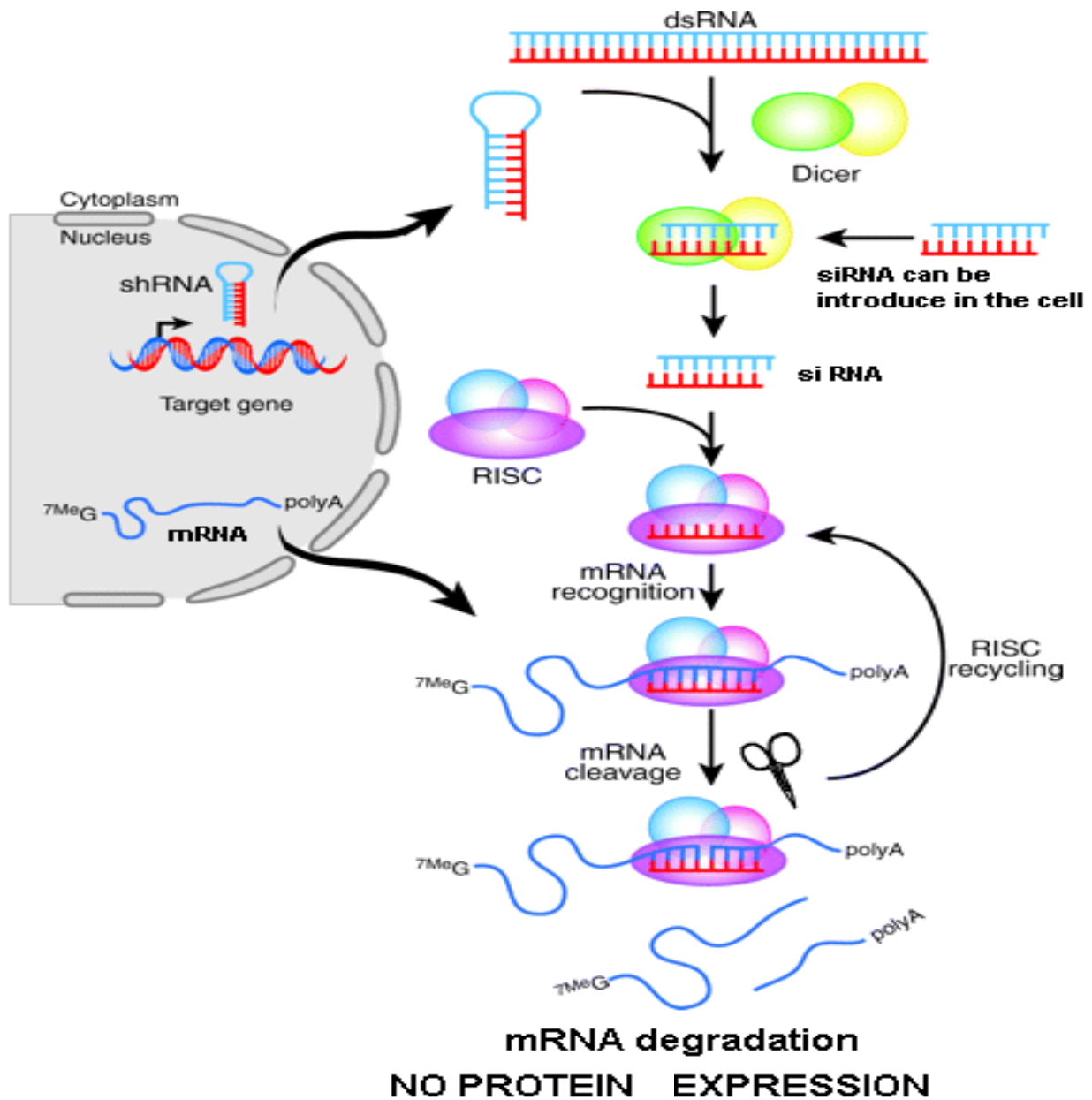


Figure 1.14: RNAi pathway.⁴⁶

II.4.c. Applications

It is now possible to design and synthesize siRNAs that can effectively silence a disease. However, a significant hurdle to realization of the potential of siRNAs as a research and therapeutic tool remains – that of efficient delivery. The work developed in this Ph.D. thesis aimed to synthesize a novel range of chemically modified siRNAs that may have enhanced delivery characteristics.

II.5. Other potential therapeutic nucleic acid analogues

II.5.a. Stimulation of the innate immune system

Some oligonucleotides exert their therapeutic effect by stimulating the natural immune response of the host cell. Oligonucleotides with sequences containing one or more CG units can bind to the TLR9 protein, so triggering the induction of cell signaling pathways that lead to the stimulation of the cell's innate immune response.⁴

II.5. b. Locked nucleic acid (LNA)

Initial reports on LNA synthesis by the group of Jesper Wengel⁴⁷ in 1998, appeared soon after the first preparation by Imanishi and co-workers⁴⁸ in 1997. A locked nucleic acid (LNA) represented in figure 1.15, often referred to as inaccessible RNA, is a modified RNA nucleotide in which the ribose moiety is modified with an extra bridge connecting the 2'-oxygen and the 4'-carbon atoms. The bridge "locks" the ribose in the 3'-endo (North) conformation, which is often found in the A-form duplexes. The locked conformation enhances base stacking and backbone pre-organization resulting in a significant increase in the hybridization properties (melting temperature) of the resulting oligonucleotides.⁴⁹

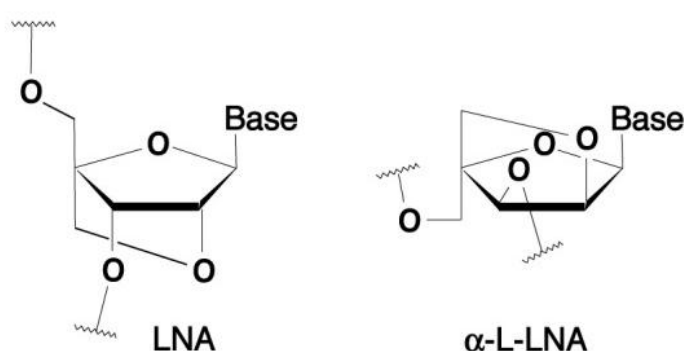


Figure 1.15: Structure of LNA.

LNA nucleotides can be mixed with DNA or RNA residues in synthetic oligonucleotides at pre-determined positions and such oligomers can be commercially sourced.

LNA nucleotides have been found to increase the sensitivity and specificity of expression in molecular biology techniques based on oligonucleotides, indeed currently the only efficient approach to in situ detection of miRNA is by way of LNA methodologies. The mechanism of action involves formation of a triplet of LNA nucleotides around a single-base pair mismatch site. The LNA probe specificity is high unless the mismatch involves the guanine base of G-T is pair.⁵⁰ Some examples are:

- DNA microarrays, a collection of microscopic DNA spots attached to a solid surface. Scientists use DNA microarrays to measure the expression levels of large numbers of genes simultaneously or to genotype multiple regions of a genome;⁵¹
- FISH (fluorescence in situ hybridization) probes, a cytogenetic technique developed by biomedical researchers in the early 1980s, that is used to detect and localize the presence or absence of specific DNA sequences on chromosomes;⁵²
- real-time PCR (polymerase chain reaction) probes, a laboratory technique based on the PCR, which is used to amplify and simultaneously quantify a targeted DNA molecule.⁵³

Using LNA based oligonucleotides therapeutically is an emerging field in biotechnology. The Danish pharmaceutical company Santaris Pharma A/S owns the sole rights to therapeutic uses of LNA technology, and is now developing a new, LNA based, hepatitis C drug called miravirsin, targeting miR-122, which is in Phase II clinical testing as of late 2010.^{54,55}

II.5. c. Peptide nucleic acid (PNA)

Peptide nucleic acids (PNA) represented in figure 1.16, not known to occur naturally were first synthesized in 1991 by the groups of Nielsen, Egholm, Berg and Buchardt (Univ. Copenhagen).⁵⁶ These artificial polymers are similar to oligonucleotides, DNA and RNA have a deoxyribose and ribose sugar backbone, respectively, whereas PNA's backbone is composed of repeating N-(2-aminoethyl)-glycine units linked by peptide bonds.⁵⁷ The name is somewhat inaccurate as PNA is not an acid.

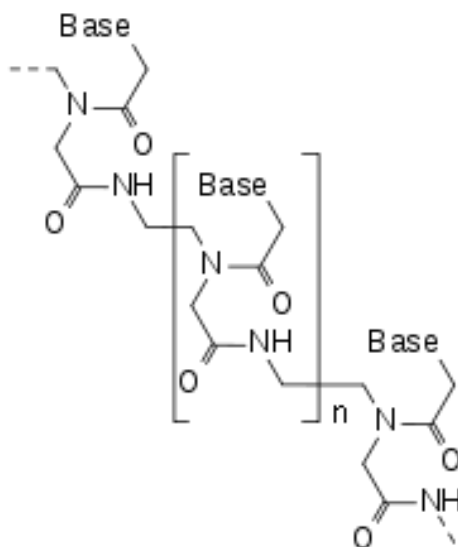


Figure 1.16: Structure of PNA.

PNA oligomers have found application in molecular biology procedures, diagnostic assays and antisense therapies. Mixed base PNA molecules are found to be true mimics of DNA molecules in terms of base-pair recognition and further, as the backbone of PNA is uncharged the lack of electrostatic repulsion actually results in stronger binding between PNA/DNA (or RNA) strands than between DNA/DNA (or RNA) strands. PNA/PNA binding is stronger than PNA/DNA binding.⁵⁶

Due to their higher binding affinity to complementary oligonucleotides PNA oligomers do not need to be as long as other oligonucleotide probes (typically 20–25 bases long). The main concern in the design of PNA-oligomers is to choose the length to optimize specificity. In this regard it is advantageous that PNA oligomers show greater specificity in binding to complementary DNAs, with a PNA/DNA base mismatch being more destabilizing than a similar mismatch in a DNA/DNA duplex. This relativity in binding strength and specificity is also observed with PNA/RNA duplexes. Further attractions of PNAs include their stability over a wide pH range and resistance to enzyme degradation - they are not easily recognized by either nucleases or proteases. Disadvantages of the uncharged backbone it that it causes PNAs to be rather hydrophobic, and thus difficult to deliver to the target cells more prior to being flushed out of the body. The hydrophobicity also renders unmodified PNAs poor at crossing cell membranes to enter the cytosol; however, it is found that covalent coupling to a cell penetrating peptide can improve cytosolic delivery.⁵⁶

III. Delivery of Nucleic Acid Therapeutics

Synthetic oligonucleotides and especially siRNAs are considered to have an exciting future as therapeutics with potential for treatment of various infectious and genetic diseases including cancer.⁵⁸ It is now chemically possible to design and synthesize siRNAs that can effectively silence a disease. Unfortunately, delivery and stability difficulties are still limiting widespread application of this technology.⁵⁹ Today, significant research efforts are being made towards directing siRNA molecules to the targeted cells in the body and making them resistant to nucleases.

Oligonucleotides have a much greater molecular mass than conventional small-molecule pharmaceutical drugs, and this is one reason why their cellular uptake by passive diffusion is inefficient. Fortunately, some cells take in oligonucleotides by a process known as receptor-mediated endocytosis,⁶⁰ which involves the specific uptake of the oligonucleotide by natural cell-surface receptors. SODNS are taken up reasonably efficiently by this process. During the process of cell uptake oligonucleotides are sometimes trapped in endosomes and separated from target mRNA by an impermeable membrane. Chemically unmodified oligonucleotides are rapidly digested in endosomes but some chemically-modified antisense oligonucleotides survive long enough for the endosomes to break down and release their contents into the cytoplasm.

Clinical siRNA delivery systems have to be prudently designed to ensure adequate stability and delivery characteristics.⁶¹ Virus-based vectors,⁶² and a number of non-viral carriers, including lipids,^{63,64} liposomes,^{65,66} polymers,^{67,68} peptides,⁶⁹ pressurized hydrodynamic injections,⁷⁰ and cationic polymers with different architectures and functionalities⁷¹ have been suggested to improve intracellular delivery. Many of these complexes are resistant to attack by extracellular nucleases and facilitate easy cellular uptake *via* an endocytic pathway. Recently, it has been reported that direct conjugation of peptides, proteins, polymers or lipids, including cholesterol derivatives, to siRNAs could improve their *in vivo* pharmacokinetic behavior.⁷² Such synthetic conjugates, either with or without forming nano-complexes with cationic carriers, were found to significantly enhance

biological half-life and to effect efficient delivery to the target tissue while maintaining sufficient gene silencing activity.⁷³ Of the multitude of synthetic possibilities for preparation of oligonucleotide conjugates “Click Chemistry”, which facilitates efficient coupling of modular building blocks, is especially attractive.

In the last decade the CuAAC reaction, the quintessential click reaction, has been successfully used for ligation and cyclization of DNA.⁷⁴⁻⁷⁷ It has also been extensively used for synthesis of modified nucleosides,⁷⁸⁻⁸¹ carbohydrates,⁸²⁻⁸⁴ fluorophores,⁸⁵⁻⁸⁹ and lipophilic oligonucleotide conjugates;^{90,91} for synthesis of chimeras of peptide-DNA/PNA oligonucleotides,^{80,92} and to explore G-quadruplex solution structures.⁹³ A recent report from Morvan’s laboratory demonstrated an efficient click chemistry approach to the synthesis of a dendrimeric oligonucleotide-glycoconjugate bearing 16 peripheral galactose moieties.⁹⁴ In addition, Best has reviewed the impact of azide-alkyne cycloaddition in chemical biology; in particular he overviews bio-orthogonal reactions for labelling of biomolecules, including proteins, viruses, sugars, nucleic acids and lipids.⁹⁵ To date, *in vivo* applications have been slow in coming to fruition. This is, in part, due to the reducing environment in the cytosol that makes Cu(I) toxic to cells, and so the CuAAC reaction is apparently inapplicable to the greater challenges associated with chemical intervention in living systems.⁹⁶⁻⁹⁸ However, important work in this area is emerging and both copper-catalysed⁹⁹ and uncatalyzed bio-benign versions¹⁰⁰ of the azide/alkyne cycloaddition reaction have been reported. Another promising approach for application in oligonucleotide bioconjugation, is the 1,3-dipolar cycloaddition between a nitrile oxide or nitron and a dipolarophile.¹⁰¹⁻¹⁰³ These reactions afford five membered isoxazol(idin)e, Δ^2 - or Δ^4 -isoxazoline rings as the conjugation linker. They proceed selectively and in high yield under mild reaction conditions. That the protocol is free from copper is significant for broader applications as it removes the need to manage potentially problematic redox interference chemistry. In addition, it is well recognised that the activities of different segments within a molecule can act in concert or confer new attributes on the molecule, and in this context the bioactivity of isoxazol(idin)e and Δ^4 -isoxazoline modified nucleosides has received much attention. Indeed those heterocycles exhibit important biological activities such as antibacterial,¹⁰⁴ antiplatelet,¹⁰⁵ antiviral,¹⁰⁶ anticonvulsant,¹⁰⁷ immunostimulatory¹⁰⁸ and antinociceptive.^{109,110}

IV. CLICK CHEMISTRY

Click chemistry is not a chemical reaction but a philosophy introduced by K. Barry Sharpless of The Scripps Research Institute (California, USA), in 2001.^{111,112} It describes chemistry tailored to generate substances quickly and reliably by joining small units together. It is inspired by nature's ability to generate substances by joining small modular units. Many of the criteria for a reaction to belong to the click chemistry group are subjective, but the concept is attractive for the synthesis of molecules having a future in biological systems.

The desired characteristics of reactions to be included within the click category are as follows:¹¹¹

- modular;
- wide in scope;
- high yielding;
- generating only inoffensive by-products;
- stereospecific;
- physiologically stable;
- exhibiting a large thermodynamic driving force $> 84 \text{ kJ.mol}^{-1}$ to favor a reaction with a single reaction product;
- and having high atom economy.

It is highly desirable that the processes:¹¹¹

- encompass simple reaction conditions;
- use readily available starting materials and reagents;
- use no solvent, a benign solvent (preferably water), or a low boiling solvent;
- provide for simple product isolation by non-chromatographic methods (crystallization or distillation).

The most common "click" reactions are the Diels-Alder reaction and the Huisgen 1,3-dipolar cycloaddition, in particular the Cu(I)-catalysed azide/alkyne cycloaddition (CuAAC), is often referred to simply as the "click reaction".

IV.1. 1,3-Dipolar Cycloaddition Reactions

Dipolar cycloaddition reactions fall within the important class of concerted reactions known as pericyclic reactions. In these reactions, all bond breaking and bond making occurs in a single step. The present understanding of the mechanism of pericyclic reactions is mainly due to the work of Woodward and Hoffmann.¹¹³ They recognized that the pathways of such reactions were determined by the symmetry properties of the orbitals that are directly involved, and that the symmetry of each participating orbital must be conserved during the concerted process.

The cycloaddition reaction is a process in which two or more π systems combine to form a stable cyclic molecule, during which sigma bonds are formed between the termini of π systems, and no fragment is lost. Two important cycloaddition reactions are the Diels-Alder reaction and the 1,3-dipolar cycloaddition reaction. The general concept of the 1,3-dipolar cycloaddition reaction evolved out of the monumental work carried out by Huisgen and his co-workers in the early 1960's.¹¹⁴ In this reaction, a five membered ring is formed by the cycloaddition of a three atom entity, (a-b-c), the 1,3-dipole, and a two atom entity, (d-e), the dipolarophile. The reaction can be represented as shown in figure 1.17. It is a [3+2]-cycloaddition reaction and in terms of orbital symmetry, it is classified as $[\pi^4_s + \pi^2_s]$ cycloaddition analogous to the Diels-Alder reaction.

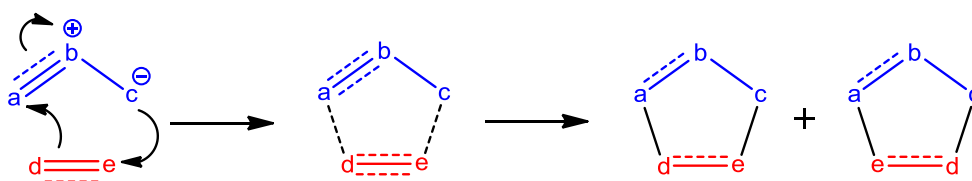


Figure 1.17: 1,3-Dipolar cycloaddition reaction leading to regioisomeric cycloadducts.

1,3-Dipoles molecules can be represented by zwitterionic octet (**14** and **15**) or sextet structures (**16** and **17**) as shown in figure 1.18. Most commonly, they include a combination of C, O and N atoms. 1,3-Dipoles containing S and P are also found.

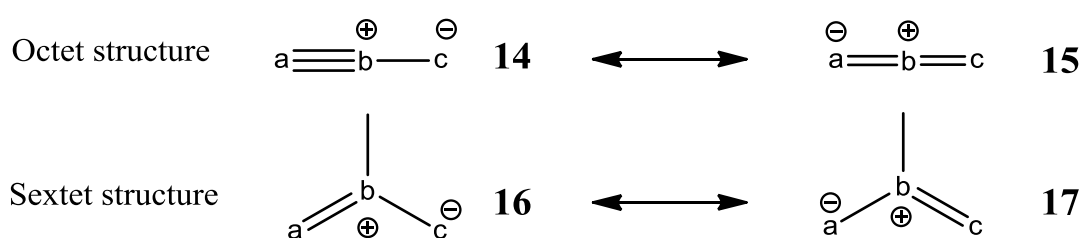


Figure 1.18: Octet and sextet structures of 1,3-dipoles.

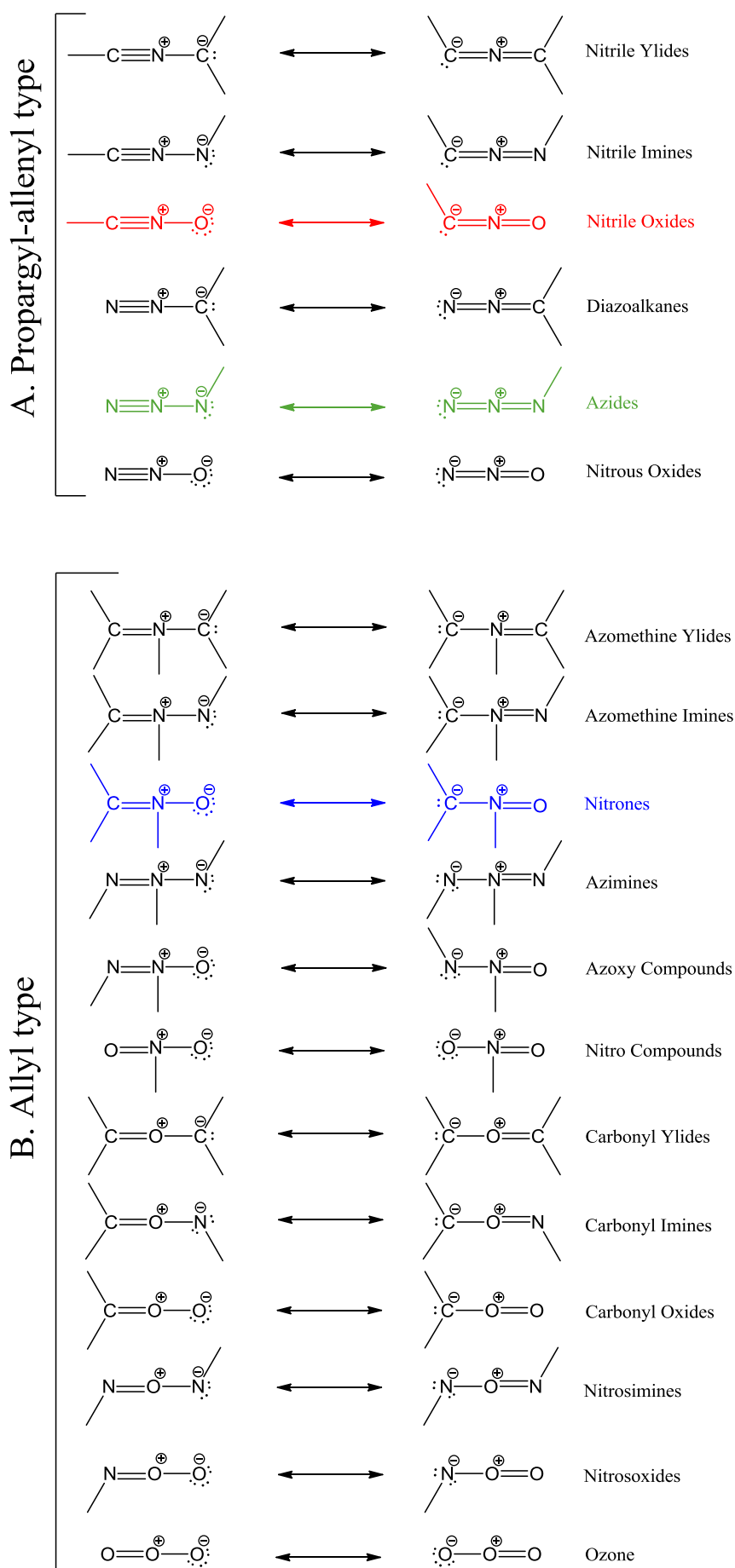
In all 1,3-dipoles (Table 1.2), there are four electrons in three parallel π orbitals. From the resonance structures contributing to the dipole, it is clear that 1,3-dipoles can be both nucleophilic and electrophilic in nature and this ambivalence is of key importance in understanding their reactivity. For any given dipole, the nucleophilic character may be stronger or weaker than its electrophilic quality, for example, nitrile ylides or diazomethane will cycloadd to electron deficient dipolarophiles much faster than to electron rich multiple bonds. The opposite is true for ozone, which combines preferably with electron rich dipolarophiles.¹¹⁵

The dipolarophile can be virtually any C=C double or C \equiv C triple bonded species. Other multiple bonded functional groups such as imines, azo and nitroso moieties can also act as a dipolarophiles. Because of the wide range of structures that can serve either as dipole or dipolarophile, 1,3-dipolar cycloaddition reactions are very useful for the construction of a wide range of five membered heterocyclic rings.

IV.1.a. Orbital analysis of the 1,3-dipolar cycloaddition reaction

Reactivity in 1,3-dipolar cycloadditions varies considerably and is best explained by the Frontier Molecular Orbital (FMO) model proposed by Fukui, for which he shared the 1981 Nobel Prize.^{116,117} In 1,3-dipolar cycloaddition reactions, two new bonds are formed by the use of π electrons of the reactants. In order to form a bond, the highest occupied molecular orbital (HOMO) of one reactant has to overlap with the lowest unoccupied molecular orbital (LUMO) of the other; in the transition state, stabilization chiefly comes from the overlap in bonding fashion.

Table 1.2: Classification of 1,3-dipoles consisting of carbon, nitrogen, and oxygen centers.



IV.1.b. The Sustmann classification

According to the Sustmann classification, 1,3-dipolar cycloadditions can be placed in one of three groups with respect to the dominant HOMO-LUMO interaction.¹¹⁸ The classification depends on the number and the nature of the heteroatoms, and on the electron donor/withdrawal properties of any substituents on the reactants.^{119,120} This Sustmann grouping indicates whether a high reactivity is expected toward electron-deficient or electron-rich olefins, or to both. The classifications, represented in figure 1.19, are as follows:

- Type I: HOMO (1,3-dipole) – LUMO (dipolarophile) controlled reaction;
- Type II: both FMO interactions are of equal importance;
- Type III: HOMO (dipolarophile) – LUMO (1,3-dipole) controlled reaction.

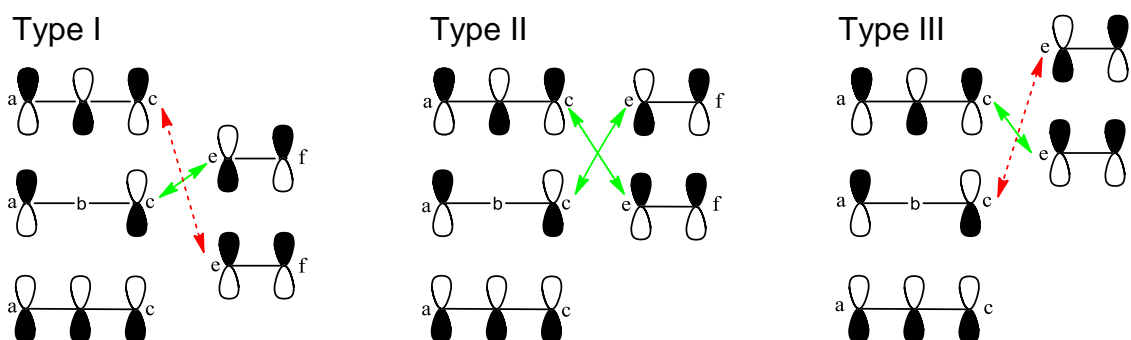


Figure 1.19: The HOMO-LUMO interaction between 1,3-dipole a-b-c and dipolarophile (e-f) depends on the orbital energies of the 1,3-dipole: — strong and - - - weak interactions.¹¹⁵

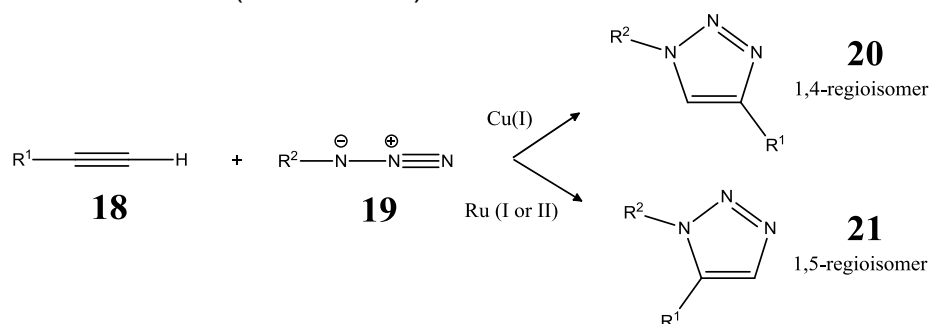
Type I: This is a HOMO (1,3-dipole) – LUMO (dipolarophile) controlled reaction. The introduction of electron withdrawing groups to ethylene (the parent dipolarophile) lowers both HOMO and LUMO energies (due to a decrease in intra-orbital electronic repulsion) and reduces the energy separation between HOMO (1,3-dipole) and LUMO (dipolarophile) thus accelerating the reaction. Electron donating substituents raise HOMO and LUMO energies in comparison to ethylene (due to an increased intra-orbital repulsion). This results in an increased energy separation between interacting FMOs which reduces the rate of the reaction. The opposite effect is true for substitution on the 1,3-dipole; acceptor substituents cause deceleration and donor substituents cause acceleration of the rate of the cycloaddition reaction.

Type II: In this case both FMO interactions are of equal importance. Therefore any substituents on the dipolarophile (acceptor or donor) accelerate the reaction rate.

Type III: This is a HOMO (dipolarophile) – LUMO (1,3-dipole) controlled reaction. Electron withdrawing substituents on the 1,3-dipole and electron donating substituents on the dipolarophile accelerate these reactions.

IV.2. Azide/Alkyne Cycloaddition Reaction

The best known reaction within the click chemistry concept is the copper or ruthenium promoted azide/alkyne cycloaddition. Alkynes are a poor electrophiles, and thus there is a high energy barrier which leads to slow cycloaddition reactions (25-26 kcal.mol⁻¹ for methyl azide and propyne)¹²¹ and the traditional reaction requires high temperatures (>100 °C). However, the reaction has been found to proceed effectively at rt under the influence of a catalyst, with Cu(I), 1,4-regioisomeric products **20** results whereas Ru (I or II) catalysis gives 1,5-disubstituted triazoles **21** (Scheme 1.1).



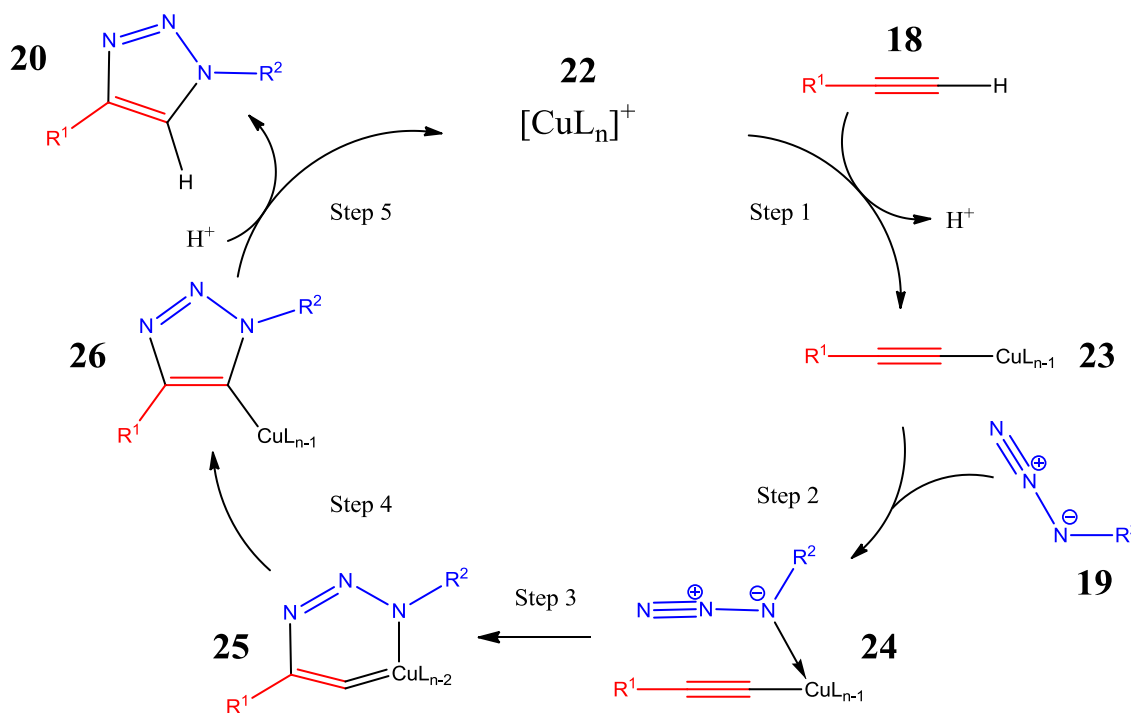
Scheme 1.1: Regiospecific cycloaddition azides/alkynes catalyzed by Cu or Ru.

IV.2.a. Copper catalysis

In 2002, the groups of Fokin/Sharpless⁹⁸ and Meldal¹²² independently reported efficient Cu(I)-catalyzed azide/alkyne cycloaddition reactions (CuAAC), selective for the formation of 1,4-disubstituted triazoles. A variety of Cu(I) catalysts can be employed.^{98,122} The attractions of this reaction include wide applicability and high tolerance of a variety of functional groups and reaction solvents, including aqueous solvents. By completely changing the mechanism, the Cu(I) catalysts overcome the high activation barrier in the non-catalyzed Huisgen reaction.

Cu(I) catalysts or pre-catalysts can be used for the CuAAC. The pre-catalyst can be a Cu(II) salt (usually CuSO_4) together with a reducing agent (usually sodium ascorbate),⁹⁸ other catalytic systems comprise Cu(I) compounds, typically CuBr or CuOAc, together with a base or amine ligand (DIPEA or NEt_3), a reducing agent often sodium ascorbate, is added in order to inhibit aerobic oxidation to Cu(II).¹²² Cu(0) can also be used in the form of copper wire, turnings, powder, or nanoparticles.^{123,124}

The mechanism of the CuAAC reaction has been investigated using kinetic studies and DFT calculations and one proposal is illustrated in scheme 1.2.^{121,125-127} Coordination between the Cu(I) species **22** and the alkyne **18** was estimated to lower the pKa of the alkyne proton by 9.8 pH units facilitating deprotonation of the π -alkyne-Cu(I) intermediate to form the σ -alkynyl-Cu(I) species **23**. In step 2, it is suggested the azide **19** attacks the Cu center on **23** forming the chelate **24**. This is followed by formation of a Cu(III) vinylidene metallacycle **25**, which after rearrangement gives the σ -triazole-Cu(I) **26**. Protonation of **26** results in formation of the 1,4-disubstituted triazole **20** and regeneration of the Cu(I) catalyst **22**.¹²⁸



Scheme 1.2: Proposed catalytic cycle for the CuAAC reaction based on DFT calculations.

According to Fokin, tris(triazolyl)methyl amine ligands are labile enough to be easily displaced by substrates, yet sufficiently strong to avoid the formation of higher unreactive or less reactive Cu(I) aggregates. In the presence of such additives, a π -complexation of the σ -alkynyl-Cu(I) species **23** was invoked as enhancing the reactivity of the alkynyl ligand by decreasing electron density on the sp carbon atoms. Consequently, the complex **24** would generate the proposed bimetallic structure **27**. DFT calculation confirmed that the second Cu(I) atom interacted with the Cu(I)-acetylide and the μ_2 -liganded σ - π -alkynyl dicopper transition state, shown in figure 1.20.^{126,125,127}

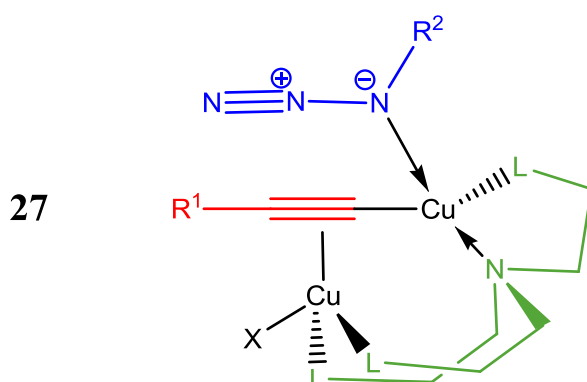


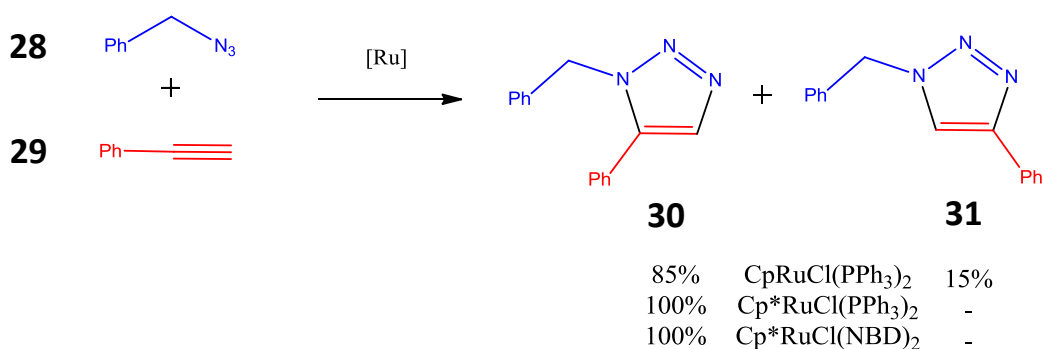
Figure 1.20: Alkyne-bridged bimetallic species 27 proposed by Fokin and Finn as the key active species for the CuAAC reaction with a [Cu(I)tris(triazolylmethyl)amine] catalyst.

The variety of solvents suitable for the CuAAC is one of the most significant features of this reaction. In their review, Meldal and Tornøe¹²² indicated that non-coordinating solvents, coordinating solvents, polar solvents, aqueous solvents, and other mixtures of two or even three solvents, all facilitate the reaction.

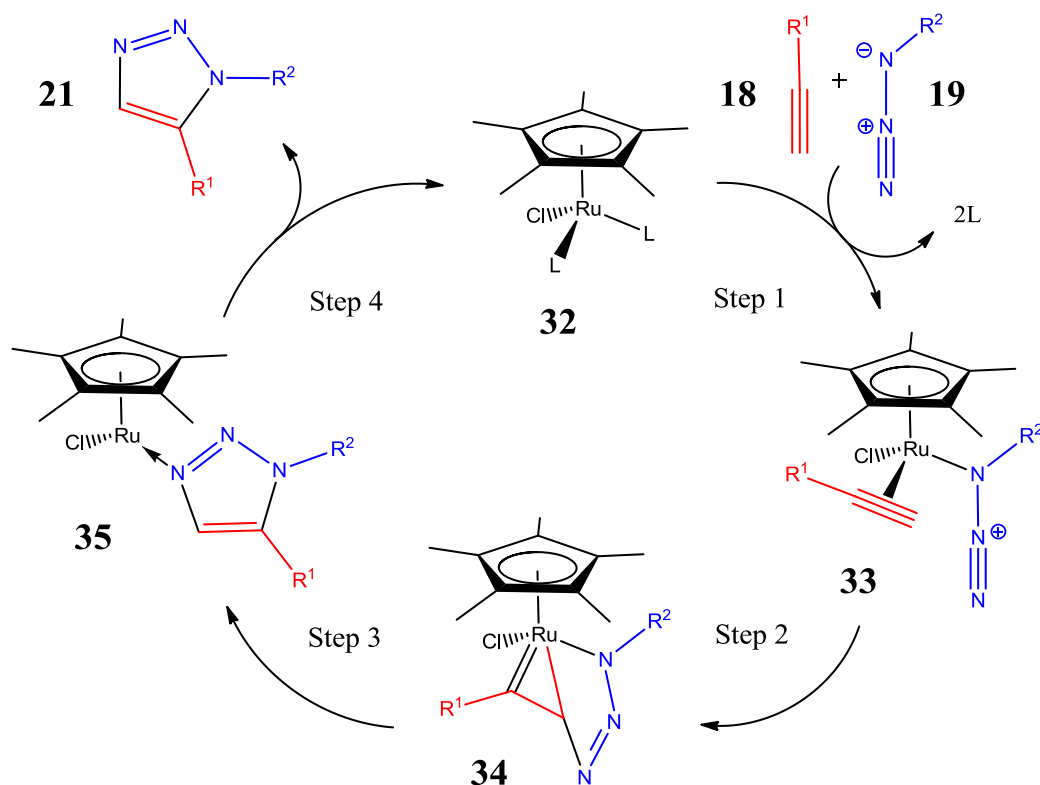
IV.2.b. Ruthenium catalysis

A more recent addition to the click tool-box is the Ru-catalyzed version of the azide/alkyne cycloadditions (RuAAC).¹²⁹ This approach provides ready access to the complementary 1,5-regioisomeric triazoles. Unlike CuAAC, which is restricted to terminal alkynes, internal alkynes also participate in the RuAAC which significantly expands the scope of this reaction. Solvents such as dioxane, benzene, 1,2-dichloroethane, toluene, or THF are all tolerated.

A range of ruthenium catalysts including $\text{Ru}(\text{OAc})_2(\text{PPh}_3)_2$, or $\text{CpRuCl}(\text{PPh}_3)_2$ containing a cyclopentadienyl group (Cp) have been used, however, better results are observed with pentamethylcyclopentadienyl (Cp^*) versions like $\text{Cp}^*\text{RuCl}(\text{PPh}_3)_2$ or $\text{Cp}^*\text{RuCl}(\text{NBD})$. The enhanced reactivity may be due to the sterically demanding Cp^* groups which facilitate displacement of the spectator ligands. The influence of the choice of catalyst on the selectivity of the reaction between benzyl azide and phenylacetylene giving regioisomers **30** and **31**, studied by Zhang, is summarized in scheme 1.3.¹³⁰



Scheme 1.3: RuAAC reaction between benzyl azide and phenylacetylene.



Scheme 1.4: Proposed catalytic cycle of the RuAAC reaction.

The proposed mechanism suggests that in the first step, the reactants displace the spectator ligands L from **32** to produce the activated complex **33**. Subsequent oxidative coupling of the alkyne and the azide unit regioselectively generates the ruthenacycle **34**. The new C-N bond forms between the more electronegative and less sterically-demanding carbon atom of the alkyne and the terminal nitrogen atom of the azide. The metallacycle **34** then undergoes reductive elimination releasing **35**. The aromatic triazole **21** formation, depending on the identity of the displacing ligand, regenerate the catalyst **32** or the activated complex **33** for further reaction cycles (Scheme 1.4).¹²⁹

V. NITRONE CHEMISTRY

Nitrones or azomethine oxides,^{131,132} first prepared by Beckmann in 1890,¹³³ were named by Pfeiffer from a shortening of “nitrogen–ketones” to emphasize their similarity to ketones.¹³⁴ While aromatic *N*-oxides also have the nitrone moiety, their reactivity is not nitrone in character. The general terms aldo- and keto-nitrones are used on occasion to distinguish between nitrones with or without a proton on the α -carbon atom. Unsymmetrical nitrones exist as (E)- and (Z)-geometrical isomers as shown in figure 1.21. The structure of the nitrone functional group can be represented by a number of canonical forms, **36** to **38**. In the case of aromatic derivatives, further conjugation with the aryl ring affords structures **39** and **40** (Figure 1.21).^{135,136}

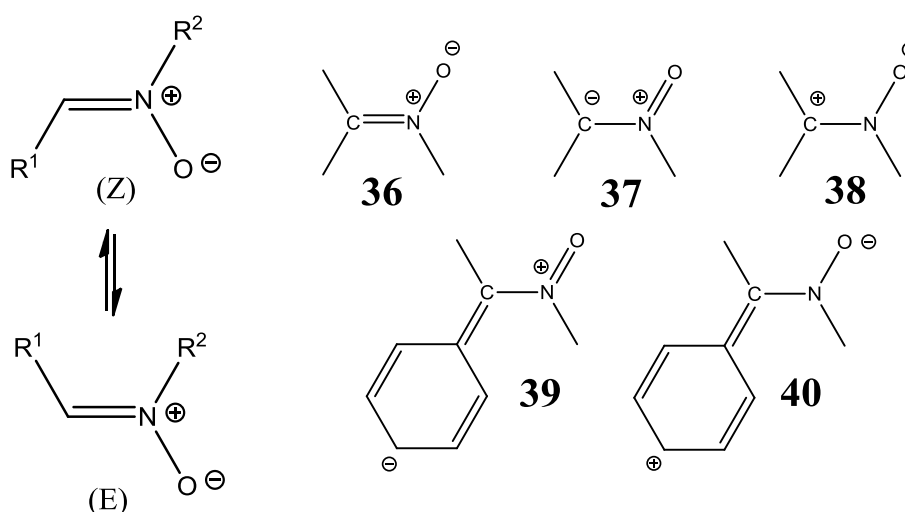
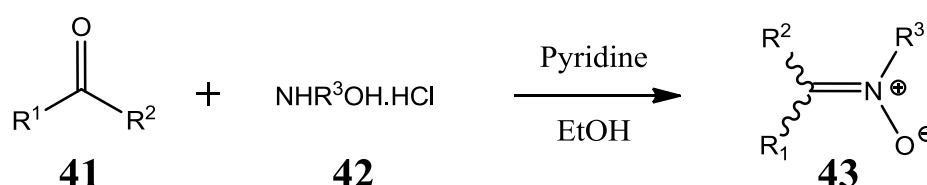


Figure 1.21: (E)- and (Z)-forms (left) and electronic structures of nitrones (right).

V.1. Generation of Nitrones

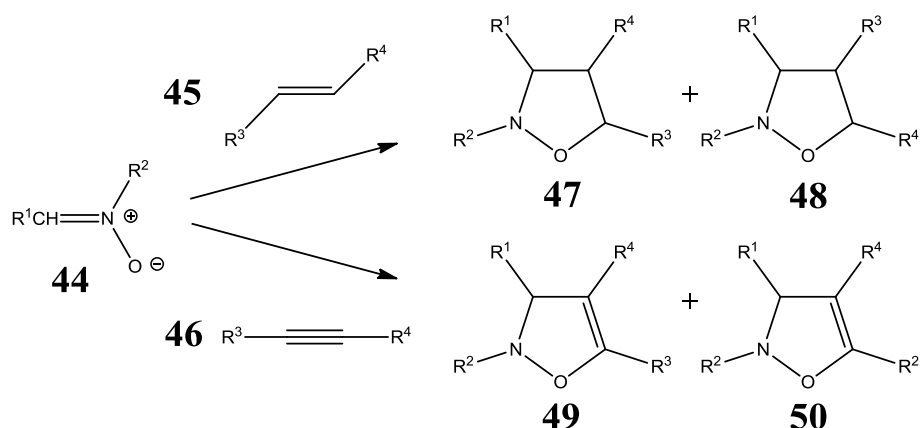
Among the most important approaches to nitrones is the condensation of *N*-substituted hydroxylamines **42** with carbonyl compounds **41**, either aldehydes or ketones. The reaction is direct and affords nitrones in good yields. Often the dipole is sufficiently stable to be isolated, in other case it must be reacted *in situ*. The condensation is carried out under mild conditions, and is largely tolerant of other functional groups. Thus, condensation of various aromatic, heteroaromatic, and aliphatic aldehydes or ketones with alkyl-hydroxylamines furnishes a wide variety of *N*-alkylnitrones **43** (Equation 1.1).¹³⁷



Equation 1.1: Nitrone formation by condensation of *N*-substituted hydroxylamines with carbonyl compounds.

V.2. 1,3-Dipolar cycloaddition of nitrones

In 1960, Huisgen proposed nitrones as 1,3-dipoles¹¹⁴ and indeed their hugely varied reactivity is dominated by their cycloaddition chemistry, the synthetic utility of which is evident from the number and scope of targets that can be prepared from the primary cycloadducts. As one of the most thoroughly investigated 1,3-dipoles, nitrones are arguably the most useful. For the last 50 years nitrones have been employed as building blocks in the synthesis of various natural and biologically active compounds. Cycloaddition of nitrones to alkenes yield regioisomeric isoxazolidines **47** and **48** while addition to alkynes gives regioisomeric Δ^4 -isoxazolines **49** and **50** (Scheme 1.5). Isoxazolidine carry up to three new chiral centers, however, as with other 1,3-dipoles, the highly ordered transition state often allows results in highly regio- and stereoselective cycloadditions.



Scheme 1.5: Cycloaddition of nitrones to olefins and alkynes.

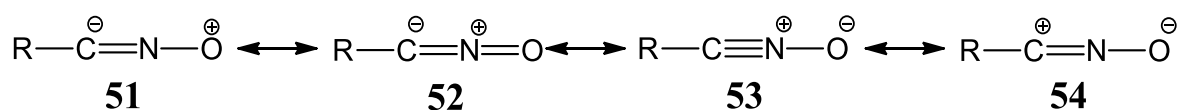
Intermolecular 1,3-dipolar cycloaddition reactions of nitrones have been exploited as key steps in the synthesis of enantiomerically pure bioactive compounds.¹³⁸ The optically active isoxazolidines can be easily transformed into biologically active β -amino acids and other important chiral building blocks, such as γ -amino alcohols and β -lactams.¹³⁹

After alkenes, alkynes constitute the second major group of dipolarophiles. They are of particular interest since isoxazolidines, the products of initial cycloadditions, undergo facile rearrangements and provide ready access to a variety of novel heterocyclic systems in synthetically useful yields.

In addition to C-C multiple bonds, 1,3-dipolar cycloadditions of nitrones to allenes,^{140,141} isocyanates,^{142,143} nitriles,^{120,144} carboxylic acid esters,¹⁴⁵ thiocarbonyls,^{146,147} have been reported.

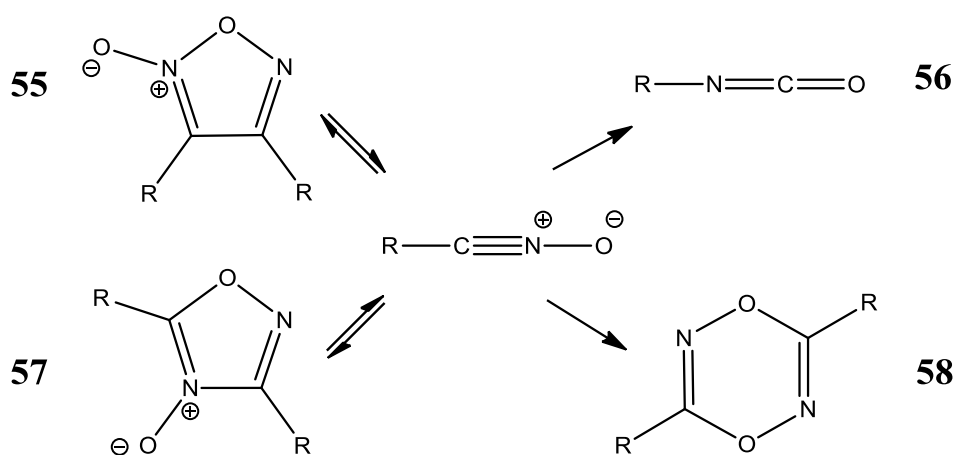
VI. NITRILE OXIDE CHEMISTRY

The parent nitrile oxide, the fulminic acid (HNCO) was discovered in 1800.¹⁴⁸ One of its most valuable derivatives, benzonitrile oxide, was generated in 1886 by Gabriel and Koppe.¹⁴⁹ The resonance forms of these important 1,3-dipoles are shown in scheme 1.6.



Scheme 1.6: Resonance forms of nitrile oxides.

Most nitrile oxides are extremely reactive, and those which are sterically unencumbered are unstable both neat and in solution. In the absence of a dipolarophile, they can rearrange to isocyanates **56**, dimerize to 6-membered 3,6-disubstituted-1,4,2,5-dioxadiazine **58** or to stable 5-membered furoxans **55** and **57** in a special [3+2]-cycloaddition reaction where the nitrile oxide acts as both dipole and dipolarophile (Scheme 1.7).^{150,151} This can happen even at 0 °C in dilute solutions within seconds or, at best, minutes. Under extreme conditions, furoxans can be cracked to regenerate nitrile oxides. Hindered nitrile oxides are stable enough to be isolated and dimerize only slowly.¹⁵² Electron donor and acceptor substituents positioned *para*- to the nitrile oxide functionality stabilize aromatic dipoles whereas electron withdrawing groups at the *ortho*-position reduce their stability.¹⁵³ The dipole instability usually means they are generated as required *in situ* from stable precursors.



Scheme 1.7: Common products of nitrile oxide self-reaction.

VI.1. Generation of nitrile oxides with CAT

Nitrile oxides can be generated directly by oxidation of aldoximes using 1-chlorobenzotriazole¹⁵⁴ or chloramine T (CAT)¹⁵⁵ as oxidant, the latter has been the reagent of choice for the work presented in this thesis.

N-Chloro-*N*-sodio-*p*-toluenesulfonamide, TsNCINa, abbreviated to CAT, is commercially available as a stable white crystalline solid trihydrate, with a slight odor

of chlorine. CAT is used for disinfection and as an algicide, bactericide, germicide for parasite control, and for drinking water disinfection. These applications are permissible due to its nontoxic character. The lack of toxicity, coupled with its solubility in H₂O, makes CAT an attractive choice for nitrile oxide generation in search of bioactive molecules.¹⁵⁶⁻¹⁵⁸

Its structure is most commonly represented as **59**, a less common resonance form is depicted by **60** (Figure 1.22). CAT is moderately soluble in cold H₂O, glycerol and alcohols but very soluble in hot H₂O. It is practically insoluble in ether and petroleum spirits. It is basic; a 5% solution has a pH of around 9. The aqueous solutions are strong electrolytes (4.1% sol. is isotonic with human serum) and mild oxidants in both acidic and alkaline media. An aqueous solution of CAT behaves like a solution of sodium hypochlorite, NaOCl, in many of its reactions (Equation 1.2).

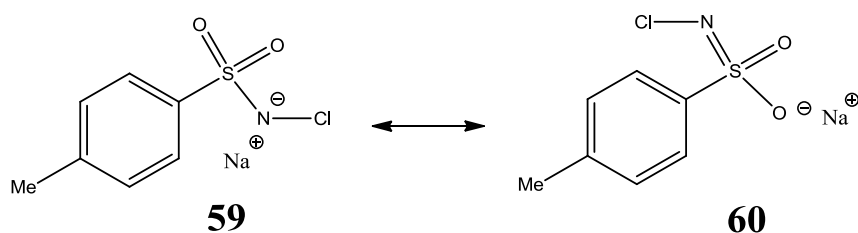
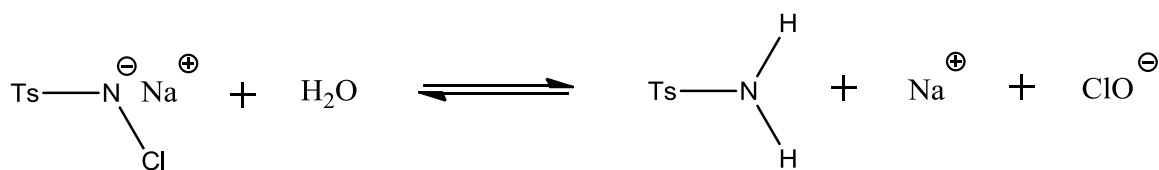
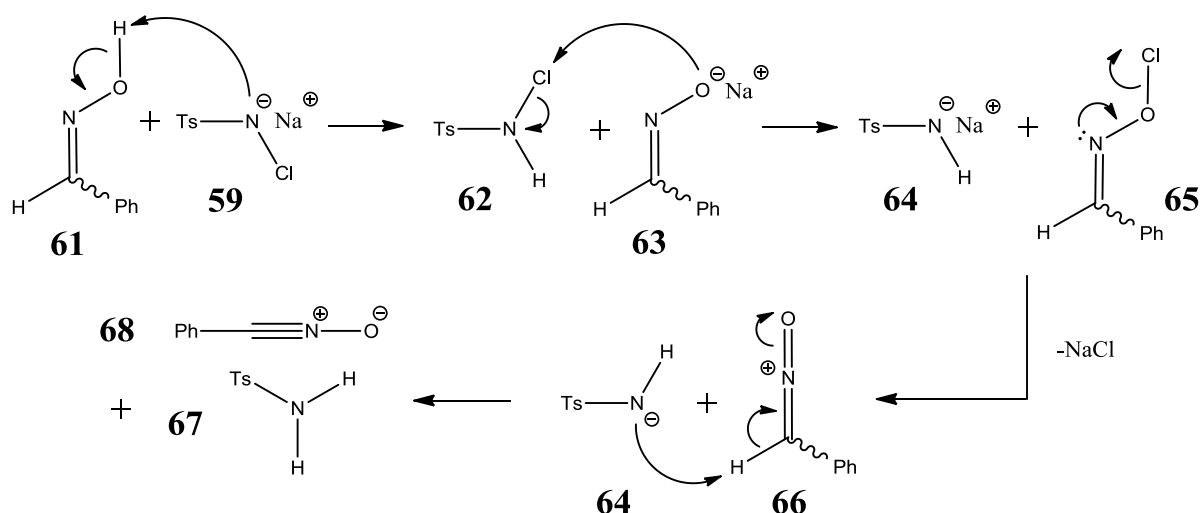


Figure 1.22: Resonance forms of CAT.



Equation 1.2: Reaction between CAT and H₂O.

It is known from the literature that NaOCl is a useful reagent for the *in situ* conversion of oximes to nitrile oxides and in 1989, Hassner and Rai¹⁵⁵ developed CAT as a new reagent for this purpose. The mechanism proposed for the transformation is illustrated for formation of benzonitrile oxide **61** in scheme 1.8.¹⁵⁹ First of all, the CAT reacts as a base to deprotonate the oxime. The alcoholate **63** can then attack the chlorine to form the unstable oxime chloride **65** which eliminates Cl⁻ to give **66** which after deprotonation gives the nitrile oxide **68**.



Scheme 1.8: Mechanism proposed by Rai for nitrile oxide generation by reaction between an oxime and CAT.

VI.3. Reactions of Nitrile Oxides

Some transformations of nitrile oxides, including dimerization to furoxans and isomerization to isocyanates, demand no additional reagents and are connected to their instability (Section VI, p 44). Other reactions, in the presence of a second reagent, e.g. deoxygenation, addition of nucleophiles, and 1,3-dipolar cycloadditions will be considered in the following sections.

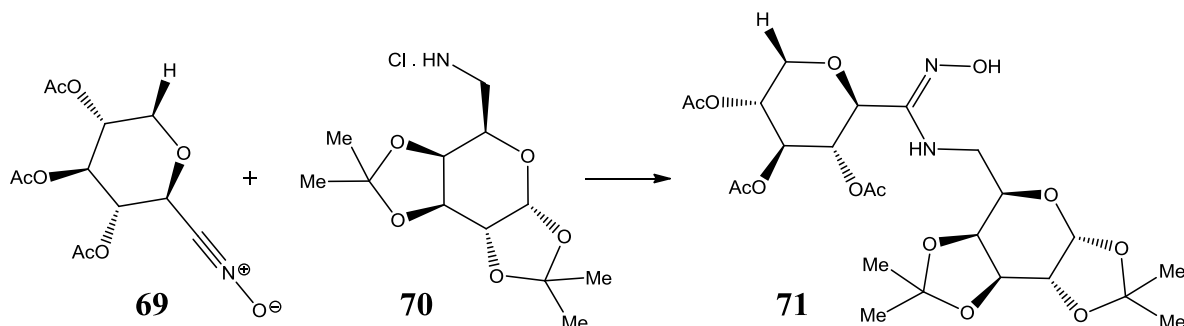
VI.3.a. Dimerization and isomerization

Dimerization and isomerization are conveniently discussed together, since for the same group of nitrile oxides the reaction route is determined by the reaction conditions or the different substituents. Unstable nitrile oxides can dimerize during their generation, while thermal or photo-stimulation are required for isomerization.¹⁶⁰⁻¹⁶² As a rule, sterically stabilized nitrile oxides do not provide furoxans, but with sufficient heat isomeric isocyanates may result. This is the case, for example, for stable bis(nitrile oxides) of the benzene series.¹⁶³

VI.3.b. Addition of nucleophiles

Nucleophiles attack to nitrile oxides nucleophilic on the carbon atom of the CNO group. One example, the synthesis of the amidoxime-bridged disaccharide **71**

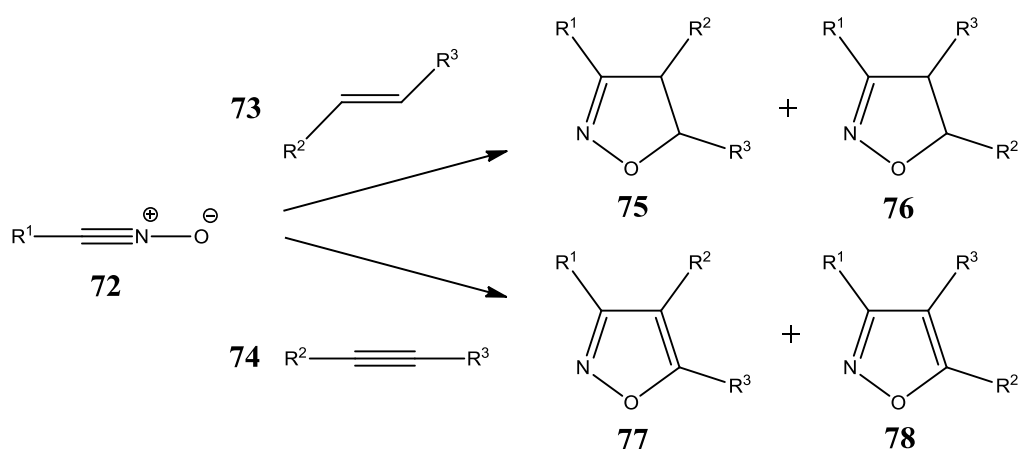
derived from D-xylose and D-galactose, is illustrated in equation 1.3. Smellie showed that pyranosyl nitrile oxides **69** react readily with primary aliphatic amines **70** to afford **71**.¹⁶⁴



Equation 1.3: Synthesis of amidoxime bridged disaccharide 71.

IV.3.d. 1,3-Dipolar cycloaddition

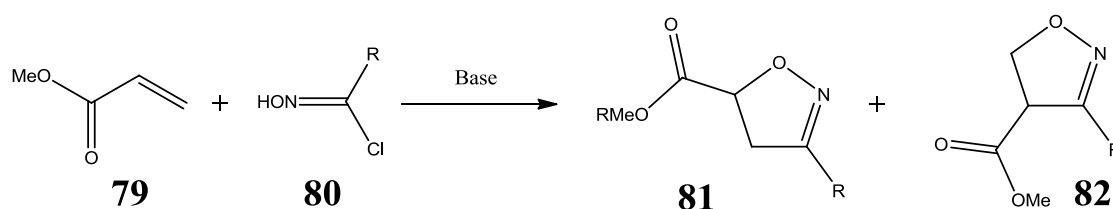
1,3-Dipolar cycloaddition reactions of nitrile oxides are central to the novel research conducted during this Ph.D. thesis. Nitrile oxides undergo 1,3-dipolar cycloaddition reactions with various dipolarophiles. There are exhaustive review articles on this topic.^{165,166} Alkenes and alkynes serve as excellent dipolarophiles and the ability of nitrile oxides to react with olefins was first recorded by Weygand in 1927.¹⁶⁷ In 1961, Huisgen categorized the nitrile oxide as a member of a broader class of 1,3-dipoles that were capable of undergoing [3+2]-cycloaddition reactions.¹¹⁴ Cycloaddition of nitrile oxides to olefins yield regioisomeric Δ^2 -isoxazolines **75** and **76** while addition to alkynes gives isoxazoles **77** and **78** (Scheme 1.9).



Scheme 1.9: Cycloaddition of nitrile oxides to olefins and alkynes.

Several reviews are devoted to analysis of regio- and stereoselectivity arising from cycloaddition of nitrile oxides to C=C double bonds.¹⁶⁸⁻¹⁷⁰ The selectivity of cycloaddition to unsymmetrically substituted alkenes/alkyne depends on the substituents present on the olefin. Mono substituted dipolarophiles preferably lead to 3,5-disubstituted isomers **75** and **77** ($R^2 = H$, scheme 1.9).¹⁷¹ This experimental result is also supported by FMO calculations.^{172,173}

The nature of the substituent on the dipole appears to have little effect on the regioselectivity and 3,5-disubstituted isomers dominate as noted for a range of dipoles in reaction with methyl acrylate (Scheme 1.10, table 1.3).^{174,175}

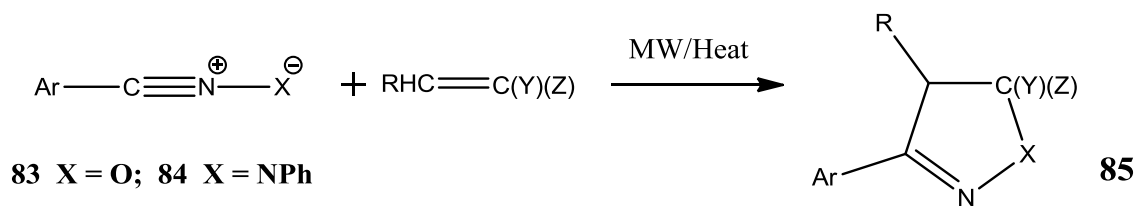


Scheme 1.10: Cycloaddition reaction between methyl acrylate and hydroximoyl chlorides.

Table 1.3: Regioselectivity of cycloaddition between methyl acrylate and hydroximoyl chlorides.

R	Yield (%)	81:82
2,6-Cl ₂ C ₆ H ₃	93	93:7
CO ₂ Et	94	>99:1
C ₆ H ₅	99	>99:1
COMe	97	>99:1
Br	89	95:5

1,3-Dipolar cycloadditions of nitrile oxides have been found to proceed rapidly upon MW activation. In many cases improved adduct yields are obtained although in others the product may differ from that obtained with conventional heating. In one example, Kaddar and co-workers have shown the superiority of the MW procedure for the cycloaddition of nitrile oxides **83** and the nitrile imines **84** with a variety of alkenes (electron rich and electron poor). Reactions were conducted in xylene at 130 °C, under MW irradiation, for 30 min in the presence of *N*-methylmorpholine (Equation 1.4). The same products are obtained with classical heating, but the yields were poorer. Results are summarized in table 1.4.¹⁷⁶



Equation 1.4: MW promoted 1,3-dipolar cycloaddition between nitrile oxides and alkenes.

Table 1.4: 1,3-Dipolar cycloaddition in xylene in the presence of *N*-methylmorpholine under MW irradiation and classical heating.

1,3-Dipole		Alkene	85 (%)	
X	Ar		MW	Heat
O	Ph	CO ₂ MeCH=CHCO ₂ Me	65	30
NPh	<i>p</i> -ClC ₆ H ₄	CO ₂ MeCH=CHCO ₂ Me	85	40
O	Ph	CO ₂ MeCH=CHCO ₂ Me	80	40
NPh	<i>p</i> -ClC ₆ H ₅	CO ₂ MeCH=CHCO ₂ Me	75	40

Several modern versions of nitrile oxide cycloadditions have appeared including solution-phase combinatorial synthesis¹⁷⁷ and polymer-supported cycloaddition.¹⁷⁸ In one example, poly(ethylene glycol)-supported dipolarophiles react with nitrile oxides, generated *in situ* from aldoximes. Following elimination from the support, the new heterocycles are obtained in good yields and with high purity.¹⁷⁹

V. OBJECTIVES OF THIS THESIS

The goal of the novel work discussed in this Ph.D. thesis was the synthesis of a range of chemically modified siRNAs with improved stability and specificity that may, one day, serve as drugs. The method of choice for producing the synthetic structures was **Click Cycloaddition Chemistry** between nitrene or nitrile oxide dipoles and maleimide or alkyne dipolarophiles. This thesis explores the potential of non-catalysed click cycloaddition chemistry to conjugate groups of interest, in particular, a cholesterol moiety, to an oligonucleotide through an isoxazolidine or isoxazole linker.

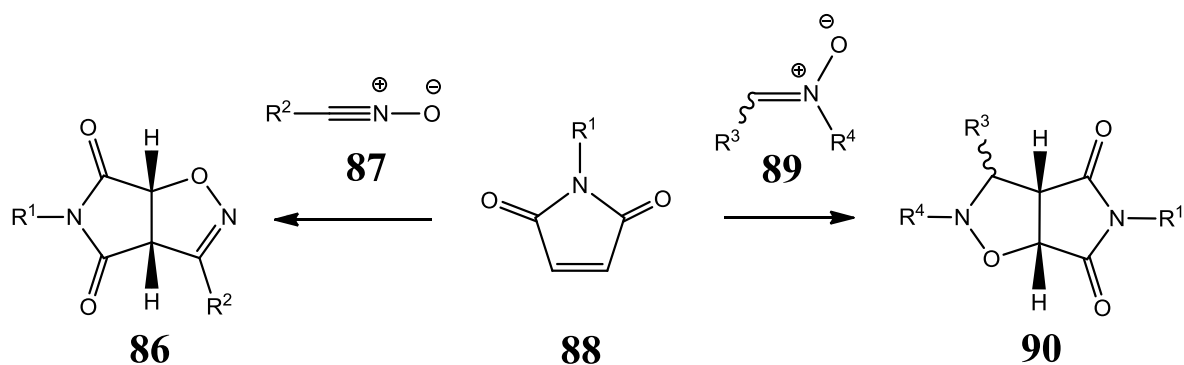
CHAPTER 2:

Optimization of Cycloaddition Between Maleimides and Nitronone or Nitrile oxide 1,3-Dipoles. Synthesis and Cycloaddition of Maleimido-Sugar Click Partners.

I. INTRODUCTION

Maleimides are important building blocks in organic synthesis, frequently employed as 2π -components in conjugate addition reactions, and in 1,3-dipolar or Diels-Alder cycloadditions. For example, in biotechnology, maleimido-terminated polyethylene glycol chains are often used as flexible linking molecules to attach proteins to surfaces.¹⁸⁰ The double bond is susceptible to react with the thiol group found on cysteine and form a stable carbon-sulfur bond. When the chain is attached to a bead or solid support, it allows an easy separation of proteins from other molecules in solution. In other new technologies, mono- and bismaleimide-based polymers are used as flexible linking molecules to reinforce rubber materials. Cross linking is achieved by Michael addition between the maleimide C=C double bond and a hydroxy or thiol group found on the matrix.¹⁸¹

The attraction of maleimides as substrates for 1,3-dipolar cycloaddition are numerous; many are commercially available; their symmetrical nature eliminates possible issues of regioselectivity; and there is potential to introduce a desired functionality through *N*-substitution. A special feature of maleimide reactivity is the double activation of the C=C bond which makes them excellent dipolarophile partners. They are widely known to readily react with a variety of dienes and 1,3-dipoles leading to various carbo- and heterocyclic products.¹¹⁴ In this research, we were interested in developing the reactivity of new “designer” maleimides with nitrones or nitrile oxides as summarized in scheme 2.1.



Scheme 2.1: General 1,3-dipolar cycloaddition of maleimides with nitrones and nitrile oxides.

The ultimate goal of the research was to apply maleimide nitrene/nitrile oxide [3+2]-cycloaddition for the generation of chemically modified oligonucleotides and finally non-natural siRNA. It was envisioned that reaction between maleimido-oligonucleotides and either nitrones or nitrile oxides, carrying, for example, a cholesterol, peptide or sugar moiety, would facilitate generation of a range of siRNA with more resistance to nucleases, more specificity in gene knock down and enhanced delivery characteristics. To achieve this goal, a maleimido-derived nucleoside was required. However, due to the numerous reactive sites, nucleoside chemistry is delicate, and before experimenting with nucleosides or nucleotides, it was deemed appropriate to begin with development of suitable sugar based click partners for ultimate application with oligonucleotides. To this end, the maleimido-sugar derivatives **91** and **92** were identified as the first synthetic targets (Figure 2.1). Their synthesis and cycloaddition potential, as well as a stability study of the resulting cycloaddition products will be discussed in the following sections.

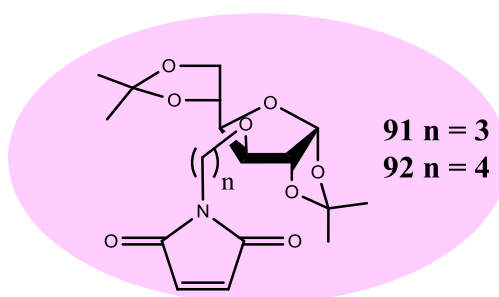


Figure 2.1: Targeted maleimido-sugars **91 ($n = 3$) and **92** ($n = 4$).**

Before exploring the cycloaddition reaction with the “designed” maleimido-sugar, the method was optimized with a range of maleimides bearing N - and/or C_4 -, C_5 - substituents as shown in figure 2.2. N -Methyl maleimide (NMM) **93**, N -benzyl maleimide **94** and N -phenyl maleimide (NPM) **95** are commercially available. The bromopropyl derivative **96** and the trimethyl species **97** are not commercially available and were prepared by the author (Scheme 2.1).

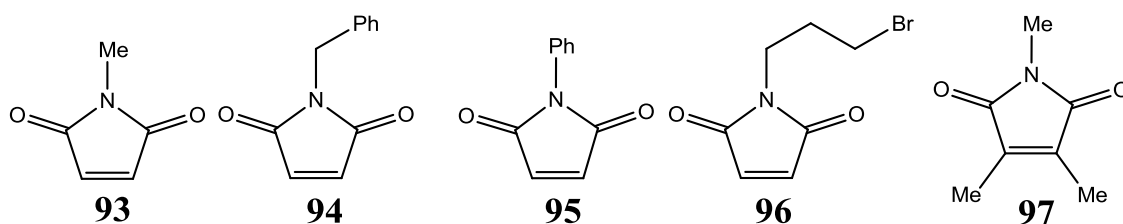
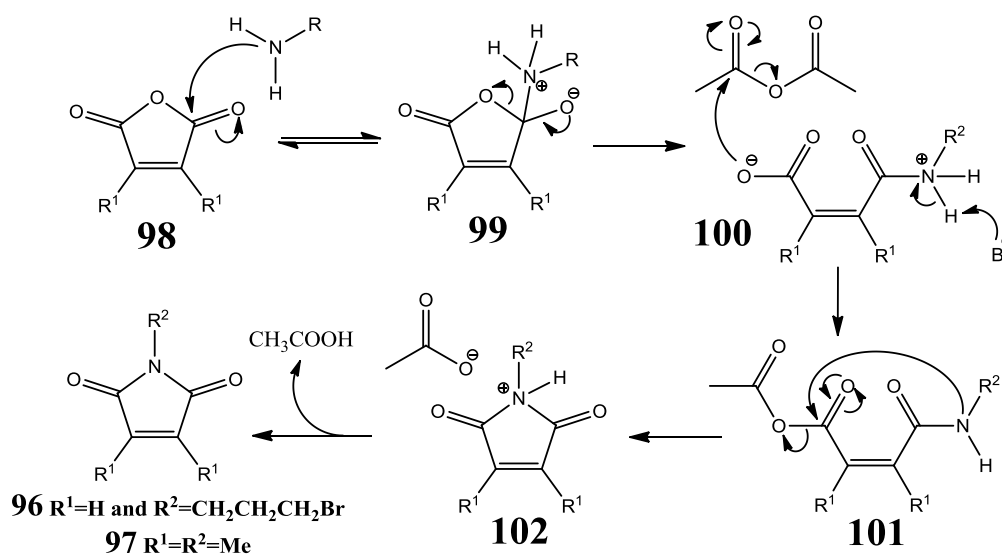


Figure 2.2: N - and C -substituted maleimides.

N-Substituted maleimides can be prepared from maleic anhydride **98** by treatment with primary amines. Nucleophilic attack on one of the carbonyl groups results in ring opening to the corresponding zwitterionic amido acid **100** which cyclizes in presence of acetic anhydride and sodium acetate; a second nucleophilic attack, followed by elimination of a molecule of acetate, gives the maleimido framework. Depending on the substitution on the starting cyclic anhydride, and the nature of the amine component, a variety of *N*- and *C*-substituted maleimides are theoretically accessible by this chemistry (Scheme 2.2).¹⁸²

The two-step synthesis of *N*-bromopropylmaleimide (NBM) **96** has been described in the literature starting from maleic anhydride and 3-bromopropylamine hydrobromide.¹⁸³⁻¹⁸⁵ In the reported methods, the second step required the addition of oxalyl chloride at 0 °C, and the desired product was obtained in 60% yield after 15 h at rt. To improve on this yield, a modification of the reported procedures was explored. Acetic anhydride and sodium acetate were used in place of oxalyl chloride. Addition was performed at rt and reaction mixture was heated at 80 °C for 2 h. These changes to the method resulted in a higher yielding reaction, and **96** was isolated in 79% yield.

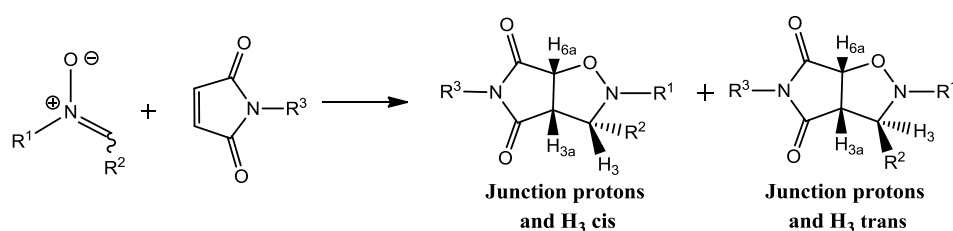
The synthesis of 1,3,4-trimethylmaleimide **97** has also been reported in the literature.¹⁸⁶ In the current work, the reported procedure, starting from 3,4-dimethyl maleic anhydride in glacial acetic acid, has been improved upon replacing methyl ammonium acetate with NH₂Me. This simple change effected an increase in yield of the desired product from 68 to 83%.



Scheme 2.2: General mechanism formation for *N*- and *C*-substituted maleimides.

II. REACTION WITH NITRONES

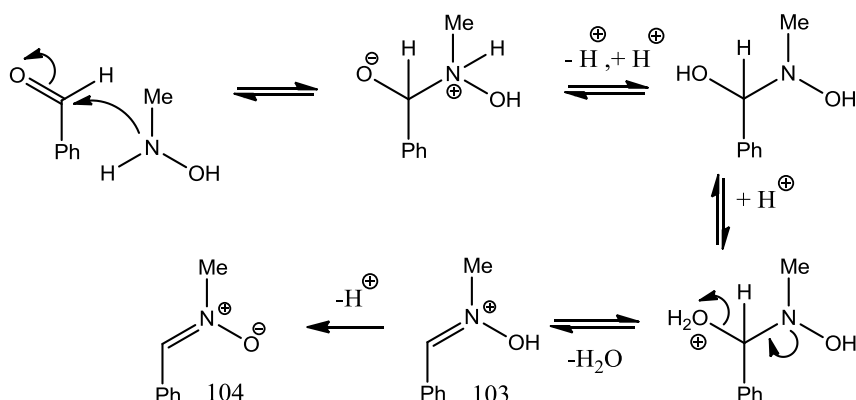
Cycloaddition of nitrones to *N*-alkyl- and *N*-arylmaleimides have frequently been reported.^{187,188} A typical reaction, shown in equation 2.1, results in formation of a new 5 membered heterocycle called an isoxazolidine. Depending on the structure of the reactants, up to four stereoisomers can result, *i.e.* two diastereoisomers, each with two enantiomers. The reaction can be conducted in aqueous or organic solvents, at elevated or room temperature, and yields are often high. The protocol is free from any catalyst and in some cases MW irradiation has been found to greatly improve reactions rates.¹⁷⁶



Equation 2.1: Diastereoisomeric cycloadducts arising from cycloaddition between maleimides and nitrones.

II.1. Nitron Preparation

N-Methyl *C*-phenyl nitron **104** was initially prepared from the corresponding aldehyde following reaction between *N*-methyl hydroxylamine hydrochloride and benzaldehyde in presence of sodium carbonate as base, in DCM at reflux. The mechanism of the well-known reaction involves formation of the iminium ion **103** followed by deprotonation of the hydroxyl group by the base (Scheme 2.3).¹⁸⁹



Scheme 2.3: Mechanism of formation of *N*-Methyl *C*-phenyl nitron 104 formation.

Applications of MW irradiation to chemical synthesis were reported for the first time in 1986 by Gedye,¹⁹⁰ and considerable rate increases were observed for a range of reactions. Since this early study, the approach has blossomed into a useful technique for a variety of organic transformations.^{191,192}

MW promoted nitron formation has been reported previously with different substrates.¹⁹³ Thus, reaction between *N*-methyl hydroxylamine hydrochloride and benzaldehyde which required 5 hours heating at reflux in DCM to give *N*-methyl *C*-phenyl nitron **104** in 95% yield, has been demonstrated to proceed to the same extent after only 30 min in the MW at 125 °C (Pmax = 300 W). Under these conditions, quantitative conversion of benzaldehyde to nitron **104** was achieved on a 2 g scale. *N*-phenyl *C*-phenyl nitron **105** was gifted by a member of the group. *N*-methyl *C*-propyl nitron **106** was obtained in 49% yield. The low yield is attributed to its volatility, with some product likely to have been lost during solvent evaporation. Nitron **107** resulting from condensation with acetone was simply too volatile to be isolated, and was trapped by NMM in solution (Figure 2.3).

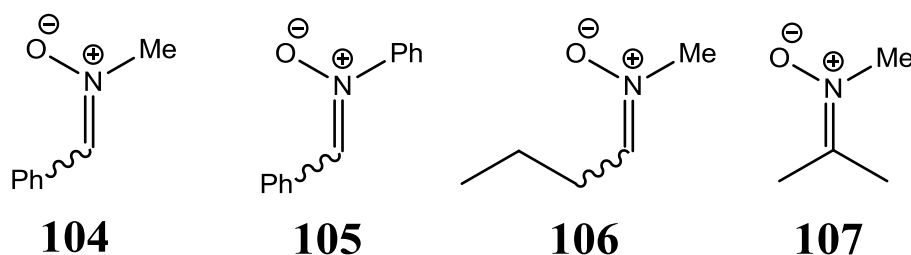
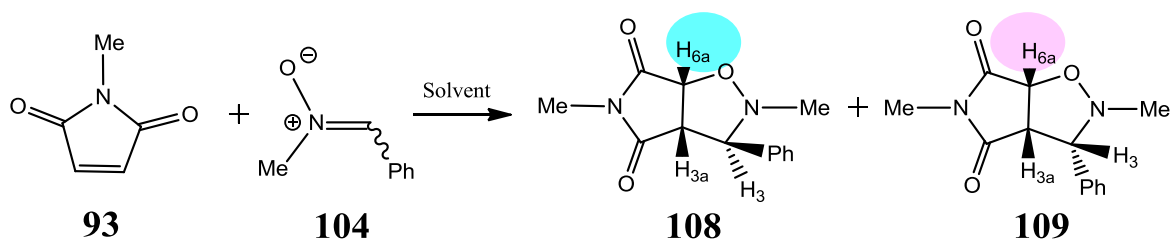


Figure 2.3: Nitrons prepared by conventional and/or MW activation approaches.

II.2. 1,3-Dipolar Cycloaddition

Cycloaddition between *N*-methyl *C*-phenyl nitron **104** and NMM has previously been reported to proceed quantitatively, giving the diastereoisomeric adducts **108** and **109** in a ~1:1 ratio, following reaction in toluene at reflux for 3 h under an N₂ atmosphere (Equation 2.2).¹⁹⁴ These isomeric products are easily distinguished on the basis of their ¹H NMR data. The ring junction protons have diagnostic signals, H_{6a} is found to resonate at 4.94 ppm in **108** where this proton is *trans* to the H₃ proton, and at 4.85 ppm in **109** where it has a *cis* relationship to the same hydrogen atom (Figure 2.4).



Equation 2.2: Cycloaddition between NMM and *N*-methyl *C*-phenyl nitronium salt **104.**

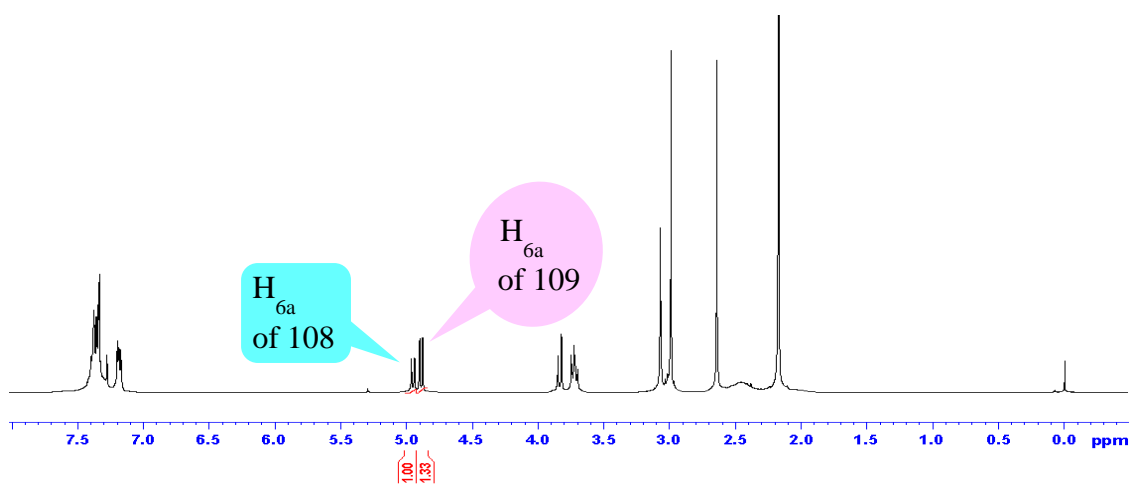


Figure 2.4: ^1H NMR spectrum of a mixture of **108 and **109**.**

The straightforward elucidation of the diastereoselectivity in this example made the reaction of *N*-Methyl *C*-phenyl nitronium salt **104** and NMM an ideal test case with which to optimize the yield and the diastereoselectivity. Solvents studied included MeOH, H₂O, EtOH, hexane, and DCM. A comparison was made between the effects of conventional heating vs. MW activation. Some of the results are summarized in table 2.1. Under classical conditions, the reaction proceeded best after 17 h stirring in DCM at rt with 10% excess of nitronium salt. Products **108** and **109**, present in ~1:1 ratio, were obtained in 98% combined yield (entry 6). In an attempt to reduce reaction duration, the temperature was increased to 50 °C, however, a significant reduction in yield was observed. Yields were also poorer in aqueous solvents (entries 2 to 4). Dramatically lower yields were obtained under the influence of MW radiation (1 h at 50 °C), in solvents including MeOH, H₂O or EtOH (entries 1 to 5).

Table 2.1: Reaction between NMM and *N*-methyl *C*-phenyl nitrone **104 leading to diastereomeric adducts **108** and **109**.**

Entry N°	Solvent	Reaction conditions					
		Conventional				MW	
		rt for 17 h		50 °C for 1 h		50 °C for 1 h P _{max} = 35 W	
		Yield (%)	ratio 108/109	Yield (%)	ratio 108/109	Yield (%)	ratio 108/109
1	MeOH	91	1:1.7	82	1:1.4	24	1:1.4
2	MeOH/H ₂ O 1:4	79	1:3.2	13	1:3.1	13	1:3.3
3	H ₂ O	92	1:3.0	12	1:4.5	24	1:5.1
4	EtOH/H ₂ O 1:4	82	1:3.2	13	1:3.0	11	1:3.0
5	EtOH	89	1:1.9	56	1:1.4	17	1:1.6
6	DCM	98	1:0.9	48	1:1.3	57	1:1.1

In all cases where the product yields were low, the crude reaction mixtures, following solvent removal under reduced pressure, were analysed by ¹H NMR spectroscopy. The spectrum shown in figure 2.5 is typical of these reactions. It shows evidence of the expected products **108** and **109** (two doublets at ~4.9 ppm), unreacted nitrone **104** (multiplet at ~8.2 ppm), and an unexpected new product (AB doublets at ~6.5 ppm). No NMM **93** was observed in the crude reaction mixture as may be expected since **93** is likely to have sublimed at low pressure during solvent removal from the crude reaction product on rotary evaporation.

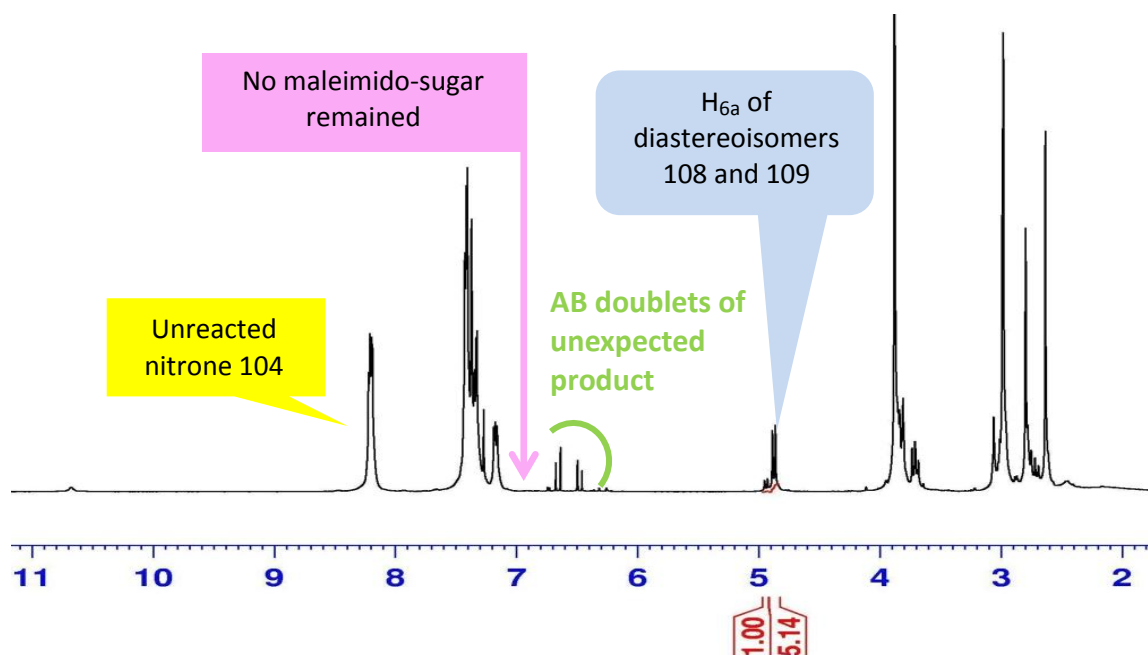
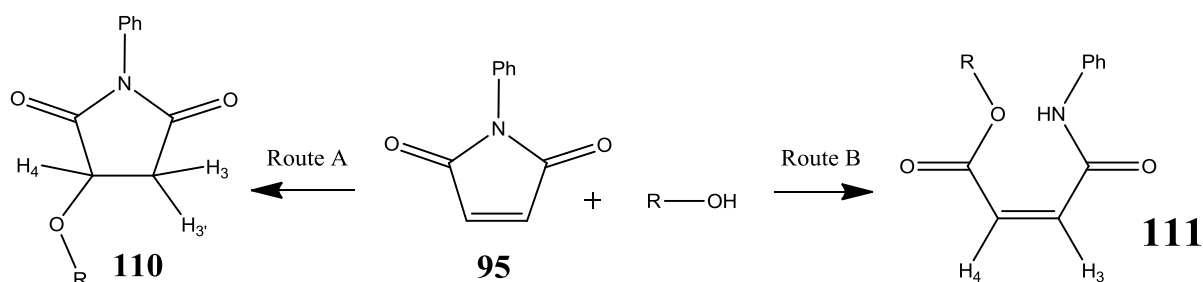


Figure 2.5: ^1H NMR spectrum of the crude reaction product resulting from reaction between NMM and *N*-methyl *C*-phenyl nitrene **104** in H_2O (MW, 50°C , 1 h)

In an attempt to identify the structure of the unexpected product, and to explain the poor cycloaddition efficiency at temperatures above rt, and conducted with MW irradiation (entries 1 to 5, table 2.1), a series of tests were conducted. NPM was selected to replace NMM as it is not expected to sublime under reduced pressure. The susceptibility of maleimides to nucleophilic attack is well known¹⁸⁰ and the first hypothesis tested was that NPM **95** may not be inert to the reaction solvent and that Michael addition may lead to a new compound **110** (Route A). A second possibility considered was solvent attack on the electrophilic carbonyl group, resulting in opening the 5 membered ring to give the amido ester **111** (Route B) (Scheme 2.4).¹⁹⁵



Scheme 2.4: Possible side products from solvent attack on NPM.

The ^1H NMR spectrum of NPM (Figure 2.6) shows a signal at 6.84 ppm for the alkene protons and signals between 7.32 and 7.55 ppm for the aryl protons. The spectrum of the product resulting from exposure of **95** to MeOH (50 °C, 17 h) is distinctly different. A singlet present at 3.85 ppm with relative integration of 3H, is typical of the resonance expected for methyl protons of an ester group ($-\text{COOCH}_3$). A broad singlet, integrating for 1H, present at 10.7 ppm, is typical of an amide proton ($-\text{CONHR}$). There is a pair of AB doublets at 6.18 and 6.45 ppm, each integrating for 1H, and aryl protons signals are also present (Figure 2.6). These resonances are consistent with formation of the unsaturated amido ester **111**. A coupling constant of 13.2 Hz between the alkene protons confirmed *cis* configuration of the double bond. Formation of the alternative Michael addition product **110** is not supported by this ^1H NMR spectral data; it would be expected to show up to three signals (doublet of doublets) for H_4 and the diastereotopic H_3 protons.¹⁹⁵

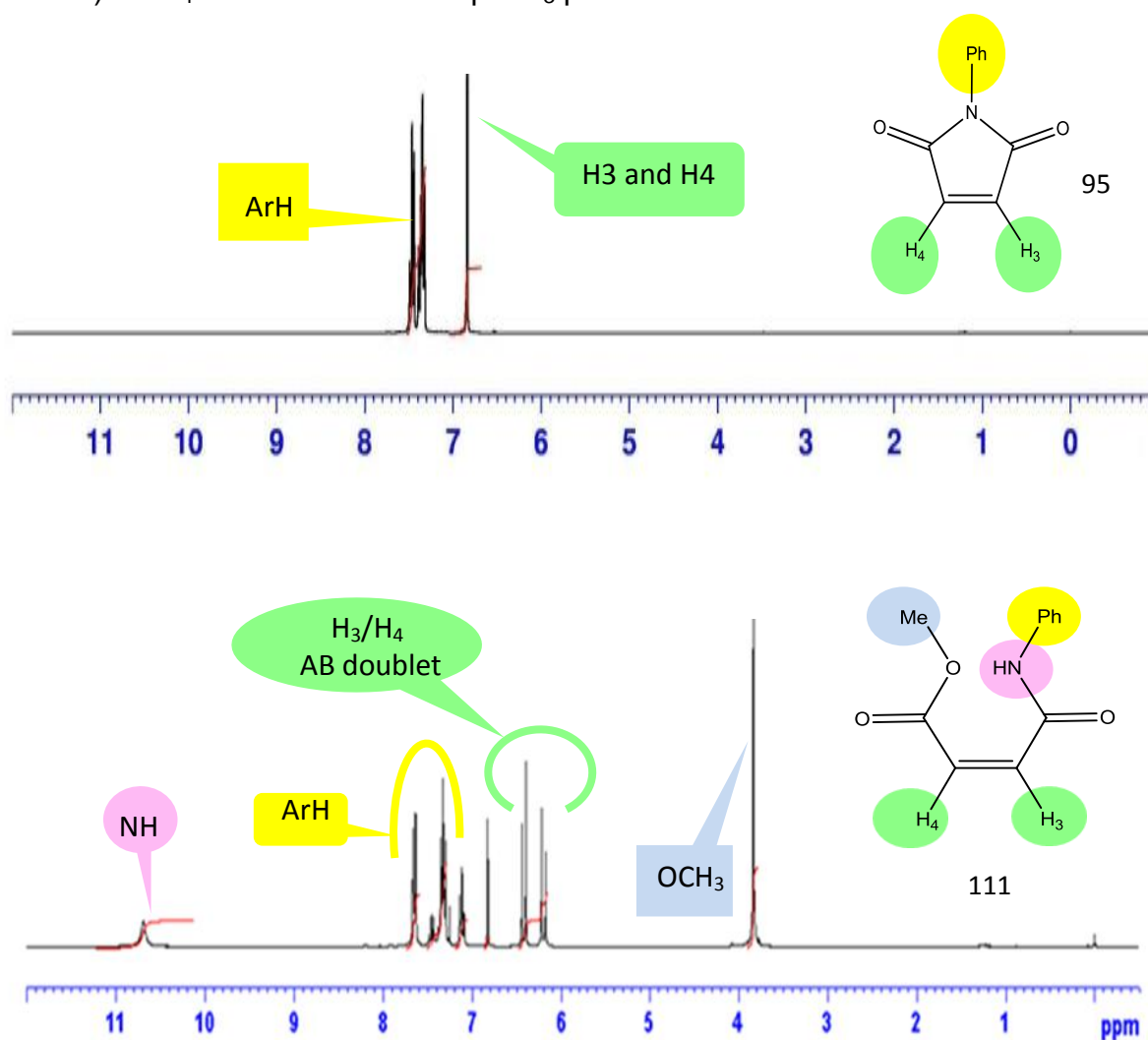


Figure 2.6: ^1H NMR spectrum of NPM (above) and of the amino ester **111** resulting from reaction between **95** and MeOH (50 °C, 17 h).

To avoid potential side reactions, non-nucleophilic solvents were selected for future nitron/maleimide reactions under MW activation; the results are summarized in table 2.2. Cycloaddition yields between 15 and 94% were observed for reactions conducted in DCM, however, diastereoselectivity was found to decrease in parallel with an increase of yield. In an effort to improve the yield and the diastereomeric ratio, hexane, the lowest MW absorbing solvent ($\epsilon'' = 0.038$), was selected for study. With such solvents, it is believed that the MW radiation is absorbed directly by the reagents as opposed to the solvent.¹⁹⁶ After 5 min at 300 W the cycloadduct yield was 94%, reaching completion upon addition of excess of NMM (entries 6 and 7), however there was little or no diastereoselectivity. A similar result was observed in the absence of solvent (entry 8); this environmentally attractive approach would be especially useful on a large scale.¹⁹⁷

Table 2.2: Reaction between NMM 93 and *N*-methyl *C*-phenyl nitron 104 leading to diastereomeric adducts 108 and 109.

Entry N°	Solvent	MW Condition	ratio 93:104	Yield (%)	d.r. 108/109
1	DCM	50 °C for 5 min, P _{max} = 35 W	1.1:1	15	1:2.3
2		50 °C for 10 min, P _{max} = 35 W		29	1:2.4
3		35 W for 5 min, T _{max} = 63 °C		33	1:2.3
4		100 W for 5 min, T _{max} = 78 °C		41	1:2.0
5		300 W for 5 min, T _{max} = 96 °C		66	1:1.6
6	Hexane	300 W for 5 min, T _{max} = 106 °C	1.1:1	94	1:0.9
7		300 W for 5 min, T _{max} = 98 °C	2.0:1	quantitative	1:1.0
8	Neat	300 W for 5 min, T _{max} = 126 °C	2.0:1	quantitative	1:1.1

Unfortunately, the diastereoselectivity ratio (d.r.) was not high in any of the solvents furnishing the cycloadducts in high chemical yield. The highest d.r. (~1:5.1), was observed following reaction in H₂O which furnished the product in just 24% yield (entry 3, table 2.1). The high yielding reactions in DCM, hexane or without solvent (entries 6, 7, and 8, table 2.2) showed little or no diastereoselectivity.

On the basis of the above studies, the method of choice for high yielding nitron/maleimide cycloadditions was deemed to involve reaction of the nitron with 2 eq of maleimide in hexane under MW activation (300 W, 5 min). Removal of the solvent under reduced pressure yielded the crude products which were purified by washing abundantly with H₂O or by flash chromatography to yield pure products. A range of cycloadducts were synthesized by this method. Their structures and isolated yields are summarized in figure 2.7.

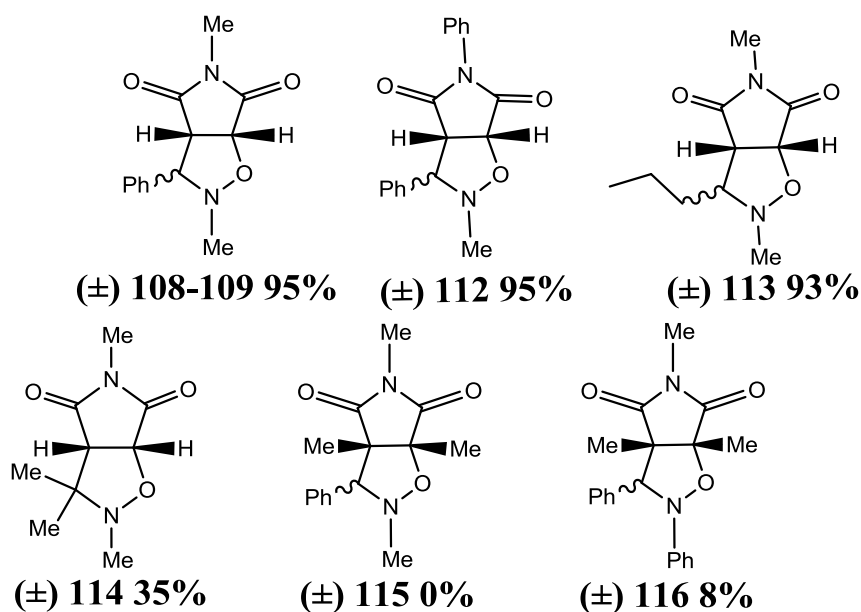
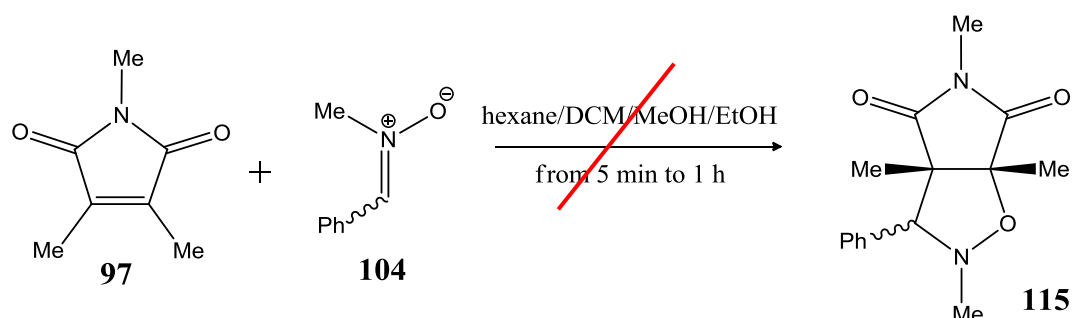


Figure 2.7: Cycloadducts prepared by nitron/maleimide cycloaddition.

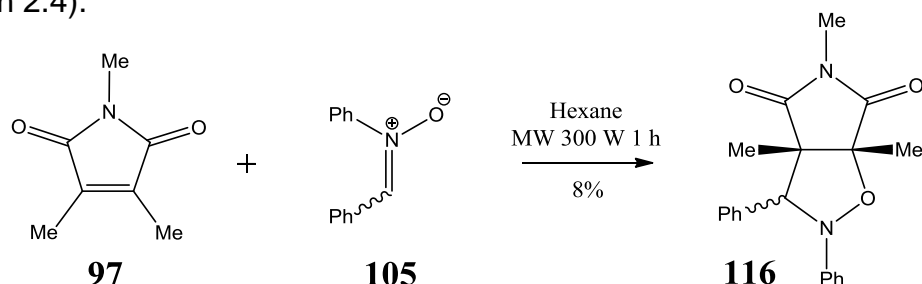
The diastereoisomers **108** and **109** (~1:1 ratio) were isolated from the crude reaction mixture in 95% combined yield, however separation of the individual isomers was difficult. Accordingly, pure samples of **108** and **109** were obtained in just 29% and 39% yield, respectively. The remaining mass was obtained as a sample of mixed diastereoisomers. The 3,3-dimethyl adduct **114** was obtained in 35% yield over two steps starting from acetone without nitron isolation; the dipole, being volatile, was directly trapped by NMM in solution. Yields of cycloadducts from

1,3,4-trimethylmaleimide **97** were poor;¹⁹⁸ *N*-methyl-*C*-phenyl nitron **104** failed to react under the standard conditions (hexane, 300 W, 5 min), nor did any cycloaddition occur in DCM, MeOH, EtOH. Neither did an increase of reaction duration from 5 min to 1 h promote product formation. It was concluded that the steric bulk of the methyl groups on the maleimide may have impeded the reaction with this dipole (Equation 2.3).



Equation 2.3: Attempted cycloaddition between 1,3,4-trimethylmaleimide **97 and *N*-methyl-*C*-phenyl nitron **104**.**

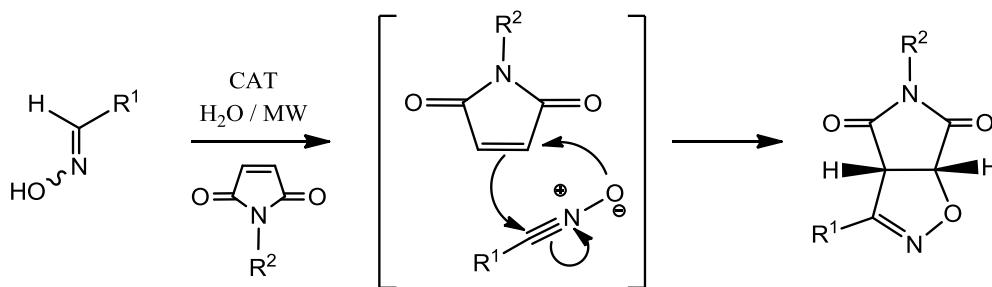
In contrast, albeit in very low yield (8%), reaction between *N*-phenyl-*C*-phenyl nitron **105** and **97** proceeded to furnish **116** after 1 h in the MW at 300 W. It is possible that the diphenyl nitron adopted a planar geometry, assisting the alignment of the reactants in the transition state leading to cycloaddition reaction (Equation 2.4).



Equation 2.4: Cycloaddition between 1,3,4-trimethylmaleimide **97 and *N*-phenyl-*C*-phenyl nitron **105**.**

III. REACTION WITH NITRILE OXIDES

Variable cycloaddition yields and low diastereoselectivity from reaction between nitrones and maleimides encouraged a change in focus to nitrile oxide dipole. The selected protocol, a practical, one pot operation, involved the use of CAT to induce *in situ* nitrile oxide formation from the parent oxime (Scheme 2.5).¹⁹⁹



Scheme 2.5: Cycloaddition between maleimides and nitrile oxides.

III.1. Oxime Preparation

Nitrile oxides were prepared *in situ* with CAT from the oximes shown in figure 2.8. 2-Nitrobenzaldehyde oxime **117** was commercially available, **118** to **120** were synthesized from the corresponding aldehydes by condensation with hydroxylamine hydrochloride.

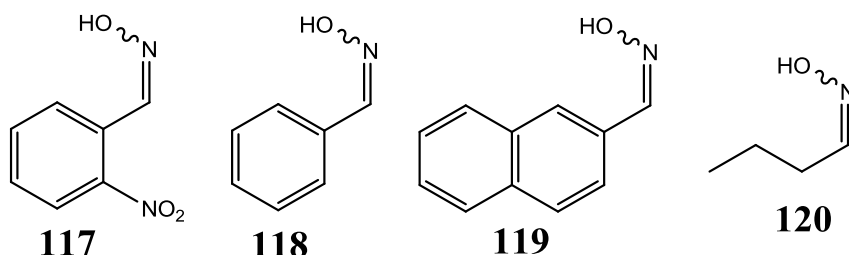
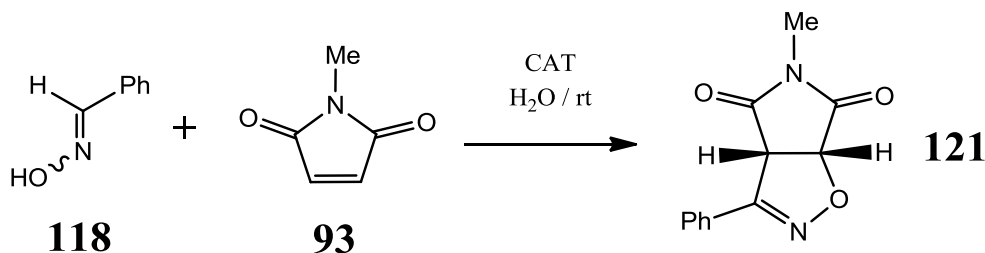


Figure 2.8: Oximes prepared by conventional heating and/or MW activation approaches.

III.2. 1,3-Dipolar Cycloaddition

Cycloaddition between *in situ* generated benzonitrile oxide and NMM was examined under a range of conditions as summarized in table 2.3 (Equation 2.5).



Equation 2.5: Cycloaddition between NMM and benzonitrile oxide.

Table 2.3: Reaction between NMM and *in situ* generated benzonitrile oxide leading to 121 from oxime 118.

Entry N°	Reaction Conditions		Ratio 118:93	Ratio CAT:93	Yield (%)
1	Conventional	2 h at RT	2:1	2.5:1	71
2	MW	8 min at 60°C			89
3		3 min at 40°C			81
4		10 min at 40°C	1.1:1	90	
5		3 min at 40°C		78	
6		14 min at 40°C	1.1:1	62	

The reaction, initially investigated at rt, employed a two fold excess of benzaldehyde oxime, and 2.5 eq of CAT. At the end of the reaction, the pure product was obtained by simple filtration and the excess reactants were removed by washing with H₂O to yield **121** in 71% yield (entry 1, table 2.3). Optimal conditions were deemed to involve reaction of the maleimide with 1.1 eq of oxime and 2.5 eq of CAT in H₂O under MW activation (40 °C, 10 min, P_{max} = 300 W) and gave the product **121** in 90% yield (entry 4). A range of cycloadducts were synthesized by this method, the structures of which are summarized in figure 2.9. Isolated yields were very good with the exception of those arising from 1,3,4-trimethylmaleimide **97**. As observed with nitrones, this is a poor dipolarophile and cycloaddition yields are too low for the reaction to be synthetically useful.

The cycloadducts were characterized on the basis of their ¹H NMR spectral data. The spectrum of **122** is shown as a representative example in figure 2.10. Two doublet resonances at ~4.80 ppm and ~5.60 ppm, diagnostic for the junction protons H_{3a} and H_{6a}, respectively, confirm formation of a pyrrolo-isoxazoline.

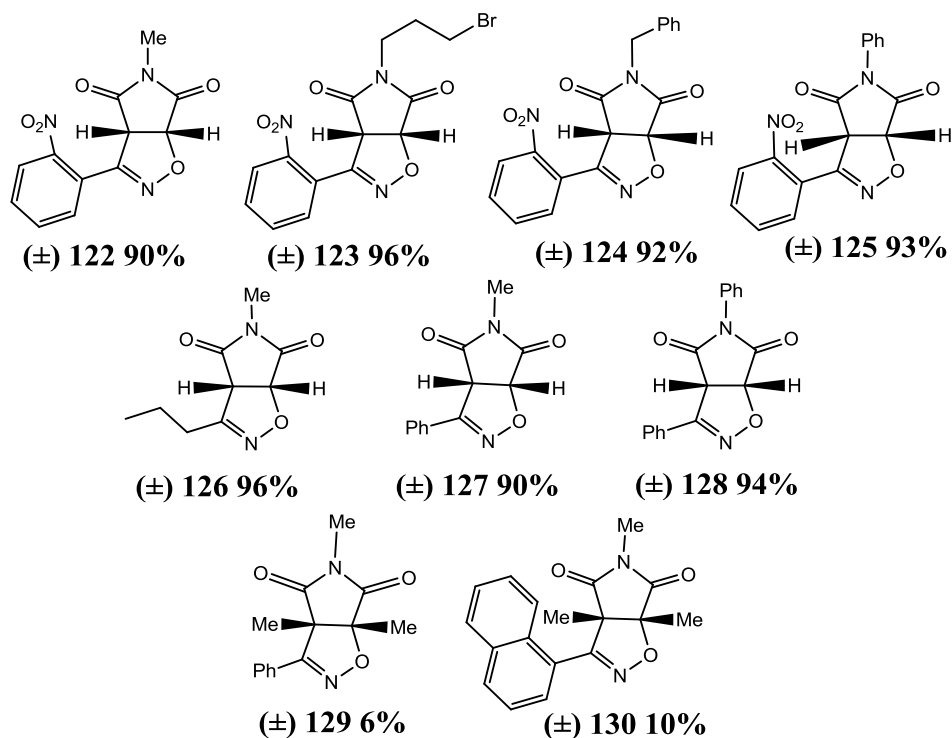


Figure 2.9: Cycloadducts arising from nitrile oxide/maleimide cycloaddition reactions.

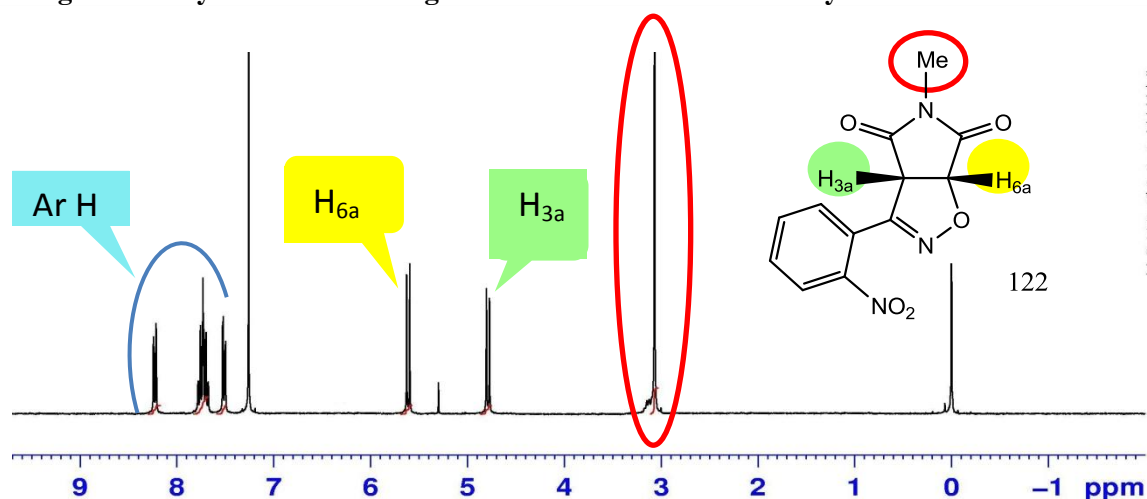
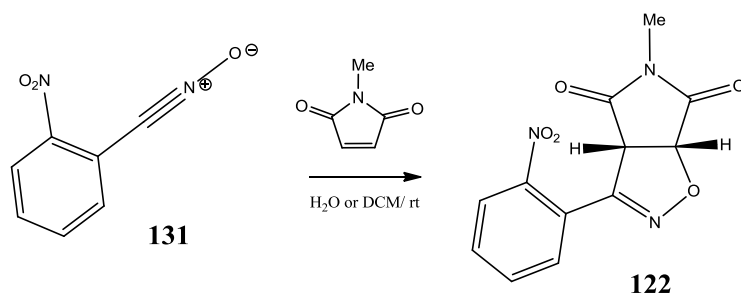


Figure 2.10: ^1H NMR spectrum of 122.

III. 3. Preformation of nitrile oxide

Nitrile oxides are not stable species and dimerization can be problematic;¹⁵¹ consequently, with few exception,¹⁵² they are not usually isolated. Rai has reported isolation of aryl nitrile oxides from reaction between oximes and CAT in DCM, with simple washing to furnish the dipole in good yield. Pre-formation, rather than *in situ* generation avoids contact between the dipolarophile and CAT, and it was felt this

approach could be potentially valuable for ultimate application to oligonucleotide substrates. For this reason, pre-formation of benzonitrile oxide was attempted; unfortunately the product was not stable enough to be isolated. The more sterically demanding 2-nitrobenzaldehyde oxime **117** was however a suitable substrate, and the corresponding nitrile oxide **131** was isolated in 98% yield. The ^1H NMR spectrum confirmed the formation of **131**, with the disappearance of the signal representing CHNOH at 8.72 ppm. This compound reacted with NMM (10% excess) to give the pyrrolo-isoxazoline **122** in 95% yield in H_2O , and 98% in DCM after 1 h at rt (Scheme 2.6).



Scheme 2.6: Cycloaddition between pre-formed nitrile oxide **131** and NMM.

IV. PREPARATION AND REACTION OF MALEIMIDO-SUGAR

Before exploring cycloaddition chemistry with nucleoside or nucleotide substrates, efforts were directed to development of suitable sugar based click partners. To this end the maleimido-sugar derivatives **91** and **92** (Figure 2.11) were identified as the first target molecules. In the following section, their synthesis and cycloaddition potential will be discussed, as well as the results of stability studies on the cycloaddition products.

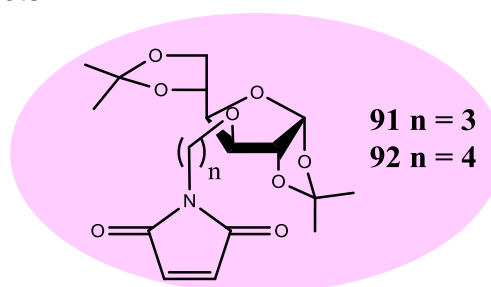
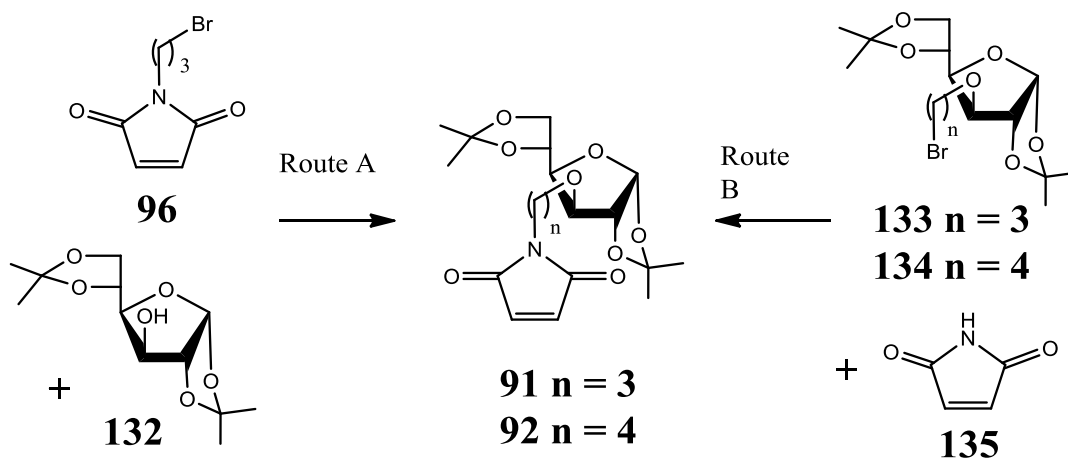


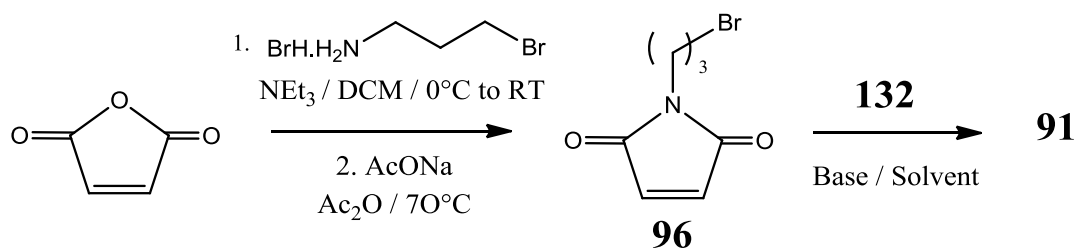
Figure 2.11: Targeted maleimido-sugars, **91** ($n = 3$) or **92** ($n = 4$).

IV.1. Synthesis of Target Maleimido-Sugar

Two synthetic routes to the target maleimido-sugars are depicted in scheme 2.7. In the first approach, route A, the synthetic sequence required selective protection of all the hydroxyl groups bar C₃, thus the already known compound **132** was prepared (89%).²⁰⁰ The formation of NBM **96** has been described scheme 2.2 (section I, p 49). Nucleophilic substitution by the deprotonated protected sugar **132** on the bromide was envisaged to yield the target compound **91** (Scheme 2.8). Unfortunately, this reaction was unsuccessful. Following exposure of the *N*-substituted maleimide to the reaction mixture, a pink color was immediately observed. The same coloration resulted when the reaction was repeated with a range of bases including NaOH, NaH or K₂CO₃ (entries 1 to 6 and 10, table 2.4). The ¹H NMR spectrum of the crude reaction products showed signals representative of the protected sugar **132** (e.g. a doublet representing H₁ at 5.92 ppm). However, with the exception of the reactions conducted in the presence of Na₂CO₃ (entries 7 to 9), no evidence was found for the presence of any remaining NBM **96**.



Scheme 2.7: Synthesis of maleimido sugars.



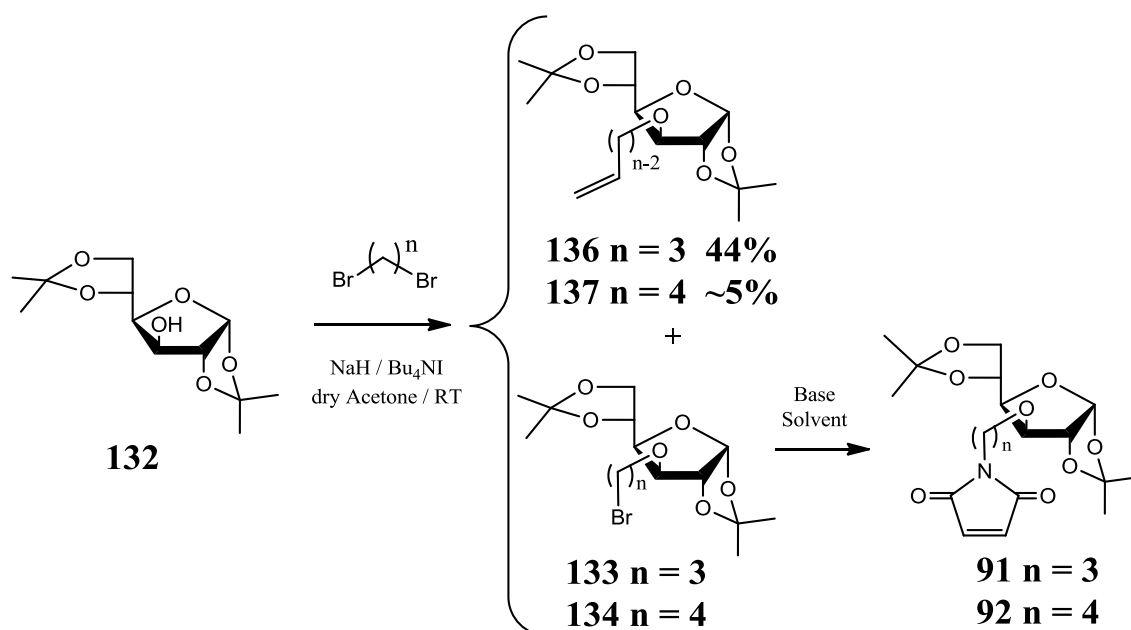
Scheme 2.8: Synthetic route A proposed to prepare maleimido-sugar **91**.

Table 2.4: Summary of results of reactions between NBM 96 and protected sugar 132 in presence of base.

Entry N°	Base	Solvent	Conditions		Results
1	NaOH	sol. 50% in H ₂ O	Reactants mixed in one pot with Bu ₄ NBr 24 h / 70°C		1. PINK coloration of reaction mixture 2. 132 returned unchanged 3. No evidence of unreacted 96
2	NaOH	sol. 50% in H ₂ O + DCM	Reactants mixed in one pot with Bu ₄ NBr 20 h / RT		
3	NaH	DMF	132 + base premixed 30 min / rt	3 h / rt	
4	NaH	DMF		20 h / rt	
5	NaH	DMF		18 h / 90 °C	
6	Na ₂ CO ₃	CH ₃ CN		24 h / rt 24 h / Δ	
7	Na ₂ CO ₃	CH ₃ CN		Addition of 96	20 h / rt
8	Na ₂ CO ₃	CH ₃ CN	3 h / Δ		1. PINK coloration of reaction mixture 2. 132 returned unchanged 3. ~25% of 96 returned
9	Na ₂ CO ₃	Acetone	20 h / rt		
10	K ₂ CO ₃	Acetone	20 h / rt		

In the second approach, route B (Scheme 2.9), a displacement by nucleophilic maleimide on the bromo-sugar 133 or 134 was envisioned. As the first step, a classic nucleophilic substitution of the protected sugar **132** by dibromoalkanes was desired. To investigate this reaction, NaH was employed as base and Bu₄NI as halogen exchange agent; the solvent was anhydrous acetone.

Reaction with 1,4-dibromobutane was successful and **134** was obtained in 67% yield. The alkene **137**, resulting from HBr elimination from either the substrate or the product, was present in the crude sample in a proportion of ~5%. Unfortunately, upon reaction with 1,3-dibromopropane, formation of the desired **133** ($n = 3$) was accompanied by large quantities of the elimination product **136**, and **133** was obtained in just 8% yield. In light of these results, experimentation continued with the sugar **134** ($n = 4$) prepared from 1,4-dibromobutane.²⁰¹



Scheme 2.9: Synthetic route B proposed to prepare maleimido-sugars **91** and **92**.

The next synthetic step to **92** envisaged a nucleophilic substitution of the brominated sugar **134** with the parent maleimide **135**. Reaction was investigated both with and without base (Na_2CO_3 or K_2CO_3). To promote reaction, anhydrous CH_3CN was chosen as solvent over acetone because of the possibility to conduct the reaction at higher temperature. Unfortunately, the substitution reaction was unsuccessful (Table 2.5). As previously observed, as soon as the maleimide was exposed to the base, a pink color appeared. In all cases, the ^1H NMR spectrum of the crude reaction mixture showed evidence of the presence of unreacted bromo-sugar **134**. There appeared to be a little or no maleimide remaining.

Table 2.5: Summary of outcome of reactions between bromo-sugar 134 and maleimide 135 in anhydrous CH₃CN.

Entry N°	Base	Reaction conditions	Result
1	No base	4 h / Δ	1. 132 returned unchanged 2. 135 returned unchanged
2	Na ₂ CO ₃	20 h / rt and 4 h / Δ	1. PINK coloration of reaction mixture 2. 132 returned unchanged 3. ~25% of 135 unreacted
3	K ₂ CO ₃	144 h / rt and 4 h / Δ	1. PINK coloration of reaction mixture 2. 132 returned unchanged 3. No evidence of unreacted 135

It was deduced that the formation of the pink coloured product following exposure of maleimides **96** or **135** to base was directly related to the failure of the reactions to lead to the desired products **91** and **92**, respectively. The identity of the pink solid was not obvious from the ¹H NMR spectrum of the crude reaction products. In a control experiment designed to shed light on this structure, maleimide was exposed to NaH. Immediately, a pink colour appeared, however, ¹H NMR spectral data still failed to provide clues to its structure. A series of tests were then conducted where NPM was selected to replace maleimide in the hope that a signature would be found from the aryl protons. After two hours exposure of **95** to NaH, a pink solid, chloroform insoluble, formed. The ¹H NMR spectrum (d₆-DMSO) revealed a number of broad signals. It was considered possible that the new product may be polymeric in nature (Figure 2.12). NPM is often used to prepared heat-resistant polymers or co-polymers.²⁰² It has been reported previously that homopolymers of maleimides could be formed and depending on the *N*-substituents, they may show no signals in ¹H NMR spectrum.²⁰³

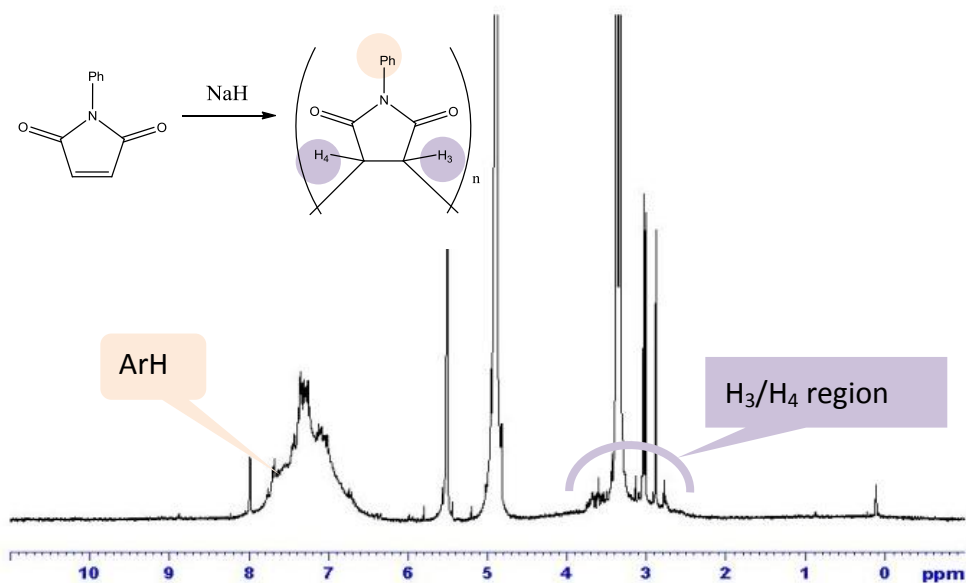
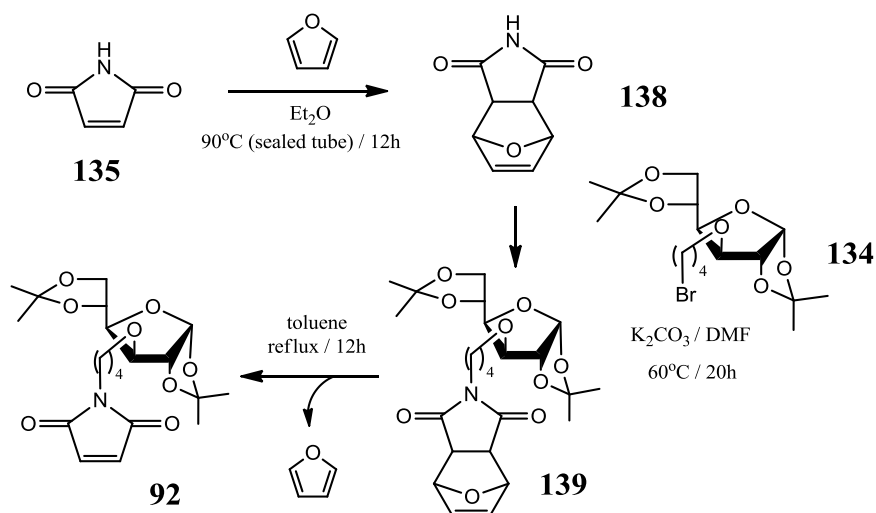


Figure 2.12: ^1H NMR spectrum (d_6 -DMSO) of product produced following exposure of NPM to NaH (2 h, rt).

A survey of the literature^{204,205} suggested it may be possible to generate the desired maleimido-sugar **92**, without exposure of the maleimide to base by protecting it as a Diels-Alder adduct with furan. Cycloaddition of maleimide to furan in Et_2O under pressure at $90\text{ }^\circ\text{C}$ gave the protected maleimide **138** in 70% yield. Subsequent reaction allowed with the bromo-sugar **134** in presence of K_2CO_3 afforded, after 20 h in anhydrous DMF at $60\text{ }^\circ\text{C}$, the protected maleimido-sugar **139** (60%). Final a quantitative retro-Diels-Alder reaction, following reflux in toluene, yielded **92** (Scheme 2.10).

The ^1H NMR spectrum provides evidence of formation of the product **92**. Concomitant with the retro-cycloaddition reaction was the disappearance of the proton resonances from the protected maleimido group, which present as three singlets at 6.52, 5.25 and 2.83 ppm. In addition, the appearance of a new signal, a singlet at 6.69 ppm, was characteristic of the maleimide $\text{CH}=\text{CH}$ protons (Figure 2.13). Those two maleimide alkene protons appear as a singlet as if the molecule was symmetric, which shows that the sugar linked by four carbons methylene bridge is too far to influence the maleimide group. This trend will be applied to more complicated structures.



Scheme 2.10: New synthesis of maleimido-sugar **92**.

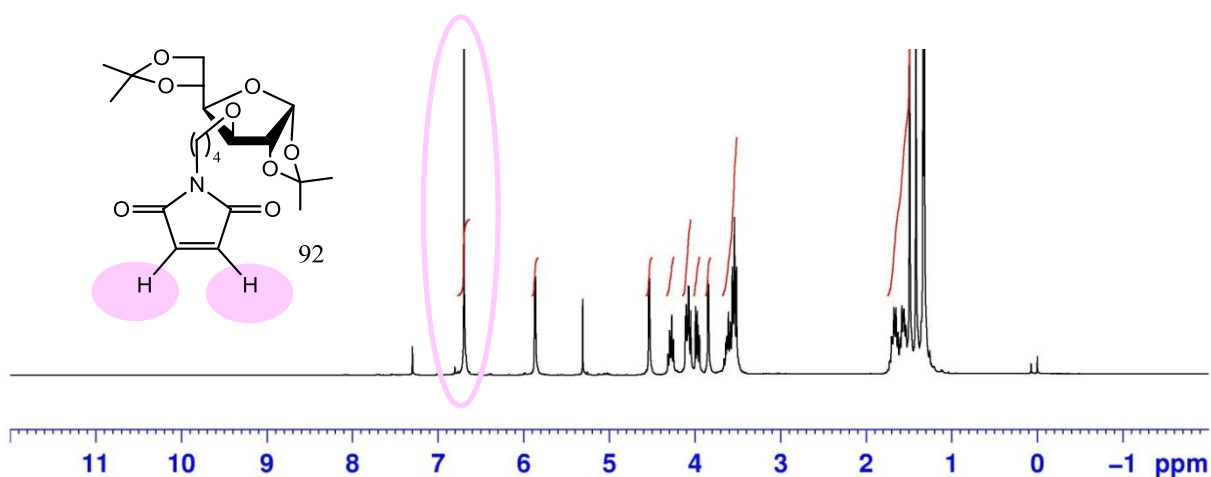
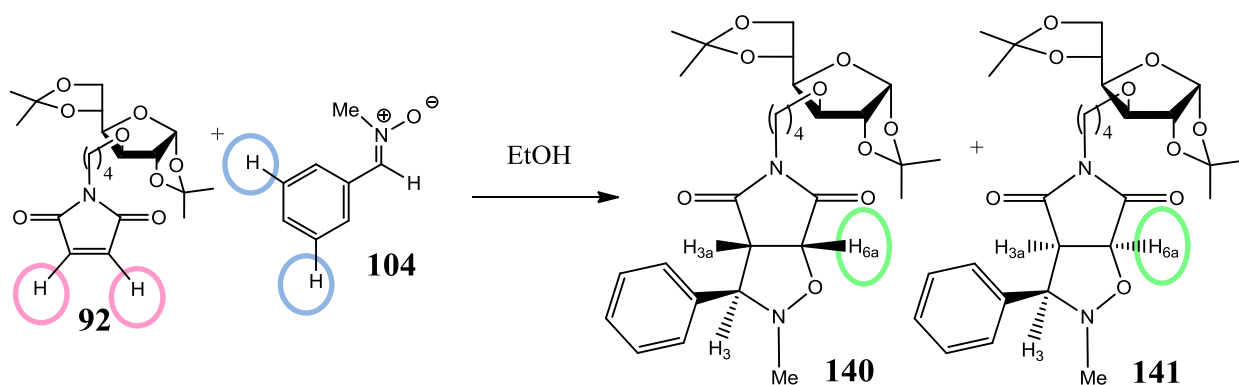


Figure 2.13: ^1H NMR spectrum of maleimido-sugar **92**.

IV.2. 1,3-Dipolar Cycloaddition

IV.2.a. Reaction of maleimido-sugar **92** with nitrones

1,3-Dipolar cycloaddition reaction of the maleimido-sugar **92** with *N*-methyl *C*-phenyl nitronone **104** was explored under the conditions optimized previously for the formation of **108/109** (Equation 2.6). To see if the sugar moiety would have an effect on the yield and diastereoselectivity, the reaction was attempted in a range of solvents including EtOH, MeOH, and H₂O; tBuOH was also tested as it was believed that its steric bulk could decrease the possibility of Michael addition between the solvent and the maleimide.



Equation 2.6: Cycloaddition between maleimido-sugar **92 and *N*-methyl *C*-phenyl nitron **104**.**

The first experiment employed an excess of nitron **104** (1.2 eq) in EtOH (Δ , 17 h, entry 1, table 2.6). After flash column chromatography, the diastereomeric products **140** and **141** were isolated in 70% combined yield.

A series of reactions followed, the aim of which was to gain information about the rate and the selectivity of the reaction under a variety of reaction conditions. The ^1H NMR data of the crude reaction products were analysed to give a picture of the extent of the product formation. The result of experiment 1 was analyzed as follows. The ^1H NMR spectra of the crude reaction mixture were compared to unreacted starting material and an isolated sample of the cycloadduct products (Figure 2.14). It was clear from a comparison of the starting nitron and the isolated products that the latter showed no signals in the region ~ 8.2 ppm. Therefore, for crude reaction products, any signals remaining in this region, must relate to the unreacted nitron. The presence (or absence) of the maleimido-sugar **92** was determined on the basis of a signal at 6.69 ppm representing the alkene protons. However, based on previous observations that maleimides have a tendency to become involved in side reactions (section II.2, p 55), the lack of signals corresponding to this reactant may have no relevance to the extent of product formation.

A comparison of the relative integrals of the signals for the H_{6a} protons of the diastereomeric products (two doublets, 4.92 and 4.86 ppm) and the signals characteristic of two aryl protons of the starting nitron **104** (multiplet, ~ 8.2 ppm), can

be interpreted to give information on the extent of product formation. Thus, for an ideal reaction furnishing cycloadducts in quantitative yield, the ratio of the signals representing H_{6a} to those representing 2H of the nitrone should be 1:0.4, this is because the nitrone was employed in 20% excess. For the reaction 1, the ¹H NMR spectrum of the crude products shows a relative integration of the product H_{6a} proton to the unreacted nitrone signal (2H) of 1:1.3. This can be divided into 0.4 excess starting material (0.2 x 2) and 0.9 unreacted starting material. Thus, the ratio of the unreacted starting material to product is 0.45 (0.9/2) to 1 which suggests ~69% conversion of nitrone **104** to cycloaddition products. With the proviso that nitrone does not enter into any reactivity other than the desired cycloaddition, this “paper” analysis fits well with the experimental finding of 70% isolated yield for reaction 1. This approach has been verified with reaction 3 conducted in MeOH, and reaction 16 conducted in tBuOH. Accordingly, it has been applied to all other reactions described in table 2.6.

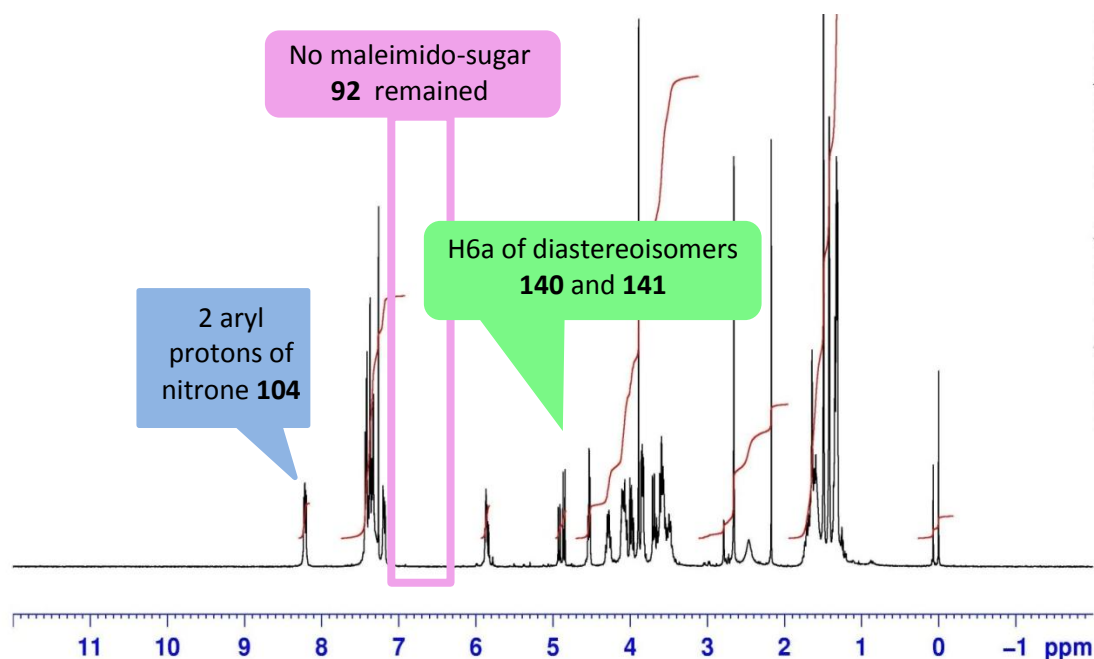


Figure 2.14: ¹H NMR spectrum of the crude product from reaction between maleimido-sugar **92** and *N*-methyl *C*-phenyl nitrone **104** in EtOH.

Under the optimized conditions, the diastereomeric cycloadducts **140** and **141** were isolated in 86% combined yield after 17 h heating at reflux in tBuOH (entry 16, table 2.6). The reactions in EtOH (entry 1) and MeOH (entry 3) also gave cycloaddition products **140** and **141** in acceptable yields, 70% and 66% respectively.

Table 2.6: Summary of outcome of reaction between maleimido-sugar 92 and *N*-methyl *C*-phenyl nitrene 104 leading to diastereomeric adducts 140 and 141.

Entry N°	Reaction conditions				Analysis of reaction products			
	Solvent	Relative quantity of 104 to 92	time	T	% maleimido-sugar 92 remaining in crude reaction product	% 104 converted to products 140/141	Isolated yield (%)	d.r. 140/141
1	EtOH	1.2 eq	17 h	Δ	0	69	70	1:1.3
2	MeOH	1.2 eq	17 h	rt	68	27	/	1:1.5
3			18 h	Δ	0	69	66	1:1.5
4	H ₂ O/MeOH 1:4	2 eq	17h	rt	4	63	/	1:2.0
5			4d	rt	0	67	/	1:2.0
6	H ₂ O/MeOH 4:1	1.2 eq	17 h	rt	23	17	/	1:3.9
7			4d	rt	0	40	/	1:2.6
8		2 eq	17 h	rt	3	20	/	1:2.1
9			4 d	rt	0	24	/	1:2.0
10	H ₂ O/tBuOH 4:1	2 eq	17 h	rt	20	12	/	1:2.5
11			4 d	rt	0	43	/	1:2.4
12	H ₂ O/tBuOH 1:4	2 eq	17 h	rt	19	19	/	1:1.8
13			4d	rt	0	36	/	1:1.9
14	tBuOH	1.2 eq	17 h	rt	14	33	/	1:1.6
15			4 d	rt	0	46	/	1:1.8
16			17h	Δ	0	89	86	1:1.5

Unfortunately, reactions giving satisfactory yields gave very limited diastereoselectivity; selectivity was optimal in aqueous MeOH (~1:4, 17%, entry 6). In search of an improvement in yield, the reaction was repeated for a longer duration (entry 7), or with a greater excess of nitrene (entries 8 and 9). Disappointingly, chemical yields increased but the diastereoselectivity decreased. It was concluded that the sugar moiety, which was linked by four carbons methylene bridge to the “maleimido” dipolarophile, was simply too far from the cycloaddition site to have an influence on the diastereoselectivity of the nitrene cycloaddition reaction.

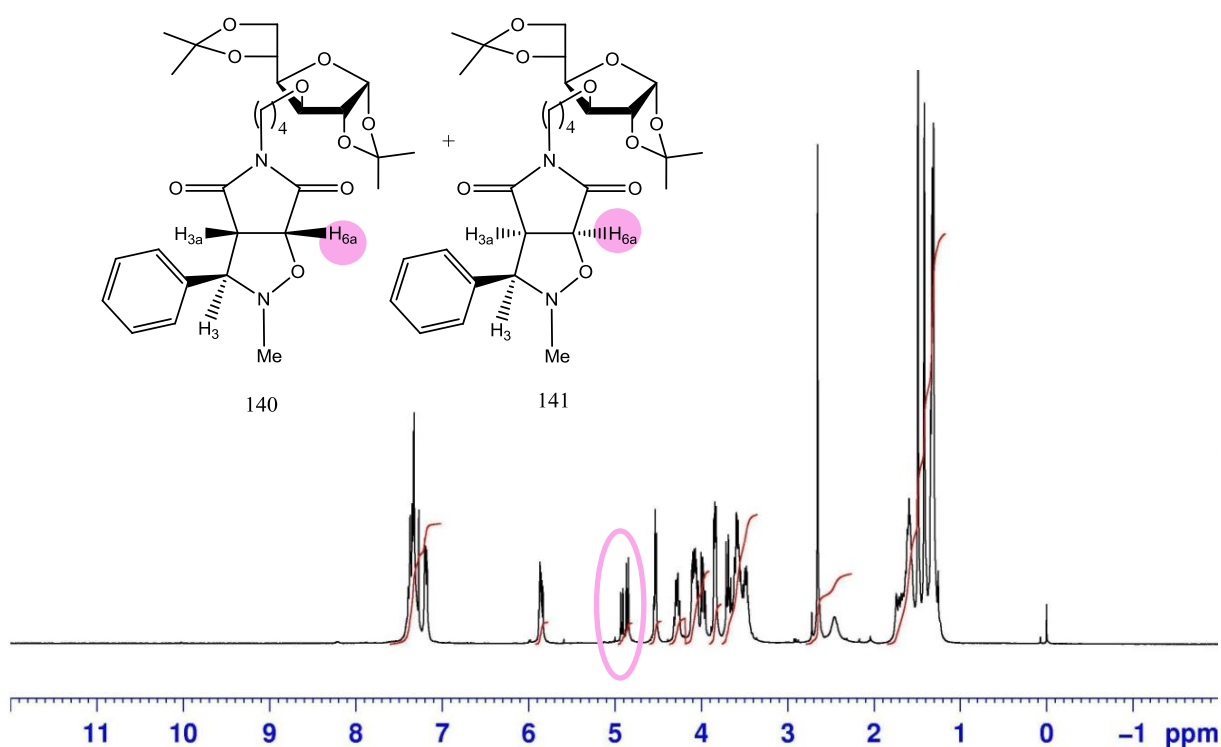
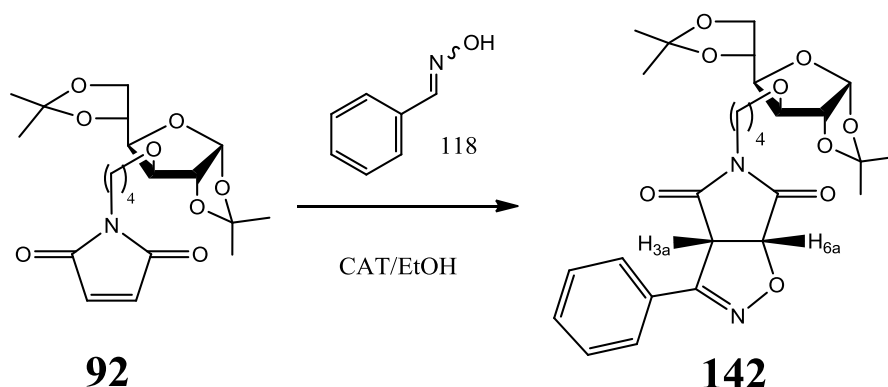


Figure 2.15: ^1H NMR spectrum of an isolated sample comprising a mixture of diastereomeric cycloadducts **140** and **141** (1:1.5).

IV.2.b. Reaction of maleimido-sugar **92** with nitrile oxides

Benzonitrile oxide, generated *in situ* following reaction of CAT with benzaldehyde oxime **118**, was the dipole of choice for investigation of the cycloaddition reaction of maleimido-sugar **92**. The reactants were combined in EtOH, and **142** was formed in 70% yield (2 h, rt) (Equation 2.7). ^1H NMR Spectral

data supports formation of product **142**; concomitant with the cycloaddition reaction was the disappearance of the resonance of the maleimide alkene protons (singlet, 6.69 ppm) and the appearance of new pair of doublets, 5.53 and 4.84 ppm representing H_{6a} and H_{3a}, respectively.



Equation 2.7: Cycloaddition between maleimido sugar **92** and benzonitrile oxide.

V. STABILITY TESTS

The various set-backs encountered during efforts to prepare the *N*-substituted maleimides desired as cycloaddition partners prompted an examination of the synthetic strategy; Michael addition of nucleophiles to the maleimide C=C bond, addition of solvent to the carbonyl groups, and base induced polymerization, all made experiments with the maleimides more tedious than expected. The poor diastereoselectivity observed during cycloaddition, coupled with the lack of chemoselectivity with maleimide substituents called into question the potential value of maleimide based cycloaddition as a strategy for preparation of chemically modified siRNAs. Before devoting more time developing this chemistry, it was deemed appropriate to begin a study of the stability of the resulting 3,5-fused cycloaddition products, and in particular, their compatibility with resin supported chemistry likely to involve base induced (NH₂Me, NH₄OH or K₂CO₃) deprotection and cleavage of the final material from the solid support. Simple 5,5-bicycles (Figure 2.16) were selected as test case compounds to investigate stability towards the basic conditions most commonly employed including NH₂Me (40%) in H₂O (30 min, 60°C), or K₂CO₃ in MeOH (0.05 M, 17 h, rt).

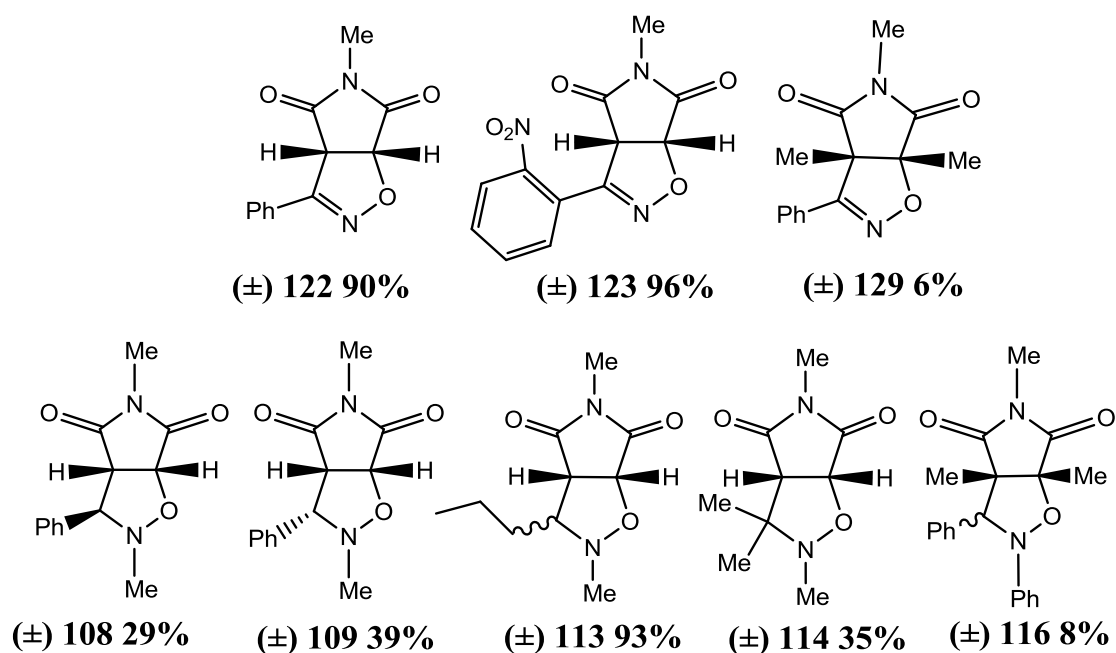
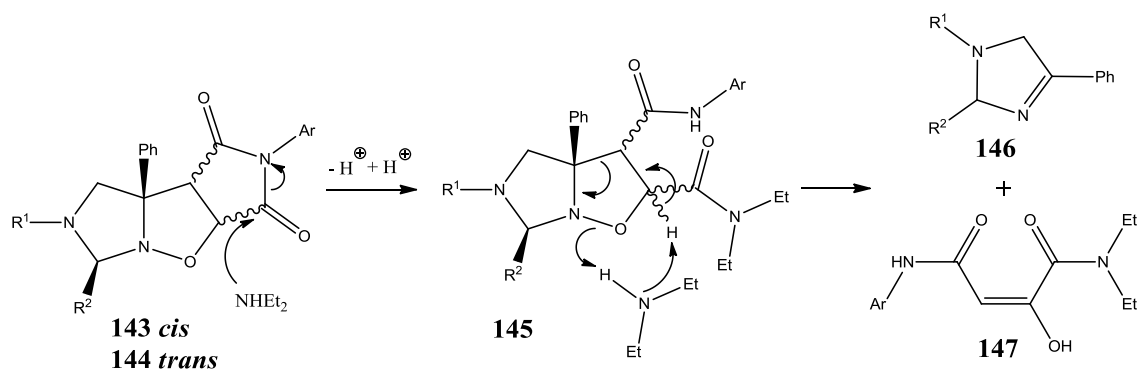


Figure 2.16: 5,5-Fused bicycles examined for stability towards base.

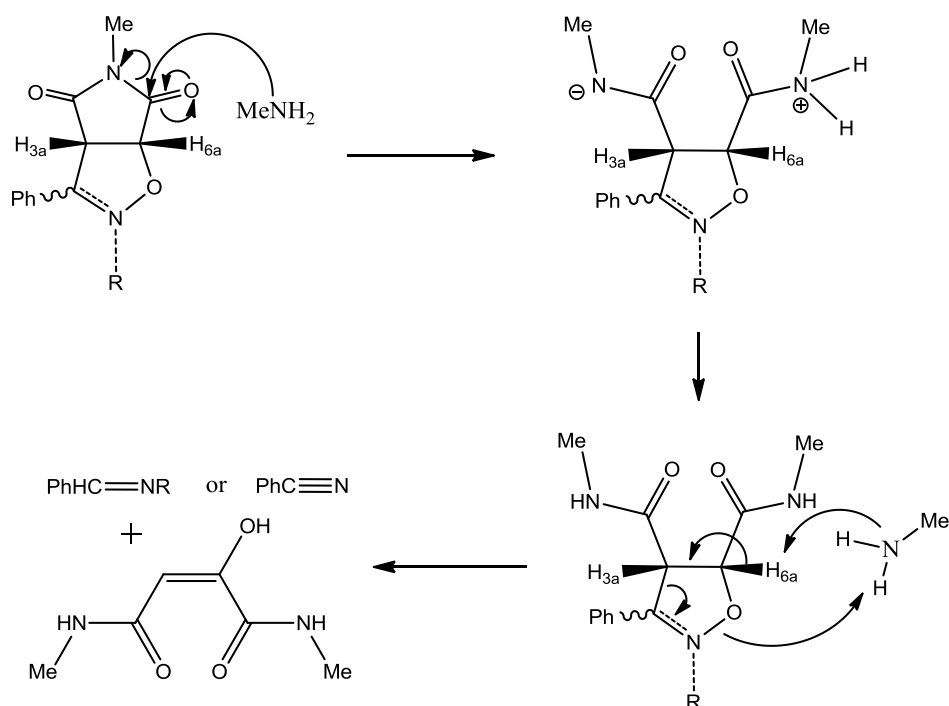
V.1. Stability Towards Methylamine

The behavior of the pyrrolo-isoxazolines/isoxazolidines was examined under the standard method of oligonucleotides cleavage, namely heating at 60 °C for 30 min in an aqueous solution of NH_2Me (40%). Unfortunately, none of the compounds examined proved resistant to this treatment (entries 1 to 9, column A, table 2.7). The ^1H NMR spectra of the crude reaction products showed a complex mixture from which it was not possible to readily identify any structures.

Coskun²⁰⁶ has described the instability of the related diastereoisomeric tricyclic adducts **143** (*cis*) and **144** (*trans*) towards NHEt_2 (Scheme 2.11). They found that nucleophilic attack of NHEt_2 lead to the intermediate **145** (isolated), which underwent NHEt_2 assisted synchronous ring-opening to give imidazolines **146** and the corresponding oxaloacetic acid amides **147**. Inspired by this report, we proposed a mechanism for the decomposition of 5,5-fused bicycles by way of nucleophilic attack by NH_2Me on the carbonyl group, resulting in a ring opening of the maleimido-framework followed by fragmentation of the isoxazol(id)ine, leading to the imine/nitrile and the succinate derivatives, as suggested in scheme 2.12.



Scheme 2.11: Mechanism proposed by Coskun for ring opening of the tricycles 143 and 144.



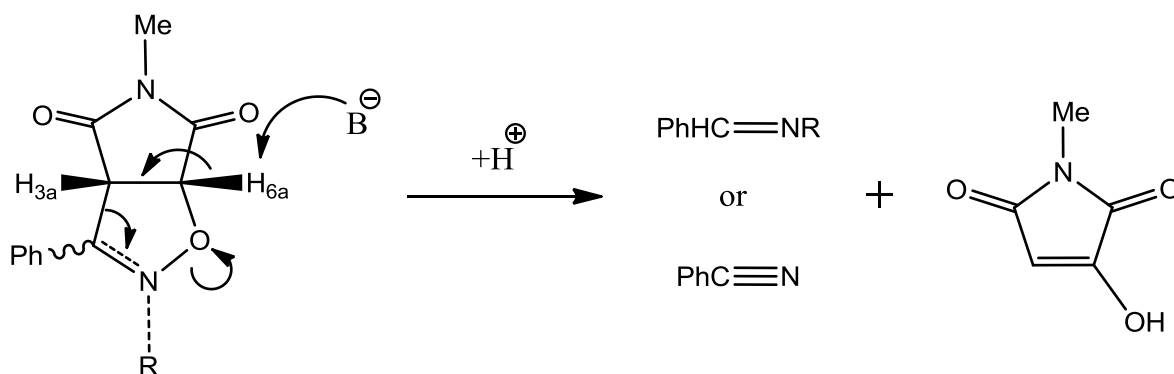
Scheme 2.12: Mechanism proposed for decomposition of pyrrolo-isoxazol(id)ines NH_2Me induced.

V.2. Stability Towards Potassium Carbonate

Cleavage and deprotection of oligonucleotides from the solid support using K_2CO_3 in MeOH (0.05 M) at rt for 17 h is recognized as a milder method than the NH_2Me approach.²⁰⁷ Under these conditions, it was observed that pyrrolo-

isoxazolines **121** and **122** decomposed completely (entries 1 and 2, column B, table 2.7) whilst the dihydro analogues **108/109** and **113** (entries 4 and 7, column B), present as 1:1.5 and 1: 1 mixtures of *trans* and *cis* isomers, displayed interesting behavior. In each case, one diastereoisomer, the *cis* form, was inert to the reaction conditions, whilst the *trans* isomer underwent decomposition. This result was subsequently confirmed by testing individual samples of isolated diastereoisomers **108** and **109** (entries 5 and 6, column B). Indeed the *cis* isomer **109** was inert, whereas the *trans* isomer **108** was not. In an attempt to explain this inconsistent reactivity, small molecular models of **108** and **109** were built in order to make the overall molecular geometry more clear and see if a base attack of H_{6a} was favored or not in the different configuration. No difference was obvious during the comparison. However, this hypothesis that the reactivity of the two isomers is different was supported by the work of Coskun,²⁰⁶ who reported that the tricyclic adducts isomers **143** (*cis*) and **144** (*trans*) have different rates of reactivity towards nucleophilic addition by NHEt₂ (Scheme 2.11, section V.2, p 75). Product formation and disappearance of adducts are faster with the *trans* isomer (1.5 h) than with the *cis* isomer (6 h).

Interestingly, it was observed that products **129** and **116**, which had no junction protons but methyl group instead, were completely stable in presence of K₂CO₃ (entries 3 and 9, column B, table 2.7). It was therefore concluded that the mode of decomposition by K₂CO₃ could involve deprotonation of the H_{6a} and so induce ring opening as depicted in equation 2.8.



Equation 2.8: Proposed mechanism for the reaction between a cycloadduct and K₂CO₃

Table 2.7: Stability results for cycloadducts towards NH₂Me and K₂CO₃.

Entry n°	Substrate	Reaction conditions	
		A	B
		40% aq. NH ₂ Me 30 min at 60°C	K ₂ CO ₃ 1 eq, 0.05 M in MeOH 17 h at rt
Outcome			
1	121 17 mg	Decomposed	Decomposed
2	122 18 mg	Decomposed	Decomposed
3	129 20 mg	Decomposed	Starting material returned unchanged 17 mg
4	108/109 (1:1.5) 50 mg	Decomposed	1. One isomer (<i>cis</i>) returned (30 mg) 2. One isomer (<i>trans</i>) decomposed
5	108 <i>cis</i> 20 mg	Decomposed	Starting material returned unchanged 17 mg
6	109 <i>trans</i> 20 mg	Decomposed	Decomposed
7	113 (1:1) 68 mg	Decomposed	1. One isomer returned (28 mg) 2. One isomer decomposed
8	114 35 mg	Decomposed	Starting material returned unchanged 17 mg
9	116 20 mg	Decomposed	Starting material returned unchanged 18 mg

VI. CONCLUSION

Pyrrolo-isoxazolidines and isoxazolines were synthesized by 1,3-dipolar cycloaddition reaction “simple” *N*-substituted maleimides and nitrones, or nitrile oxides derived *in situ* by the action of CAT on precursor oximes. The cycloadducts were formed in a practical and efficient manner in very good yields. Optimal reaction conditions were found to involve MW irradiation; all the isolated cycloadducts were characterized by spectral studies.

Following the success with the “simple” *N*-substituted maleimides, the target maleimido-sugar **92** was prepared. Several synthetic problems required addressing, however, the desired sugar was finally obtained in 42% yield over three steps. The successful strategy involved protection/deprotection of the maleimide with furan. Some cycloadditions were attempted with **92** in order to study the influence of the sugar moiety on the diastereoselectivity of the reaction. It was concluded that the reaction conditions, solvent, temperature and reaction duration had a significant effect on the diastereoselectivity of the reaction. However, the sugar was found to be too far from the reaction site to have an influence on the selectivity of the reaction.

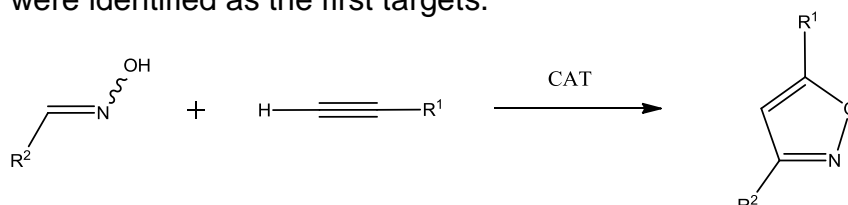
Unfortunately, initial experiments indicate the bicyclic isoxazolidine ring skeleton may not be stable to the standard conditions of oligonucleotide cleavage. Two different sets of conditions have been explored including NH_2Me (40% solution in H_2O at 60 °C for 30 min) and K_2CO_3 (0,05 M in MeOH at rt, 17 h); these results suggest that none of the compounds were stable towards NH_2Me and only the diastereomeric adducts where $\text{H}_{3a}\text{H}_{6a}$ are *cis* was stable towards K_2CO_3 . The compounds having methyl substituents at positions 3a and 6a were stable towards K_2CO_3 but unfortunately 1,3,4-trimethylmaleimide **97** was a poor dipolarophile and yields of cycloaddition reactions were too low for the reaction to be synthetically useful. For all these reasons, we concluded that the maleimide approach was not likely to be successful for oligonucleotide applications, therefore we changed tack and set out to develop nitrile oxide/alkyne cycloaddition as an alternative strategy.

CHAPTER 3:

Synthesis of Thymidine-Alkynes and their
Cycloaddition to Nitrile Oxides.

I. INTRODUCTION

The next approach envisaged was the 1,3-dipolar cycloaddition between a nitrile oxide and a mono substituted alkyne which was shown to be an effective copper-free click chemistry reaction.¹⁰³ It proceeds selectively and in high yield under mild reaction conditions. That the protocol is free from copper is significant for broader applications in oligonucleotide bioconjugation.^{101,208} This key reaction affords five membered isoxazole ring as the conjugation linker (Equation 3.1). In this section, the utility of this reaction is demonstrated in the solution phase synthesis of sugar ($C^{3'}-O$) and nucleobase (N^3 -) tethered isoxazoles. Initial experimentation focused on thymidine derivatives as it is the most robust nucleoside. The molecules in figure 3.1 were identified as the first targets.



Equation 3.1: Cycloaddition reaction between a nitrile oxide and a monosubstituted alkyne.

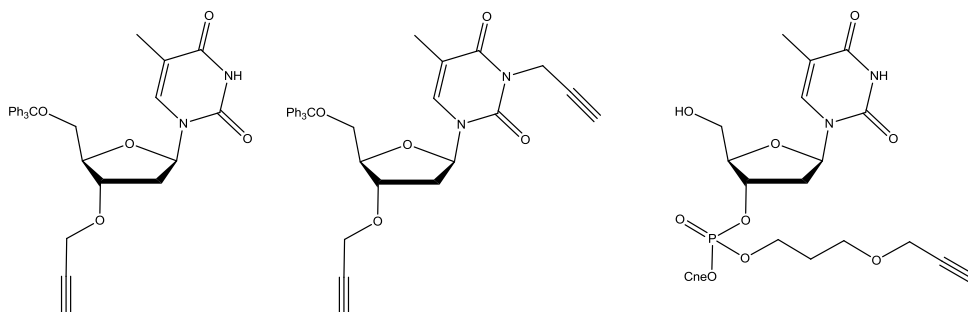
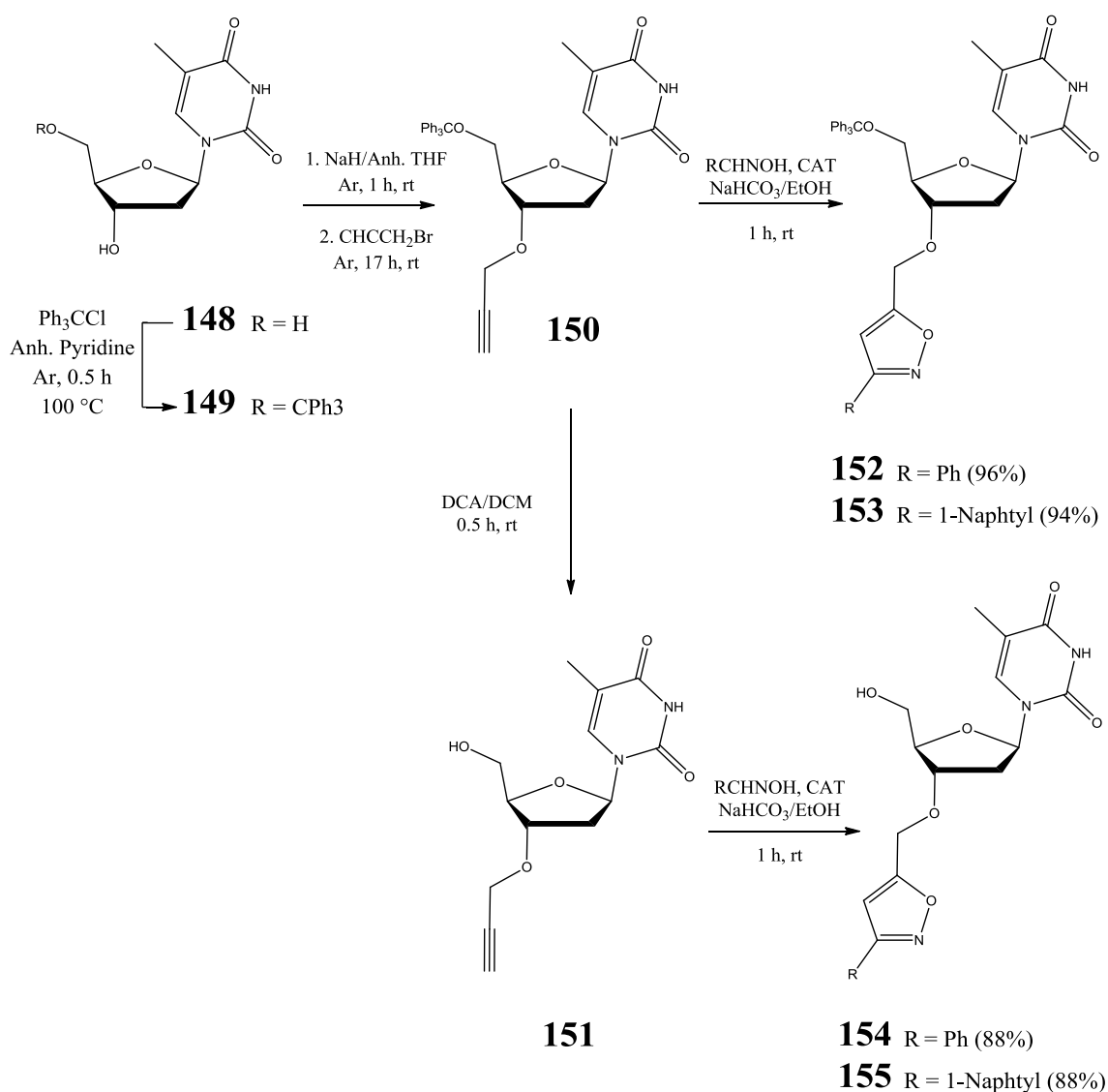


Figure 3.1: Target molecules to synthesized in this chapter.

II. SYNTHESIS AND CYCLOADDITION OF $C^{3'}-O$ -PROPARGYL THYMIDINES

The first step of this synthesis was the already known selective protection of the 5'-OH of thymidine.²⁰⁹ The primary 5'-OH, being more reactive than the 3'-OH, was directly protected by reaction with trityl chloride under the influence of

anhydrous pyridine. The protected thymidine **149** was obtained in 86% yield (Scheme 3.1). Introduction of the propargyl group proceeded by nucleophilic displacement. Propargyl bromide was selected as the alkylating agent and NaH as the base in THF as solvent. The nucleoside **149** was exposed to the base for 1 h at rt in order to form the alcoholate prior to the addition of the propargyl bromide. To ensure chemoselective formation of **150**, it was necessary to exercise caution, a solution of the bromide (80% in toluene) was added dropwise to the reaction mixture, at 0 °C. Without this precaution the C^{3'}-O, N³-bisalkylated product (Figure 3.2) was found as a side product in up to 26% yield.



Scheme 3.1: Synthesis of propargyl 150-151 and isoxazole 152 to 155.

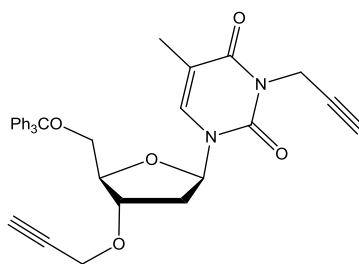


Figure 3.2: C^{3'}-O, N³-bisalkylated product.

Cycloaddition reaction between the propargyl modified nucleoside **150** and nitrile oxides was explored. Aromatic appendages are interesting for biological activity induced by π stacking (also called π - π stacking). It refers to attractive, non-covalent interactions between aromatic rings. These interactions are important in base stacking of DNA nucleotides, protein folding, materials science, and molecular recognition; accordingly benzaldehyde oxime and 1-naphthaldehyde oxime were selected as the nitrile oxide precursors. The solvent of choice was aqueous ethanolic NaHCO₃ and CAT was used as the dipole generating agent.¹⁵⁵ It was deemed important to explore the cycloaddition reaction with the 5'-OH group both protected and unprotected, thus DCA (dichloroacetic acid) mediated detritylation of **150** furnished the known **151** in 96% yield.²¹⁰ To explore the cycloadditions, the reaction components were simply mixed together in aqueous ethanolic NaHCO₃ at rt. The reaction was very fast, reaching completion upon stirring for 1 h under atmospheric conditions. Following purification by column chromatography, **152** (R = Ph) and **153** (R = 1-Naphtyl), were isolated in 96% and 94% yield respectively. The reaction was equally successful with the 5'-deprotected substrate **151**, and the adducts **154** (R = Ph) and **155** (R = 1-Naphtyl), resulting from cycloaddition to benzonitrile oxide and 1-naphtonitrile oxide, were both obtained in 88%.

¹H NMR Spectral data of the crude reaction products indicated regiospecific formation of 3,5-disubstituted isoxazoles in high yielding. A singlet resonance in the region 6.52-6.62 ppm, diagnostic for the H₄ proton of the isoxazole ring, confirms the presence of only one isomer. The expected position for the analogous proton in the regioisomeric 3,4-disubstituted isoxazole would be ~1 ppm further downfield.²¹¹ The regioselectivity of the reaction is also supported by the presence of only one signal representing the OCH₂-isoxazole diastereotopic methylene protons. In each case, it

presents as an AB doublet, at ~4.6 ppm, integrating for 2H. In the starting propargylated thymidines **150**, the corresponding protons appeared ~0.5 ppm upfield as part of a multiplet signal together with the resonance of the H_{4'} proton (Figure 3.3).

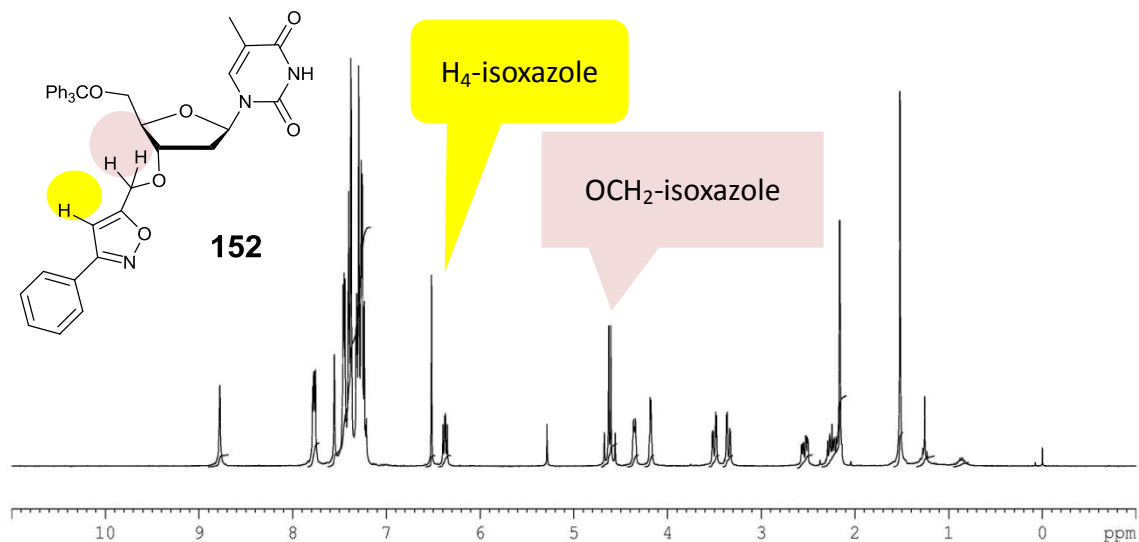
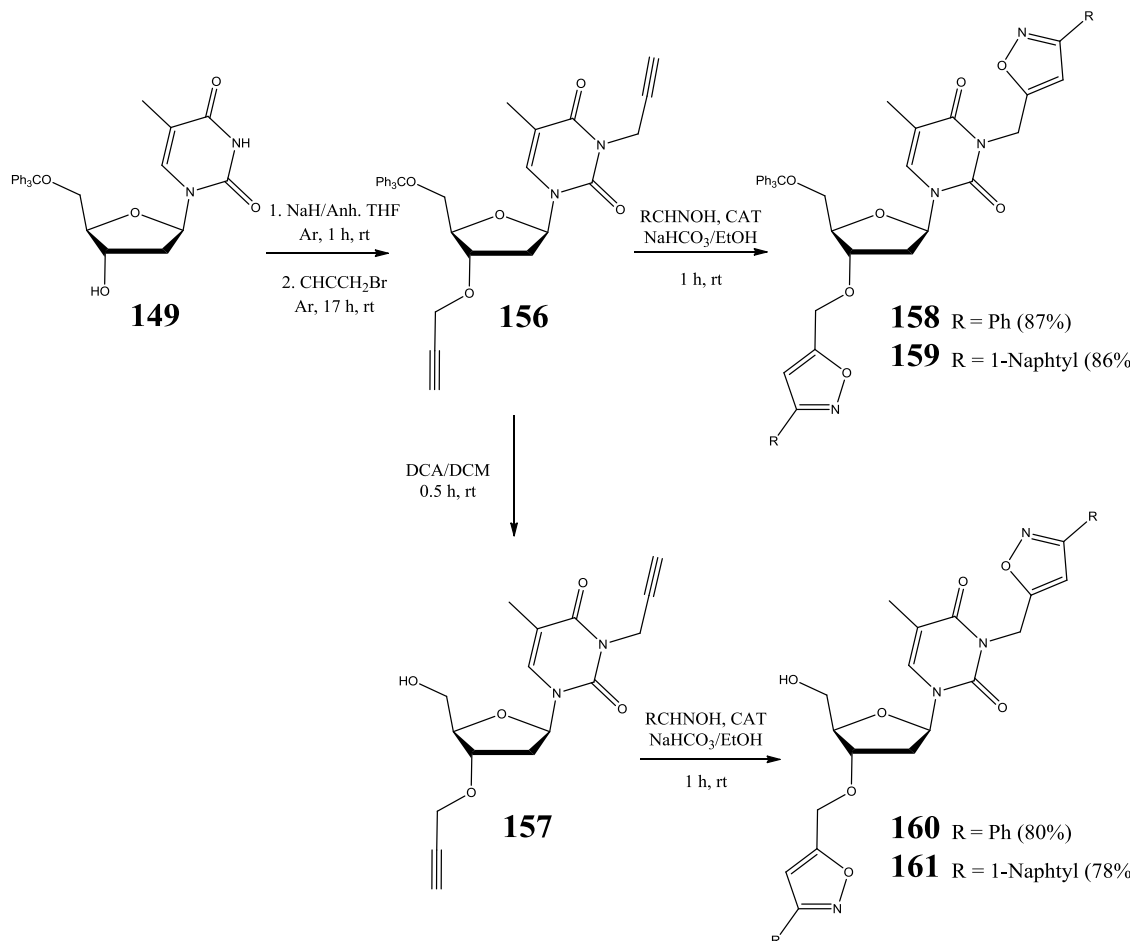


Figure 3.3: ¹H NMR spectrum of **152**.

III. SYNTHESIS AND CYCLOADDITION OF C^{3'}-O-N³-BISPROPARGYL THYMIDINES

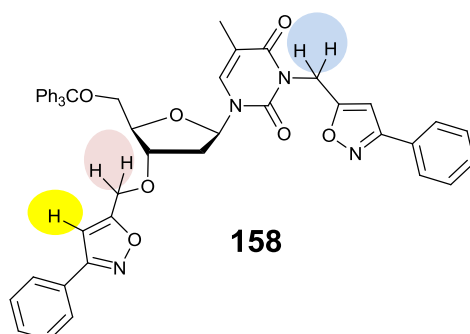
During the synthesis of mono-alkylated compound **150**, it was observed that with a significant excess of NaH, the C^{3'}-O-N³-(bis)propargyl thymidine **156** dominated the reaction product. The possibility to modify the nucleobase is attractive, thus, it was deemed important to explore the double cycloaddition reaction. The *bis* propargyl derivative **156** was prepared in 77% yield from **159** following deprotonation with NaH (6 eq) and double alkylation with propargyl bromide (3 eq). The successful formation of the diyne nucleoside was supported by the appearance of resonances representing the two inequivalent alkyne protons, present as two triplets at 2.41 and 2.17 ppm in the ¹H NMR spectrum. The methylene protons of the propargyl moiety appeared as doublets (4.25 ppm, OCH₂ and 4.77 ppm, NCH₂). The cycloaddition reaction was explored with both **156** and **157**, *i.e.* with and without trityl protection on the 5'-position. The 1,3-dipole partners were the

benzonitrile oxide or 1-naphthyl nitrile oxide with CAT. The reaction was conducted under atmospheric conditions, in ethanolic NaHCO_3 at rt. No compromise in regioselectivity was noted in formation of the double cycloaddition products **158** to **161** which were isolated in 78-87% yield (Scheme 3.2).



Scheme 3.2: Synthesis of bispropargyl nucleosides 156-157 and their double cycloaddition products 158 to 161.

Once again ^1H NMR spectral data supports formation of the 3,5-disubstituted regioisomeric isoxazoles; in all cases, concomitant with cycloaddition, was the disappearance of the alkyne proton resonance and a downfield shift (~ 0.5 ppm) in the position of both the NCH_2 and the OCH_2 methylene protons. No other regioisomer could be found amongst the crude products (Figure 3.4).



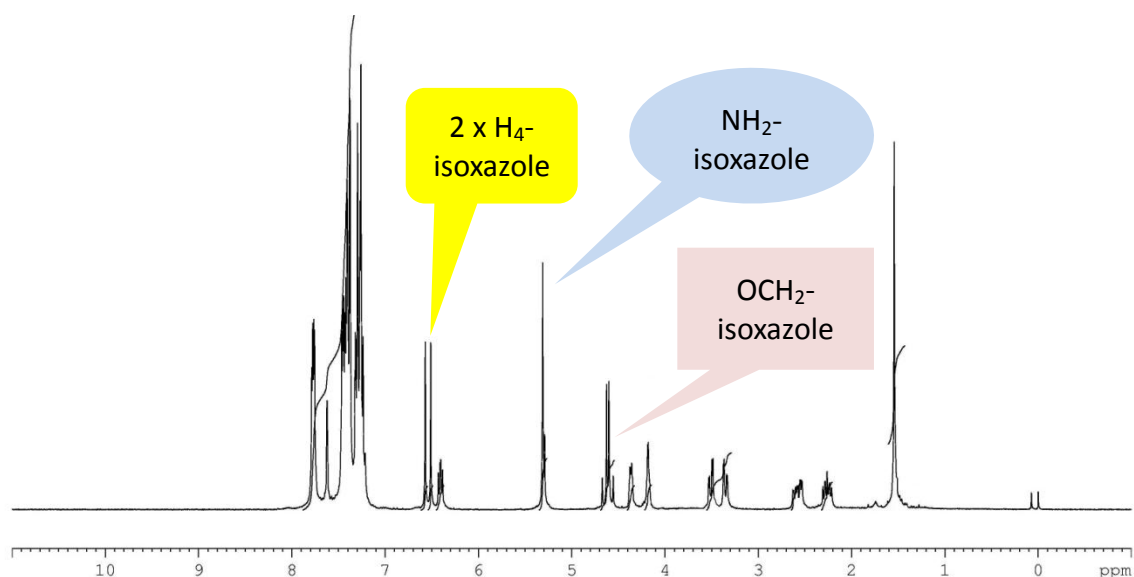
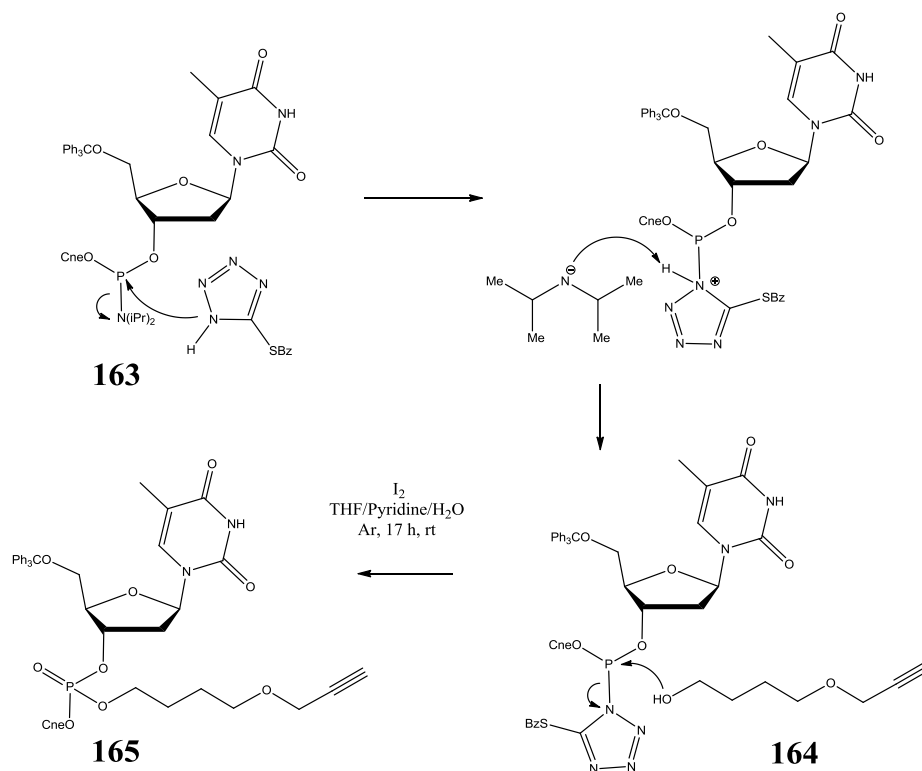


Figure 3.4: ^1H NMR spectrum of **158**.

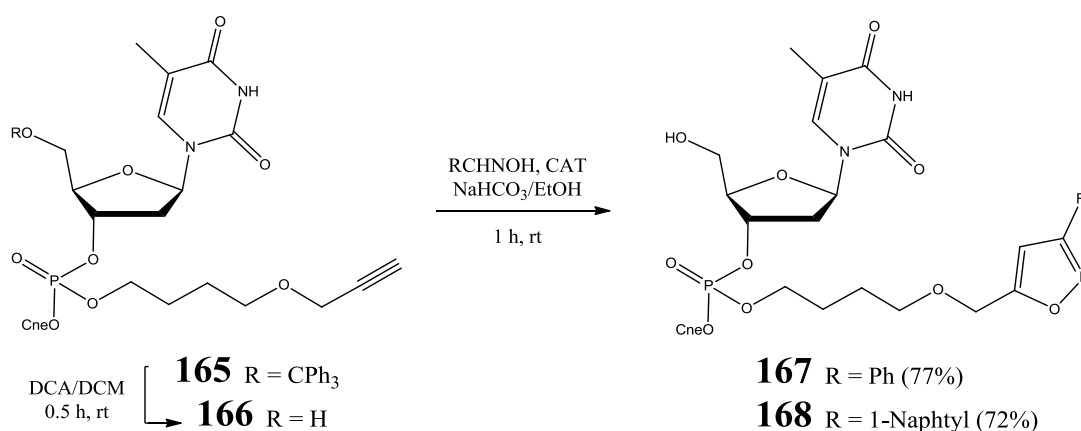
IV. SYNTHESIS AND CYCLOADDITION OF THYMIDINE NUCLEOTIDE

To show compatibility of the CAT induced nitrile oxide click protocol with the nucleotide phosphodiester backbone, the “dimer” **166** was prepared. The first step towards **166** involved the coupling between the alkynyl alcohol **164**¹⁰¹ and the 5'-trityl protected thymidine phosphoramidite **163**. This coupling requires initial activation of the phosphoramidite, which is conducted in presence of 5-(benzylmercapto)-1H-tetrazole (BMT) (Scheme 3.3).²¹² The resulting activated phosphorous is attacked by active 5'-OH group of the nucleoside base. Following oxidation and work-up, removal of the protecting group from **165**, by treatment with DCA, afforded **166** in 53% yield over the two steps (Scheme 3.4). Its structure was supported by ^{31}P , ^{13}C and ^1H NMR spectra; HRMS data confirmed the expected molecular formula (m/z $\text{C}_{20}\text{H}_{28}\text{KN}_3\text{O}_9\text{P}$ requires 524.1195 $[\text{M}+\text{K}]^+$, found 524.1196). A signal at ~ 2.6 ppm in the ^{31}P NMR spectrum is diagnostic for the P(V); nucleus P(III) resonances are expected around 150 ppm;²¹³ the ^1H and ^{13}C assignments were supported by 2D-COSY experiments.

The cycloaddition potential of the nucleotide **166** was confirmed through formation of the phenyl and 1-naphthyl substituted isoxazole derivative nucleotides **167** and **168**, in 77% and 72% yield respectively, following reaction with the appropriate oxime and CAT in ethanolic NaHCO₃ (1 h, rt) as shown in scheme 3.4. Nucleotide compounds are less stable due to the reactivity of the P atom that explains the slightly lower cycloadduct yield for nucleotide compared to nucleoside substrates.²¹⁴



Scheme 3.3: Synthesis of nucleotide alkyne 165 in presence of BMT.



Scheme 3.4: Cycloaddition of nucleotides alkyne 165 with nitrile oxides.

^1H NMR spectra for cycloadducts **167** (Figure 3.5) and **168**, both show a singlet resonance in the region 6.58–6.59 ppm, diagnostic for the isoxazole ring proton, which confirms formation of a 3,5-disubstituted isoxazole. Further validation of the regiochemistry of the reaction is supported by the appearance of the OCH_2 isoxazole protons as a singlet at ~ 4.7 ppm.

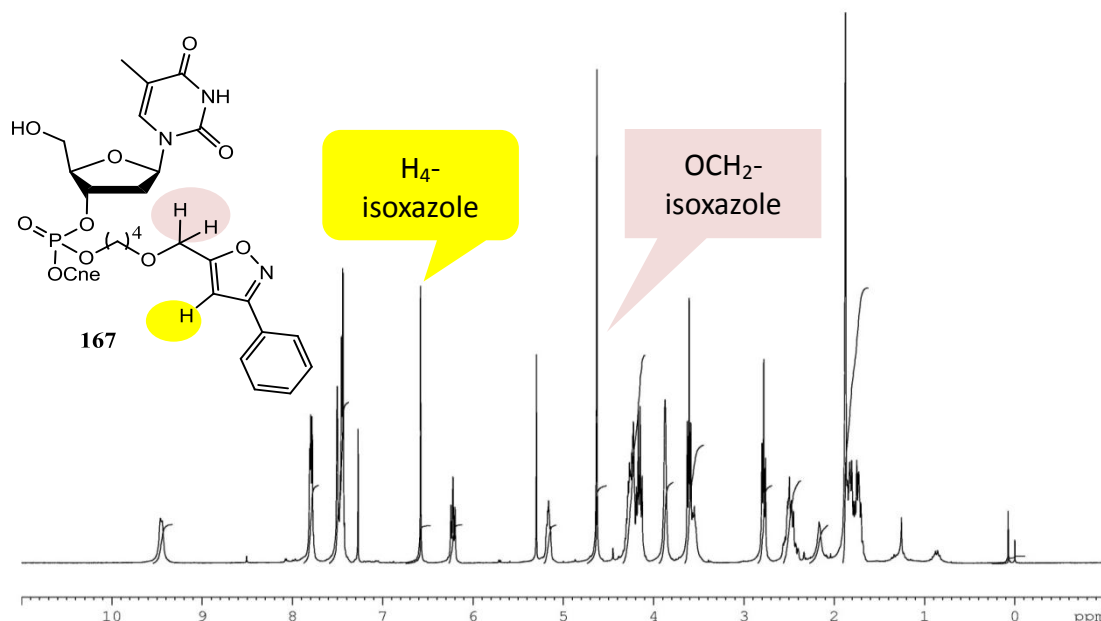


Figure 3.5: ^1H NMR spectrum (d_6 -DMSO) of nucleotide-isoxazole **167**.

V. CONCLUSION

In conclusion, nitrile oxide/alkyne click cycloaddition chemistry offers a robust route to novel isoxazole conjugated nucleosides and nucleotides. The reaction has been shown to be efficient with either 5'-trityl protection or with a free 5'-OH, available for subsequent structural elaboration. The ability to incorporate an isoxazole nucleus in the design of new thymidine receptor agonists is potentially very valuable, and the significance of the current work lies in the demonstration of a high yielding CAT protocol for rapid, catalyst free nucleoside and nucleotide elaboration under very mild conditions (rt, atmospheric conditions and an aqueous environment). The synthetic utility of the nitrile oxide reaction, which reaches completion in 60 min at rt, compares favorably with the observed copper catalyzed formation of triazole linked dithymidines which requires 24 h to reach $\sim 40\%$ completion at rt.²¹⁵

CHAPTER 4:

Synthesis and Cycloaddition of Click
Partners Bearing a Cholesterol Core.

I. INTRODUCTION

In this chapter, the novel work presented by the author concerns generation of cholesterol derivatised click reaction partners, both alkynes and oximes, as shown in figure 4.1.

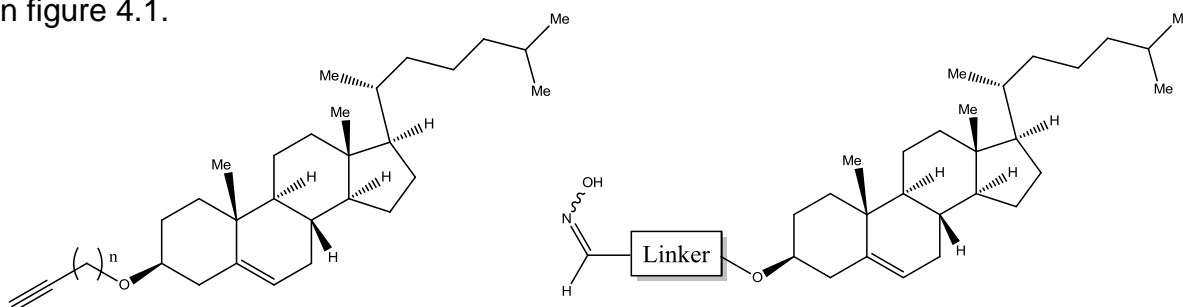


Figure 4.1: Key cholesterol derivatised molecules carrying a click cycloaddition partner.

II. CHOLESTEROL DERIVATIVES AS CLICK REACTION PARTNERS

II.1. Structure of Cholesterol

Cholesterol, an amphipathic molecule has three distinct regions: a tetracyclic core (shown in green, figure 4.2), a hydrocarbon tail (shown in blue), and a hydroxy group (shown in red.). The cyclic core is the signature of all steroid hormones. The combination of the steroid ring structure and the hydroxy group classifies cholesterol as a "sterol." It is an important animal sterol produced in the liver or intestines and used in the construction of cell membranes where it is required to maintain permeability and fluidity. Plants only produce trace amounts of cholesterol.

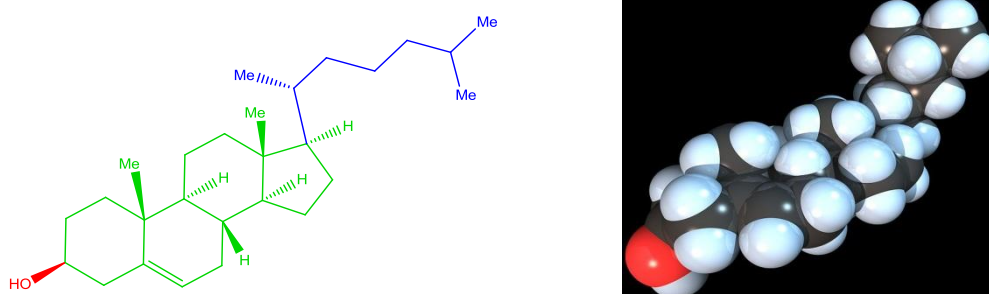


Figure 4.2: The structure of cholesterol, color coded to highlight its key regions

II.2. Synthesis and Cycloaddition of Cholesterol Alkyne Derivatives

The first approach involved the introduction of a mono-substituted alkyne to the cholesterol moiety which would have the potential to function as a dipolarophilic click partner in subsequent nitrile oxide/alkyne cycloaddition reactions. The cholesterol core is large, and an early priority was to establish the optimal length of linker between the terminal alkyne and the cholesterol moiety as well as ideal conditions for the nitrile oxide click cycloaddition reaction with this bulky substrate. To this end, the alkynes **169** to **171** were identified as the first target molecules (Figure 4.3).

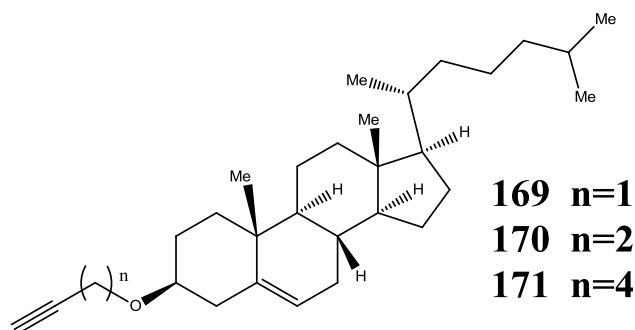
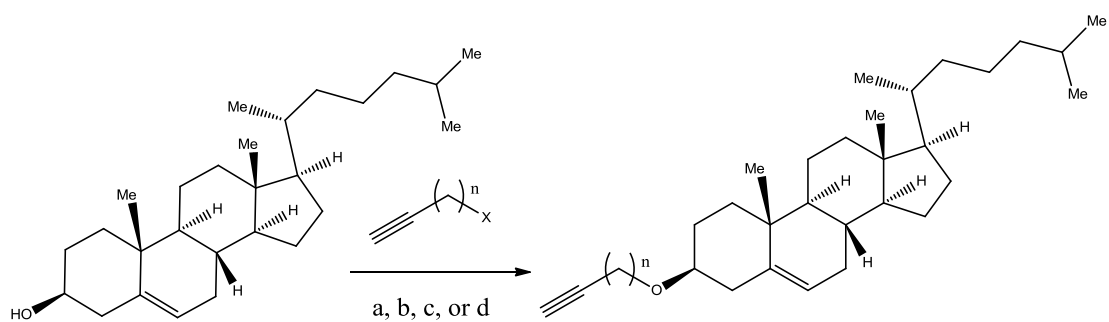


Figure 4.3: Targeted cholesterol alkyne derivatives **169** to **171**.

The first compound investigated was the previously reported propargyl cholesteryl ether **169** ($n = 1$).⁹⁰ Its preparation involved base induced nucleophilic substitution of commercially available cholesterol, with propargyl bromide. With NaH as base and anhydrous DMF as solvent, the target compound was obtained in 44% yield after 17 h at rt. This represents a small increase over the 36% achieved in the reported article. To prepare the homologous compounds **170** and **171**, parallel reactions were attempted with 4-bromobut-1-yne and 6-chlorohex-1-yne respectively. Unfortunately both reactions failed under the conditions described above for **169**. Even under more forceful conditions, *viz* MW activation (12 h, 125 °C), either the products were obtained in very low yield or no reaction occurred. Significantly, to date, neither compound has been reported in the literature by synthetic methodologies involving base promoted nucleophilic attack on halide substrates. One supposes this might be explained by a tendency of the halo-alkyne substrates to undergo a base induced dehydrohalogenation.²⁰¹

In a further attempt to synthesize **170** and **171**, inspiration was taken from the report by Lu²¹⁶ on the use of pre-activated Montmorillonite K-10 (MK-10), to promote etherification of sterols. MK-10 is a soft phyllosilicate that forms microscopic crystals and is named after Montmorillon in France. It is a hydrated sodium calcium aluminium magnesium silicate hydroxide $[(\text{Na},\text{Ca})_{0.33}(\text{Al},\text{Mg})_2(\text{Si}_4\text{O}_{10})(\text{OH})_2 \cdot n\text{H}_2\text{O}]$ and appears to be an efficient acid catalyst for many reactions including etherifications,²¹⁷ the synthesis of bismaleimides or bisphthalimides,²¹⁸ the deprotection of hydroxyl groups of carbohydrates or nucleosides^{219,220} and aldol-type reactions with aldehydes.²²¹ It is commercially available, environmentally friendly and cheap. Rega and co-workers²²² have described MK-10 promoted formation of the propargyl and butynyl cholesteryl ethers **169** and **170**. On the basis of these reports, it was proposed that the alkyne tethered cholesterol derivatives **170** and **171** could be accessed by a clay promoted etherification between cholesterol and the appropriate alkyne alcohol. The substrates, and pre-activated (17 h, 120 °C) catalyst were simply combined in chloroform and reaction progressed to give the corresponding sterol ethers **170** and **171** in 62-70% yield after reflux for 7 days in CHCl_3 . Reaction times have been dramatically improved, from 7 days to one night, by using MW activation (90 °C, 17 h) (Equation 4.1).



169 $n = 1$, **a** 44%, **b** -- , **c** 80%, **d** 68%,
170 $n = 2$, **a** 0%, **b** 0%, **c** 85%, **d** 62%,
171 $n = 4$, **a** 0%, **b** 9%, **c** 71%, **d** 70%

- X = Br or Cl, NaH, DMF, 17 h, rt;
- X = Br or Cl, NaH, DMF, 12 h, 125 °C, MW;
- X = OH, MK-10, CH_3Cl , 7 days, 55 °C;
- X = OH, MK-10, CH_3Cl , 17 h, 90 °C, MW.

Equation 4.1: Synthesis of propargylated cholesterol derivatives 169 to 171.

Structural characterization of the new ethers were supported by ^1H NMR spectral data. For example, concomitant with ether formation, in the case of **169**, was the appearance of a singlet resonance at 4.19 ppm, diagnostic of the OCH_2 protons (Figure 4.4). The corresponding protons in **170** and **171**, appear as triplet signals at 3.60 and 3.48 ppm respectively.

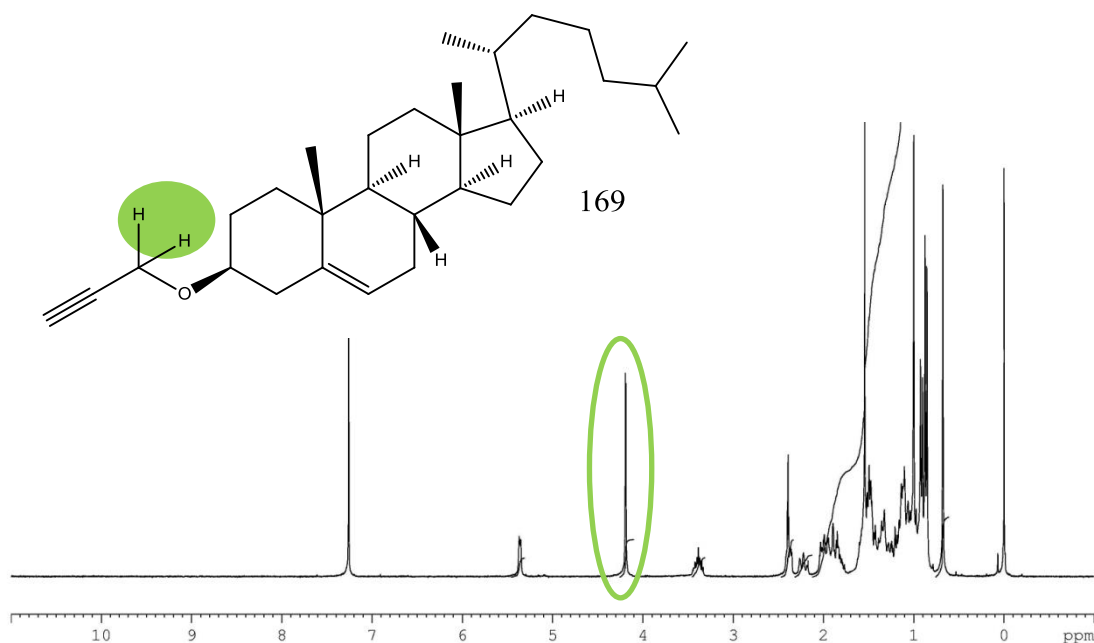
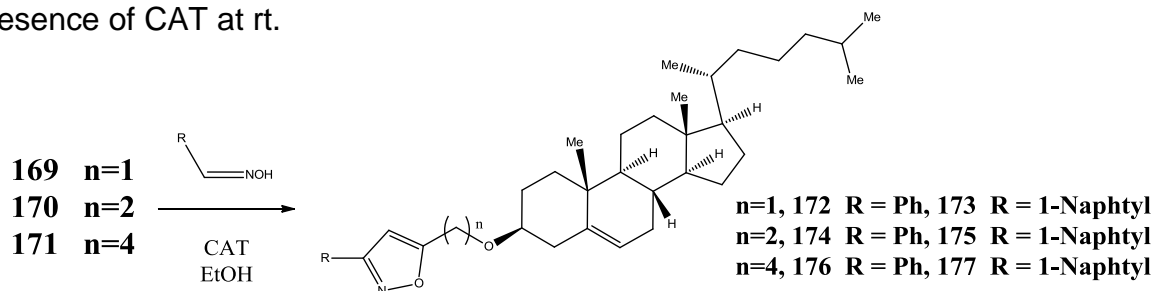


Figure 4.4: ^1H NMR spectrum of propargyl cholesteryl ether **169**.

1,3-Dipolar cycloadditions between the cholesterol ethers **169** to **171** and “simple” nitrile oxides were explored. Benzaldehyde oxime and 1-naphthaldehyde oxime were selected as the dipole precursors. In each case, formation of the nitrile oxide was induced *in situ* by reaction with CAT and reaction solvent was EtOH (Equation 4.2). The results of the experiments conducted under a range of conditions are summarized in table 4.1. Initial reactions, conducted at rt, failed to furnish cycloadducts in reasonable yield. Reaction between the propargyl ether **169**, and aryl nitrile oxides furnished the products **172** (R = Ph) and **173** (R = 1-Naphtyl), in just 19% and 43% yields, respectively after 17 h. Cycloadduct yields were subsequently increased to acceptable levels (78% for **172**, 96% for **173**) following heating in a scientific MW. One possible explanation for the poor reactivity at rt is the steric bulk of the cholesterol moiety in the vicinity of the reaction site. The

improved yields of cycloadducts arising from reaction of **170**, where the alkyne partner is further removed from the cholesterol core, are testament to this hypothesis. Thus, after 1 h at rt, **174** (R = Ph) and **175** (R = 1-Naphtyl), were obtained in 44% and 54% yield respectively. A further increase in yield was observed for the homologous substrate **171** where four carbon atoms separate the cholesterol moiety from the alkyne functionality. Thus, the cycloadducts **176** and **177**, were both obtained in 90% yield following mixing of the reactants in the presence of CAT at rt.



Equation 4.2: Synthesis of cholesterol-isoxazole conjugates 172 to 177.

Table 4.1: Conditions explored for reaction of 169, 170 and 171 with benzonitrile oxide and 1-naphtonitrile oxide .

		Product	Conditions		Isolated yield
			T	Reaction time	
R= 1-Naphtyl	n = 1	173	rt	17 h	43%
			60 °C / MW	1 h	96%
	n = 2	175	rt	1 h	54%
	n = 4	177	rt	1 h	90%
R= Ph	n = 1	172	rt	17 h	19%
			60 °C / MW	1 h	26%
			100 °C / MW	1 h	78%
	n = 2	174	rt	1 h	44%
n = 4	176	rt	1 h	90%	

Successful formation of the isoxazole cycloadducts is supported by their ^1H NMR spectral data. In each case, concomitant with isoxazole formation was the appearance of a new singlet between 6.30 and 6.60 ppm representing the isoxazole ring proton and the disappearance of the alkyne proton resonance, a triplet around 2.3 ppm. The spectrum of **173** is shown in figure 4.5 as a representative example.

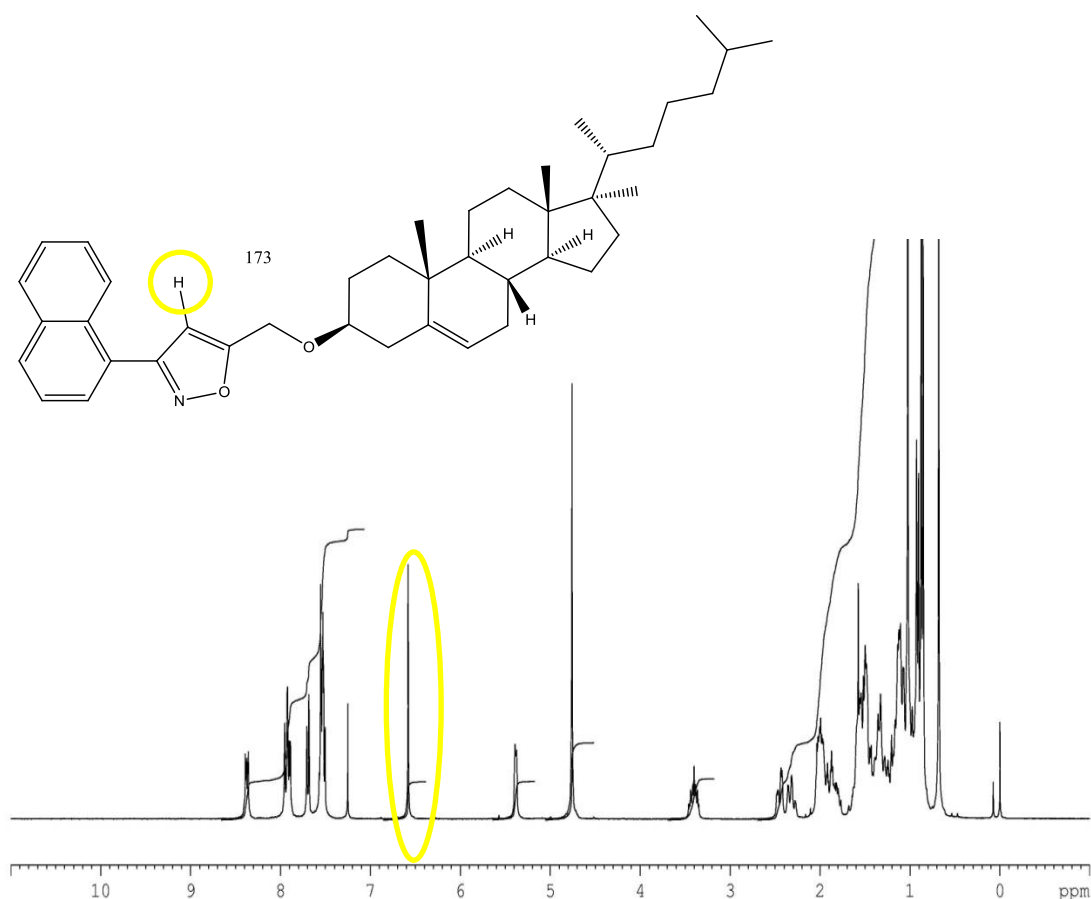


Figure 4.5: ^1H NMR spectrum of **173**.

To conclude, the cholesterol alkyne partners **169** to **171** were successfully prepared with the assistance of MK-10 as an acid catalyst for promotion of the condensation reaction. Their success as click reaction partners related to the length of spacer between the propargyl moiety and the cholesterol core. MW heating could, to some extent, compensate for sluggish reactivity relating to the steric bulk of the steroid core. Substrates with longer linkers between the cholesterol moiety and the terminal alkyne gave better yields of cycloaddition products.

II.3. Synthesis and Cycloaddition of Amido-Carbamate Linked Cholesterol Oximes

With a long term goal of click conjugation where the oligonucleotide substrate bears the alkyne moieties, it was deemed necessary to prepare cholesterol partners carrying nitrile oxide precursors. To this end, the sterol oxime **178** with an amido-carbamate linker, was identified as the next target molecule (Figure 4.6).

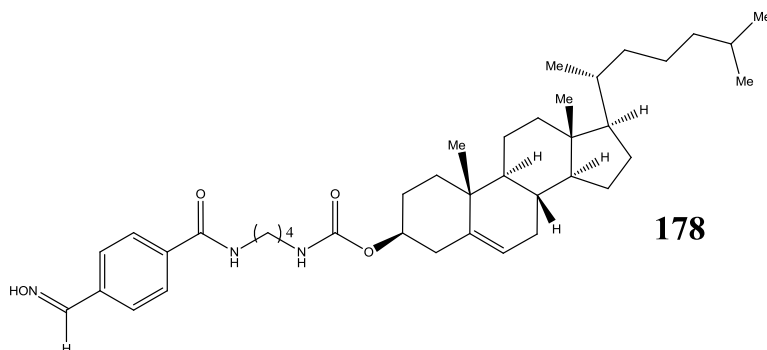
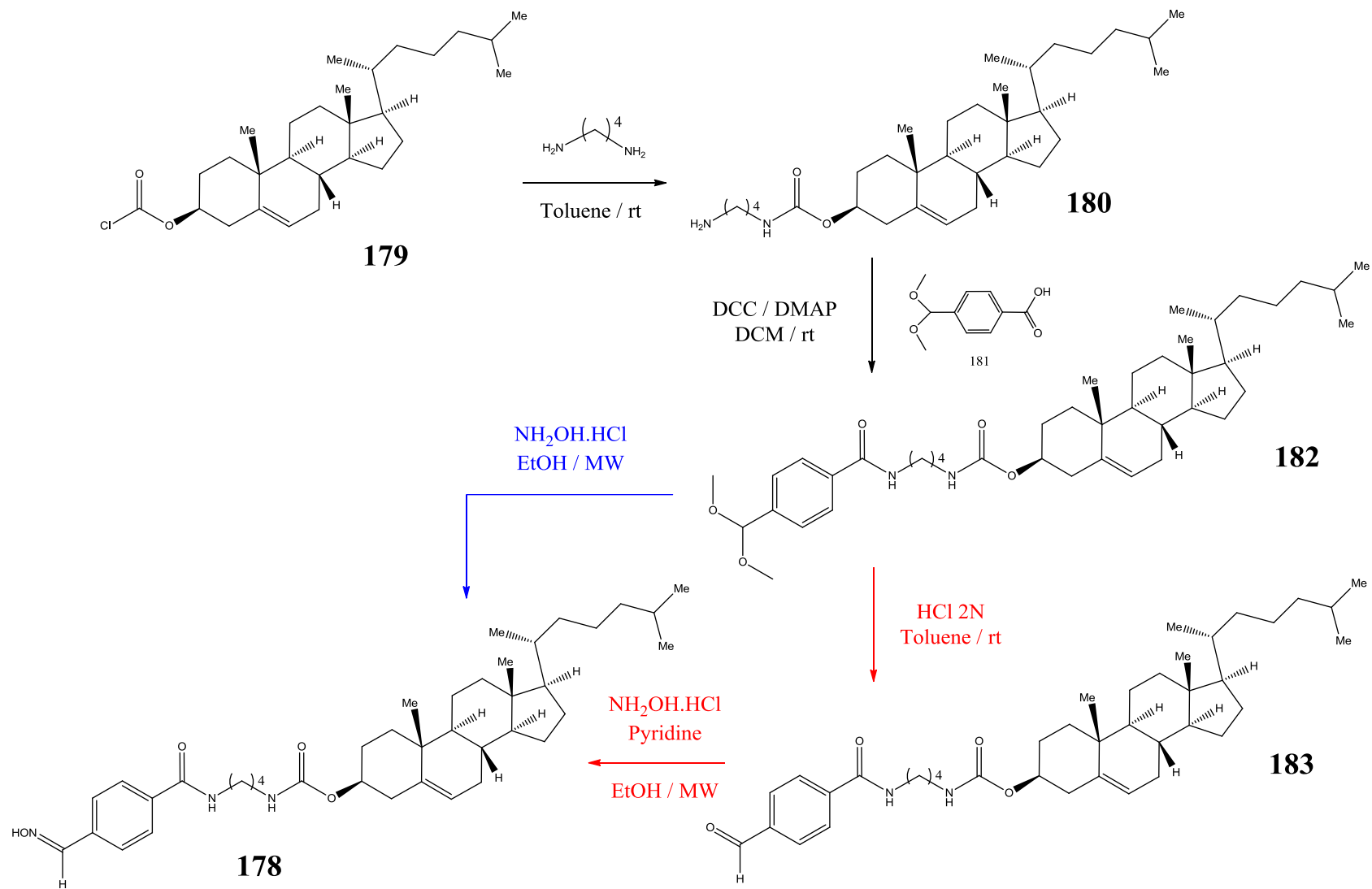


Figure 4.6: Targeted amido-carbamate linked cholesterol oxime **178**.

The convergent synthetic route to the target cholesterol oxime **178** is depicted in scheme 4.1. The synthesis begins with the preparation of the already known amino terminated cholesterol carbamate **180**, derived from the commercially available cholesterol chloroformate **179** following by treatment with diaminobutane.²²³ The product **180** was obtained in 88% yield which represents a huge improvement over the 21% achieved in the reported article. The dramatic improvement is attributed to the slow addition of cholesterol chloroformate **179** to prevent formation of the bis-carbamate. The next step required preparation of the protected aldehyde **181**, the dimethyl acetal of 4-formylbenzoic acid was achieved according to a literature procedure.²²⁴ Thus, treatment of 4-formylbenzoic acid with ammonium chloride in dry methanol at reflux for 3 h gave the diacetal **181** in 89% yield. The subsequent DCC/DMAP mediated condensation of the protected aldehyde with the cholesterol bearing amine **180** was achieved in 53% yield in anhydrous DCM. Using an emulsion of HCl (2 N) in toluene the crude condensation products **182** were deprotected to reveal the aldehyde **183**. Disappointingly, **183** was obtained in just 10% yield over the condensation/deprotection step. Never the less, we persisted in search of the desired cholesterol tethered oxime **178** which was



Scheme 4.1: Synthesis of the amido-carbamate linked cholesterol oxime 178.

obtained in 48% yield following reaction with hydroxylamine hydrochloride and pyridine in EtOH (MW, 80 °C, 1 h). If the aldehyde **183** starting material was sufficiently pure, only a work up was necessary to yield the desired compound. In a subsequent refinement of the synthetic route to **178**, we have discovered that a significant improvement in oxime yield can be achieved. If the protected cholesterol aldehyde **182** was directly treated with hydroxylamine hydrochloride, shown in blue in scheme 4.1, the oxime was prepared in 91% yield. With this modification, the overall yield of the desired oxime from commercially available cholesterol chloroformate was improved from 4% over 4 steps (red arrows; scheme 4.1), to 44% over 3 steps (blue arrows).

^1H NMR spectral evidence in support of formation of the oxime **178** rests with the disappearance of the aldehyde proton resonance (a singlet at 10.08 ppm), and the appearance of a new singlet signal at 8.15 ppm characteristic of the aldoxime CHNOH proton (Figure 4.7).

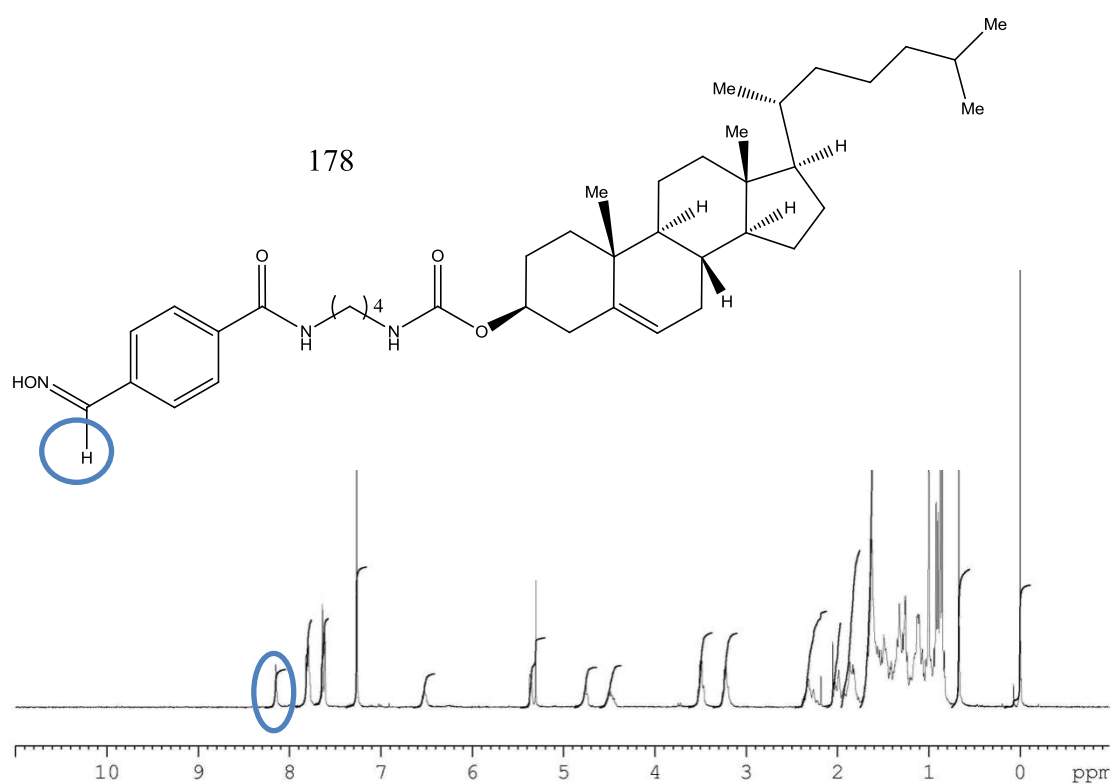
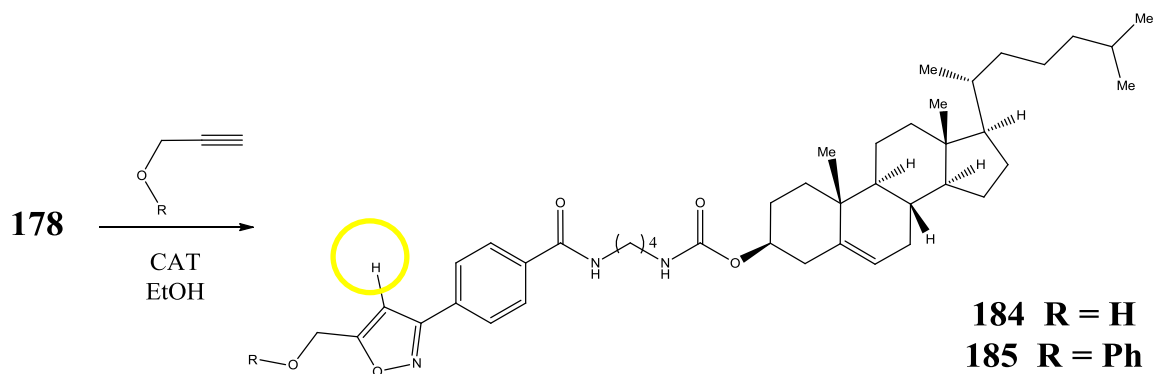


Figure 4.7: ^1H NMR spectrum of the amido-carbamate linked cholesterol oxime **178**.

1,3-Dipolar cycloadditions between the oxime **178** and mono-substituted alkynes, propargyl alcohol and (prop-2-yn-1-yloxy)benzene were explored (Equation 4.3). Both reactions furnished the expected cycloaddition products, albeit in low yields (**184** (21%); **185** (37%)). The ^1H NMR spectra of products **184** (R = H) and **185** (R = Ph) provided evidence in support of isoxazole formation; in particular a new singlet signal appearing, around 6.50 ppm is representative of the isoxazole proton in each product (Figure 4.8).



Equation 4.3: 1,3-Dipolar cycloaddition between amido carbamate linked cholesterol oxime 178 and propargyl alcohol / (prop-2-yn-1-yloxy)benzene.

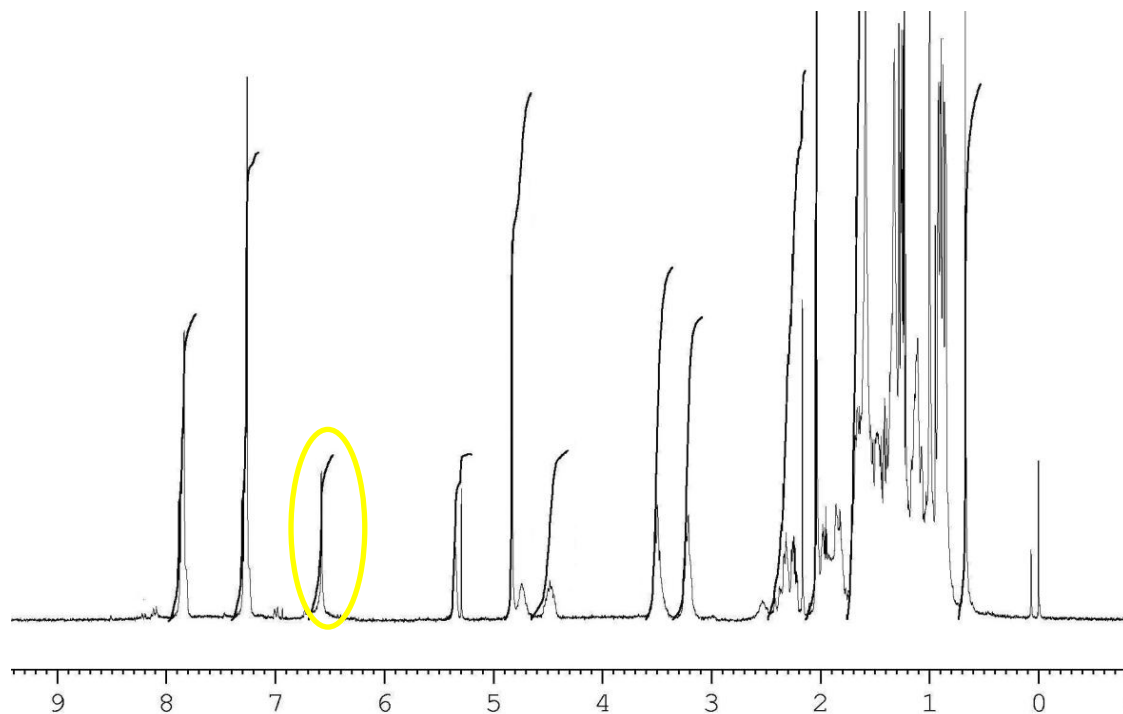


Figure 4.8: ^1H NMR spectrum of **184 (R = H).**

From the very beginning, synthesis of the amido-carbamate linked cholesterol conjugates were plagued by poor solubility. Indeed, these compounds, carrying a lipophilic moiety and a polar group were insoluble in most solvents and consequently were hard to purify. The oxime derivative **178** was particularly unstable during column chromatography on silica gel. Perhaps its lability also accounts for the low yields of cycloaddition products. For this reason the cholesterol oxime **178** was considered an unsuitable substrate for further experimentation with oligonucleotides substrates.

II.4. Synthesis and Cycloaddition of Ether Linked Cholesterol Oximes

The difficulties encountered during efforts to prepare the amido-carbamate linked cholesterol oxime **178** prompted an examination of ether linked analogues which we believed may be more easily synthesized and more stable. In this section, the synthesis and cycloaddition potential of **186a-c** are reported (Figure 4.9).

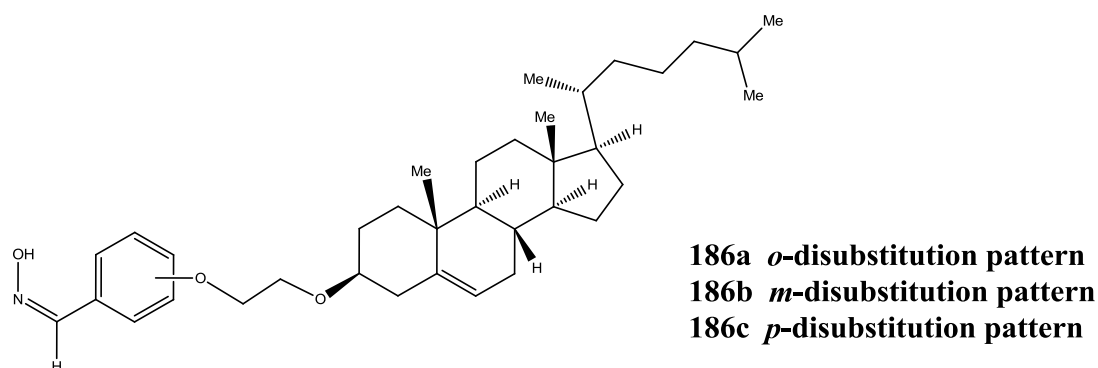
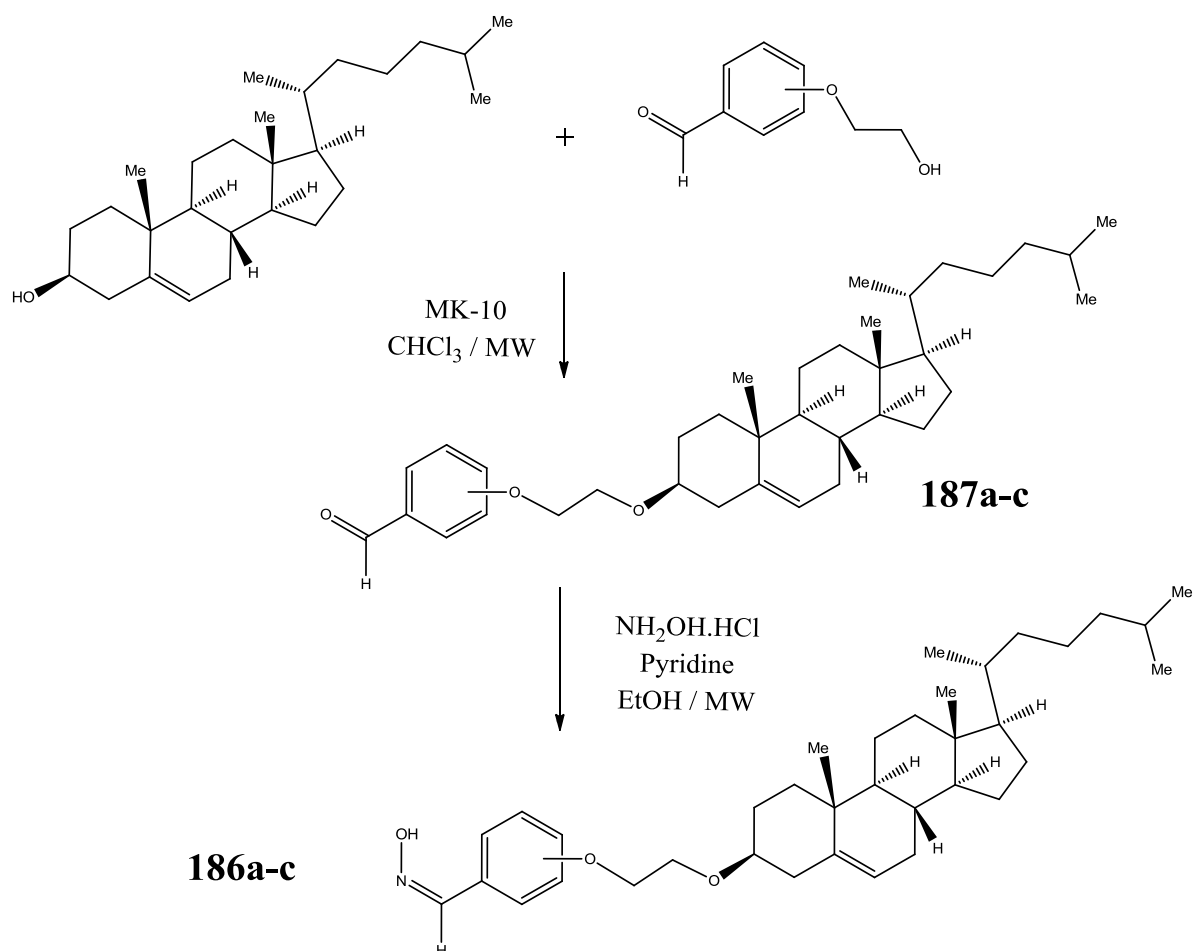


Figure 4.9: Targeted ether linked cholesterol oximes **186a-c**.

The first step in the synthesis of **186c** involved a coupling reaction between cholesterol and 4-(2-hydroxyethoxy)benzaldehyde, both of which commercially available. The condensation reaction was conducted in the presence of activated MK-10 as catalyst and CHCl_3 as solvent; heating to 80 °C was achieved with MW irradiation. Under these conditions the desired ether **187c** was obtained in 58% yield after 8 h. An increase in yield to 68% was observed upon further heating (17 h). As expected, in the case of non-activated MK-10, the yield was dramatically lower (9%).

Condensation with the isomeric 2- and 3-(2-hydroxyethoxy) benzaldehydes, under parallel conditions, yielded the analogous ethers **187a** and **187b** in 35% and 58% yields, respectively. With the regioisomeric aldehydes **187a-c** to hand, the next step was oximation which progressed in quantitative yield with either conventional or MW heating (Scheme 4.2).



Scheme 4.2: Synthesis of ether linked cholesterol oxime 186a-c.

The structures of the new compounds **186a-c** were supported by their ^1H NMR spectra; concomitant with oxime formation was the disappearance of the aldehyde proton (singlet ~10 ppm) and the appearance of new singlet signals representing the oxime proton CHNOH resonance; singlets at 8.55 ppm for **186a**, 8.08 ppm for **186b** and 8.07 ppm for **186c**. The ^1H NMR spectra of the aldehyde **187a** and the oxime **186b** are shown as representative examples in figures 4.10 and 4.11.

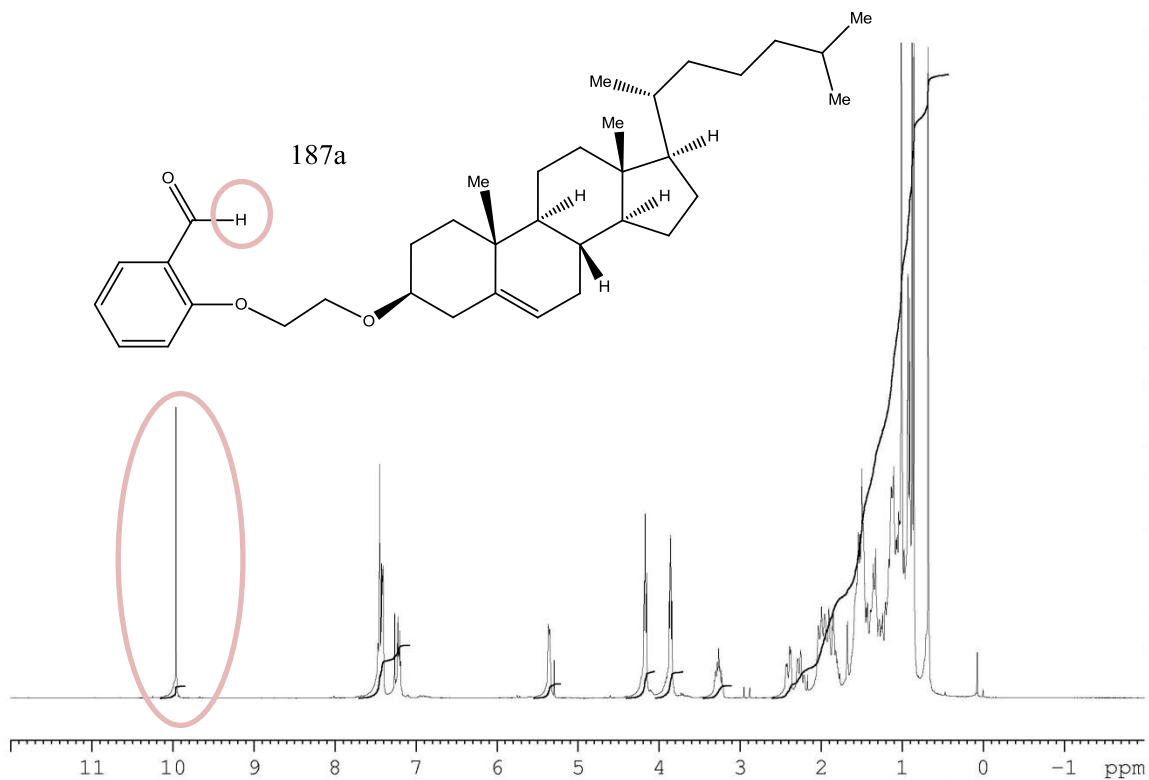


Figure 4.10: ^1H NMR spectrum of ether linked cholesterol aldehyde 187a.

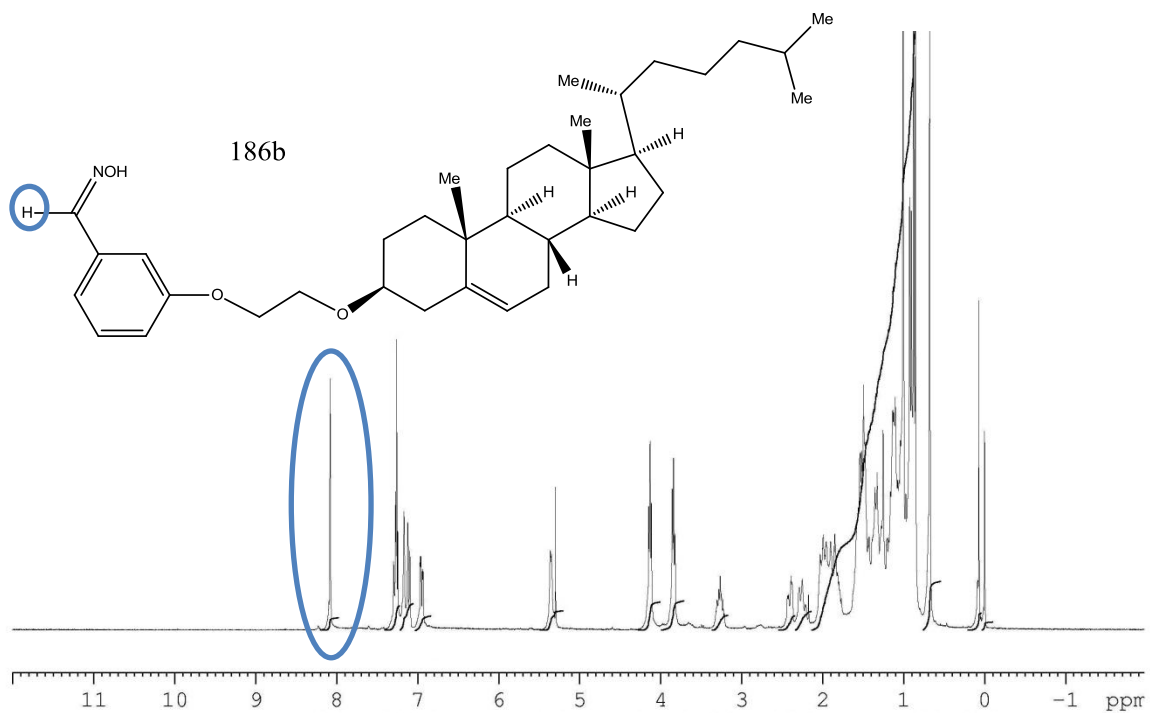
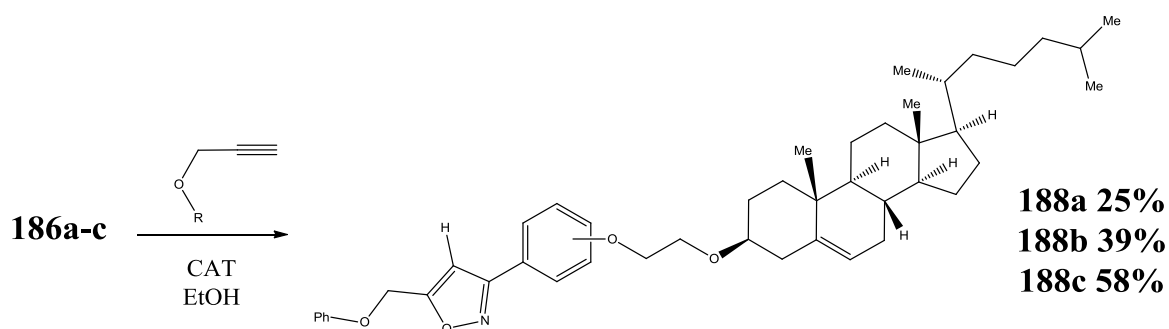


Figure 4.11: ^1H NMR spectrum of ether linked cholesterol oxime 186b.

(Prop-2-yn-1-yloxy)benzene was the dipolarophile of choice for investigation of the cycloaddition potential of steroidal nitrile oxides, generated *in situ* following reaction of cholesterol oximes **186a-c** (1.5 eq) with CAT (2 eq) (Equation 4.4). The reactants were combined together, with no specific attention to the order of addition, and allowed to stir for 17 h at rt. The first compound studied was the 1,4-disubstituted steroid oxime **186c**. The cycloaddition reaction was examined with a range of solvents. The reaction failed in EtOH/H₂O (1:2), most likely because of the insolubility of steroid type compounds in aqueous media. Cycloadduct **188c** was formed in 58% in EtOH, however a significant proportion of what appeared to remain insoluble in that solvent. The reaction was repeated in CHCl₃/EtOH (2:1). In this case, the oxime was completely soluble but a reduction in yield was observed and the desired compound was obtained in only 12% yield. The susceptibility of nitrile oxides to dimerize is well known,¹⁵¹ and one possibility is that the cholesterol oxime derivative **186c** underwent a competitive side-reaction.

The optimal reaction conditions (EtOH, 17 h, rt) were applied to the 1,2- and 1,3-disubstituted oximes, **186a** and **186b**, and cycloadducts **188a** and **188b** were obtained in 25% and 39% respectively (Equation 4.4). The bulkiness of the cholesterol core likely provides the explanation for the modest yields, in particular for **188a** with the *o*-disubstitution pattern.



Equation 4.4: Synthesis of ether linked cholesterol-isoxazole conjugates 188a-c.

The ¹H NMR spectra of cycloadducts **188a-c** support isoxazole formation; in particular a new singlet signal appearing, around 6.50 ppm is characteristic of the isoxazole proton. The spectrum of **188c**, as a representative example, is shown in figure 4.12.

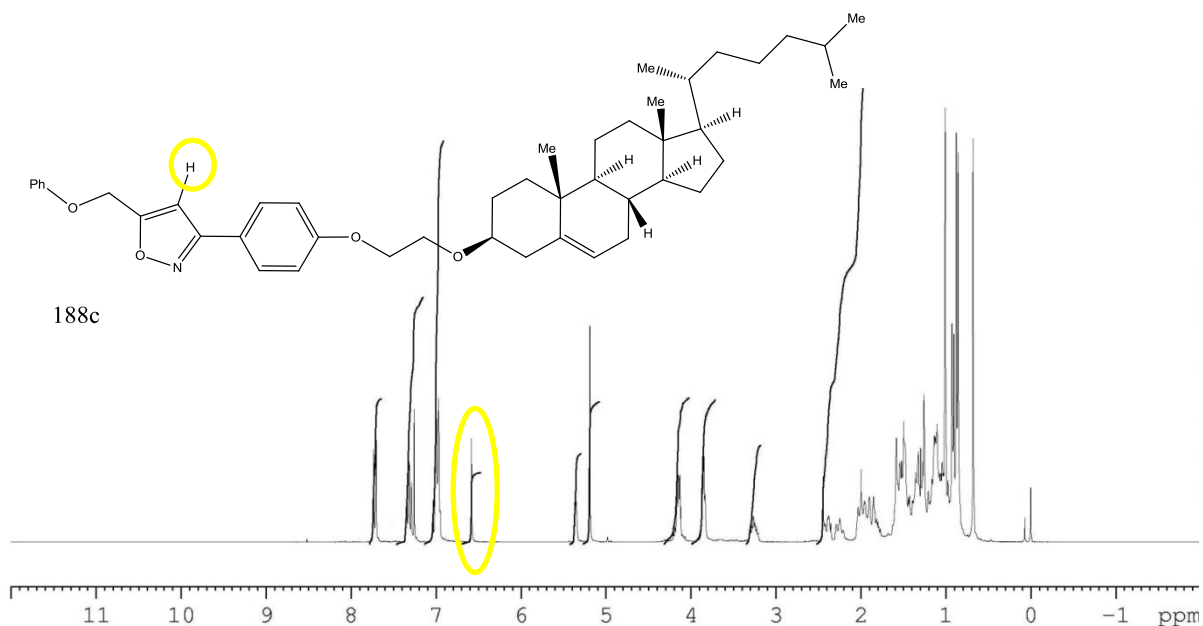
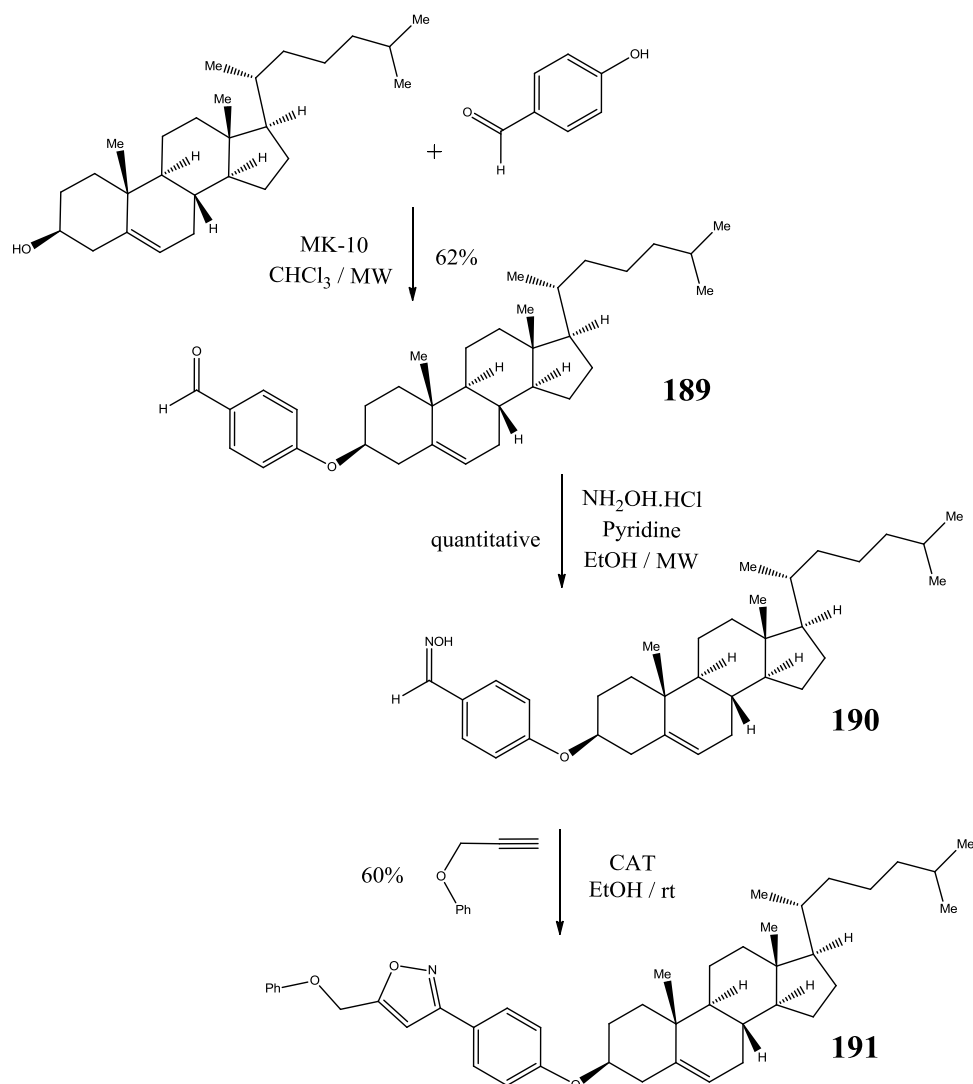


Figure 4.12: ^1H NMR spectrum of ether linked cholesterol-isoxazole conjugate **188c**.

In order to improve the cycloaddition yield, and assuming that the stability of the nitrile oxide may be an issue, the experimental conditions were altered. Instead of mixing all reactants together, the oxime **186c** and the CAT were added by portion to a solution containing the alkyne. Optimum conditions consisted of the addition of 0.75 eq of oxime with 1 eq of CAT (relative to the alkyne) at the beginning of the reaction followed by a second dose 4 h later and stirred for 17 h at rt. With this method, the yield of product **188c** increased to 80%.

Another possible reason for the poor cycloaddition yields in EtOH, pertains to the solubility of steroidal compounds. It was observed that oximes **186a-c** were not completely soluble in EtOH. Thus, we designed a new oxime, **190**, which lacks the carbon chain linker, in the hope of an increased solubility in EtOH. Its synthesis and cycloaddition reaction are shown in scheme 4.3. The reaction conditions resulting in oxime **190** formation from cholesterol were the parallel to those discussed for **186c**. Cycloaddition to **190** was explored, using (prop-2-yn-1-yloxy)benzene as dipolarophile, and CAT to generate the nitrile oxide *in situ* in EtOH (17 h, rt). Cycloadduct **191** was obtained in 60% yield, which is almost identical with that obtained for the cycloaddition with **186c**, under the same conditions (58%). The removal of the $-\text{OCH}_2\text{CH}_2$ linker, therefore, did not appear to influence the solubility or the yield of the cycloaddition reaction.



Scheme 4.3: Synthesis of 191.

III. CONCLUSION

The cholesterol alkynes **169** to **171** were synthesized and their potential as dipolarophiles in nitrile oxide cycloaddition chemistry was explored. It was found that the length of the linker between the cholesterol core and the terminal propargyl moiety significantly influenced the success of the reaction. It was concluded that whilst the steroidal core was compatible with the CAT induced nitrile oxide/alkyne cycloaddition reaction, its steric bulk necessitated it to be kept at a distance of at least four atoms from the reaction site.

Cholesterol bearing oximes **178** and **186a-c** were synthesized and their potential as dipole precursors for nitrile oxide alkyne cycloaddition chemistry was explored. In pursuit of the oximes, several synthetic problems required addressing. Two families were targeted with different linkers between the cholesterol core and the terminal oxime functionality. The amido carbamate family presented difficulties with solubility and purification opportunities, whereas the ether linked substrates proved much easier to prepare and more robust.

1,3-Dipolar cycloaddition reactions were explored between mono-substituted alkynes and nitrile oxides derived *in situ* by the action of CAT on precursor, ether linked steroid oximes **186a-c**. The cycloadduct **188c** was formed in a practical and efficient manner in very good yields in EtOH at rt. Optimum reaction conditions were found to involve the portion wise addition of the oxime/CAT pair (0.5 eq oxime / 1 eq CAT at the beginning of the reaction and the same dose 4 h later). It was concluded that the cholesterol oxime derivative **186c** with the *p*-disubstitution pattern, shown in figure 4.13 would be a suitable click cycloaddition partner for oligonucleotide conjugations.

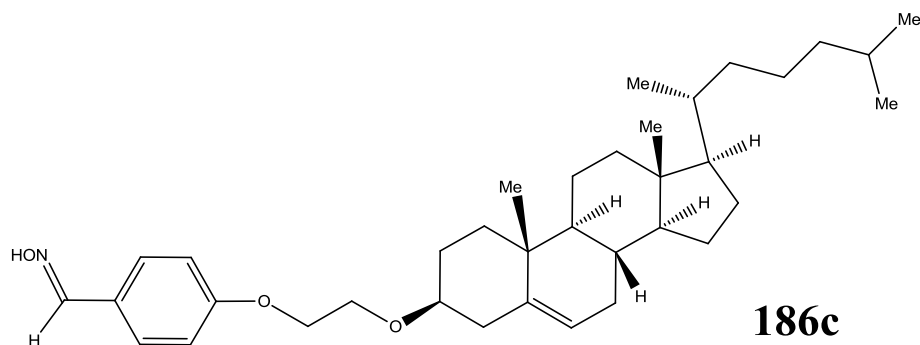


Figure 4.13: Cholesterol oxime derivative 186c chosen for oligonucleotide applications.

CHAPTER 5:

Application of the Nitrile Oxide/Alkyne
Cycloaddition to Oligonucleotides.

I. INTRODUCTION

Click Chemistry facilitates efficient coupling of modular building blocks. In the last decade, the Cu promoted azide/alkyne cycloaddition has been successfully applied to DNA ligation and cyclization.⁷⁴⁻⁷⁷ In the previous chapters, the author has demonstrated an efficient solution phase, copper free, cycloaddition for conjugation of “small” molecules employing nitrile oxide dipole partners. Owing to the enormous potential of oligonucleotide/ligand conjugates for delivery of nucleic acid therapeutics, the next goal of the project was to investigate the utility of nitrile oxide/alkyne cycloaddition for the synthesis of modified oligonucleotides. In the following chapter, the hypothesis that solid supported nitrile oxide/alkyne cycloaddition is a valid route to modify oligonucleotides will be studied.

II. AUTOMATED OLIGONUCLEOTIDE SYNTHESIS

Oligonucleotides of up to 200 nucleotides length²²⁵ are commonly synthesized on the solid phase using standard phosphoramidite coupling chemistry on a DNA/RNA synthesizer (Figure 5.1).²²⁶



Figure 5.1: Expedite DNA/RNA synthesiser

The first base of the oligonucleotide sequence to be grown is covalently bound to the resin via its 3'-terminal hydroxyl group and remains attached to it over the entire course of the chain assembly. The most common resins are macroporous polystyrene (MPPS) and Controlled Pore Glass (CPG),²²⁷ the latter has been employed by the author (Figure 5.2). The solid support is contained in columns sized according to the scale of synthesis.

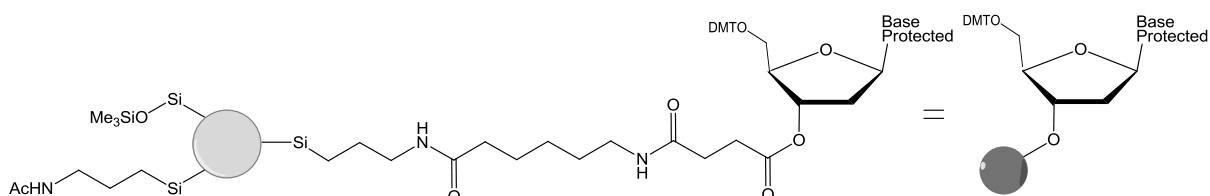
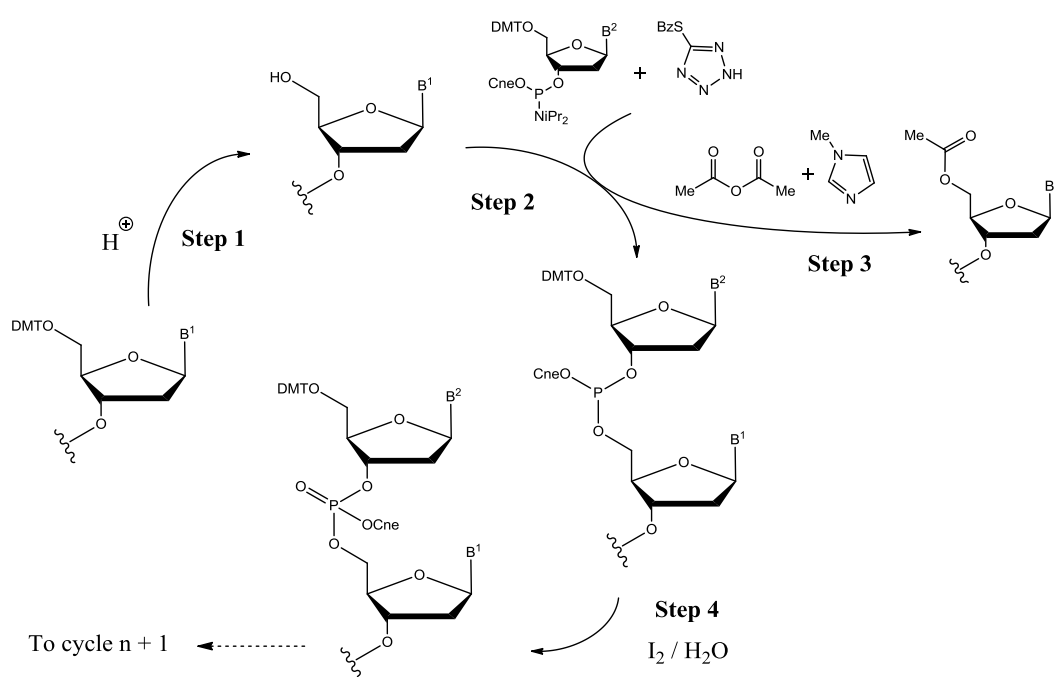


Figure 5.2: General CPG structure (Synbase™) employed by the author.

Whereas enzymes synthesize DNA and RNA in a 5'- to 3'- direction,²²⁸ chemical oligonucleotide synthesis is carried out in the 3'- to 5'- direction. The synthesis involves stepwise addition of nucleotide residues to the 5'-terminus of the growing chain until the desired sequence is assembled. Each addition is referred to as a synthetic cycle and each cycle consists of four chemical reactions: de-blocking (Step 1), coupling (Step 2), capping (Step 3), and oxidation (Step 4) (Scheme 5.1).



Scheme 5.1: Synthetic cycle for preparation of oligonucleotides by phosphoramidite chemistry.

II.1. Building Blocks

Naturally occurring nucleotides, nucleoside 3'- or 5'-phosphates and their phosphodiester analogs, are insufficiently reactive to afford synthetic oligonucleotides in high yields. The selectivity and the rate of the formation of inter-nucleosidic linkages is dramatically improved by using 3'-*O*-*N,N*-diisopropyl phosphoramidite 2'-deoxynucleosides (dA, dC, dG, and T), ribonucleosides (A, C, G, and U), or chemically modified nucleoside phosphoramidites. To prevent undesired side reactions, reactive functionalities on the nucleoside are protected. The 5'-hydroxyl group is commonly protected by an acid-labile **4,4'-dimethoxytrityl group (DMT)**. The phosphite group is protected by a base-labile **2-cyanoethyl group (Cne)** (Figure 5.3). Individual bases have their own protecting groups as discussed in the following section.

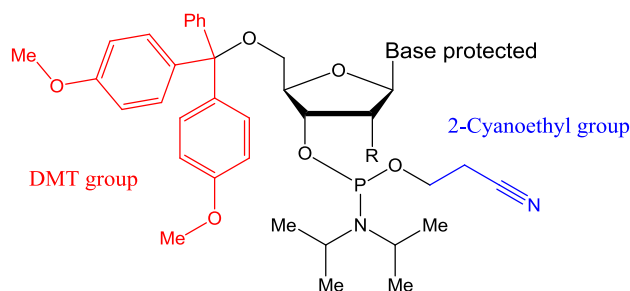


Figure 5.3: Phosphite and 5'- *O*-Protected 2'-deoxyribonucleoside (R = H) or ribonucleoside (R = OH) phosphoramidites

II.2. Deblocking (Step 1)

The DMT group is typically removed with 2% trichloroacetic acid (TCA) or 3% dichloroacetic acid (DCA), in DCM or toluene. The reaction column is then washed to remove excess acid and by-products, including the orange-colored DMT cation (Figure 5.4); this step results in the solid support-bound oligonucleotide bearing a free 5'-terminal hydroxyl group (Scheme 5.2).

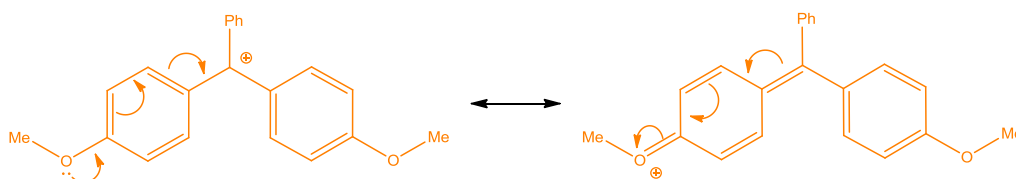
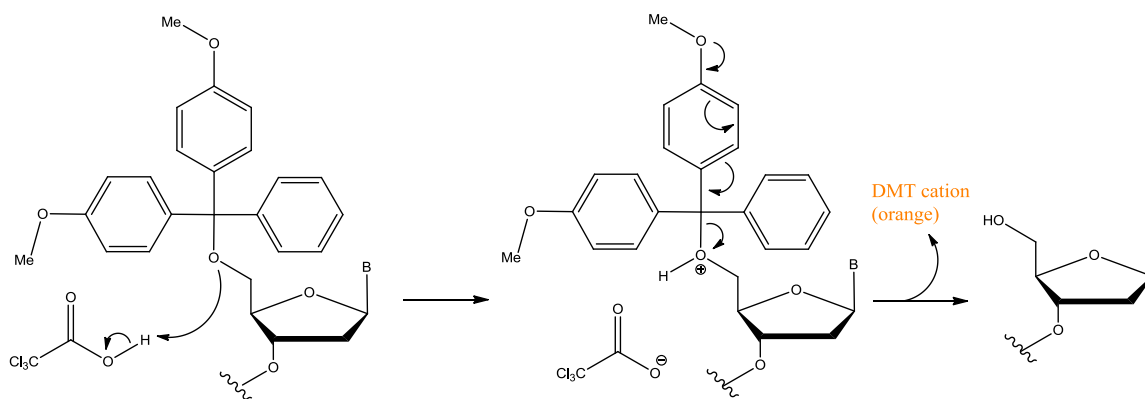


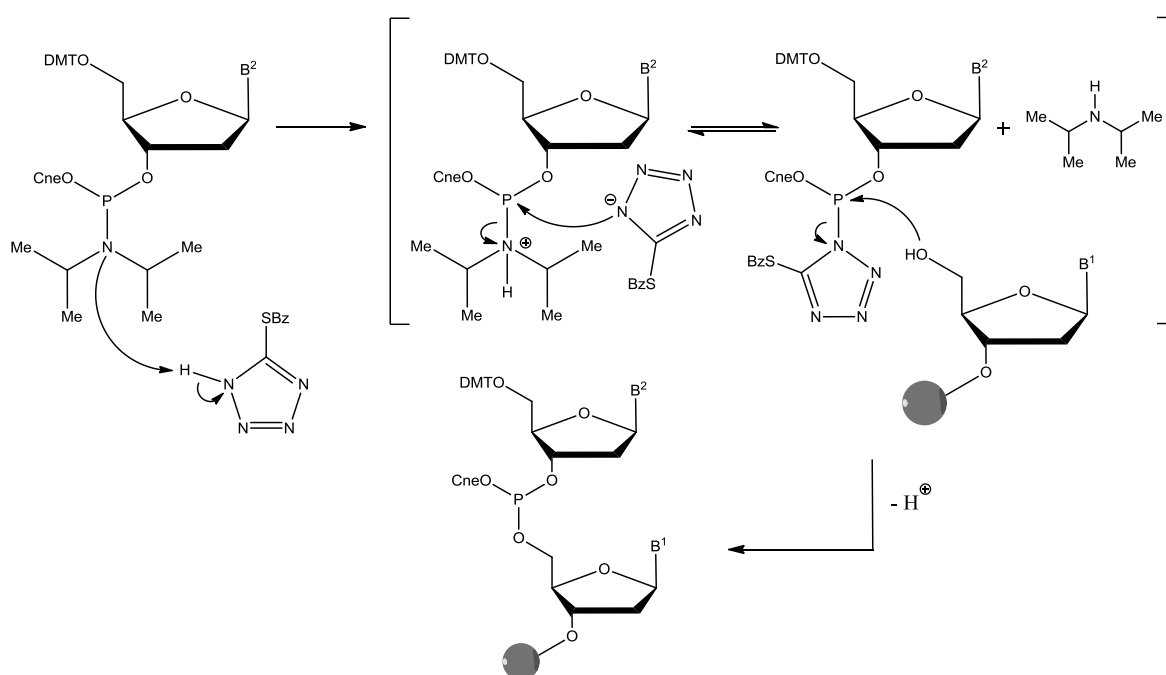
Figure 5.4: Resonance forms of DMT cation.



Scheme 5.2: Mechanism of the deblocking step in oligonucleotide synthesis.

II.3. Coupling (Step 2)

The next monomer is added following activation by treatment of a solution of nucleoside phosphoramidite 0.02-0.2 M with a solution of an acidic azole catalyst 0.2-0.7 M (BMT). The activated phosphoramidite, in 1.5-20 fold excess over the support-bound material, is then brought in contact with the 5'-hydroxyl group of the preceding base resulting in formation of an unstable phosphite linkage (Scheme 5.3). The reaction column is then washed to remove any extra reactant, unbound base and by-products.



Scheme 5.3: Mechanism of the phosphoramidite coupling reaction in oligonucleotide synthesis.

II.6. Cleavage/Deprotection and Purification

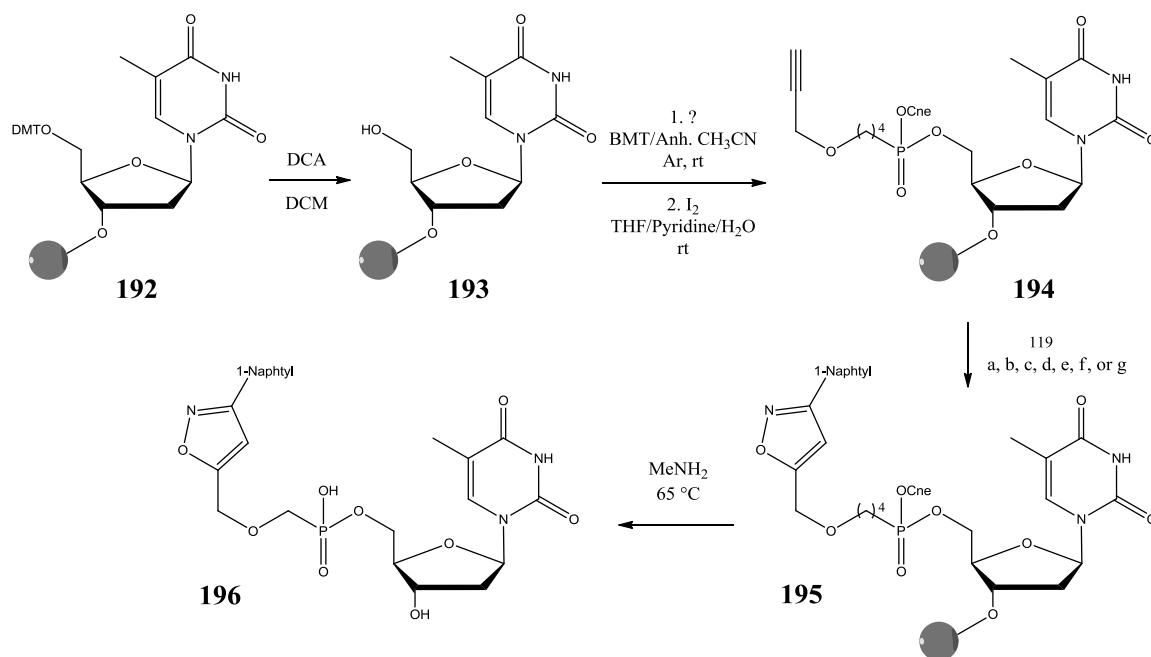
The four steps are repeated until all desired bases have been added. If the reagents and solvents are good quality, each cycle is approximately 98-99% efficient. Upon completion of the required sequence, the support-bound oligonucleotide remains fully protected. The 5'-terminal 5'-hydroxyl group is protected with DMT, the inter-nucleosidic phosphates are protected with Cne and the exocyclic amino groups on the nucleic bases are also protected. Most often, the 5'-DMT group is removed as the final step of the automated synthesis. The oligonucleotides are then released from the solid support by treatment with a base, most commonly MeNH₂, NH₄OH or K₂CO₃.^{159,229} These conditions also remove the Cne and the base protection groups. The crude mixture comprises the desired oligonucleotide, the cleaved protective groups and failed oligonucleotide sequences. Most commonly, the final product is purified and desalted by EtOH precipitation, size exclusion chromatography, or reverse-phase HPLC.

III. CONJUGATION TO DNA

With a long term goal of conjugation to RNA, the hypothesis that nitrile oxide/alkyne click chemistry offers a reliable tool to chemically modify oligonucleotides was initially tested on the chemically more robust DNA.

III.1. Conjugation of “Small” Ligands to [T]-(CPG)

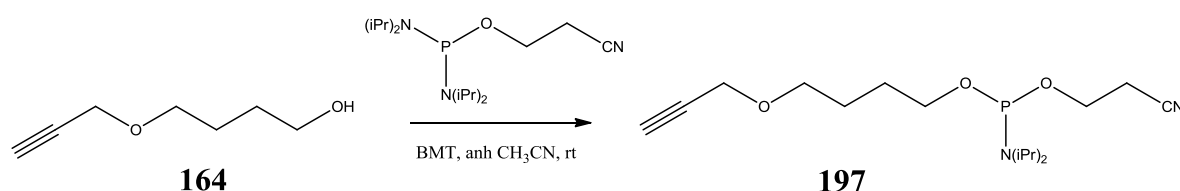
The first resin supported 1,3-dipolar cycloaddition reaction employed the thymidine **194** bearing a 5'-alkyne. The synthesis began with the deprotection of the DMT group at the 5'-position of the commercially available 500 Å CPG-succinyl thymidine **192** using 3% DCA in DCM to give the 5'-OH CPG-loaded thymidine **193** (Scheme 5.6). The phosphoramidite alkyne **197** was prepared according to a procedure developed within the group (Equation 5.1),¹⁰¹ and attached directly to the 5'-position of **193**. After deprotection/cleavage of an analytical portion, reversed-phase HPLC analysis indicated quantitative conversion to the thymidine-alkyne **194**; the retention time of which **194** was ~12 min longer than that of the parent nucleoside 5'-OH (Figure 5.5).



Cycloaddition conditions:

- 100 eq ox, 200 eq CAT, EtOH/NaHCO₃ 4% in H₂O (1:2), 30 min, rt (quantitative);
- 100 eq ox, 200 eq CAT, MeOH/NaHCO₃ 4% in H₂O (1:2), 30 min, rt (quantitative);
- 100 eq ox, 200 eq CAT, EtOH/H₂O (1:2), 30 min, rt (quantitative);
- 100 eq ox, 100 eq CAT, EtOH/NaHCO₃ 4% in H₂O (1:2), 30 min, rt (96%);
- 100 eq ox, 200 eq CAT, EtOH, 30 min, rt (quantitative);
- 100 eq ox, 200 eq CAT, CHCl₃/EtOH (2:1), 30 min, rt (17%);
- 100 eq ox, 200 eq CAT, THF, 30 min, rt (26%).

Scheme 5.6: Synthesis of isoxazole ligated thymidine 196.



Equation 5.1: Synthesis of the phosphitylating agent 197.

The reactivity of the support-bound alkyne **194** in nitrile oxide click cycloaddition chemistry was tested by exposing it to 1-naphthaldehyde oxime **119** (100 eq) and CAT (200 eq) in ethanolic NaHCO₃ (conditions **a**). Following deprotection and cleavage from the resin, quantitative conversion to the isoxazole-nucleotide conjugate **196** was evidenced by reverse-phase HPLC analysis (entry 1, table 5.1, p 125). The retention time of the cycloadduct **196** was ~12 min longer than the precursor alkyne (Figure 5.5).

To optimize the reaction conditions, a range of experiments were conducted. First, the EtOH was replaced by MeOH (conditions **b**). The click reaction was equally successful and isoxazole **196** was prepared in quantitative yield as evidenced from HPLC analysis. The next reaction was conducted with the purpose of evaluating the requirement for the base (conditions **c**). Initially NaHCO₃ was added to neutralize the sulfonamide TsNH₂, by-product from the CAT induced nitrile oxide formation (see chapter 1, section IV.2, p 38). Even in the absence of base, the click reaction progressed in quantitative yield as evident from HPLC analysis. Importantly there was no indication of product decomposition in the absence of base. Reducing the CAT to 100 eq, apparently resulted in a slower reaction and gave the desired compound **196** in 96% (conditions **d**).

Lipid type compounds might not be soluble in aqueous media, thus, it was deemed useful to study the reaction in a range of solvents. Reaction in neat EtOH (conditions **e**) gave **196** in quantitative yield, however, significant lower yields resulted from reactions in organic solvents CHCl₃/EtOH (2:1) 17% (conditions **f**) and THF 26% (conditions **g**). In light of these results, optimal conditions were deemed to involve rt reaction with 100 eq of oxime, 200 eq of CAT, and aqueous EtOH or EtOH as solvent.

Applying these conditions a range of aryl-isoxazole ligated thymidines were prepared. The phenyl and 2-nitrophenyl isoxazoles, **198** and **199** formed from reactions with benzonitrile oxide and 2-nitrobenzonitrile oxide, respectively (entries 2 and 3, table 5.1). Both reactions reached completion after 30 min. Reactions with the anthracene and pyrene analogues required 3 h (entries 4-7). It is likely that the poor solubilities of anthracene-9-carbaldehyde oxime and pyrene-4-carbaldehyde oxime in aqueous EtOH are responsible for the slower reaction. For the same reason, with these two substrates, extensive washing of the support with DMF, was necessary to remove the excess of reactants before the classical washes with CH₃CN and H₂O.

In all cases, the purity of the ligated products was checked by reverse-phase HPLC. As expected, the retention time of the cycloadducts increased progressively with the hydrophobicity of the isoxazole substituents (Ph, 2-NO₂-C₆H₄, 1-Naphtyl, 9-Anth and 4-Pyr) (Figure 5.5).

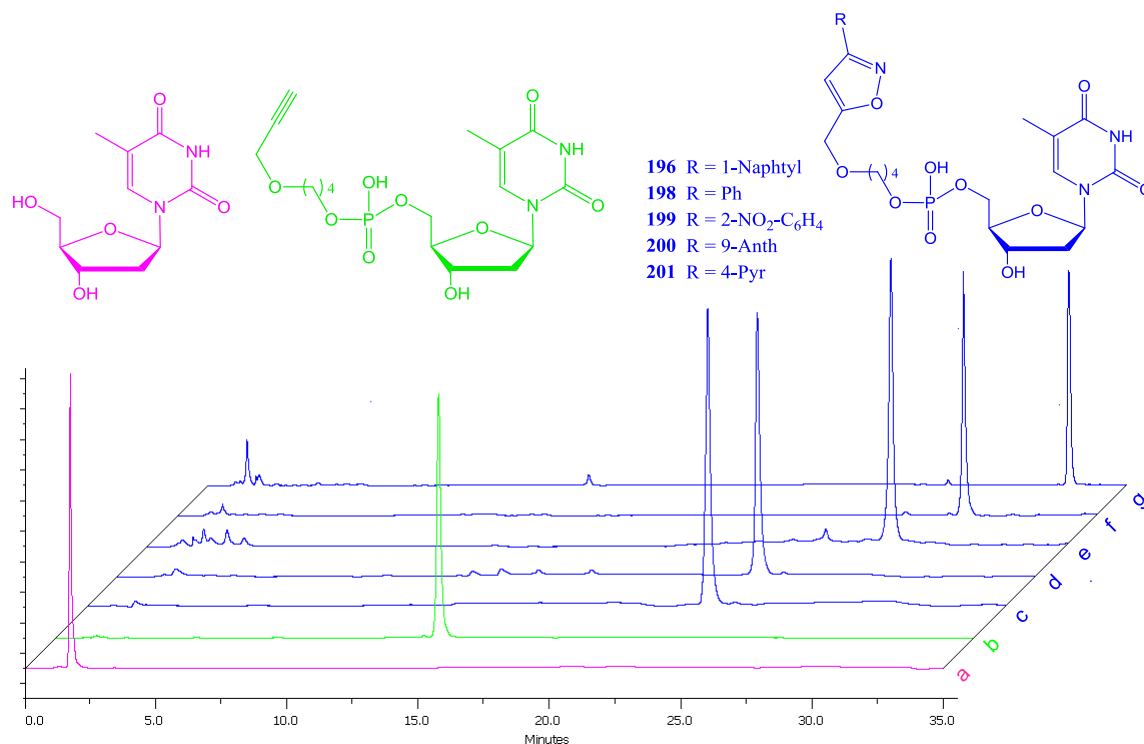


Figure 5.5: HPLC traces of crude products a) Thymidine, b) (5'-alkyl)T, isoxazoles c) (5'-(1-Naphtyl))T, d) (5'-Ph)T, e) (5'-(2-NO₂-C₆H₄)T, f) (5'-(9-Anth))T and g) (5'-(4-Pyr))T.
 (a, b, c, d and e are recorded with C₁₈ column; f and g are recorded with the C₈ column)

III.2. Conjugation of “Small” Ligands to [DNA]-(CPG)

Having successfully achieved conjugation of ligands to the 5'-end of the resin-supported monomer T₁, the next step was the application of the nitrile oxide/alkyne cycloaddition reaction to more complex DNA substrates. The initial goal was the preparation of substrates suitable for modification at the 5'-position of the 5'-terminus of the sequence. These we regarded as the “*grow and click*” strategy. In other words, the desired oligonucleotide sequence was grown before the click reaction was conducted.

In first instance, aromatic oximes were chosen as precursor to “simple” nitrile oxides suitable for the cycloaddition reaction. 1-Naphthaldehyde oxime, benzaldehyde oxime, and 2-nitrobenzaldehyde oxime were selected. CAT was the reactant of choice to generate the dipoles *in situ*. The solvent was aqueous EtOH. In all cases, quantitative reaction was observed after 30 min at rt, with 100 eq of oxime and 200 eq of CAT (relative to the alkyne). After cycloaddition, the oligonucleotides were cleaved/deprotected, and, if necessary, purified to furnish the desired molecules (Scheme 5.7).

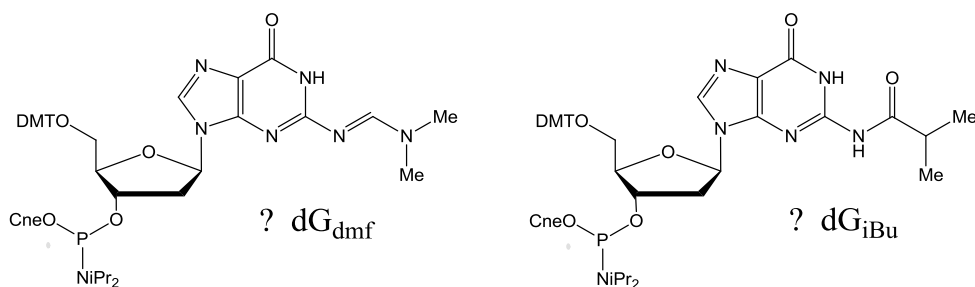


Figure 5.6: Commercially available base protected 5'-O-DMT-2'-deoxyguanosine phosphoramidites.

To determine the compatibility of resin-supported protected dG to alkyne introduction and cycloaddition, parallel reactions to those already discussed for [T]-(CPG) were conducted with both [dG_{iBu}]- (CPG) and [dG_{dmf}]- (CPG). Following preparation of each alkyne and CAT induced cycloaddition, deprotection/cleavage with aqueous MeNH₂ (40%, 60 °C, 30 min) afforded the conjugate (5'-(1-Naphtyl))dG **203** in quantitative yield (entries 8 and 9, table 5.1). The HPLC chromatogram, in each case, showed a single peak as seeing in figure 5.7 for dG_{iBu}. On this basis there was no good reason to choose one protecting group over the other. However, it has been reported that the dmf group can be deprotected under milder conditions than the iBu group, which can make the dmf protected phosphoramidites prone to unintended cleavage during storage in solution.²³⁰ For this reason, building blocks G or dG bearing iBu protecting groups were selected as the reactants of choice for final application to DNAs/RNAs.

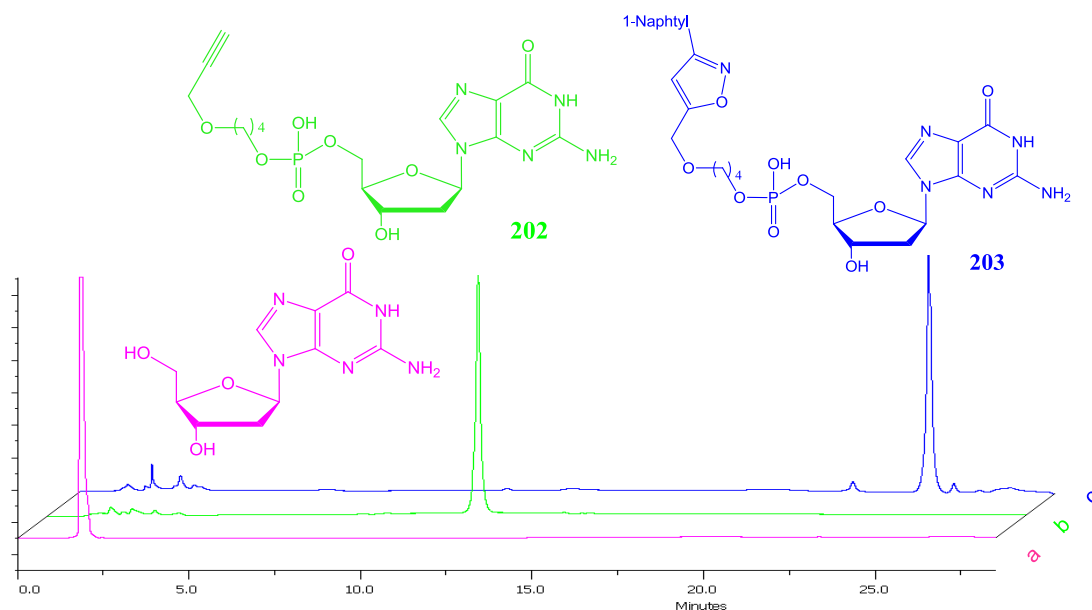


Figure 5.7: HPLC traces of crude a) dG, b) (5'-alk)dG, and c) (5'-(1-Naphtyl))dG.

To facilitate characterization of isoxazole conjugates by MALDI-TOF MS, it was deemed attractive to continue the investigations of the stability of the base protecting group to the conditions of the desired CAT-cycloaddition protocol with trimer substrates TXT (X = dG, dC or dA). Thus, starting with [TdG_{iBu}T]-(CPG) and following introduction of the alkyne as described for T₁, cycloaddition was conducted with the 1-naphtonitrile oxide yielding the product (5'-(1-Naphtyl))TdGT **204** in quantitative yield after 30 min at rt (entry 10).

III.2.b. Deoxycytosine/cytosine

The exocyclic amino groups of deoxycytosine (dC) and cytosine (C) must be protected to prevent side reaction with phosphoramidites during the coupling step of oligonucleotide synthesis. Both C and dC are commercially available with a choice of protecting groups, benzoyl group (Bz) and acetyl group (Ac), as represented for dC in figure 5.8. It is known that the Bz group is susceptible to transamination during cleavage with aqueous MeNH₂, as described in equation 5.2 while the Ac group allows deprotection with a variety of strong organic bases.²²⁹

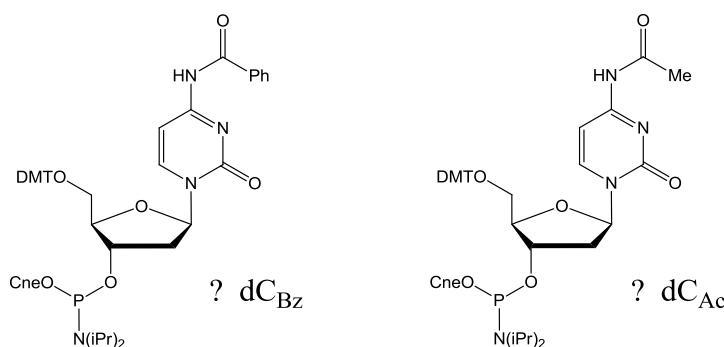
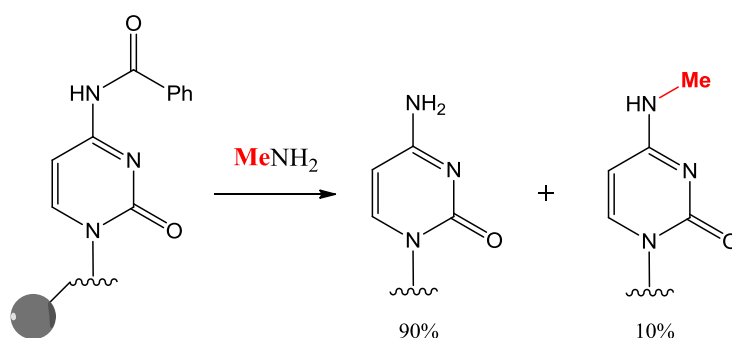


Figure 5.8: Commercially available base, protected 5'-O-DMT-2'-deoxycytosine phosphoramidites.



Equation 5.2: Transamination during oligonucleotide cleavage from the resin with MeNH₂.

In an attempt to gauge the relative stability of the Ac and the Bz protecting groups towards the experiments designed to introduce the alkyne, the cycloaddition and the cleavage/deprotection protocol, experiments were conducted with [TdC_{Bz}T]-(CPG) and [TdC_{Ac}T]-(CPG). After alkyne introduction, the oligonucleotides were cleaved from the resin and deprotected with aqueous MeNH₂ (40%, 60 °C, 30 min). For the substrate protected with Bz, HPLC analysis of the resulting alkyne showed two peaks. The major, present in 89%, was judged to be the hydrolyzed product (5'-alk)TdCT **205**, and the minor the transamination product, (5'-alk)TdC_{Me}T **206** (11%) (Figure 5.9). The structures of the alkynes **205** and **206** are supported by MALDI-TOF MS data ((5'-alk)TdCT **205** *calc* 1025.8, *found* 1026.5; (5'-alk)TdC_{Me}T **206** *calc* 1039.8, *found* 1040.9). With the substrate bearing the Ac protecting group, only the desired alkyne **205** was formed (Figure 5.9).

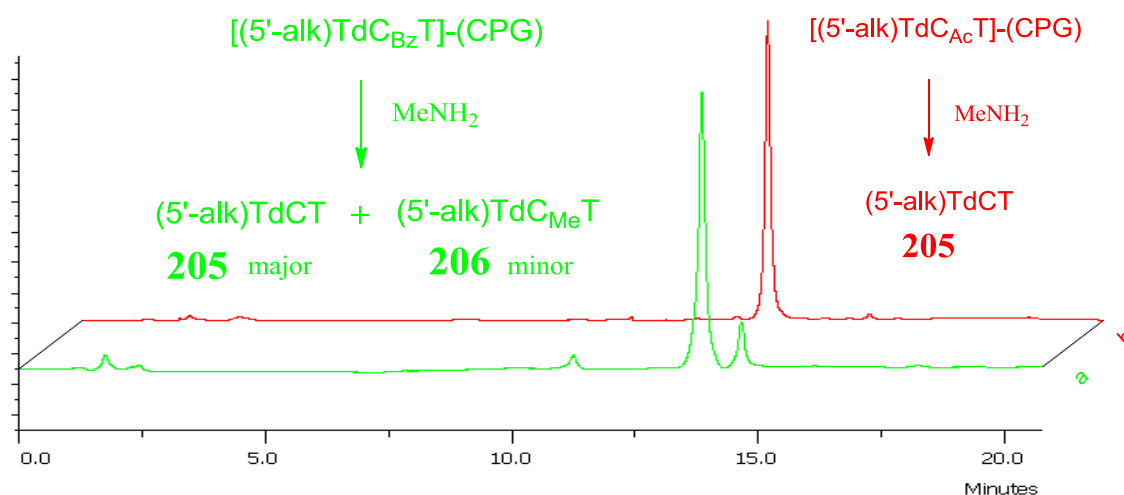


Figure 5.9: HPLC traces of crude reaction products after deprotection of a) [(5'-alk)TdC_{Bz}T]-(CPG) and b) [(5'-alk)TdC_{Ac}T]-(CPG) with MeNH₂

The cycloaddition reaction was subsequently explored between the trimer-alkyne bearing the Ac protecting group and 1-naphthaldehyde oxime **119**. The isoxazole (5'-(1-Naphtyl))TdCT **207** was obtained in quantitative yield (entry 11), after 30 min at rt (Figure 5.10). Accordingly, it was concluded that future experiments should employ the Ac protecting group on cytosine bases. Thus, a range of aryl-isoxazole ligated trimers TCT-aryl-isoxazole were prepared. Formation of the phenyl and 2-nitrophenyl substrates, **208** and **209**, respectively, was achieved after 30 min at rt (entries 12 and 13, table 5.1).

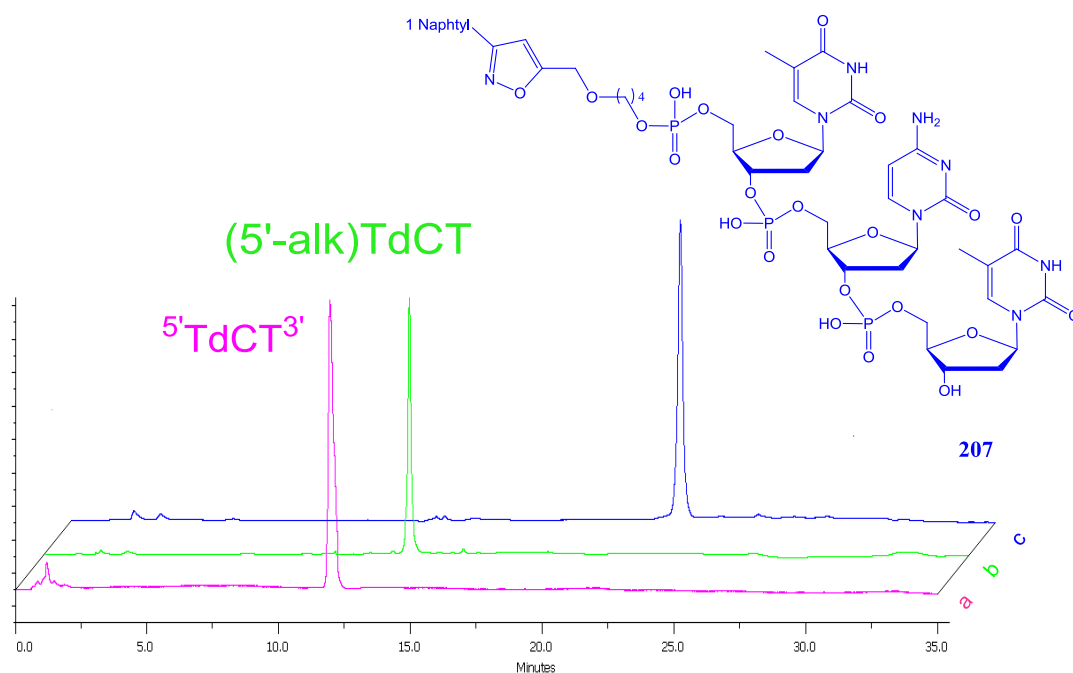


Figure 5.10: HPLC traces of crude reaction product of a) TdCT, b) (5'-alk)TdCT, and c) (5'-(1-Naphtyl))TdCT.

Having established the protecting group of choice for C and dC, it was then necessary to demonstrate the compatibility of the strategy directly on dC. Parallel behavior was observed with the monomer, and the preparation of the (5'-(1-Naphtyl)C conjugate **210** was equally successful (quantitative reaction) (entry 14).

III.2.c. Deoxyadenosine/adenosine

Nucleic bases deoxyadenosine (dA) and adenosine (A) also bear reactive exocyclic amino groups which must be protected during the coupling reaction. The Bz group is the only commonly available protecting group for A and dA. As expected from the result with C, exposure to MeNH₂ resulted in the formation of (5'-alk)TdA_{Me}T together with the desired product (Figure 5.11). To prevent any difficulties with transamination, cleavage/deprotection of substrates, bearing A_{Bz}, were effected by treatment with aqueous NH₄OH (28%, 17 h, rt). With this protocol, deprotection/cleavage of [(5'-(1-Naphtyl))TdA_{Bz}T]-(CPG) resulted in the formation of a single product **213**, eluting at 24.2 min (entry 15, table 5.1). The HPLC traces, shown in figure 5.11, suggest that the NH₄OH cleavage protocol affords clean samples of 5'-alkylated and isoxazole-ligated TAT derivatives. Following parallel experimental conditions, the phenyl analogue **214** was also synthesized in

quantitative yield (entry 16). As discussed for the monomer dC, this approach was proven compatible with the monomer dA and the conjugate (5'-(1-Naphtyl))dA **215** was obtained in quantitative yield as evidenced by reverse-phase HPLC (entry 17) (Figure 5.12).

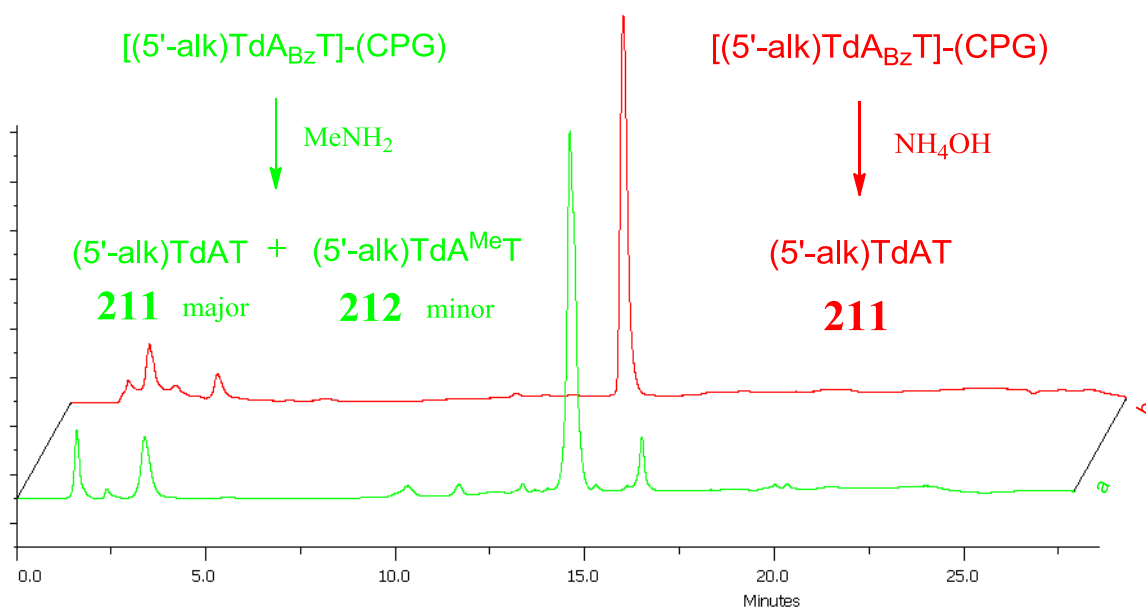


Figure 5.11: HPLC traces of crude reaction product after cleavage/deprotection of $[(5'\text{-alk})\text{TdA}_{\text{BzT}}]\text{-(CPG)}$ with a) MeNH_2 and b) NH_4OH .

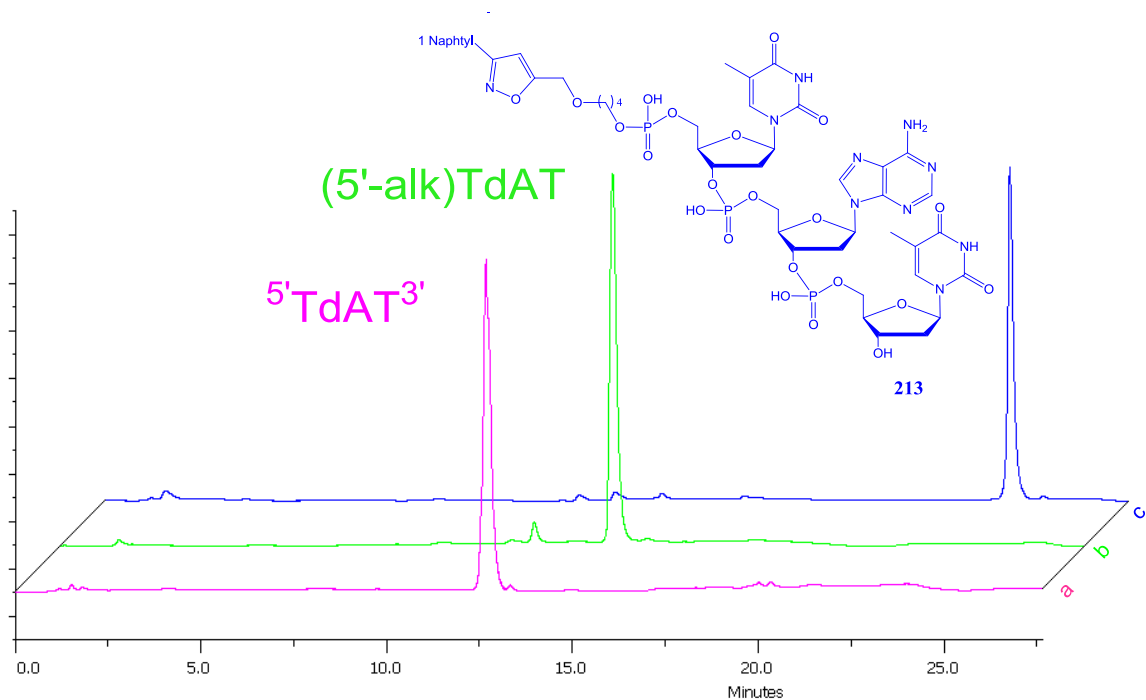


Figure 5.12: HPLC traces of crude a) TdAT , b) $(5'\text{-alk})\text{TdAT}$, and c) $(5'\text{-}(1\text{-Naphtyl isoxazole}))\text{TdAT}$.

III.2.d. Pentamer substrate [TTTTT]-(CPG)

Experiments with CPG-supported pentathymidylate, [TTTTT]-(CPG), confirmed compatibility with longer chain oligonucleotides and the isoxazole-ligated pentamers **217**, **218** and **219** (R = 1-Naphtyl, Ph, 2-NO₂-C₆H₄, entries 18-20, table 5.1) were formed from the precursor alkyne. Quantitative yields for the alkyne coupling and the click conjugation reactions were evident from HPLC analysis as seen in figure 5.13. MALDI-TOF MS data confirmed the structure of the alkyne and the isoxazole-ligated-T₅ products **217-219**.

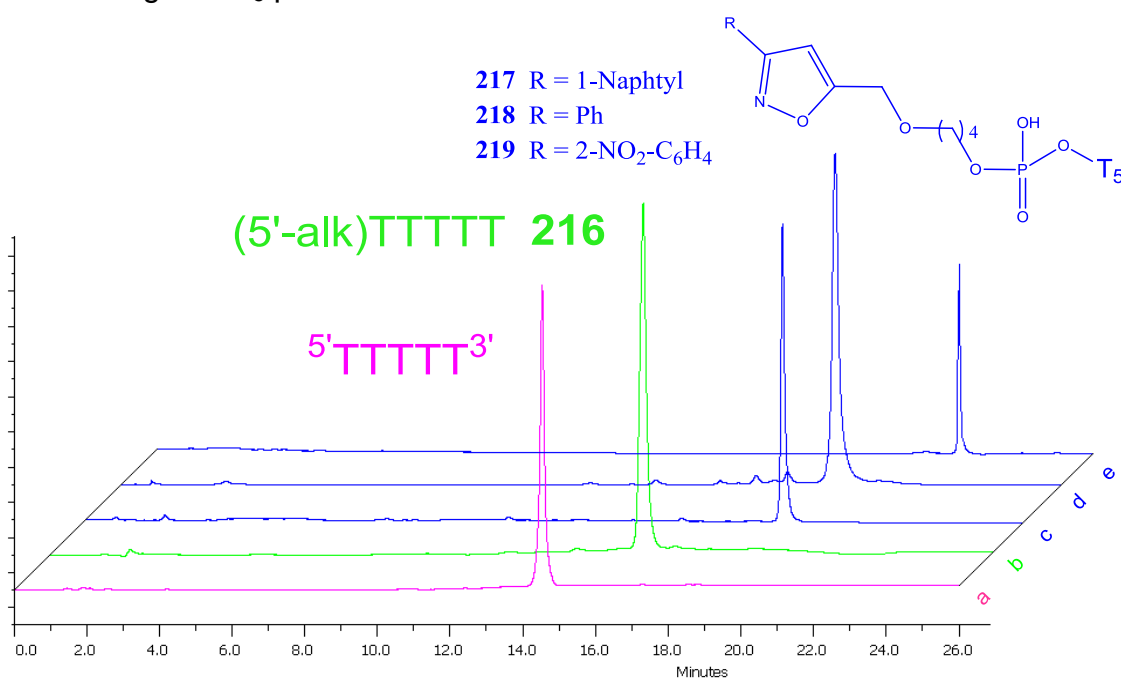


Figure 13: HPLC traces of crude a) T₅, b) (5'-alk)TTTTT, and isoxazole conjugates c) (5'-(1-Naphtyl))TTTTT, c) (5'-Ph)TTTTT e) (5'-(2-NO₂-C₆H₄))TTTTT.

III.2.e. Dodecamer substrate [5'TdCdGdCdAdCdAdCdAdCdGdC3]-(CPG)

Having established that the nitrile oxide/alkyne cycloaddition is compatible with all four nucleobases, the scope of the reaction was further demonstrated with the resin-bound dodecamixer. The alkyne was introduced to the [DNA]-(CPG) in a parallel fashion to that described above and cycloaddition to aryl nitrile oxides proceeded uneventfully, to yield the 5'-isoxazoles **221** and **222** (R = 1-Naphtyl, Ph, entries 21 and 22). HPLC analysis, figure 5.14, and MALDI-TOF MS data confirmed the success of the alkyne attachment and of the click reactions.

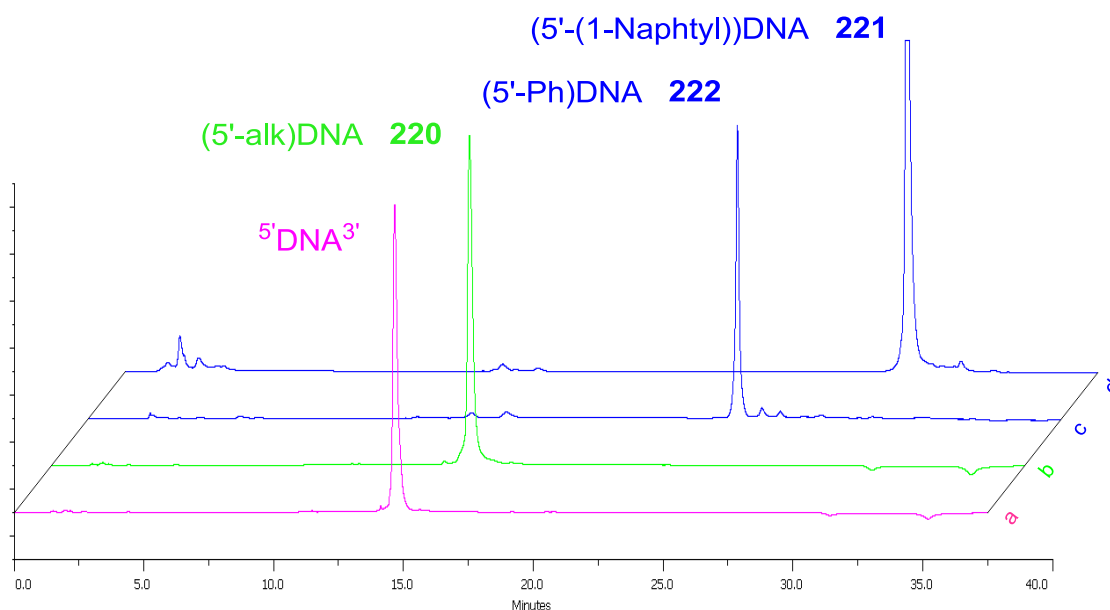


Figure 5.14: HPLC traces of crude reaction products **a) DNA**, **b) (5-alk)DNA**, **isoxazoles c) (5'-(1-Naphtyl))DNA** and **d) (5'-Ph)DNA**; DNA = $5'$ TdCdGdCdAdCdAdCdAdCdGdC $3'$.

III.2.e. Melting temperature studies

To demonstrate the influence, if any, of the isoxazole nucleus on duplex stability a sequence complementary **223** to the click functionalized was prepared. The unmodified oligonucleotide, $5'$ dGdCdGTdGTdGTdGdCdGdA $3'$ **223**, and the isoxazole ligated **221** and **222** (R = 1-Naphtyl, Ph) were hybridized. The thermal consequences of the isoxazole modification were evaluated by UV melting experiments. The duplexes **221/223** (Figure 5.15) and **222/223** show T_m values of 70.0 °C and 72.8 °C, respectively, whilst the reference duplex shows a T_m value of 67.5 °C.¹⁰¹ Thus, it is clear that the phenyl-isoxazole moiety enhances DNA duplex stability.

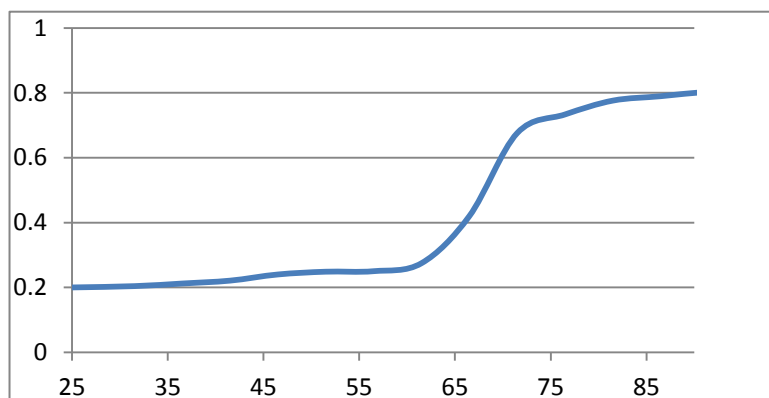


Figure 5.15: Melting curves of duplex **221/223**.

Table 5.1: Overview of the structures of the new aryl isoxazole DNA conjugates.

Entry	Precursor sequences 5'-3'	Product	Product sequences 5'-3'	Reaction time (h)	conversion (%)
1	[(5'-alk)T]-(CPG)	196	(5'-(1-Naphtyl))T	0.5	Quant.
2		198	(5'-Ph)T	0.5	Quant.
3		199	(5'-(2-NO ₂ Ph))T	0.5	Quant.
5		200	(5'-(9-Anth))T	3	Quant.
7		201	(5'-(4-Pyr))T	3	Quant.
8	[(5'-alk)dG _{IBu}]- (CPG)	203	(5'-(1-Naphtyl))dG	0.5	Quant.
9	[(5'-alk)dG _{dmf}]- (CPG)			0.5	Quant.
10	[(5'-alk)TdG _{ibu} T]-(CPG)	204	(5'-(1-Naphtyl))TdGT	0.5	Quant.
12	[(5'-alk)TdC _{Ac} T]-(CPG)	207	(5'-(1-Naphtyl))TdCT	0.5	Quant.
13		208	(5'-Ph)TdCT	0.5	Quant.
14		209	(5'-(2-NO ₂ Ph))TdCT	0.5	Quant.
15	[(5'-alk)dC _{Ac}]- (CPG)	210	(5'-(1-Naphtyl))dC	0.5	Quant.
16	[(5'-alk)TdA _{Bz} T]-(CPG)	213	(5'-1Naphtyl)TdAT	0.5	Quant.
17		214	(5'-Ph)TdAT	0.5	Quant.
18	[(5'-alk)dA _{Bz}]- (CPG)	215	(5'-(1-Naphtyl))dA	0.5	Quant.
19	[(5'-alk)TTTTT]-(CPG)	217	(5'-(1-Naphtyl))TTTTT	0.5	Quant.
20		218	(5'-Ph)TTTTT	0.5	Quant.
21		219	(5'-(2-NO ₂ Ph))TTTTT	0.5	Quant.
22	[(5'-alk)TdCdGdCdAdCdAdCdAdCdGdC]-(CPG)	221	(5'-(1-Naphtyl))TdCdGdCdAdCdAdCdAdCdGdC	0.5	Quant.
23		222	(5'-Ph)TdCdGdCdAdCdAdCdAdCdGdC	0.5	Quant.

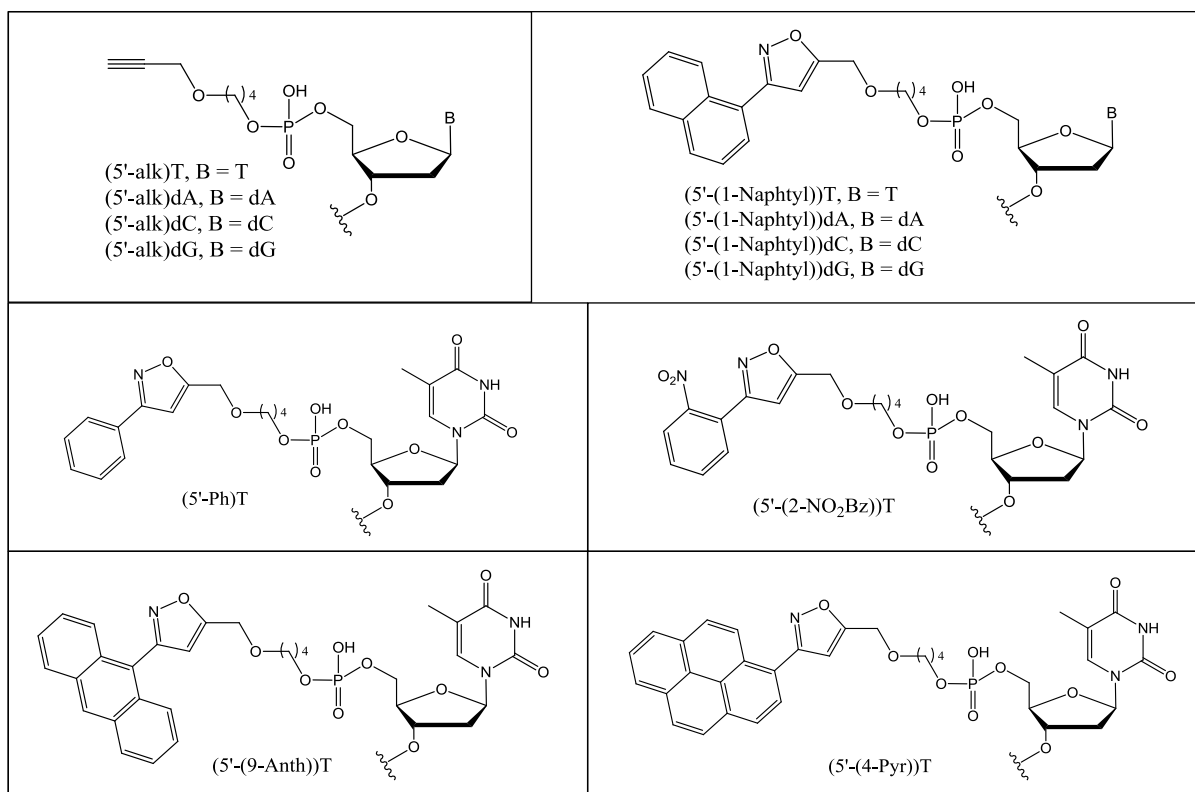


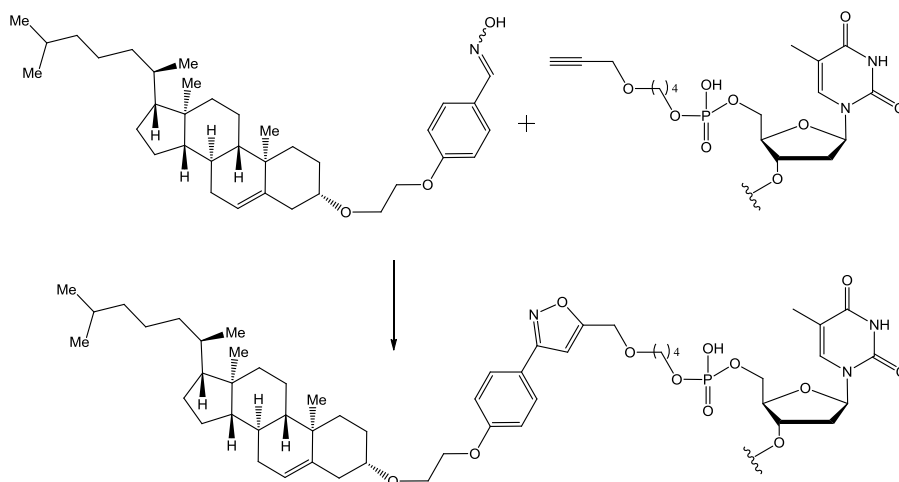
Figure 5.16: Structural representation of the nomenclature used in table 5.1.

III.3. Conjugation to Steroidal Oximes

Conjugation of a lipid to assist the cellular uptake of therapeutic oligonucleotides is currently a hot topic of interest. Cholesterol-modified oligonucleotides have been associated with an increased cellular association and improved transfection efficiency.^{231,232} In addition, their delivery into cells can be achieved by using less toxic particles (e.g. low-density lipoproteins), thus avoiding the use of cationic phospholipids.²³³

Resin-supported cycloaddition of alkyne appended DNA substrates and cholesterol nitrile oxides, was explored beginning with the [(5'-alk)T]-(CPG) and the dipole derived from the oxime **186c**, (Equation 5.3). As previously discovered during this research (chapter 4, section II.4, p 100), cycloaddition with steroidal nitrile oxides proceed best with portion wise addition of the oxime/CAT pair. Accordingly, a suspension of [(5'-alk)T]-(CPG), with 30 eq of oxime **186c** and 60 eq of CAT, was

stirred in EtOH for 6 h, at rt, before addition of a second dose of reactants and stirring for a further 17 h, at rt.



Equation 5.3: Synthesis of resin-support (5'-Chol)T.

Unfortunately, “small” cholesterol adducts were difficult to characterize; compounds with less than 5 bases did not have attractive elution profiles on reverse-phase HPLC. Their high lipophilic character resulted in very broad peaks, in fact, it was impossible to be confident that the cycloaddition reaction had been successful. Following analysis with either a C₁₈ or a C₈ column, all that could be unambiguously concluded was that very little of the starting material remained, as seen for T₁ in figure 5.17. The “small” cholesterol conjugates did not respond to ESI MS and in the case of monomers neither was MALDI-TOF MS useful as the molecular weight of the products were too small to be detected.

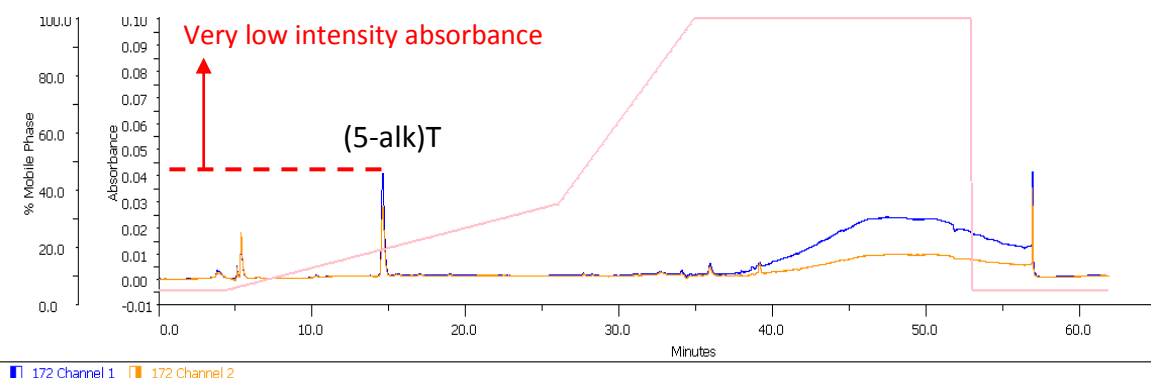


Figure 5.17: HPLC trace of the crude product from reaction designed to generate (5'-Chol)T (C₈ column, channel 1: detection at 254 nm, channel 2: detection at 260 nm).

In spite of the inconclusive outcome designed to conjugate a cholesterol moiety to resin-supported T₁-alkyne, a study with longer oligonucleotide alkynes, viz the pentamer [(5'-alk)TTTTT]-(CPG) and the decamer [(5'-alk)TTTTTTTTTT]-(CPG) was undertaken. Following addition, to a suspension of oligonucleotide alkyne in EtOH, of 30 eq of oxime and 60 eq of CAT (relative to the alkyne) at the beginning of the reaction and a second dose of same magnitude 6 h later, and stirring for 17 h at rt (5'-Chol)TTTTT **226** and (5'-Chol)TTTTTTTTTT **227** (entries 2 and 3, table 5.2) were obtained in 53% and 62% yields, respectively. These same experimental conditions were successfully applied for formation of the isoxazole ligated cholesterol dodecamer **228** (entry 4).

In each case, HPLC analysis suggested successful conjugation. The retention times of the cholesterol appended molecules were significantly longer than the precursor alkynes (Figure 5.18). The conjugates have been purified following a number of rounds of HPLC, and the structure of the 5'-conjugates were confirmed by MALDI-TOF MS.

Table 5.2: Overview of the structures of the isoxazole ligated cholesterol oligonucleotides

Entry	Product	Sequences 5'-3'	Post-click conversion (%)
1	225	(5'-Chol)T	/ *
2	226	(5'-Chol)TTTTT	53
3	227	(5'-Chol)TTTTTTTTTT	62
4	228	(5'-Chol)TdCdGdCdAdCdAdCdAdCdGdC	68

* Almost complete consumption of starting material

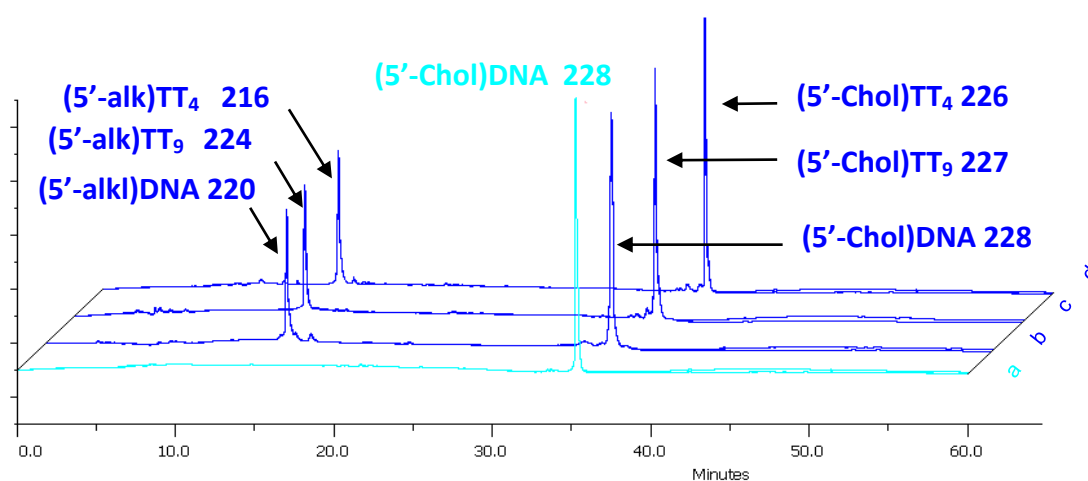


Figure 5.18: HPLC trace of the crude (5'-Chol)TTTTT **226, (5'-Chol)TTTTTTTTTT **227**, (5'-Chol)DNA **228** and purified (5'-Chol)DNA **228**.**

IV. CONJUGATION TO RNA

Having successfully achieved conjugation of ligands to the 5'-end of DNA molecules, the final synthetic goal of this project was modification of the chemically more sensitive RNA substrates in search of synthetic siRNAs.⁷³ Since siRNA is a hybridized product of two complementary strands (sense and antisense), there are four termini potentially attractive as conjugation sites. The choice of which terminus to modify is dictated by the biological mechanism of RNAi. After cellular uptake, the anti-sense strand of siRNA, the strand having a complementary sequence to the target mRNA, is incorporated into the RISC. This characteristic strand bias could be significantly influenced by chemical modification and it has been shown that the integrity of the 5'-terminus of the antisense strand is important for the initiation of an RNAi mechanism.^{234,235} Therefore, either terminus of the sense strand, or the 3'-terminus of the antisense strand are considered the most attractive sites for conjugation. The objective of the current work was to develop a solid phase, catalyst free, click methodology suited to RNA modification(s) at either a terminal or an internal position. In particular, we were interested in resin-supported formation of isoxazole linked 2'-OMe oligoribonucleotide cholesterol conjugates.

IV.1. Conjugation at the 2'-Position of the 3'-Terminus

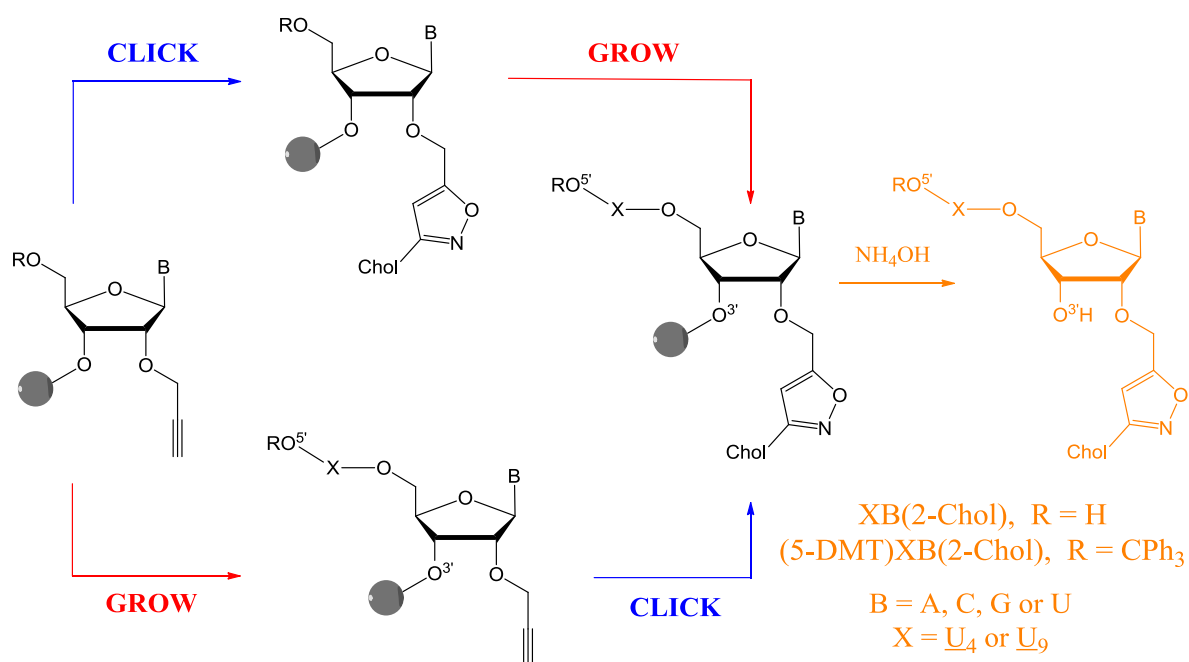
Among the potential sites for oligonucleotide modification, the 2'-position is attractive as substitution at this position locks the pento-furanose sugar in the *C*^{3'}-*endo* conformation which is the structure preferred by the RNAi intracellular machinery.²³⁶ For oligonucleotide modification at the 3'-end, cycloaddition of the nitrile oxide derived from cholesterol oxime **186c** to commercially available CPG-succinyl 2'-O-propargyl nucleosides (with 5'-DMT protection and with standard base protecting groups) was explored.

A range of experimental conditions were investigated to promote the cycloaddition reaction:

- Method **A**: 50 eq of oxime **186c** and 100 eq of CAT, were employed. The reaction was conducted for 17 h at rt.
- Method **B**: 30 eq of oxime **186c** and 60 eq of CAT were added at the beginning of the reaction, and the same dose 6 h later. The reaction was then stirred for another 17 h at rt.
- Method **C**: 30 eq of oxime **186c** and 60 eq of CAT were again employed, this time the reactions were left for 17 h at rt, and the beads were washed free of any by-products before adding a fresh batch of oxime **186c**/CAT, 30 eq and 60 eq, respectively, for a further 17 h reaction at rt.

HPLC analyses of these test case reactions lead to the conclusion that Method **C** was the most attractive for this substrates combination (table 5.3).

Two strategies were considered for the preparation of isoxazole linked cholesterol-oligonucleotide conjugates. These we classified as “**grow** and **click**”, where the cycloaddition reaction was conducted on the solid support post oligonucleotide synthesis, and the “**click** and **grow**” tactic where the cycloaddition was conducted on resin-supported monomer alkyne prior synthesis of the oligonucleotide sequence (Scheme 5.8).



Scheme 5.8: Synthesis of isoxazole linked cholesterol--RNA conjugates by the “**grow** and **click**” and the “**click** and **grow**” approaches.

V.1.a. Uridine derivatives

To demonstrate the “**grow** and **click**” approach, [(5'-DMT)UUUUU(2'-alk)]-(CPG) was prepared and the nitrile oxide/alkyne cycloaddition was attempted with the cholesterol oxime **186c** (Method A, entry 1, table 5.3). Disappointingly, the cycloaddition reaction failed. It is likely that the DMT, which is hydrophobic and bulky, impeded access of the cholesterol derivative to the reaction site. This hypothesis was confirmed when the reaction repeated with the same alkyne minus the DMT group, [UUUUU(2'-alk)]-(CPG), furnished the cholesterol conjugate UUUUU(2'-Chol) **230** albeit in low yield, 17% (entry 2).

The “**click** and **grow**” strategy was also examined. Cycloaddition was initially explored between commercially available 500A^o CPG-succinyl 2'-O-propargyl uridine with 5'-DMT protection, and cholesterol oxime **186c**. As seen previously with T₁ substrates, cholesterol ligated monomers are difficult to characterize, and it was found necessary to grow the oligonucleotide after the attempted cycloaddition to interpret the success, or otherwise, of the reaction. HPLC analyses of the samples obtained following deprotection/cleavage of the click reaction between cholesterol nitrile oxide and [U(2'-alk)]-(CPG) followed by chain extension to UUUUUU(2'-Chol) **230** or to UUUUUUUUUU(2'-Chol) **231**, suggested successful conjugations. The retention times of the cholesterol appended molecules were significantly longer than the control alkyne. The pentamer **230** was prepared in 56% and 40% yields by method A (entry 3) and B (entry 4), respectively. A significant improvement in yield was observed when the reaction was repeated with 500A^o CPG-succinyl 2'-O-propargyl uridine having the 5'-OH group deprotected. Under these circumstances the free 5'-OH conjugate **230** was obtained in up to 89% yield (Method A: 77%, entry 5; Method B: 73%, entry 6; Method C: 89%, entry 7). Parallel reactions confirmed compatibility with longer chain oligonucleotides and the cholesterol-isoxazole decamer, UUUUUUUUUU(2'-Chol) **231** was obtained in 91% yield (Method C, entry 8). In each case, the HPLC traces of the crude reaction products show only two peaks; one representative of unreacted alkyne, and one for the isoxazole conjugate.

To extend the versatility of the reaction, the decamer **231** was prepared after elongation of the shorter, pentamer, oligonucleotide UUUUU(2'-Chol) **230** (entry 9),

which validated the hypothesis that the synthesis of the modified oligonucleotide can be stopped and carried on at any time. The 2'-cholesterol conjugates were purified following a number of rounds of HPLC. Their structures were confirmed by MALDI-TOF MS. The compatibility of the nitrile oxide/alkyne click reaction with the other RNA nucleobases, G, C and A, was next investigated.

V.1.b. Guanosine derivatives

To directly compare the results achieved with the “**click** and **grow**” approach on the uridine derivatives, cycloaddition between the steroidal oxime **186c** and commercially available 500 Å CPG-succinyl 2'-O-propargyl guanosine, with 5'-DMT protection, was examined. After deprotection/cleavage from the resin, the pentamer UUUUG(2'-Chol) **232** was found in 40-50% yield (Method A, Method B, entries 10 and 11). The decamer UUUUUUUUG(2'-Chol) **233** accessed by a parallel route, was prepared in 62% yield (Method A, entry 12). As expected, reactions with substrates free of the DMT group, gave the final products **232** and **233** in significantly enhanced yields; quantitative conversion to the conjugates was observed by method C (entries 13 and 14). The cholesterol appended decamer **233** was also prepared by elongation of the shorter conjugate **232** (entry 15). HPLC analysis suggested successful conjugation and crude reaction products show only peaks attributed to the isoxazole linked cholesterol-oligonucleotides (plus any remaining oligonucleotide alkyne when the reaction did not reach completion). The compound structures were supported by MALDI-TOF MS.

V.1.c. Cytosine derivatives

The “**grow** and **click**” approach was examined with the pentamer alkyne (DMT off), UUUUC(2'-alk). As expected from the result with the U analogues, the desired product, UUUUC(2'-Chol) **234**, was obtained in very low yield, 9% (entry 16).

In the “**click** and **grow**” strategy, one experiment was conducted with [(5'-DMT)C(2'-alk)]-(CPG), the product UUUUUUUUC(2'-Chol) **235** was synthesized in 65% (Method A, entry 17). In another experiment with “DMT off”, the pentamer UUUUC(2'-Chol) **234** was prepared in excellent yields as evidenced by HPLC data (Method A: 81%; Method C: quantitative, entries 18-19). The elongation of the

pentamer **234** afforded the longer oligonucleotide UUUUUUUUUC(2'-Chol) **235** (entry 20).

V.1.d. Adenosine derivatives

Parallel behavior was observed with adenosine analogues. Products UUUUA(2'-Chol) **236** (entry 21) and UUUUUUUUUA(2'-Chol) **237** (entry 22) were synthesized in quantitative yields by method C. The elongation from **236** to **237** was also successful (entry 23) as evidenced by HPLC.

As representative examples the reverse-phase HPLC traces of the crude reaction products UUUUA(2'-Chol) **236** and UUUUUUUUUA(2'-Chol) **237** are shown, in figure 5.19. Their structures are supported by MALDI-TOF MS.

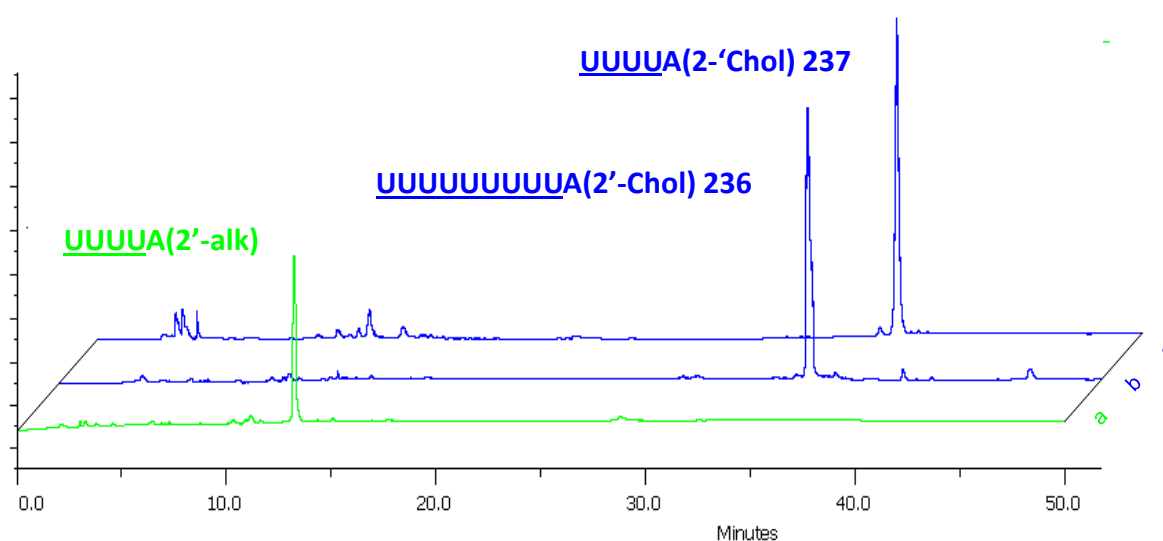
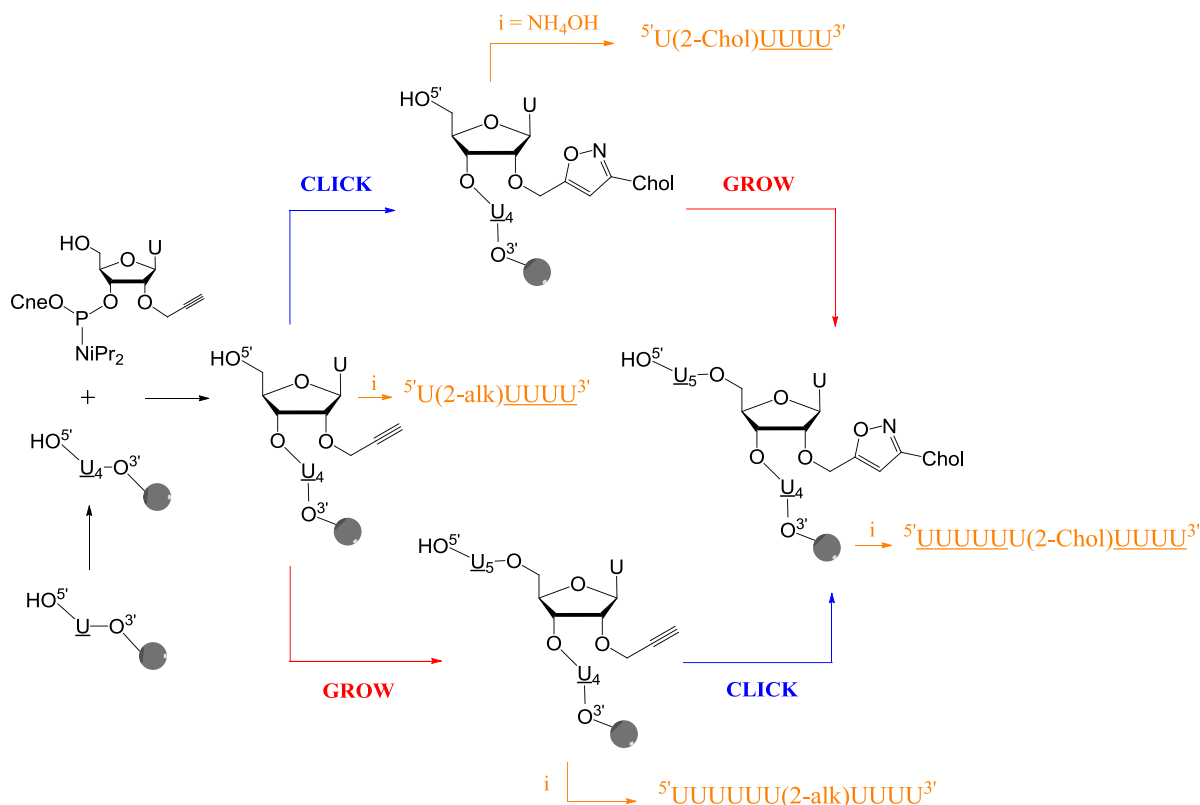


Figure 5.19: HPLC traces of crude a) UUUUA(2'-alk), isoxazoles UUUUA(2'-Chol) **236** and UUUUUUUUUA(2'-Chol) **237**.

IV.2. Conjugation at the 2'-Position at the 5'-Terminus or at an Internal Position

To prepare substrates suited to modification at the 5'-terminus or at an internal position, the commercially available 2'-O-propargyl uridine phosphoramidite was employed. As depicted in the scheme 5.9, the preparation of 5'- or internal conjugates begins with the synthesis of the oligonucleotide, U₄, to which the alkyne-phosphoramidite was coupled to afford [U(2'-alk)UUUUU]-(CPG). Firstly, cycloaddition was conducted directly at the 5'-end to give the 5'-conjugate U(2'-Chol)UUUUU **238** in quantitative yield (Method C, entry 24).

The decamer UUUUUU(2'-Chol)UUUU **239** with an internal cholesterol modification was successfully prepared by two different strategies. Following the “**click** and **grow**” approach, the cholesterol ligated pentamer **238** was elongated to the decamer (entry 25). With the “**grow** and **click**” tactic, the cycloaddition was achieved post synthesis of [UUUUUU(2'-alk)UUUU]-(CPG) (Method A: 44%, entry 26). A comparison of the yields of **239** obtained by each method, shows “**click** and **grow**” approach to be more efficient than the “**grow** and **click**” alternative.

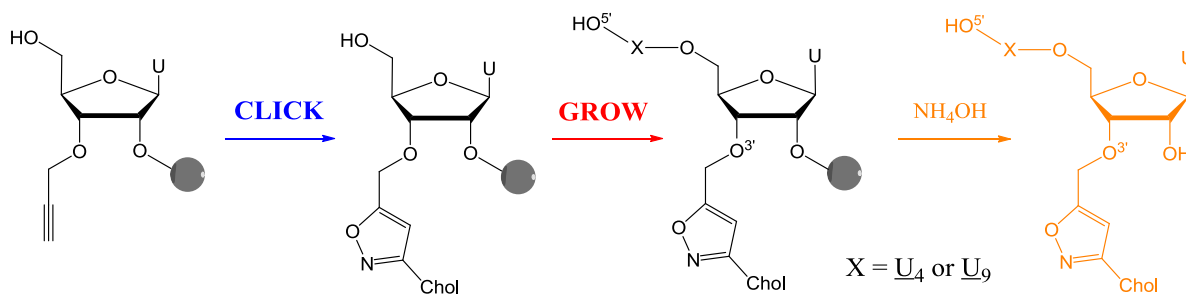


Scheme 5.9: Synthesis of cholesterol-RNA conjugates where the cholesterol, borne on the 2'-position of a ribose unit, is introduced at the 5-terminus or at an internal position

IV.3. Conjugation at the 3'-Position of the 3'-Terminus

500A° CPG-succinyl 3'-O-propargyl uridine is also commercially available, thus it was deemed interesting to explore ligation at the 3'-position of a ribose moiety at the 3'-terminus of an oligonucleotide (Scheme 5.10). Gratifyingly, following

experimentation parallel with that conducted with the 2'-analogues, conjugates UUUUU(3'-Chol) **240** and UUUUUUUUUUU(3'-Chol) **241** (entries 27 and 28) were prepared in quantitative yields by method C.



Scheme 5.10: Synthesis of 3'-cholesterol-RNA conjugates at the 3'-end.

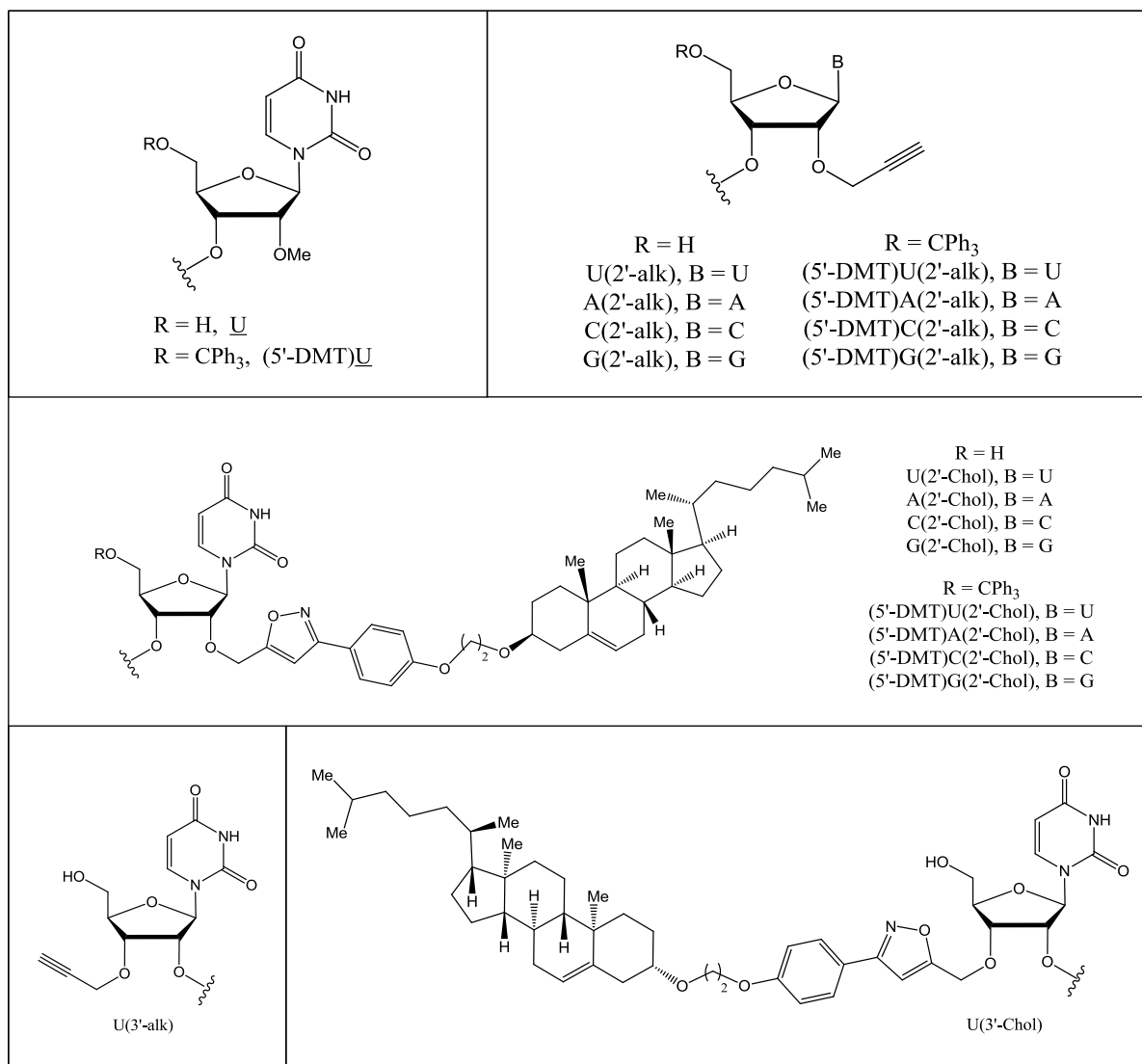


Figure 5.20: Structural representation of the nomenclature used in table 5.3.

Table 5.3: Overview of isoxazole linked cholesterol RNA conjugates synthesized.

Entry	Precursor sequences 5'-3'	Precursor or intermediary sequences 5'-3'	Product	Sequences 5'-3'	Click method	Click conversion (%)
1	[U(2'-alk)]-(CPG)	(5'-DMT)UUUUU(2'-alk)	229	(5'-DMT)UUUUU(2'-Chol)	A	0
2	[U(2'-alk)]-(CPG)	UUUUU(2'-alk)	230	UUUUU(2'-Chol)	A	17
3	[(5'-DMT)U(2'-alk)]-(CPG)	[(5'-DMT)U(2'-Chol)]-(CPG)	230	UUUUU(2'-Chol)	A	56
4	[(5'-DMT)U(2'-alk)]-(CPG)	[(5'-DMT)U(2'-Chol)]-(CPG)	230	UUUUU(2'-Chol)	B	40
5	[U(2'-alk)]-(CPG)	[U(2'-Chol)]-(CPG)	230	UUUUU(2'-Chol)	A	77
6	[U(2'-alk)]-(CPG)	[U(2'-Chol)]-(CPG)	230	UUUUU(2'-Chol)	B	73
7	[U(2'-alk)]-(CPG)	[U(2'-Chol)]-(CPG)	230	UUUUU(2'-Chol)	C	89
8	[U(2'-alk)]-(CPG)	[U(2'-Chol)]-(CPG)	231	UUUUUUUUUU(2'-Chol)	C	91
9		[UUUUU(2'-Chol)]-(CPG)	231	UUUUUUUUUU(2'-Chol)	/	/
10	[(5'-DMT)G(2'-alk)]-(CPG)	[(5'-DMT)G(2'-Chol)]-(CPG)	232	UUUUU(2'-Chol)	A	50
11	[(5'-DMT)G(2'-alk)]-(CPG)	[(5'-DMT)G(2'-Chol)]-(CPG)	232	UUUUU(2'-Chol)	B	41
12	[(5'-DMT)G(2'-alk)]-(CPG)	[(5'-DMT)G(2'-Chol)]-(CPG)	233	UUUUUUUUUU(2'-Chol)	A	62
13	[G(2'-alk)]-(CPG)	[G(2'-Chol)]-(CPG)	232	UUUUU(2'-Chol)	C	Quant.
14	[G(2'-alk)]-(CPG)	[G(2'-Chol)]-(CPG)	233	UUUUUUUUUU(2'-Chol)	C	Quant.
15		[UUUUU(2'-Chol)]-(CPG)	233	UUUUUUUUUU(2'-Chol)	/	/

Table 5.3: Continued.

16	[C(2'-alk)]-(CPG)	[UUUUC(2'-alk)]-(CPG)	234	<u>UUUUC(2'-Chol)</u>	A	9
17	[(5'-DMT)C(2'-alk)]-(CPG)	[(5'-DMT)C(2'-Chol)]-(CPG)	235	<u>UUUUUUUUUC(2'-Chol)</u>	A	65
18	[C(2'-alk)]-(CPG)	[C(2'-Chol)]-(CPG)	234	<u>UUUUC(2'-Chol)</u>	A	81
19	[C(2'-alk)]-(CPG)	[C(2'-Chol)]-(CPG)	234	<u>UUUUC(2'-Chol)</u>	C	Quant.
20		[UUUUC(2'-Chol)]-(CPG)	235	<u>UUUUUUUUUC(2'-Chol)</u>	/	/
21	[A(2'-alk)]-(CPG)	[A(2'-Chol)]-(CPG)	236	<u>UUUUA(2'-Chol)</u>	C	Quant.
22	[A(2'-alk)]-(CPG)	[A(2'-Chol)]-(CPG)	237	<u>UUUUUUUUUA(2'-Chol)</u>	C	Quant.
23		[UUUUA(2'-Chol)]-(CPG)	237	<u>UUUUUUUUUA(2'-Chol)</u>	/	/
24	[U]- (CPG)	<u>U(2'-alk)UUUU</u>	238	<u>U(2'-Chol)UUUU</u>	C	Quant.
25		[<u>U(2'-Chol)UUUU</u>]- (CPG)	239	<u>UUUUUU(2'-Chol)UUUU</u>	/	/
26	[<u>U(2'-alk)UUUU</u>]- (CPG)	<u>UUUUUU(2'-alk)UUUU</u>	239	<u>UUUUUU(2'-Chol)UUUU</u>	A	44
27	[U(3'-alk)]-(CPG)	[U(3'-Chol)]-(CPG)	240	<u>UUUUU(3'-Chol)</u>	C	Quant.
28	[U(3'-alk)]-(CPG)	[U(3'-Chol)]-(CPG)	241	<u>UUUUUUUUUU(3'-Chol)</u>	C	Quant.

Method A (50 eq of oxime **186c** and 100 eq of CAT relative to the alkyne, 17 h, at rt);

Method B (addition of 30 eq of oxime **186c** and 60 eq of CAT, after 6 h at rt, addition of the same dose following by stirring for another 17 h, at rt);

Method C (addition of 30 eq of oxime **186c** and 60 eq of CAT, after 17 h at rt, wash of the beads, and addition of the same dose following by stirring for another 17 h, at rt).

V. ASSAYS FOR RNA INTERFERENCE EVALUATION

Having established the suitability of the nitrile oxide/alkyne cycloaddition for generation of modified RNAs, the final objective was to evaluate the biological consequences of the chemical modifications introduced.

V.1. siRNA Transfection into Cho-K1 cells for eGFP gene knockdown.

The first series of experiments were designed to determine the effect, if any, of the introduction, at the 3'-end, of an aryl isoxazole on gene silencing by an siRNA designed to target the eGFP gene in CHO-K1 cells. We hypothesized this addition to the oligonucleotide may have no effect, or may help the process by enhancing the duplex stability by π stacking, with attractive, noncovalent interactions between aromatic rings.

An siRNA designed to target the eGFP gene in CHO-K1 cells was prepared and tested within the group of Dr. Sean Doyle (NUIM). The sequence of the 19 nt long sense strand was ^{5'}CAGCCACAACGUCUAUAUC^{3'} **242**; all sugars bore 2'-OMe blocking groups. The anti-sense sequence was ^{5'}GAUUAUAGACGUUGUGGCUG^{3'} **243**, it too was 19 nt long and also employed 2'-OMe building blocks.^{67,237} The design having no overhangs at the 3'-termini, is known as a "blunt". The chemically modified sequences considered for study introduced an isoxazole ligated phenyl ring at the 2'-position of the ribo-sugar at the 3'-terminus of either the sense strand (**244**), or the anti-sense strand (**245**). The duplexes envisaged were:



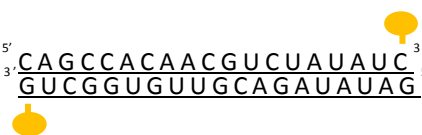
- **siRNA 1**: both strands unmodified synthetic control (entry 1, table 5.4);
- **siRNA 2**: bearing an isoxazole ligated phenyl moiety at the 2'-position of the ribo-sugar at the **3'-terminus** of the **sense strand** (entry 2);

- **siRNA 3:** bearing an isoxazole ligated phenyl moiety at the 2'-position of the ribo-sugar at the **3'-terminus** of the **anti-sense strand** (entry 3);
- **siRNA 4:** bearing an isoxazole ligated phenyl moiety at the 2'-position the ribo-sugar at the **3'-terminus** of **both**, the **sense** and the **anti-sense, strands** (entry4);

RNAs were transfected into cells using Lipofectamine™ 2000. The oligonucleotides synthesized are summarized in table 5.4; their characterizations were based on reverse-phase HPLC, micro-volume UV-vis and MALDI-TOF MS.

Table 5.4: Overview of the siRNAs studied in the CHO-K1 cells.

Orange color: site of introduction of aryl isoxazole

Entry n°	Duplex		
	Name	Strands	Structure: sense 5'-----3' 3'-----5' anti-sense
1	siRNA 1	242/243	$\begin{array}{c} 5' \text{ CAGCCACAACGUCUAUAUC } 3' \\ 3' \text{ GUCGGUGUUGCAGAUUAUAG } 5' \end{array}$
2	siRNA 2	244/243	$\begin{array}{c} 5' \text{ CAGCCACAACGUCUAUAUC } 3' \\ 3' \text{ GUCGGUGUUGCAGAUUAUAG } 5' \end{array}$ 
3	siRNA 3	242/245	$\begin{array}{c} 5' \text{ CAGCCACAACGUCUAUAUC } 3' \\ 3' \text{ GUCGGUGUUGCAGAUUAUAG } 5' \end{array}$ 
4	siRNA 4	244/245	$\begin{array}{c} 5' \text{ CAGCCACAACGUCUAUAUC } 3' \\ 3' \text{ GUCGGUGUUGCAGAUUAUAG } 5' \end{array}$ 

The first experiment examined **siRNA 1** at variety of concentrations (0 picoM, 50 picoM, 100 picoM, 200 picoM, 300 picoM, and 400 picoM) to establish the optimal concentration needed for satisfactory knockdown (Figure 5.21). Mean fluorescence intensity was measured on Fluorescence Plate Reader at the following setting: excitation 485 nm, emission 530 nm. A buffer only control was used as a blank

(HEPES buffer) and its reading was subtracted from each mean reading prior to plotting the graph. At 400 picoM, control **siRNA 1** effected 85% eGFP knockdown. Subsequent experiments used this concentration to compare the activities of the isoxazole conjugates with that of the “control”. Having established the efficacy of the sequence of the “synthetic control”, **siRNA 1**, the mean fluorescence intensity, indicating the extent of the gene knockdown for each modified siRNA sample (1-4) was established following the method described above. The results are summarized in figure 5.22.

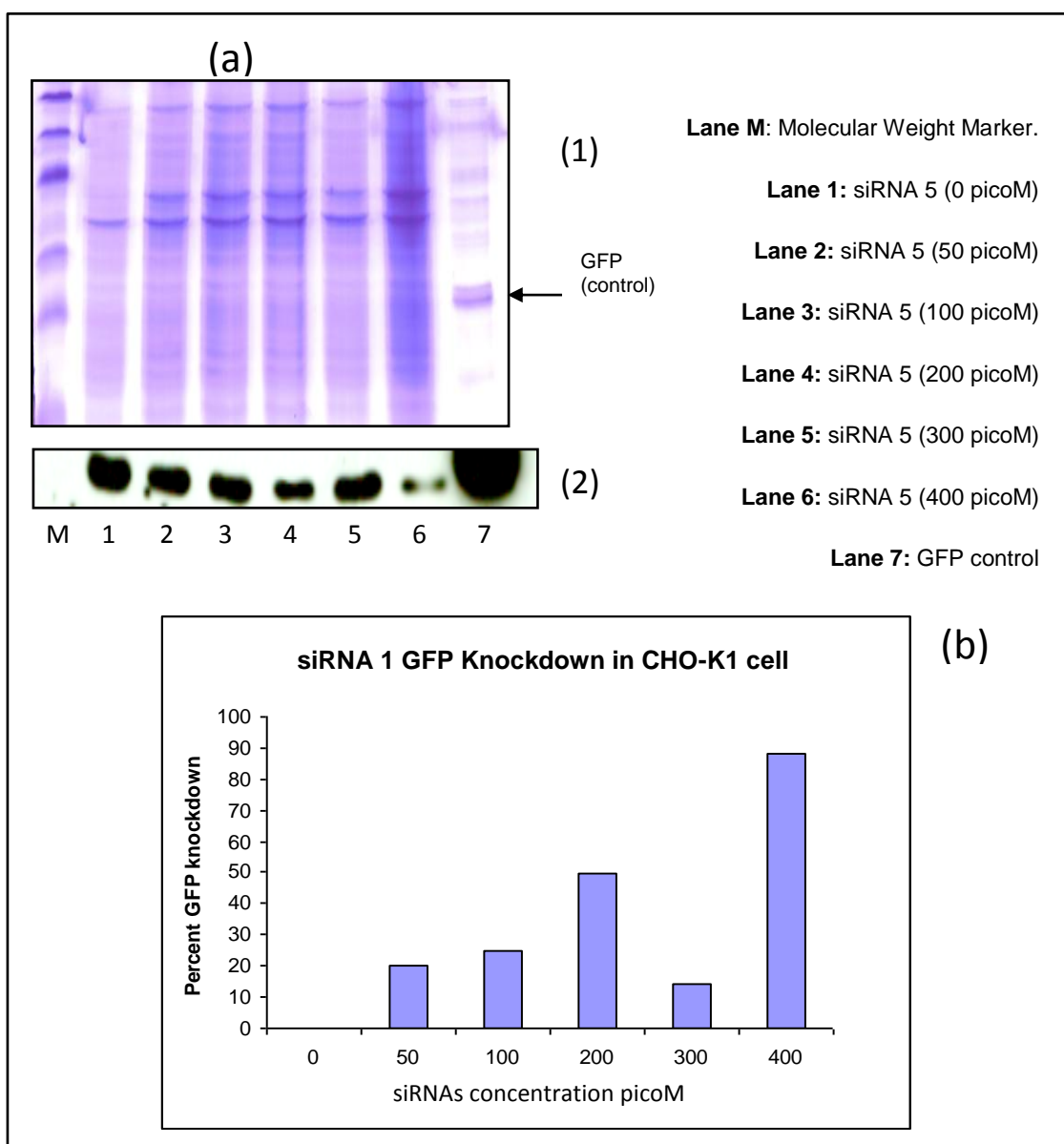


Figure 5.21: (a) SDS PAGE (1) and Western blot Analysis (2), representation of the GFP knockdown for different concentrations (b).

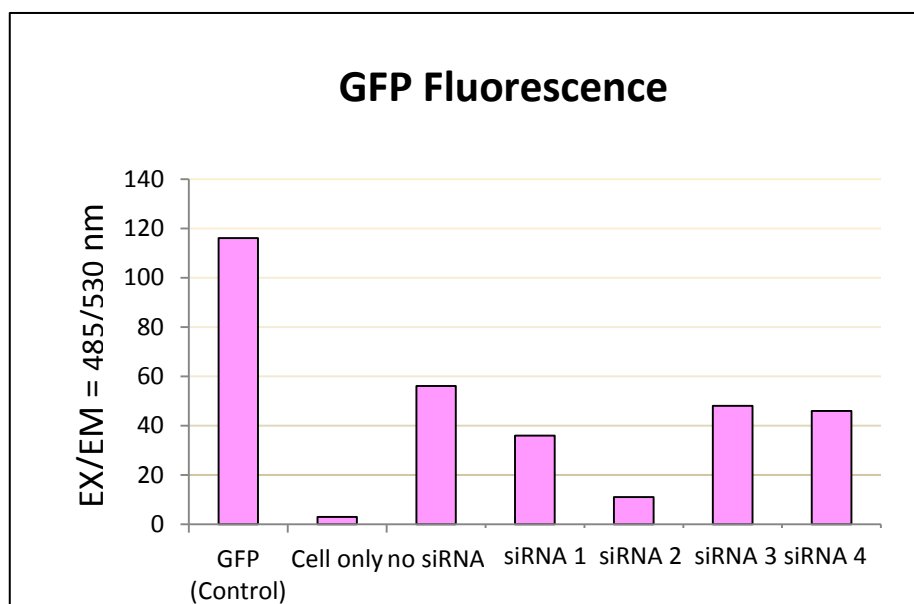


Figure 5.22: Mean fluorescence intensity indicating the extent of the gene knockdown (excitation at 485 nm and emission at 530 nm).

Without siRNA, the mean fluorescence intensity indicating the extent of the gene knockdown was 55. After introduction of **siRNA 1, 2, 3 and 4**, experiments gave respectively an intensity of 36, 11, 48 and 46.

From these results, the extent of knockdown of GFP for each sample is represented in figure 5.23. Approximately 30% knockdown of the GFP gene expression in CHO-K1 cells was achieved by transfecting 400 picoM of **siRNA 1** (control unmodified) and 80% was achieved by transfecting the same concentration of **siRNA 2** (sense 3'-modified). Transfection of **siRNA 3** (anti-sense 3'-modified) and **siRNA 4** (sense and anti-sense 3'-modified) had little effect on gene expression, 15% and 18% knockdown were observed, respectively.

These preliminary findings suggest introduction of an aryl isoxazole at the 3'-terminus of the sense strand, if an siRNA construct may enhance its silencing activity, however, whilst it is appreciated that all results in this experiment need to be duplicated for validation they were considered to be sufficiently positive to encourage future experiments with more complex siRNAs bearing a biological active group.

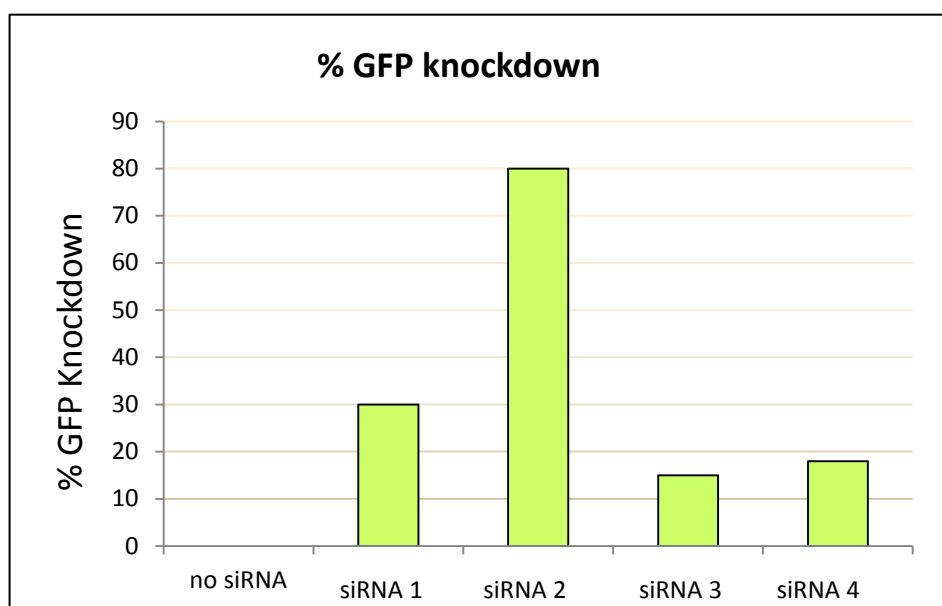


Figure 5.23: siRNA Knockdown of GFP in CHO-K1 cells.

V.1. Luciferase reporter assay

A second analysis of the silencing activity of isoxazole modified siRNA constructs was conducted within the group of Dr. Paul Moynagh (NUIM). A dual-luciferase assay was used to evaluate gene silencing by siRNAs formed from oligonucleotide strands bearing isoxazole linked cholesterol moieties, introduced by the nitrile oxide/alkyne cycloaddition chemistry discussed in the preceding section. The siRNA sequences were designed to target the Renilla and firefly luciferase gene (interleukin 17 receptor D) in HEK293 cells using a pRL-TK reporter vector. siRNAs were transfected into cells using Lipofectamine2000. The objective of the experiment was to compare the activities in the knock-out process of the siRNAs constructed from the cholesterol-RNAs conjugates, prepared in this research, with the commercial siRNA already well-studied by Dr. Moynagh's group.

V.1.a. Preparation and characterization of the siRNA samples

The siRNA sequence studied by Moynagh laboratory is 19 bp long with a 2 nt, TT, 3'-overhang on the sense strand. The chemically modified sequences designed for study introduced an additional U, at the 3'-terminus giving 3 nt, TTU, 3'-overhang sense strand. The first strand **246**, the synthetic control, had an unmodified U. The

second and third strands had an isoxazole linked cholesterol modification at the 2'- or 3'-position of the ribo-sugar, **247** and **248**, respectively:

- $5' \underline{\text{GGAGCAAACUACAGAGAUGTTU}} 3'$ **246** (control);
- $5' \underline{\text{GGAGCAAACUACAGAGAUGTTU}}(2'\text{-Chol}) 3'$ **247**;
- $5' \underline{\text{GGAGCAAACUACAGAGAUGTTU}}(3'\text{-Chol}) 3'$ **248**.

The fourth sequence was designed bearing an extra U(2'-Chol) at the 5'-end to give the sense strand $5' \text{U}(2'\text{-Chol}) \underline{\text{GGAGCAAACUACAGAGAUGTT}} 3'$ **249**.⁹¹

The complementary strand was designed with no additional base to hybridize to the additional U. In keeping with the design of Moynagh's commercial construction, a 2 nt, dGT, 3'-overhang $5' \underline{\text{CAUCUCUGUAGUUUGCUCCT}} \text{dG} 3'$ **250** was synthesized as the anti-sense strand.

All bases of RNAs prepared carried 2'-OMe blocks on the ribo-sugar, even though the commercial control siRNA has all the 2'-OH free. Synthetic RNAs for siRNA studies commonly select 2'-OMe blocks as these units are chemically robust and appeared not to negatively impact their biological activity.⁹¹ The synthetic RNAs were purified following a number of rounds of HPLC. Their characterizations were based on reverse-phase HPLC data (Figure 5.24), micro-volume UV-vis data (Figure 5.26 and 5.27) and MALDI-TOF MS data.

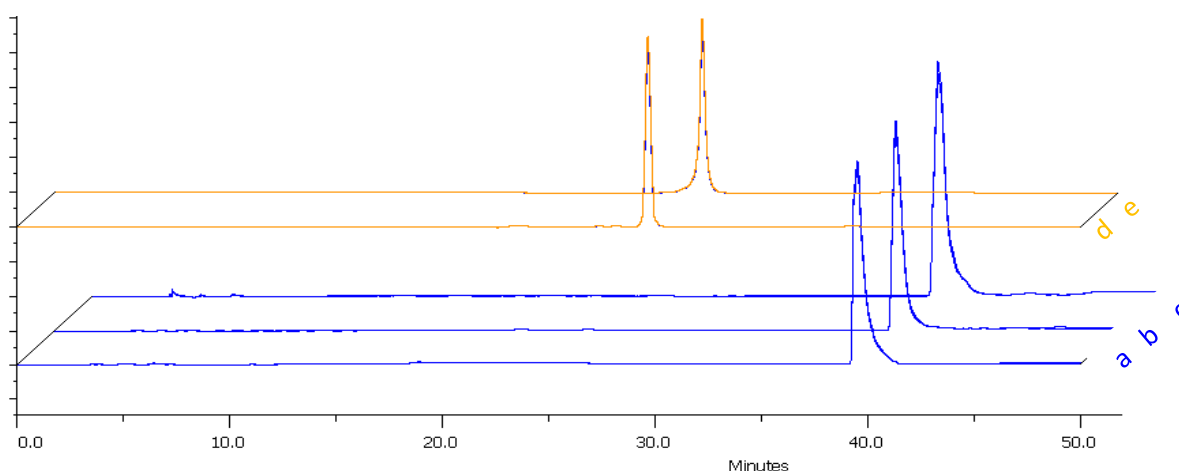


Figure 5.24: HPLC traces of purified cholesterol-RNA conjugates a) 247, b) 248, c) 249, purified d) sense strand synthetic control 246 and e) synthetic anti-sense strand 250.

Nucleic acid samples can be readily checked for concentration and quality using the NanoDrop 1000 Spectrophotometer (Figure 5.25). It accurately measures DNA samples up to 3700 ng/ul and RNA samples up to 3000 ng/ul



Figure 5.25: NanoDrop 1000 Spectrophotometer.

Concentration Calculation²³⁸ (Beer's Law): the Beer-Lambert equation is used to correlate the measured UV absorbance with concentration:

$$A = E * I * c$$

A is the absorbance represented in absorbance units, **E** is the wavelength-dependent molar absorptivity coefficient (or extinction coefficient) with units of $L \cdot mol^{-1} \cdot cm^{-1}$, **I** is the path length in cm, and **c** is the analyte concentration in $mol \cdot L^{-1}$.

Analysis of the data from the NanoDrop spectrophotometer furnished three important pieces of information (Figure 5.26 and 5.27):

- **ng/ul (red arrows):** the sample concentration in ng/ul based on the intensity of the absorbance at 260 nm. The concentration in ng/ul divided by the molecular weight gives the concentration in mmol/L;
- **260/280 (blue arrows):** the ratio of sample absorbance at 260 and 280 nm. The ratio of absorbance at 260 and 280 nm is used to assess the purity of DNA and RNA. A ratio of ~2.0 is generally interpreted to mean the RNA is "pure";
- **260/230 (green arrows):** the ratio of sample absorbance at 260 and 230 nm. This is a secondary measure of nucleic acid purity. The 260/230 values for "pure" nucleic acids may be higher than the respective 260/280 values. They are commonly in the range of 1.8-2.2.

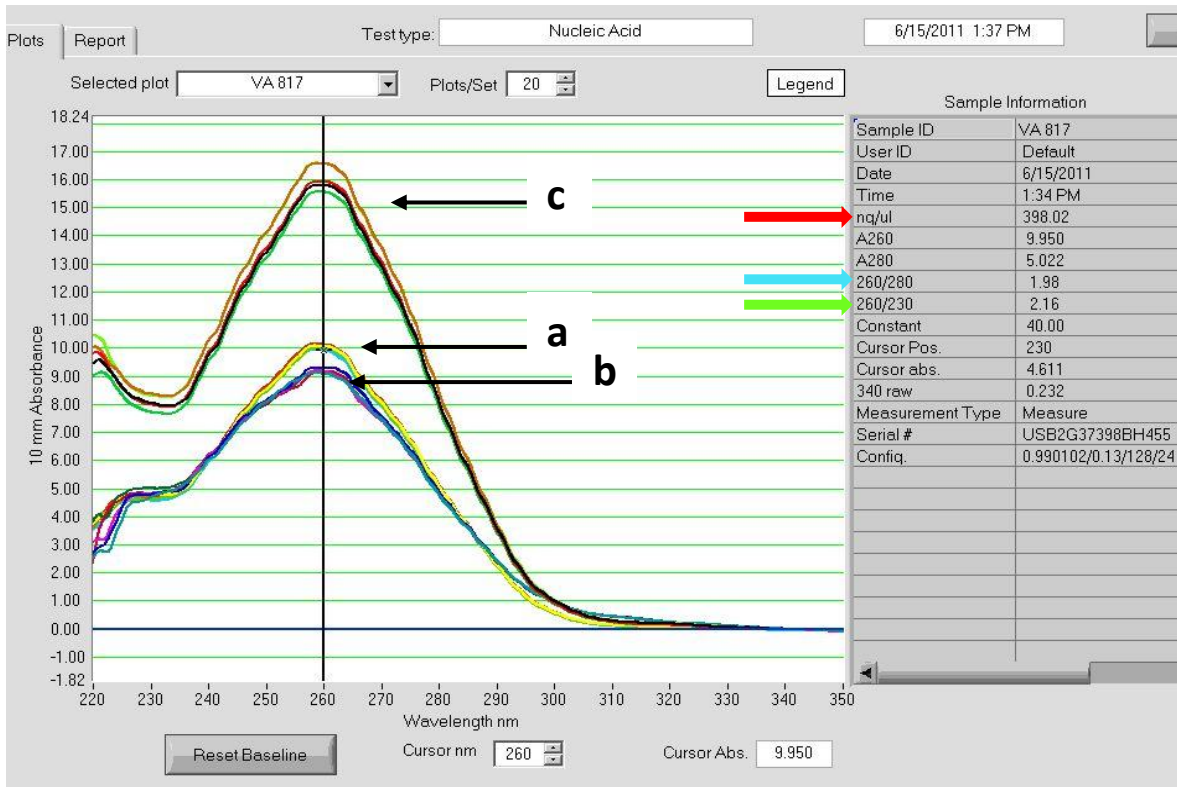


Figure 5.26: Micro-volume UV-vis spectra of purified cholesterol-RNA conjugates a) 247, b) 248, and c) 249.

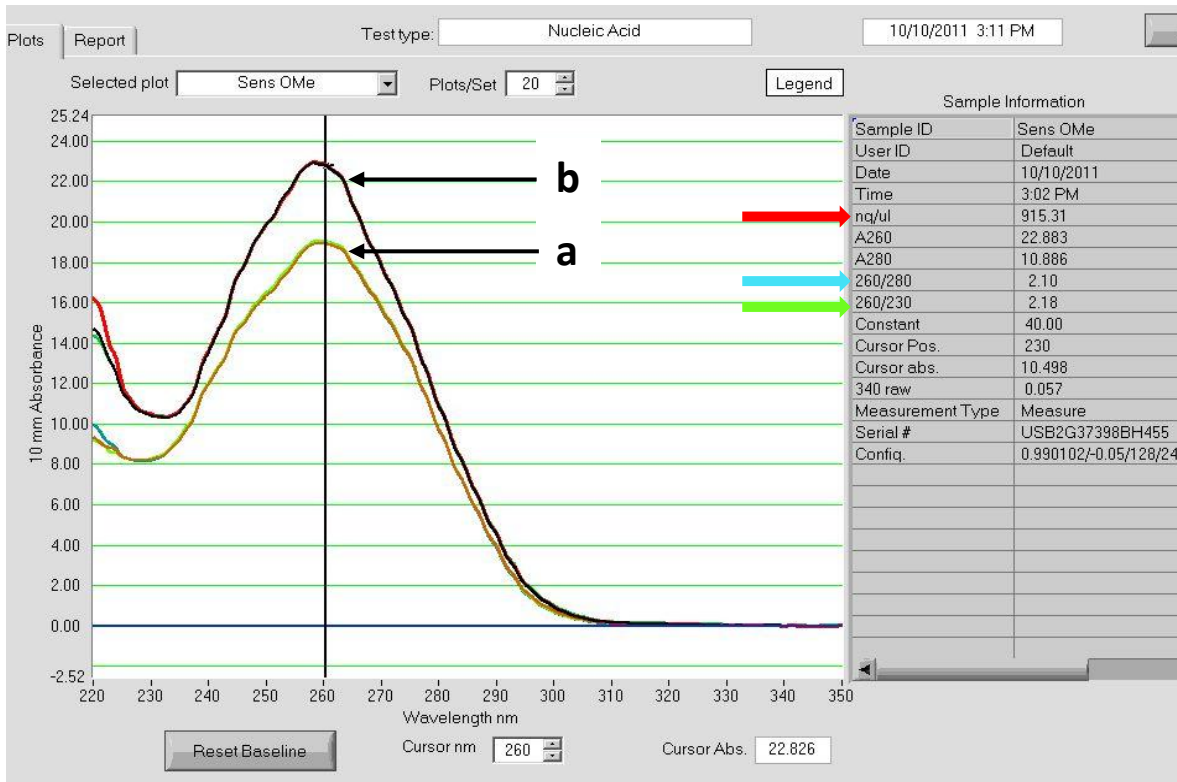


Figure 5.27: Micro-volume UV-vis spectra of purified a) sense strand synthetic control 246 and b) synthetic anti-sense strand 250.


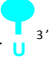

The duplexes envisaged were:

- **siRNA 5: synthetic control**, bearing an additional U unmodified at the 3'-terminus of the sense strand (entry 1, table 5.5);
- **siRNA 6**: bearing an additional U with an isoxazole ligated cholesterol moiety at the **2'-position** of the ribo-sugar at the **3'-terminus** of the sense strand (entry 2);
- **siRNA 7**: bearing an additional U with an isoxazole ligated cholesterol moiety at the **3'-position** of the ribo-sugar at the **5'-terminus** of the sense strand (entry3);
- **siRNA 8**: bearing an additional U with an isoxazole ligated cholesterol moiety at the **2'-position** of the ribo-sugar at the **3'-terminus** of the sense strand (entry 4).

The modified duplex activities were compared to the commercial siRNA used by the Moynagh's laboratory, **IL-17RD** (entry 5), and the **scrambled commercial siRNA** (entry 6). They both have free 2'-OH on the ribo-sugar units.

Table 5.5: Overview of the siRNA studied in HEK 293 cells.

Underlined bases carry a 2'-OMe block. Color code: green U(2'-Chol) and blue U(3'-Chol)

Entry n°	Duplex		
	Name	Strands	Structure: sense 5'-----3' 3'-----5' anti-sense
1	siRNA 5	246/250	$ \begin{array}{c} 5' \quad \underline{G} \underline{G} \underline{A} \underline{G} \underline{C} \underline{A} \underline{A} \underline{A} \underline{C} \underline{U} \underline{A} \underline{C} \underline{A} \underline{G} \underline{A} \underline{G} \underline{A} \underline{U} \underline{G} \underline{T} \underline{T} \underline{U} \quad 3' \\ 3' \quad \text{dG} \underline{T} \underline{C} \underline{C} \underline{U} \underline{C} \underline{G} \underline{U} \underline{U} \underline{U} \underline{G} \underline{A} \underline{U} \underline{G} \underline{U} \underline{C} \underline{U} \underline{C} \underline{U} \underline{A} \underline{C} \end{array} $
2	siRNA 6	247/250	$ \begin{array}{c} 5' \quad \underline{G} \underline{G} \underline{A} \underline{G} \underline{C} \underline{A} \underline{A} \underline{A} \underline{C} \underline{U} \underline{A} \underline{C} \underline{A} \underline{G} \underline{A} \underline{G} \underline{A} \underline{U} \underline{G} \underline{T} \underline{T} \underline{U} \quad 3' \\ 3' \quad \text{dG} \underline{T} \underline{C} \underline{C} \underline{U} \underline{C} \underline{G} \underline{U} \underline{U} \underline{U} \underline{G} \underline{A} \underline{U} \underline{G} \underline{U} \underline{C} \underline{U} \underline{C} \underline{U} \underline{A} \underline{C} \end{array} $ 
3	siRNA 7	248/250	$ \begin{array}{c} 5' \quad \underline{G} \underline{G} \underline{A} \underline{G} \underline{C} \underline{A} \underline{A} \underline{A} \underline{C} \underline{U} \underline{A} \underline{C} \underline{A} \underline{G} \underline{A} \underline{G} \underline{A} \underline{U} \underline{G} \underline{T} \underline{T} \underline{U} \quad 3' \\ 3' \quad \text{dG} \underline{T} \underline{C} \underline{C} \underline{U} \underline{C} \underline{G} \underline{U} \underline{U} \underline{U} \underline{G} \underline{A} \underline{U} \underline{G} \underline{U} \underline{C} \underline{U} \underline{C} \underline{U} \underline{A} \underline{C} \end{array} $ 
4	siRNA 8	249/250	$ \begin{array}{c} 5' \quad \underline{U} \underline{G} \underline{G} \underline{A} \underline{G} \underline{C} \underline{A} \underline{A} \underline{A} \underline{C} \underline{U} \underline{A} \underline{C} \underline{A} \underline{G} \underline{A} \underline{G} \underline{A} \underline{U} \underline{G} \underline{T} \underline{T} \quad 3' \\ 3' \quad \text{dG} \underline{T} \underline{C} \underline{C} \underline{U} \underline{C} \underline{G} \underline{U} \underline{U} \underline{U} \underline{G} \underline{A} \underline{U} \underline{G} \underline{U} \underline{C} \underline{U} \underline{C} \underline{U} \underline{A} \underline{C} \end{array} $ 
5	IL-17RD	/	$ \begin{array}{c} 5' \quad \underline{G} \underline{G} \underline{A} \underline{G} \underline{C} \underline{A} \underline{A} \underline{A} \underline{C} \underline{U} \underline{A} \underline{C} \underline{A} \underline{G} \underline{A} \underline{G} \underline{A} \underline{U} \underline{G} \underline{T} \underline{T} \quad 3' \\ 3' \quad \text{dG} \underline{T} \underline{C} \underline{C} \underline{U} \underline{C} \underline{G} \underline{U} \underline{U} \underline{U} \underline{G} \underline{A} \underline{U} \underline{G} \underline{U} \underline{C} \underline{U} \underline{C} \underline{U} \underline{A} \underline{C} \quad 5' \end{array} $
6	Scrambled siRNA	/	$ \begin{array}{c} 5' \quad \underline{G} \underline{G} \underline{A} \underline{C} \underline{A} \underline{G} \underline{A} \underline{A} \underline{C} \underline{A} \underline{C} \underline{U} \underline{A} \underline{G} \underline{A} \underline{U} \underline{G} \underline{A} \underline{G} \underline{T} \underline{T} \quad 3' \\ 3' \quad \text{dG} \underline{T} \underline{C} \underline{C} \underline{U} \underline{G} \underline{U} \underline{C} \underline{U} \underline{U} \underline{G} \underline{U} \underline{G} \underline{A} \underline{U} \underline{G} \underline{U} \underline{A} \underline{C} \underline{U} \underline{C} \quad 5' \end{array} $

The successes of the annealing experiments were checked by Polyacrylamide Gel Electrophoresis (PAGE) (Figure 5.28) which separates molecules according to size. Samples of each of the synthetic **siRNAs 5, 6, 7 and 8**, were loaded, as well as the individual sense **246**, and anti-sense **250** strands used to prepare the synthetic control **siRNA 5**. To validate the analysis, a further sample comprising a mixture of **siRNA 5** and the sense strand **246** was also loaded. Each of the four siRNA samples showed only one purple band; in contrast the single strands **246** and **250** gave a blue colored band. There was no trace of single strands in any of the duplexes. Thus, it was then concluded that all hybridizations were successful.

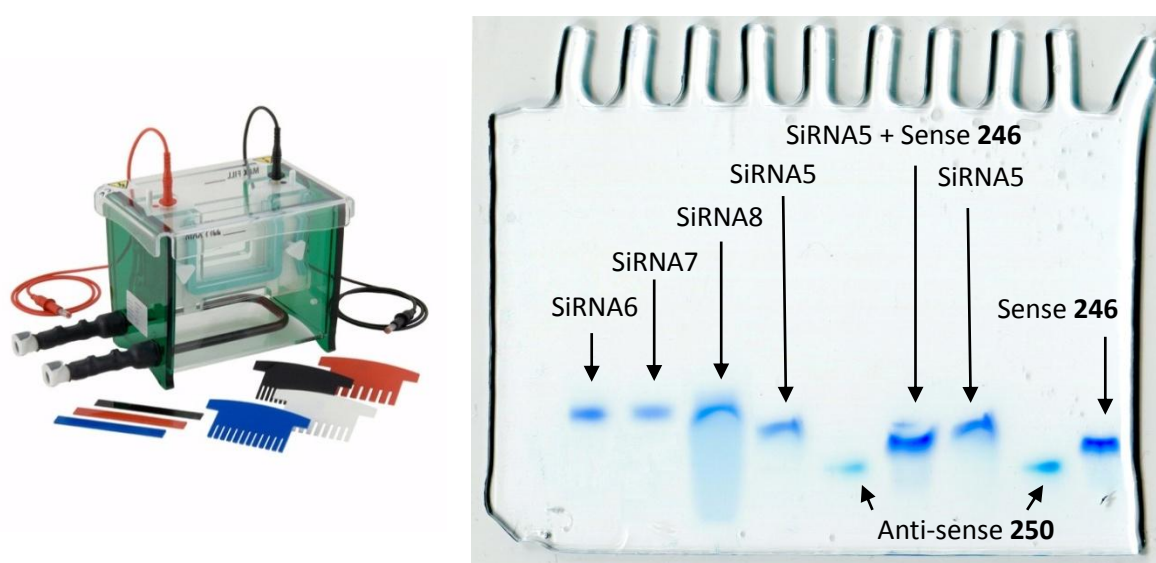


Figure 5.28: Gel electrophoresis unit (left) and SDS-PAGE used to judge success of hybridization of siRNAs 5-8.

V.1.b. Luciferase assay results

Assays were performed in duplicate with each of the four siRNAs, the synthetic control and the three cholesterol modified samples. They were compared to the commercial siRNA (**IL-17RD**) and the scrambled sequence. That the cells were viable, and that the assay was conducted successfully, is clear from the data obtained for **IL-17RD**, the commercial sequence, and thus it was disappointing that, whilst **siRNAs 6 and 7** (with 3'-modification to the sense strand), do show marginally better activity than **siRNA 8** (with a 5'-modification on the same strand), none of the siRNA constructs offer any evidence for real gene knockdown (Figure 5.29). At this

junction the synthetic control **siRNA 5** was tested separately; it did not show any activity either and thus, with the available data, one possible conclusion is that the introduction of the additional U within the overhang was a fundamental design problem. Experimentation beyond the time available to this author is required to examine such a hypothesis.

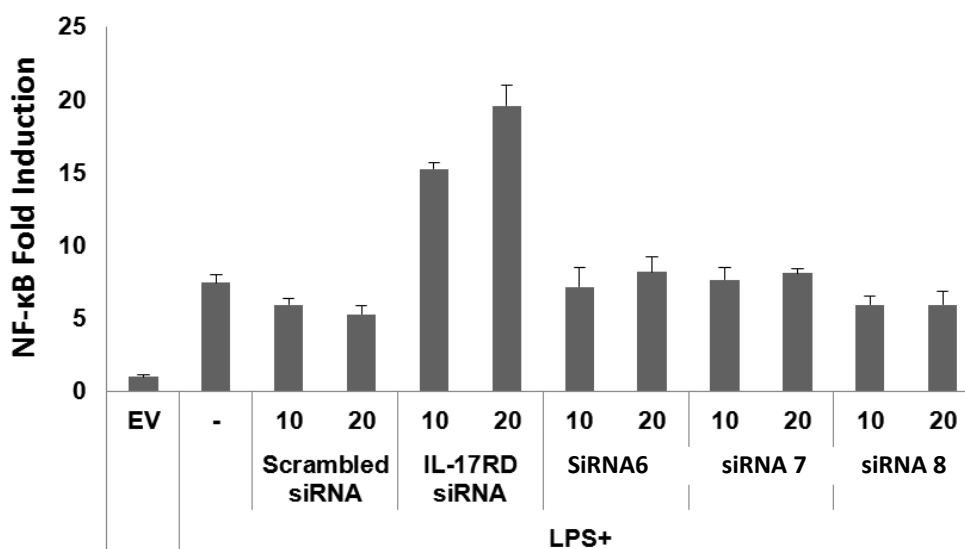


Figure 5.29: Knockdown representation of isoxazole linked cholesterol siRNAs 6, 7, and 8 compared to negative control, commercial IL-17RD and scrambled siRNAs.

VI. CONCLUSION

In this chapter, we developed and compared various approaches to conjugate a cholesterol moiety to oligonucleotide sequences, before concluding that the nitrile oxide/alkyne cycloaddition reaction offers an efficient and reliable tool for provision of chemically modified siRNAs.

Initially using the 5'-alkyne-oligonucleotide scaffold and a range of nitrile oxides, isoxazole functionalized ligands have been introduced at the 5'-end of DNAs through cycloaddition at the 5'-position of the sugar moiety.

Following optimization of the reaction conditions for conjugation, on the solid support, of oligoribonucleotides bearing 2'- or 3'-O-propargyl ribonucleosides, steroidal ligands have been introduced at pre-determined sites within an oligoribonucleotide sequence.

The conjugation procedure was established to be compatible with all four natural nucleobases bearing the standard protecting groups. It is selective, convenient, fast, economical, and allowed the synthesis of a wide variety of conjugates. The reaction occurs under atmospheric conditions, in aqueous solvents, is high yielding, highly regioselective and catalyst free which makes it very attractive for bio-conjugation.

In the final part of this project, two distinct families of chemically modified, 2'-OMe blocked siRNAs were prepared. The first family had no overhang and bore an isoxazole linked phenyl group at the 3'-terminus of the sense and/or the anti-sense strand. The biological consequences of the chemical modifications introduced were evaluated. In the second family, siRNAs with 3'-overhang containing an additional U base, with or without a 2'- or 3'-isoxazole linked cholesterol modification were designed.

The results obtained from transfection of the first family, into CHO-K1 cells for eGFP gene, conducted in the laboratory of Dr. Sean Doyle group appear promising; however, those assays do need to be duplicated for validation. The early results suggest the presence of the isoxazole linked aryl moiety has a beneficial effect on the gene knock down. Unfortunately, the Luciferase assay conducted with the second family, within the group of Dr. Paul Moynagh, did not show convincing evidence of knock-down activity. It has been reported that effective siRNA duplexes are frequently composed of 21 nt sense and 21 nt antisense strands which form a 19 bp double helix with 2 nt 3'-overhanging ends.²³⁹⁻²⁴² It is also known that the length of the 3'-overhang regions can influence the activity of the siRNA. Whilst the 2-nt 3'-overhang is most efficient using 21 nt siRNA, it is reported that 2'-deoxy monomers within the 2 nt 3'-overhang do not affect RNAi²³⁹ but incorporation of same does help to reduce the costs of RNA synthesis and may enhance RNase resistance of siRNA duplexes. More extensive 2'-deoxy or 2'-O-methyl modifications are reported to reduce the ability of siRNAs to mediate RNAi, probably by interfering with protein association for siRNP assembly.²⁴² Thus, it is likely that either the addition of the extra U within the 3'-overhang, or the exhaustive presence of the methoxy blocks on the ribose moieties, might have interfered with the silencing activity. Therefore, this author suggests future designs should reduce 3'-overhanging to 2 nt in length and should work either with ribose gapmer or alternates sequence

EXPERIMENTAL

GENERAL

Chemical agents, unless noted otherwise, were purchased from the Aldrich Chemical Company and were used without further purification.

The anhydrous solvents were redistilled over calcium chloride, calcium hydride, potassium hydroxide or sodium as appropriate.²⁴³

Analytical TLC was performed on precoated (250 mm) silica gel 60 F-254 plates from Merck, all plates were visualized by UV irradiation, and/or staining with 5% H₂SO₄ in ethanol, followed by heating.

Flash chromatography grade silica gel 60 (230-400 mesh) was obtained from Merck.

ESI Mass analysis was performed on a LC/TOF-MS instrument: model 6210 Time-Of-Flight LC/MS (Agilent Corp, SantaClara, CA) with an electrospray source, operated in either positive and negative mode (ESI ±), capillary 3,500 V, nebulizer spray 30 psig, drying gas 5 L min⁻¹ source temperature 325 °C. The fragmentor was used at 175 V. Reference/calibration solution, purchased from Agilent had *m/z* 121.050873, 149.02332, 322.048121, 922.009798, 1221.990633, 1521.971475, and 2421.91399.

MALDI-TOF Mass analysis were generally performed with a LASER-TOF LT3 from Scientific Analytical Instruments by Metabion (Germany) or an Ettan Pro from Amersham Biosciences (England), with 3-hydroxypicolinic acid or 2,4',6'-trihydroxyacetophenone as matrix.

NMR spectra were obtained for ¹H at 300 MHz, for ¹³C at 75 MHz and for ³¹P at 121 MHz, on a BRUKER Advance DPX-300 at 25 °C. All samples for NMR analysis were prepared in CDCl₃ unless otherwise stated. Chemical shifts are reported in ppm downfield from TMS as standard and coupling constants are reported in Hz.

IR spectra were recorded on disposable polyethylene card (19 mm, type 61, 3M) on a Perkin-Elmer Spectrum 100 RX-I series FT IR: spectrophotometer.

The scientific microwave (MW) is a Discover SP (CEM, Matthews North Carolina, USA), with an Explorer controlled by the software Synergy™.

Melting points (Mp) were determined on a Stuart equipment SMP 11.

Automated oligonucleotide synthesis was performed on an Expedite 8909 DNA/RNA synthesizer on a 1.0 μmol scale using standard reagents from Link Technologies, and Chemgene. Standard coupling cycles were conducted with BMT (0.2 M in CH_3CN) as activating agent; oxidation was performed using 8:1:1 THF:pyridine:H₂O, 0.02 M I₂.

The concentrator was an Eppendorf model 5301.

HPLC was conducted on a model GX-271 Series (Gilson Inc. Middleton, WI, USA), 500 μL injection loop, pump (model 322), 172 diode array detector (detection at 254 nm and 260 nm), injection volume was from 35 μL to 350 μL . The columns were a C₁₈ Macherey-Nagel (250/4 Nucleosil 100-5 C₁₈ length 250 nm ID 4mm) or a C₈ Phenomenex (Luna 5u C₈ (2) 100A, 250 x 4.60 mm 5 micron). The flow rate was 1 $\text{mL}\cdot\text{min}^{-1}$ and the mobile phases comprised A = 5% CH_3CN in 1M solution of triethylamine acetate (pH 6.5) and B = CH_3CN .

Three different methods were used:

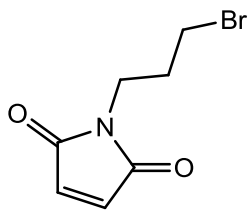
- Method 1: For C₁₈ column gradient 0-5 min 5% of B, 5-26 min 5-35%, 26 min to the end 100% B.
- Method 2: For C₈ column gradient 0-5 min 5% of B, 5-26 min 5-35%, 26 min to the end 100% B
- Method 3: For both columns gradient 0-5 min 5% of B, 5-35 min 5-17%, 35 min to the end 100% B

Purification of oligonucleotides has been achieved following a number of HPLC rounds eluting by method 3. The C₈ column was used for cholesterol conjugates and the C₁₈ column for the others.

Desalting was conducted with Sep-Pak® classic C₁₈ cartridges from Waters.

UV-absorbance for oligonucleotide quantification at 260 nm was performed on a NanoDrop® ND-1000 spectrophotometer v3.7. Molar extinction coefficients of oligonucleotides were calculated from the nearest neighbour model.²⁴⁴

UV Melting experiments of oligonucleotides were determined using a JASCO V-630 Bio spectrophotometer (Cary100 Scan) combined with a JULABO AWC 100 to regulate the temperature. The absorbances at 260 nm of degassed solutions of duplex oligonucleotides was recorded (5 μM of each oligomer in 100 mM NaCl, 10 mM Na-phosphate, 1 mM Na.EDTA, pH 7.0 - 500 μl) every 0.5 °C between 15 and 95 °C, using a gradient of 1 °C/min and this was repeated triplicate. Prior to recording the data, the solutions were heated to 90 °C and allowed to cool slowly to ambient temperature.

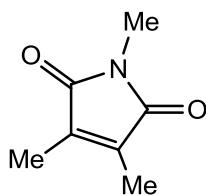


N-3-Bromopropylmaleimide 96

To a solution of maleic anhydride (500 mg, 5.10 mmol) and 3-bromopropylamine hydrobromide (1.116 g, 5.10 mmol) in dry DCM (10 mL) was slowly added triethylamine (0.8 mL, 5.77 mmol) drop by drop over 2 min, at 0 °C (ice bath) under argon atmosphere. The reaction mixture was stirred for 17 h at rt. The reaction mixture was then washed with a solution of 1N HCl (3 x 20 mL). The organic layer was dried over anhydrous Na₂SO₄, filtered and evaporated to dryness.

The residue was dissolved in acetic anhydride (10 mL), anhydrous sodium acetate (418 mg, 5.10 mmol) was added and the mixture was stirred for 2 h with heating at 80 °C. After cooling to rt, 20 mL of 1N NaOH was added and the product was extracted with DCM (3 x 20 mL). The combined organic layers were dried over anhydrous Na₂SO₄, filtered and evaporated to dryness. The crude reaction product was purified by flash column chromatography (SiO₂, hexane, AcOEt, 1:1) to give the title compound as an off-white solid (79%, 859 mg). The data agreed with that reported in the literature.¹⁸⁵

HRMS (ESI): calcd for [M+H]⁺, C₇H₉NO₂, 216.9700, found 216.9698 (-0.92 ppm).



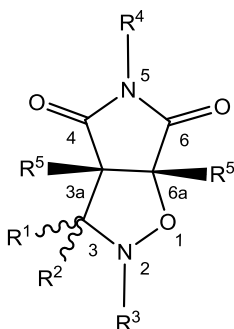
1,3,4-Trimethyl-1H-pyrrole-2,5-dione 97

A solution of 3,4-dimethyl maleic anhydride (200 mg, 1.59 mmol) in glacial acetic acid (2 mL) was cooled to 0 °C (ice bath) under an argon atmosphere. Methylamine (99 mg, 3.17 mmol, 2 eq) was added very slowly (drop by drop over 2 min). The reaction mixture was warmed to rt before stirring for 2 h with heating at reflux. The solvent was then carefully evaporated.

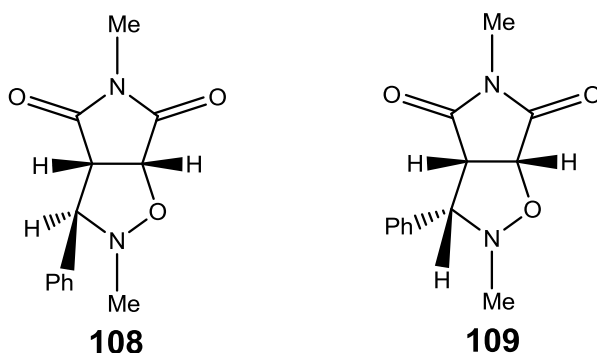
The residue was dissolved in acetic anhydride (2 mL), anhydrous sodium acetate (130 mg, 1.59 mmol, 1 eq) was added and the mixture was stirred for 2 h with heating at 80 °C. After cooling to rt, a solution of 1N NaOH (5 mL) was added and the product was

extracted with DCM (3 x 5 mL). The combined organic layers were dried over anhydrous Na₂SO₄, filtered and evaporated to dryness. The residue was purified by flash column chromatography (SiO₂, hexane, AcOEt, 1:1) to give the title compound as a colorless oil (53%, 158 mg). The data agreed with that reported in the literature.¹⁸⁶

¹H NMR: δ 3.03 (3H, s, NCH₃), 1.99 (6H, s, 2 x Me).



General procedure for cycloaddition between nitrones and maleimides: A suspension of the appropriate nitron (0.90 mmol, 1 eq) and maleimide (1.80 mmol, 2 eq) in hexane (3 mL), was inserted into the cavity of a scientific MW in a pressure tube. The mixture was irradiated at 300 W with stirring for 10 min (air cooling was selected to ensure internal T_{max} < 125 °C). Solvent removal under reduced pressure yielded the residues which were purified by washing abundantly with distilled H₂O or by flash column chromatography.

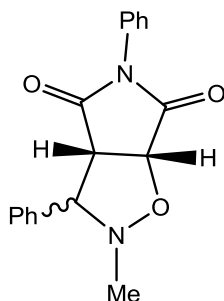


2,5-Dimethyl-3-phenylperhydropyrrolo[3,4-d]isoxazole-4,6-diones

The title compounds, an off-white solid, were isolated in 95% yield (210 mg) as a 1:1 mixture of diastereoisomers, which were separated by flash column chromatography (SiO₂, hexane, AcOEt, 7:3). The ¹H NMR data agreed with that reported in the literature.¹⁹⁴

108: off-white solid (39%, 64 mg); ¹³C NMR: δ 176.4 (C=O), 173.3 (C=O), 133.8 (Ar-C), 128.8, 128.8, 127.7 (5 x Ar-CH), 77.0 (C₃), 75.1 (C_{6a}), 54.2 (C_{3a}), 42.5 (NCH₃ isoxazolidine), 25.1 (NCH₃ maleimide); IR: 1709, 1435, 1287, 730, 720, 701 cm⁻¹; HRMS (ESI): calcd for [M+H]⁺, C₁₃H₁₅N₂O₃, 247.2601, found 247.2603 (1.21 ppm).

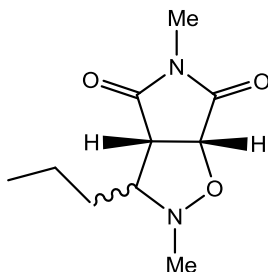
109: off-white solid (29%, 86 mg); ^{13}C NMR: δ 175.6 (C=O), 173.1 (C=O), 133.7 (Ar-C), 128.5, 128.5, 128.1 (5 x Ar-CH), 76.3 (C₃), 75.4 (C_{6a}), 54.5 (C_{3a}), 42.5 (NCH₃ isoxazolidine), 24.8 (NCH₃); IR: 1709, 1435, 1287, 730, 720, 701 cm⁻¹; HRMS (ESI): calcd for [M+H]⁺, C₁₃H₁₅N₂O₃, 247.2601, found 247.2609 (3.24 ppm).



2-Methyl-3,5-diphenyldihydro-2H-pyrrolo[3,4-d]isoxazole-4,6(5H,6aH)-dione 112

The title compound, an off-white solid, was isolated in 95% yield (258 mg) as a 1:1 mixture of diastereoisomers. Purification involved washing abundantly with distilled H₂O. The data agreed with that reported in the literature.¹⁹⁴

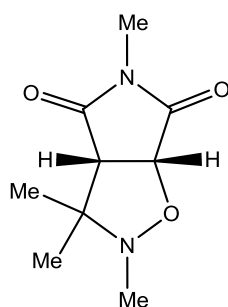
HRMS (ESI): calcd for [M+H]⁺, C₁₈H₁₇N₂O₃, 309.3401, found 309.3408 (2.27 ppm).



**2,5-Dimethyl-3-propyldihydro-2H-pyrrolo[3,4-d]isoxazole-4,6(5H,6aH)-dione
113 I and 113 II**

The title compound, an off-white solid, was isolated in 93% (219 mg) yield as a 1:1 mixture of diastereoisomers. Purification involved washing abundantly with distilled H₂O.

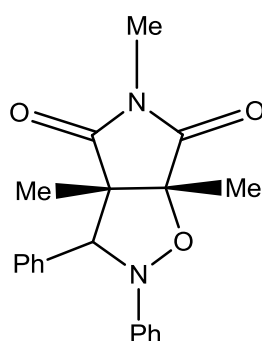
Rf: 0.45 (Hexane, AcOEt, 7:3); Mp: 136-138 °C; ^1H NMR: δ 4.47 (2H, d, ^3J 7.5, H_{6a}), 3.33 (1H, t, ^3J 7.5, H_{3a} of **113 I**), 3.19 (1H, t, ^3J 7.50, H_{3a} of **113 II**), 2.90-2.51 (7H, m, 2 x NCH₃ maleimide + H₃ of **113 I**), 2.46-2.22 (7H, m, 2 x NCH₃ isoxazolidine + H₃ of **113 II**), 1.58-1.03 (8H, m, 4 x CH₂), 0.79-0.51 (6H, m, 2 x CH₂CH₃). ^{13}C NMR: δ 175.8 (C=O), 175.2 (C=O), 173.9 (C=O), 76.1 (C₃), 75.1 (C₃), 71.1 (C_{6a}), 50.9 (C_{3a}), 42.3 (NCH₃), 29.8 (C_{1'}), 29.5 (C_{1'}), 24.6 (NCH₃), 24.27 (NCH₃), 19.4 (C_{2'}), 19.0 (C_{2'}), 14.0 (C_{3'}), 13.8 (C_{3'}); IR: 1710, 1436, 1285, 1135, 730, 720 cm⁻¹; HRMS (ESI): calcd for [M+H]⁺, C₁₀H₁₆N₂O₃, 213.1234, found 213.1244 (4.69 ppm).



2,3,3,5-Tetramethyldihydro-2H-pyrrolo[3,4-d]isoxazole-4,6(5H,6aH)-dione 114

A suspension of *N*-methylhydroxylamine hydrochloride (250 mg, 2.99 mmol), sodium hydrogen carbonate (505 mg, 6.00 mmol, 2 eq) and sodium sulfate (1.704 g, 12.00 mmol, 4 eq) in anhydrous acetone (5 mL) was inserted into the cavity of a scientific MW in a pressure tube and the mixture was irradiated stirring at 80 °C for 30 min ($P_{\max} = 300$ W). The solution was filtered, washed with DCM (5 mL) and the solvent evaporated carefully under pressure (350 mbar) to afford the crude nitron (140 mg). The residue and NMM (665 mg, 6.00 mmol, 2 eq) were mixed in hexane (3 mL), in a pressure tube, and irradiated at 300 W for 10 min (air cooling was selected to ensure internal $T_{\max} < 80$ °C). Solvent removal under reduced pressure yielded a residue which was purified by washing abundantly with distilled H₂O. The title compound was obtained as an off-white solid (35%, 112 mg).

Rf: 0.40 (Hexane, AcOEt, 6:4); Mp: 142-144 °C; ¹H NMR: δ 4.67 (1H, d, ³J 7.2, H_{6a}), 3.05 (1H, d, ³J 7.2, H_{3a}), 2.61 (3H, s, NCH₃ maleimide), 2.18 (3H, s, NCH₃ isoxazolidine), 1.20, 1.16 (3H each, s, 2 x Me). ¹³C NMR: δ 174.6 (C=O), 170.8 (C=O), 76.6 (C₃), 74.8 (C_{6a}), 57.7 (C_{3a}), 43.9 (NCH₃), 25.3 (Me), 24.9 (Me), 23.7 (NCH₃); IR: 1702, 1463, 1381, 1287, 1125, 730, 720 cm⁻¹; HRMS (ESI): calcd for [M+H]⁺, C₉H₁₄N₂O₃, 199.107, found 199.1080 (1.51 ppm).

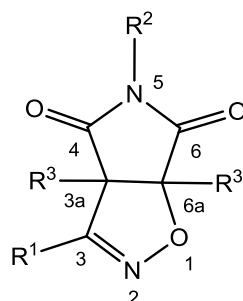


3a,5,6a-Trimethyl-2,3-diphenyldihydro-2H-pyrrolo[3,4-d]isoxazole-4,6(5H,6aH)-dione 116

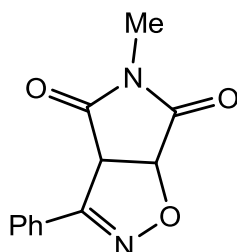
A suspension of 1,3,4-trimethylmaleimide **97** (150 mg, 1.08 mmol) and *N*-phenyl-*C*-phenyl nitron **105** (426 mg, 2.16 mmol, 2 eq) in hexane (3 mL), was inserted into the cavity

of a scientific MW in a pressure tube and irradiated stirring at 300 W for 1H (air cooling was selected to ensure internal $T_{\max} < 125$ °C). Solvent removal under reduced pressure yielded the crude product which was purified by flash column chromatography (SiO_2 , hexane, AcOEt, 6:4). The title compound was obtained as an off-white solid (8%, 29 mg).

Rf: 0.30 (Hexane, AcOEt, 6:4); Mp: 127-129 °C; ^1H NMR: δ 7.48-7.41 (2H, m, Ar-H), 7.37-7.25 (3H, m, Ar-H), 7.20-7.12 (2H, m, Ar-H), 6.95-6.82 (3H, m, Ar-H), 5.32 (1H, s, H₃), 2.72 (3H, s, NCH₃), 1.49, 0.97 (3H each, s, 2 x Me). ^{13}C NMR: δ 170.8 (C=O), 169.9 (C=O), 150.1, 147.8 (2 x Ar-C), 134.1, 134.1, 131.8, 131.4, 128.9, 127.9, 126.2, 122.8 (10 x Ar-CH), 90.3 (C_{6a}), 76.9 (C₃), 62.2 (C_{3a}), 25.7 (NCH₃), 15.7 (Me), 14.8 (Me); IR: 1702, 1473, 1463, 1162, 730, 720 cm^{-1} ; HRMS (ESI): calcd for $[\text{M}+\text{H}]^+$, $\text{C}_{20}\text{H}_{21}\text{N}_2\text{O}_3$, 337.1580, found 337.1588 (2.37 ppm).



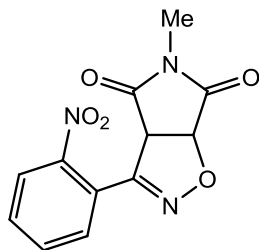
General procedure for cycloaddition between nitrile oxides and maleimides: A suspension of oxime (1.10 mmol, 1.1 eq), CAT (2.50 mmol, 2.5 eq) in H_2O (3 mL) with the appropriate maleimide (1 mmol, 1 eq) was inserted into the cavity of a scientific MW in a pressure tube. The mixture was irradiated stirring at 40 °C for 10 min ($P_{\max} = 300$ W). Solvent removal under reduced pressure yielded the crude product. Purification by washing abundantly with water or by flash column chromatography afforded the pure products as off-white solids.



5-Methyl-3-phenyl-3aH-pyrrolo[3,4-d]isoxazole-4,6(5H,6aH)-dione 121

The title compound, an off-white solid, was isolated in 90% yield (207 mg) after purification by washing abundantly with distilled H_2O . The data agreed with that reported in the literature.²⁴⁵

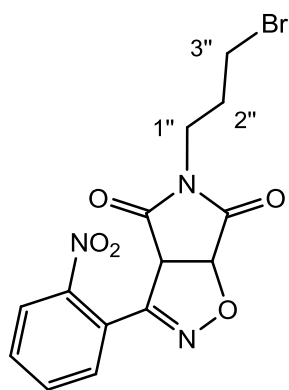
HRMS (ESI): calcd for $[M+H]^+$, $C_{12}H_{11}N_2O_3$, 231.0764, found 231.0765 (0.43 ppm).



5-Methyl-3-(2-nitrophenyl)-3aH-pyrrolo[3,4-d]isoxazole-4,6(5H,6aH)-dione 122

The title compound, an off-white solid, was isolated in 93% yield (230 mg) after purification by washing abundantly with distilled H_2O .

Rf: 0.32 (hexane, AcOEt, 6:4); Mp: 170-172 °C; 1H NMR: δ 8.24-8.21 (1H, m, Ar-H), 7.79-7.67 (2H, m, Ar-H), 7.54-7.49 (1H, m, Ar-H), 5.61 (1H, d, 3J 9.6, H_{6a}), 4.79 (1H, d, 3J 9.6, H_{3a}), 3.05 (3H, s, Me). ^{13}C NMR: δ 172.0 (C=O), 170.6 (C=O), 151.8 (C_3), 147.7 ($C_{1'}$), 134.1, 131.8, 125.5 (4 x Ar-CH), 122.8 ($C_{2'}$), 80.4 (C_{6a}), 57.3 (C_{3a}), 25.6 (NCH₃). ; IR: 1719, 1473, 1463, 730, 720 cm^{-1} ; HRMS (ESI): calcd for $[M+H]^+$, $C_{12}H_{10}N_3O_5$, 276.0615, found 276.0622 (2.54 ppm).

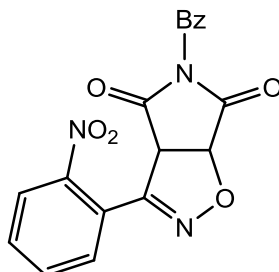


5-(3-Bromopropyl)-3-(2-nitrophenyl)-3aH-pyrrolo[3,4-d]isoxazole-4,6(5H,6aH)-dione 123

The title compound, an off-white solid, was isolated in 96% yield (291 mg) after purification by washing abundantly with distilled H_2O .

Rf: 0.30 (hexane, AcOEt, 6:4); Mp: 141-143 °C; 1H NMR: δ 8.24-8.21 (1H, m, Ar-H), 7.79-7.68 (2H, m, Ar-H), 7.53-7.49 (1H, m, Ar-H), 5.61 (1H, d, 3J 9.6, H_{6a}), 4.79 (1H, d, 3J 9.6, H_{3a}), 3.75-3.70 (2H, m, $H_{1''}$), 3.37 (3H, t, 3J 6.4, $H_{3''}$), 2.24-2.15 (2H, m, $H_{2''}$). ^{13}C NMR: δ 171.8 (C=O), 170.4 (C=O), 151.7 (C_3), 147.8 (Ar-C), 134.1 (Ar-C), 131.7, 131.6, 125.5 (4

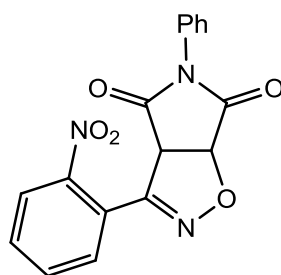
x Ar-CH), 122.8 (C₂), 80.9 (C_{6a}), 57.2 (C_{3a}), 38.6 (C_{1''}), 30.0 (C_{2''}), 29.5 (C_{3''}); IR: 1717, 1529, 1348, 730, 720, 558 cm⁻¹; HRMS (ESI): calcd for [M+H]⁺, C₁₄H₁₃BrN₃O₅, 382.0033, found 382.0051 (4.71 ppm).



5-Benzyl-3-(2-nitrophenyl)-3aH-pyrrolo[3,4-d]isoxazole-4,6(5H,6aH)-dione 124

The title compound, an off-white solid, was isolated in 92% yield (291 mg) after purification by washing abundantly with distilled H₂O.

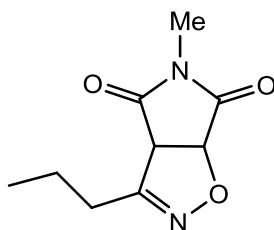
Rf: 0.24 (hexane, AcOEt, 6:4); Mp: 182-184 °C; ¹H NMR: δ 8.17-8.09 (1H, m, Ar-H), 7.68-7.59 (2H, m, Ar-H), 7.34-7.19 (6H, m, Ar-H), 5.52 (1H, d, ³J 9.3, H_{6a}), 4.75 (d, 1H, ³J 9.3, H_{3a}), 4.63 (2H, s, NCH₂). ¹³C NMR: δ 172.0 (C=O), 170.4 (C=O), 152.2 (C₃), 134.7, 134.2, 134.1 (3 x Ar-C), 131.8, 131.6, 128.9, 128.7, 128.4, 126.3, 122.6 (9 x Ar-CH), 80.5 (C_{6a}), 57.2 (C_{3a}), 43.1 (NCH₂); IR: 1718, 1462, 1347, 1173, 731, 720 cm⁻¹; HRMS (ESI): calcd for [M+H]⁺, C₁₈H₁₄N₃O₅, 352.0928, found 352.0943 (4.30 ppm).



3-(2-Nitrophenyl)-5-phenyl-3aH-pyrrolo[3,4-d]isoxazole-4,6(5H,6aH)-dione 125

The title compound, an off-white solid, was isolated in 93% yield (282 mg) after purification by washing abundantly with distilled H₂O.

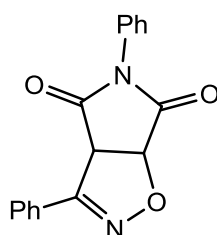
Rf: 0.32 (hexane, AcOEt, 6:4); Mp: 170-172 °C; ¹H NMR: δ 8.07 (1H, d, ³J 7.80, Ar-H), 7.78-7.63 (2H, m, Ar-H), 7.62-7.23 (6H, m, Ar-H), 5.71 (1H, d, ³J 9.60, H_{6a}), 4.92 (d, 1H, ³J 9.60, H_{3a}). ¹³C NMR: δ 171.9 (C=O), 170.0 (C=O), 151.9 (C₃), 134.2 (Ar-C), 134.1 (Ar-C), 131.7, 131.5, 131.2, 130.8, 129.4, 129.2, 128.0, 126.3, 126.1, 125.5 (Ar-C + 9 x Ar-CH), 80.6 (C_{6a}), 57.8 (C_{3a}); IR: 1717, 1473, 1463, 1196, 730, 720 cm⁻¹; HRMS (ESI): calcd for [M+H]⁺, C₁₁H₁₂N₃O₅, 338.0771, found 338.0769 (-0.60 ppm).



5-Methyl-3-propyl-3aH-pyrrolo[3,4-d]isoxazole-4,6(5H,6aH)-dione 126

The title compound, an off-white solid, was isolated in 96% yield (180 mg) after purification by flash column chromatography (SiO₂, hexane, AcOEt, 7:3).

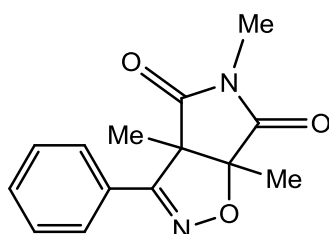
Rf: 0.28 (hexane, AcOEt, 7:3); Mp: 152-154 °C; ¹H NMR: δ 5.32 (1H, d, ³J 9.30, H_{6a}), 4.30 (1H, d, ³J 9.30, H_{3a}), 3.02 (3H, s, NCH₃), 1.89-1.19 (4H, m, H_{1'} + H_{2'}), 0.97 (3H, t, ³J 8.0, H_{3'}). ¹³C NMR: δ 172.7 (C=O), 171.2 (C=O), 154.6 (C₃), 78.7 (C_{6a}), 57.0 (C_{3a}), 28.2 (C_{1'}), 25.4 (NCH₃), 19.2 (C_{2'}), 13.7 (C_{3'}); IR: 1715, 1462, 1163, 730, 720 cm⁻¹; HRMS (ESI): calcd for [M+H]⁺, C₉H₁₃N₂O₃, 197.0921, found 197.0934 (4.38 ppm).



3,5-Diphenyl-3aH-pyrrolo[3,4-d]isoxazole-4,6(5H,6aH)-dione 128

The title compound, an off-white solid, was isolated in 94% yield (260 mg) after purification by washing abundantly with distilled H₂O. The data agreed with that reported in the literature.²⁴⁶

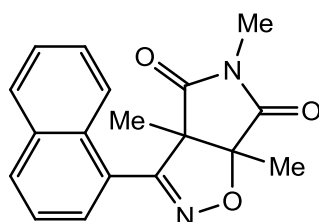
HRMS (ESI): calcd for [M+H]⁺, C₁₂H₁₁N₂O₃, 292.0852, found 292.0848 (1.37 ppm).



3a,5,6a-Trimethyl-3-phenyl-3aH-pyrrolo[3,4-d]isoxazole-4,6(5H,6aH)-dione 129

The title compound, an off-white solid, was isolated in 6% yield (14 mg) after purification by purified by flash column chromatography (SiO₂, hexane, AcOEt, 6:4).

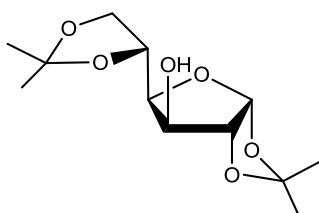
Rf: 0.40 (hexane, AcOEt, 7:3); Mp: 141-143 °C; ¹H NMR: δ 8.09-8.00 (2H, m, Ar-H), 7.49-7.38 (3H, m, Ar-H), 3.09 (3H, s, NCH₃), 1.64, 1.58 (3H each, s, 2 x Me). ¹³C NMR: δ 174.9 (C=O), 174.6 (C=O), 156.3 (C₃), 130.7 (Ar-C), 128.8, 128.1, 127.4 (5 x Ar-CH), 90.5 (C_{6a}), 62.5 (C_{3a}), 25.8 (NCH₃), 15.7 (Me), 14.8 (Me); IR: 1708, 1473, 1463, 1162, 731, 720 cm⁻¹; HRMS (ESI): calcd for [M+H]⁺, C₁₄H₁₅N₂O₃, 259.1082, found 259.1085 (1.16 ppm).



3a,5,6a-Trimethyl-3-(naphthalen-1-yl)-3aH-pyrrolo[3,4-d]isoxazole-4,6(5H,6aH)-dione
130

The title compound, an off-white solid, was isolated in 10% yield (28 mg) after purification by purified by flash column chromatography (SiO₂, hexane, AcOEt, 6:4).

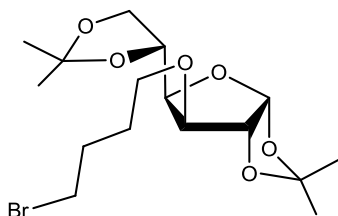
Rf: 0.35 (hexane, AcOEt, 7:3); Mp: 149-151 °C; ¹H NMR: δ 8.01-7.86 (3H, m, Ar-H), 7.79-7.67 (1H, m, Ar-H), 7.58-7.44(3H, m, Ar-H), 3.12 (3H, s, NCH₃), 1.74, 1.41 (3H each, s, 2 x Me). ¹³C NMR: δ 174.5 (C=O), 174.4 (C=O), 155.8 (C₃), 133.8, 132.2, 130.8 (3 x Ar-C), 129.0, 128.6, 127.9, 127.3, 126.7, 126.4, 125.2 (7 x Ar-CH), 89.3 (C_{6a}), 64.6 (C_{3a}), 25.7 (NCH₃), 15.5 (Me), 14.1 (Me); IR: 1708, 1473, 1463, 1162, 731, 720 cm⁻¹; HRMS (ESI): calcd for [M+H]⁺, C₁₈H₁₇N₂O₃, 309.1234, found 309.1242 (2.70 ppm).



1,2:5,6-Di-O-isopropylidene-α-D-glucufuranoside 132

This compound, prepared according to a literature procedure, was obtained as a white solid (5.1 g, 89%). The data agreed with that reported.²⁰⁰

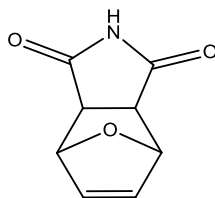
¹H NMR: δ 5.92 (1H, d, ³J 3.7, H₁), 4.51 (1H, d, ³J 3.7, H₂), 4.38-4.25 (2H, m, H₃, H₅), 4.15 (1H, dd, ²J 8.7, ³J 6.6, H_{6a}), 4.04 (1H, dd, ²J 8.0, ³J 2.9, H₄), 3.97 (1H, dd, ²J 8.7, ³J 5.1, H_{6b}), 1.48, 1.43, 1.35, 1.30 (3H each, s, 4 x Me).



3-O-(4-Bromobutyl)-1,2:5,6-di-O-isopropylidene- α -D-glucopyranoside **134**

This compound, prepared according to a literature procedure, was obtained as a white solid (269 mg, 74%). The data agreed with that reported.²⁴⁷

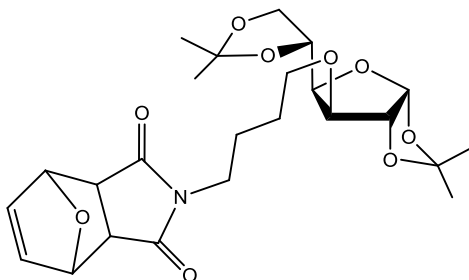
^1H NMR: δ 5.87 (1H, d, 3J 3.8, H₁), 4.52 (1H, d, 3J 3.8, H₂), 4.32–4.23 (1H, m, H₅), 4.13–4.05 (2H, m, H_{6a}, H₄), 4.20–3.94 (1H, m, H_{6b}), 3.85 (1H, d, 3J 3.0, H₃), 3.71–3.62 (1H, m, OCH₂), 3.60–3.50 (1H, m, OCH₂), 3.44 (2H, t, 3J 6.6, BrCH₂), 2.02–1.90 (1H, m, OCH₂CH₂), 1.78–1.67 (1H, m, OCH₂CH₂), 1.49, 1.42, 1.35, 1.32 (3H each, s, 4 x Me).



7-Oxabicyclo[2.2.1]hept-5-ene-2,3-dicarboximide **138**

This compound, prepared according to a literature procedure, was obtained as a white solid (503 mg, 95%).²⁴⁸ The data agreed with that reported.²⁴⁹

^1H NMR (d₆-DMSO): δ 7.96 (1H, s, NH), 6.52 (2H, s, CH=CH), 5.32 (2H, s, OCH), 2.89 (2H, s, CHCO).

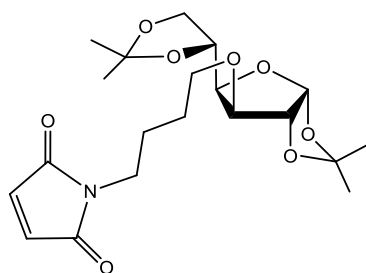


Protected maleimido-sugar **139**

The protected bromo-sugar **134** (125 mg, 0.38 mmol) and the protected maleimide **138** (95 mg, 0.57 mmol, 1.5 eq) were dissolved in dry acetone (10 mL). Dry potassium carbonate (107 mg, 0.76 mmol, 2 eq) was added and the resulting mixture stirred with heating at reflux overnight. After solvent removal under pressure the residue was dissolved

in DCM (20 mL). The organic layer was washed with a sat. aq. solution of NH_4Cl (3 x 10 mL), dried over anhydrous Na_2SO_4 and the solvents were removed under reduced pressure. The residue was purified by flash column chromatography (SiO_2 , DCM, MeOH, 98:2) to give the title compound as a yellow oil in 79% yield (144 mg).

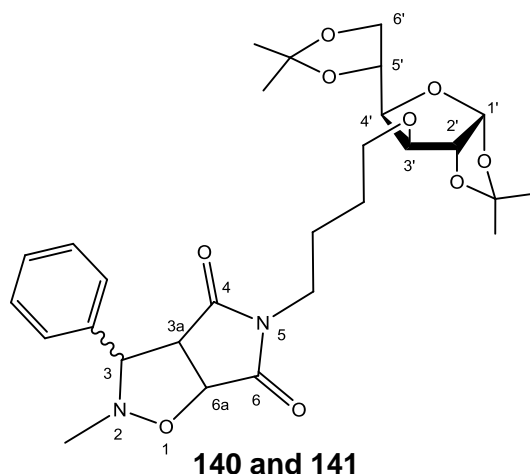
Rf: 0.77 (DCM, MeOH, 98:2); ^1H NMR: δ 6.52 (2H, s, 2 x CH=CH), 5.86 (1H, d, ^3J 3.6, H_1), 5.25 (2H, s, 2 x OCH), 4.53 (1H, d, ^3J 3.6, H_2), 4.32–4.23 (1H, m, H_5), 4.13–4.05 (2H, m, H_{6a} , H_4), 4.20–3.94 (1H, m, H_{6b}), 3.85 (1H, d, ^3J 3.0, H_3), 3.64–3.44 (4H, m, OCH_2 , NCH_2), 2.83 (2H, s, 2 x CH), 1.71–1.50 (4H, m, $\text{OCH}_2\text{CH}_2\text{CH}_2$), 1.49, 1.42, 1.34, 1.32 (3H each, s, 4 x Me); ^{13}C NMR (DMSO- d_6): δ 177.8 (2 x C=O), 136.4 (2 x CH=CH), 110.4 ($\underline{\text{C}}(\text{CH}_3)_2$), 110.3 ($\underline{\text{C}}(\text{CH}_3)_2$), 104.5 (C_1), 84.6 (C_2), 80.3 (2 x OCH), 80.0 (C_4), 79.9 (C_3), 73.2 (C_5), 68.4 (OCH_2), 63.6 (C_6), 48.4 (2 x CH), 40.8 (NCH_2), 29.4 (CH_2), 28.5 (CH_2), 26.8, 26.7, 26.2, 25.5 (4 x Me); IR: 1718, 1473, 1463, 730, 720 cm^{-1} ; HRMS (ESI): calcd for $[\text{M}+\text{H}]^+$, $\text{C}_{24}\text{H}_{36}\text{NO}_9$, 482.2459, found 482.2477 (3.32 ppm).



Maleimido-sugar 92

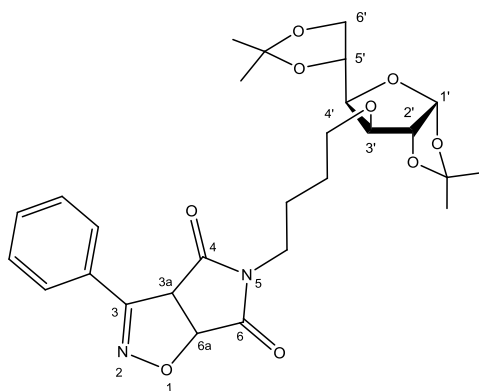
The protected maleimido sugar **139** (120 mg, 0.25 mmol) was heated at reflux in toluene (5 mL) overnight. After solvent removal, the residue was purified by flash column chromatography (SiO_2 , DCM, MeOH, 98:2) to give the title compound as a yellow oil in quantitative yield (100 mg).

Rf: 0.52 (DCM, MeOH, 98:2); ^1H NMR: δ 6.69 (2H, s, 2 x CH=CH), 5.87 (1H, d, ^3J 3.6, H_1), 4.53 (1H, d, ^3J 3.6, H_2), 4.33–4.20 (1H, m, H_5), 4.14–4.04 (2H, m, H_{6a} , H_4), 4.01–3.93 (1H, m, H_{6b}), 3.86–3.80 (1H, m, H_3), 3.67–3.45 (4H, m, OCH_2 , NCH_2), 1.74–1.50 (4H, m, $\text{OCH}_2\text{CH}_2\text{CH}_2$), 1.49 (3H, s, Me), 1.42 (3H, s, Me), 1.33 (3H, s, Me), 1.32 (3H, s, Me); ^{13}C NMR: δ 170.5 (2 x C=O), 133.9 (2 x CH=CH), 111.8 ($\underline{\text{C}}(\text{CH}_3)_2$), 109.0 ($\underline{\text{C}}(\text{CH}_3)_2$), 105.3 (C_1), 82.6 (C_2), 82.5 (C_4), 81.2 (C_3), 72.6 (C_5), 69.4 (OCH_2), 67.2 (C_6), 41.8 (NCH_2), 28.5 (CH_2), 27.5 (CH_2), 26.9, 26.8, 26.3, 25.6 (4 x Me); IR: 1720, 1473, 1463, 1067, 730, 720 cm^{-1} ; HRMS (ESI): calcd for $[\text{M}+\text{H}]^+$, $\text{C}_{20}\text{H}_{30}\text{NO}_8$, 412.2001, found 412.2008 (1.70 ppm).



To a solution of the maleimido sugar **92** (28 mg, 0.07 mmol) in tBuOH (2 mL) was added the *N*-methyl *C*-phenyl nitron **104** (11 mg, 0.08 mmol, 1.1 eq). The mixture was stirred for 17 h with heating at reflux. After solvent removal, the residue was purified by flash column chromatography (SiO₂, DCM) to give the title compound, a yellow oil, as a 2:3 mixture of diastereoisomers **140** and **141**, in 86% yield (32 mg).

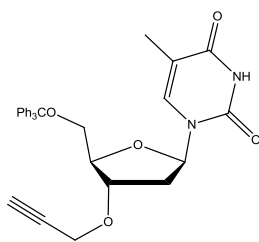
Rf: 0.62 (DCM, MeOH, 98:2); ¹H NMR: δ 7.47-7.24 (10H, m, Ar-H), 7.21-7.13 (2.5H, m, Ar-H), 5.93-5.81 (2.5H, m, H_{1'}), 4.92 (1.5H, d, ³J 7.5, H_{6a} of **140**), 4.86 (1H, d, ³J 7.5, H_{6a} of **141**), 4.58-4.48 (2.5H, m, H_{2'}), 4.34-4.23 (2.5H, m, H_{5'}), 4.15-4.02 (7.5H, m, H_{6'a}, H_{6'b}, H_{4'}), 3.88-3.78 (2.5H, m, H_{3'}), 3.76-3.39 (12.5H, m, H_{3a}, OCH₂, NCH₂), 1.78-1.53 (10H, m, OCH₂CH₂CH₂), 2.65 (4.5H, s, NCH₃), 2.42 (3H, s, NCH₃), 1.49, 1.42, 1.32, 1.31 (7.5H each, s, 8 x Me); ¹³C NMR: δ 175.4 (C=O), 173.6 (C=O), 133.9 (Ar-C), 128.9, 128.8, 128.5, 128.1, 127.8 (5 x Ar-CH), 111.3 (C(CH₃)₂), 108.7 (C(CH₃)₂), 105.0 (C_{1'}), 82.1 (C₂), 82.0 (C_{4'}), 80.9 (C_{3'}), 77.1 (C₃), 76.6 (C₃), 75.4 (C_{6a}), 75.1 (C_{6a}), 72.0 (C_{5'}), 69.3 (OCH₂), 67.0 (C_{6'}), 54.4 (C_{3a}), 42.5 (NCH₃), 40.4 (NCH₂), 29.3 (CH₂), 28.3 (CH₂), 26.8, 26.7, 26.1, 25.4 (4 x Me); IR: 1712, 1473, 1463, 730, 720 cm⁻¹; HRMS (ESI): calcd for [M+H]⁺, C₂₄H₃₆NO₉, 547.2650, found 547.2665 (2.74 ppm).



To a solution of the maleimido sugar **92** (28 mg, 0.07 mmol) in EtOH (2 mL) was added benzaldehyde oxime **118** (11 mg, 0.08 mmol, 1.1 eq), and CAT (41 mg, 0.18 mmol, 2.5 eq). The mixture was stirred for 2 h at rt. After solvent removal, the residue was purified by flash column chromatography (SiO₂, DCM) to give the title compound as a yellow oil in 70% yield (26 mg).

Rf: 0.53 (DCM, MeOH, 98:2); ¹H NMR: δ 8.05-7.91 (2H, m, Ar-H), 7.51-7.41 (3H, m, Ar-H), 5.86 (1H, d, ³J 3.6, H₁), 5.53 (1H, d, ²J 9.5, H_{6a}), 4.84 (1H, d, ²J 9.5, H_{3a}), 4.53 (1H, d, ³J 3.6, H₂), 4.33–4.23 (1H, m, H₅), 4.16-4.02 (3H, m, H_{6a}, H_{6b}, H₄), 3.86-3.79 (1H, m, H₃), 3.74-3.42 (4H, m, OCH₂, NCH₂), 1.72-1.49 (4H, m, OCH₂CH₂CH₂), 1.49, 1.42, 1.32, 1.31 (3H each, s, 4 x Me); ¹³C NMR: δ 174.9 (C=O), 174.1 (C=O), 157.5 (C₃), 130.7 (Ar-C), 128.7, 128.0, 127.4 (5 x Ar-CH), 111.3 (C(CH₃)₂), 108.7 (C(CH₃)₂), 105.0 (C_{1'}), 90.5 (C_{6a}), 82.1 (C_{2'}), 82.0 (C_{4'}), 80.9 (C_{3'}), 72.0 (C_{5'}), 69.3 (OCH₂), 67.0 (C_{6'}), 62.5 (C_{3a}), 40.5 (NCH₂), 29.3 (CH₂), 28.3 (CH₂), 26.8, 26.6, 26.2, 25.4 (4 x Me); IR: 1708, 1473, 1463, 1074, 730, 720 cm⁻¹; HRMS (ESI): calcd for [M+H]⁺, C₂₄H₃₆NO₉, 531.2335, found 531.2353 (3.39 ppm).

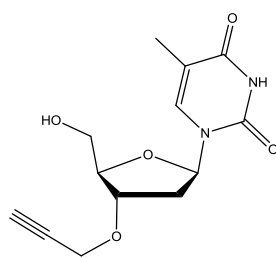
Compounds **150** to **168**, prepared by the author, have been reported.¹⁰³ Full characterization data is included in the paper which is placed in the Appendix section of this thesis. ¹H NMR spectra are recorded in the current section.



3'-O-(2-Propynyl)-5'-O-(triphenylmethyl)thymidine **150**

This compound prepared according to a literature procedure, was obtained as an off-white foam (501 mg, 93%). The data agreed with that reported.¹⁰³

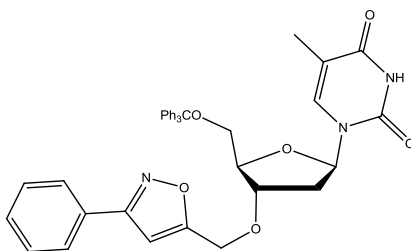
¹H NMR: δ 8.88 (1H, br s, NH), 7.58 (1H, s, H₆), 7.50-7.18 (15H, m, Ar-H), 6.37-6.30 (1H, m, H₁), 4.56-4.49 (1H, m, H₃), 4.19-4.11 (3H, m, H₄, OCH₂), 3.47 (1H, dd, ²J 10.6, ³J 3.0, H_{5'}), 3.38 (1H, dd, ²J 10.6, ³J 3.0, H₅), 2.58-2.47 (1H, m, H₂), 2.41 (1H, t, ⁴J 2.4, C≡CH), 2.29-2.19 (1H, m, H₂), 1.49 (3H, s, Me).



3'-O-(2-Propynyl)thymidine 151

This compound prepared according to a literature procedure, was obtained as an off-white foam (257mg, 96%). The data agreed with that reported.¹⁰³

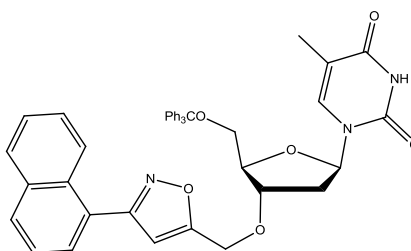
¹H NMR: δ 9.45 (1H, br s, NH), 7.44 (1H, s, H₆), 6.12 (1H, t, ³J 6.6, H_{1'}), 4.46-4.38 (1H, m, H_{3'}), 4.29-4.09 (3H, m, H_{4'}, OCH₂), 3.95 (1H, dd, ²J 12.1, ³J 2.7, H_{5'}), 3.82 (1H, dd, ²J 12.1, ³J 3.0, H_{5'}), 3.58 (1H, br s, OH), 2.49 (1H, t, ⁴J 2.4, C \equiv CH), 2.46-2.30 (2H, m, H_{2'}), 1.90 (3H, s, Me).



3'-O-[(3-Phenylisoxazol-5-yl)methyl]-5'-O-(triphenylmethyl)thymidine 152

This compound prepared according to a literature procedure, was obtained as an off-white foam (118 mg, 96%). The data agreed with that reported.¹⁰³

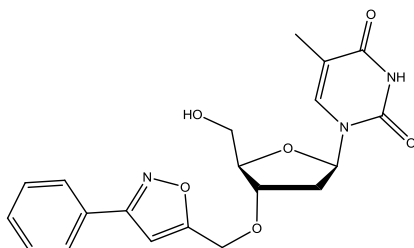
¹H NMR: δ 8.78 (1H, br s, NH), 7.83-7.18 (21H, m, H₆, Ar-H), 6.52 (1H, s, Isoxazole-H), 6.41-6.34 (1H, m, H_{1'}), 4.65 (1H, d, ²J 13.9, OCH₂), 4.58 (1H, d, ²J 13.9, OCH₂), 4.38-4.32 (1H, m, H_{3'}), 4.21-4.16 (1H, m, H_{4'}), 3.50 (1H, dd, ²J 10.6, ³J 3.3, H_{5'}), 3.35 (1H, dd, ²J 10.6, ³J 2.7, H_{5'}), 2.59-2.49 (1H, m, H_{2'}), 2.31-2.18 (1H, m, H_{2'}), 1.52 (3H, s, Me).



3'-O-[3-[(1-Naphthyl)isoxazol-5-yl]methyl]-5'-O-(triphenylmethyl)thymidine 153

This compound prepared according to a literature procedure, was obtained as an off-white foam (124 mg, 94%). The data agreed with that reported.¹⁰³

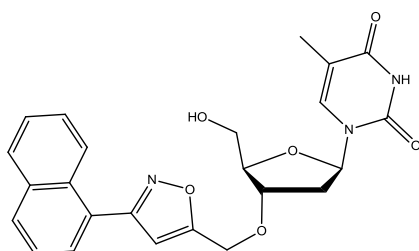
¹H NMR: δ 8.41 (1H, br s, NH), 8.38-7.17 (23H, m, H₆, Ar-H), 6.53 (1H, s, Isoxazole-H), 6.42-6.35 (1H, m, H_{1'}), 4.73 (1H, d, ²J 13.6, OCH₂), 4.65 (1H, d, ²J 13.6, OCH₂), 4.45-4.38 (1H, m, H_{3'}), 4.24-4.17 (1H, m, H_{4'}), 3.52 (1H, dd, ²J 10.7, ³J 3.3, H_{5'}), 3.37 (1H, dd, ²J 10.6, ³J 3.0, H_{5'}), 2.65-2.51 (1H, m, H_{2'}), 2.34-2.21 (1H, m, H_{2'}), 1.52 (3H, s, Me).



3'-O-[(3-Phenylisoxazol-5-yl)methyl]thymidine 154

This compound prepared according to a literature procedure, was obtained as an off-white solid (125 mg, 88%). The data agreed with that reported.¹⁰³

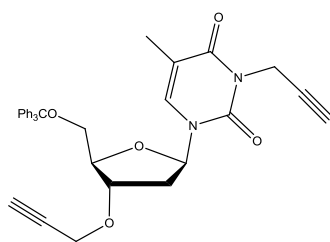
¹H NMR: δ 8.55 (1H, br s, NH), 7.81-7.78 (2H, m, Ar-H), 7.46-7.44 (3H, m, Ar-H), 7.38 (1H, s, H₆), 6.59 (1H, s, Isoxazole-H), 6.13 (1H, t, ²J 7.2, H_{1'}), 4.72 (1H, d, ²J 13.8, OCH₂), 4.66 (1H, d, ²J 13.8, OCH₂), 4.40-4.37 (1H, m, H_{3'}), 4.15 (1H, d, ²J 2.7, H_{4'}), 3.92 (1H, dd, ²J 11.7, ³J 2.7, H_{5'}), 3.80 (1H, dd, ²J 11.7, ³J 3.0, H_{5'}), 2.41-2.37 (2H, m, H_{2'}), 1.89 (3H, s, Me).



3'-O-[3-[(1-Naphthyl)isoxazol-5-yl]methyl]thymidine 155

This compound prepared according to a literature procedure, was obtained as an off-white solid (141 mg, 88%). The data agreed with that reported.¹⁰³

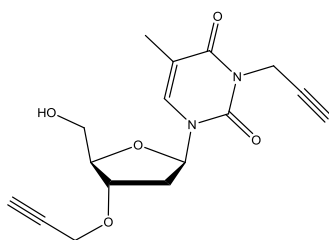
¹H NMR: δ 8.39-8.32 (1H, m, Ar-H), 7.99-7.89 (2H, m, Ar-H), 7.72-7.67 (1H, m, Ar-H), 7.60-7.50 (3H, m, Ar-H), 7.38 (1H, s, H₆), 6.62 (1H, s, Isoxazole-H), 6.14 (1H, t, ³J 9.9, H_{1'}), 4.78 (1H, d, ²J 13.9, OCH₂), 4.73 (1H, d, ²J 13.9, OCH₂), 4.49-4.41 (1H, m, H_{3'}), 4.23-4.16 (1H, m, H_{4'}), 3.96 (1H, dd, ²J 12.5, ³J 3.3, H_{5'}), 3.83 (1H, dd, ²J 12.4, ³J 2.7, H_{5'}), 2.49-2.40 (2H, m, H_{2'}), 1.92 (3H, s, Me).



3-(2-Propynyl)-3'-O-(2-propynyl)-5'-O-(triphenylmethyl)thymidine 156

This compound prepared according to a literature procedure, was obtained as an off-white foam (433mg, 77%). The data agreed with that reported.¹⁰³

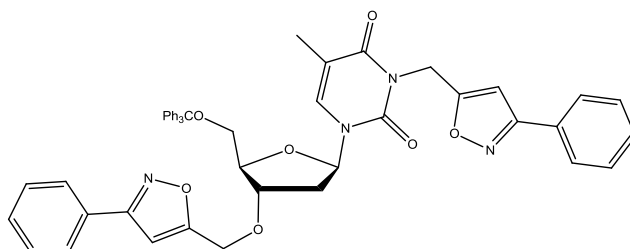
¹H NMR: δ 7.62 (1H, s, H₆), 7.50-7.20 (15H, m, Ar-H), 6.42-6.34 (1H, m, H_{1'}), 4.77 (2H, d, ⁴J 2.4, NCH₂), 4.58-4.49 (1H, m, H_{3'}), 4.25-4.07 (3H, m, H_{4'}, OCH₂), 3.47 (1H, dd, ²J 10.7, ³J 3.0, H_{5'}), 3.38 (1H, dd, ²J 10.7, ³J 3.0, H_{5'}), 2.61-2.50 (1H, m, H_{2'}), 2.41 (1H, t, ⁴J 2.4, OCH₂C \equiv CH), 2.32-2.19 (1H, m, H_{2'}), 2.17 (1H, t, ⁴J 2.4, NCH₂C \equiv CH), 1.51 (3H, s, Me).



3-(2-Propynyl)-3'-O-(2-propynyl)thymidine 157

This compound prepared according to a literature procedure, was obtained as an off-white foam (213 mg, 94%). The data agreed with that reported.¹⁰³

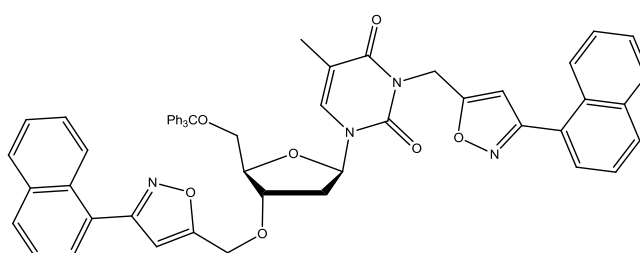
¹H NMR: δ 7.43 (1H, s, H₆), 6.14 (1H, t, ³J 7.5, H_{1'}), 4.72 (2H, d, ⁴J 2.4, NCH₂), 4.47-4.40 (1H, m, H_{3'}), 4.28-4.05 (4H, m, H_{4'}, OCH₂, OH), 3.97 (1H, dd, ²J 12.5, ³J 2.7, H_{5'}), 3.85 (1H, dd, ²J 12.5, ³J 3.0, H_{5'}), 2.49 (1H, t, ⁴J 2.4, OCH₂C \equiv CH), 2.47-2.36 (2H, m, H_{2'}), 2.17 (1H, t, ⁴J 2.4, NCH₂C \equiv CH), 1.96 (3H, s, Me).



3-[(3-Phenylisoxazol-5-yl)methyl]-3'-O-[(3-phenylisoxazol-5-yl)methyl]-5'-O-(triphenylmethyl)thymidine 158

This compound prepared according to a literature procedure, was obtained as an off-white solid (123 mg, 87%). The data agreed with that reported.¹⁰³

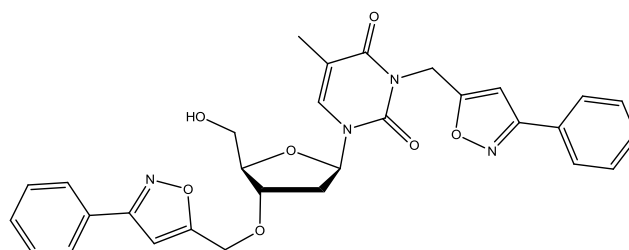
¹H NMR: δ 7.81-7.73 (5H, m, Ar-H), 7.62 (1H, s, H₆), 7.49-7.20 (20H, m, Ar-H), 6.57 (1H, s, Isoxazole-H), 6.51 (1H, s, Isoxazole-H), 6.44-6.37 (1H, m, H_{1'}), 5.31 (2H, m, NCH₂), 4.65 (1H, d, ²J 13.6, OCH₂), 4.58 (1H, d, ²J 13.6, OCH₂), 4.40-4.33 (1H, m, H₃), 4.21-4.15 (1H, m, H₄), 3.51 (1H, dd, ²J 10.9, ³J 3.3, H₅), 3.35 (1H, dd, ²J 10.7, ³J 2.7, H₅), 2.61-2.52 (1H, m, H₂), 2.32-2.20 (1H, m, H₂), 1.54 (3H, s, Me).



3-[3-[(Naphthyl)isoxazol-5-yl]methyl]-3'-O-[3-[(naphthyl)isoxazol-5-yl]methyl]-5'-O-(triphenylmethyl)thymidine 159

This compound prepared according to a literature procedure, was obtained as an off-white solid (138 mg, 86%). The data agreed with that reported.¹⁰³

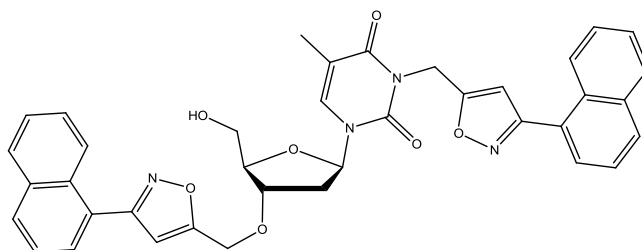
¹H NMR: δ 8.43-8.29 (2H, m, Ar-H), 7.99-7.84 (4H, m, Ar-H), 7.70-7.17 (24H, m, H₆, Ar-H), 6.59 (1H, s, Isoxazole-H), 6.52 (1H, s, Isoxazole-H), 6.49-6.42 (1H, m, H_{1'}), 5.38 (2H, s, NCH₂), 4.72 (1H, d, ²J 13.4, OCH₂), 4.64 (1H, d, ²J 13.4, OCH₂), 4.49-4.39 (1H, m, H₃), 4.26-4.18 (1H, m, H₄), 3.54 (1H, dd, ²J 10.7, ³J 3.0, H₅), 3.38 (1H, dd, ²J 10.7, ³J 2.7, H₅), 2.67-2.56 (1H, m, H₂), 2.38-2.26 (1H, m, H₂), 1.56 (3H, s, Me).



3-[(3-Phenylisoxazol-5-yl)methyl]-3'-O-[(3-phenylisoxazol-5-yl)methyl] thymidine 160

This compound prepared according to a literature procedure, was obtained as an off-white solid (140 mg, 80%). The data agreed with that reported.¹⁰³

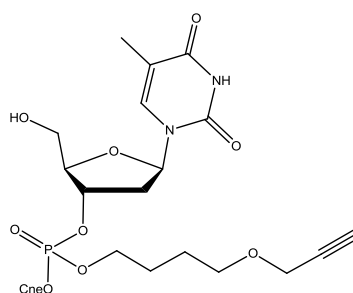
^1H NMR: δ 7.78-7.64 (4H, m, Ar-H), 7.44-7.28 (7H, m, H_6 , Ar-H), 6.52 (1H, s, Isoxazole-H), 6.49 (1H, s, Isoxazole-H), 6.11 (1H, t, ^3J 7.7, $\text{H}_{1'}$), 5.22 (2H, s, NCH_2), 4.63 (1H, d, ^2J 13.4, OCH_2), 4.58 (1H, d, ^2J 13.4, OCH_2), 4.36-4.28 (1H, m, H_3'), 4.12-4.06 (1H, m, H_4'), 3.88 (1H, dd, ^2J 11.6, ^3J 2.4, H_5'), 3.74 (1H, br d, ^2J 11.5, H_5'), 2.52-2.25 (3H, m, H_2' , OH), 1.88 (3H, s, Me).



**3-[3-[(Naphthyl)isoxazol-5-yl]methyl]-3'-O-[3-[(naphthyl)isoxazol-5-yl]methyl] thymidine
161**

This compound prepared according to a literature procedure, was obtained as an off-white solid (160 mg, 78%). The data agreed with that reported.¹⁰³

^1H NMR: δ 8.40-8.31 (2H, m, Ar-H), 7.99-7.83 (4H, m, Ar-H), 7.73-7.44 (9H, m, H_6 , Ar-H), 6.60 (1H, s, Isoxazole-H), 6.58 (1H, s, Isoxazole-H), 6.26-6.19 (1H, m, $\text{H}_{1'}$), 5.37 (2H, s, NCH_2), 4.76 (1H, d, ^2J 13.6, OCH_2), 4.70 (1H, d, ^2J 13.6, OCH_2), 4.48-4.39 (1H, m, H_3'), 4.22-4.14 (1H, m, H_4'), 3.79-3.40 (2H, m, H_5'), 2.68 (1H, s, OH), 2.54-2.33 (2H, m, H_2'), 1.95 (3H, s, Me).

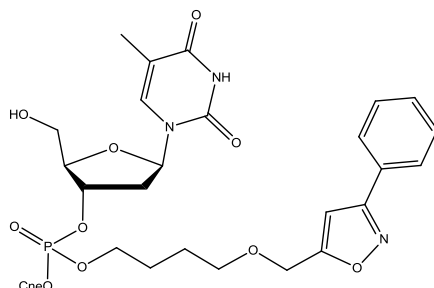


3'-Thymidylic acid, 2-cyanoethyl 4-(2-propynyl-1-yloxy)butyl ester 166

This compound prepared according to a literature procedure, was obtained as an off-yellow oil (144 mg, 53%). The data agreed with that reported.¹⁰³

^1H NMR (d_6 -DMSO): δ 9.71 (1H, br s, NH), 7.55 (1H, s, H_6), 6.24 (1H, t, ^3J 7.2, $\text{H}_{1'}$), 5.17 (1H, br s, H_3'), 4.35-4.10 (7H, m, H_4' , OCH_2 isoxazole, 2 x POCH_2), 3.88 (1H, br s, H_5'),

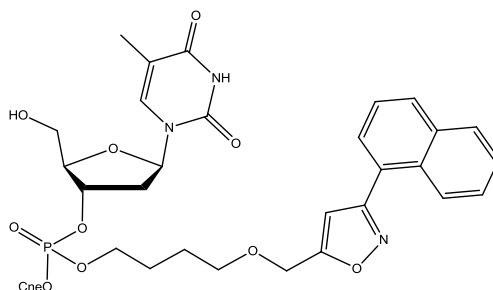
3.76 (1H, br s, OH), 3.56 (2H, t, 3J 5.6, OCH_2CH_2), 2.82 (2H, t, 3J 5.6, CH_2CN), 2.60-2.35 (3H, m, 2 x H_2 , $C\equiv CH$), 1.90 (3H, s, Me), 1.86-1.63 (4H, m, $CH_2CH_2CH_2CH_2$).



3'-Thymidylic acid, 2-cyanoethyl 4-[[3-(phenylisoxazole-5-yl)methyl]oxy]butyl ester
167

This compound prepared according to a literature procedure, was obtained as an off-yellow oil (48 mg, 77%). The data agreed with that reported.¹⁰³

1H NMR (d_6 -DMSO): δ 9.45 (1H, br s, NH), 7.82-7.75 (2H, m, Ar-H), 7.51 (1H, s, H_6), 7.48-7.41 (3H, m, Ar-H), 6.58 (1H, s, Isoxazole-H), 6.22 (1H, t, 3J 7.5, H_1), 5.19-5.12 (1H, m, H_3), 4.63 (2H, m, OCH_2 -iso), 4.33-4.11 (5H, m, H_4 , 2 x OCH_2), 3.87 (2H, br s, H_5), 3.61 (2H, t, 3J 6.0, OCH_2CH_2), 2.78 (2H, t, 3J 6.0, CH_2CN), 2.59-2.40 (2H, m, H_2), 2.17 (1H, br s, OH), 1.92-1.69 (7H, m, Me, $CH_2CH_2CH_2CH_2$).

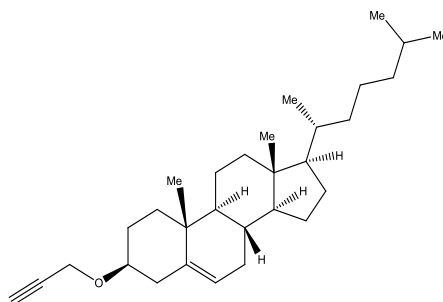


3'-Thymidylic acid, 2-cyanoethyl 4-[[3-[(1-naphthyl)isoxazole-5-yl]methyl]oxy]butyl ester 168

This compound prepared according to a literature procedure, was obtained as an off-yellow oil (49 mg, 72%). The data agreed with that reported.¹⁰³

1H NMR (d_6 -DMSO): δ 8.91 (1H, br s, NH), 8.38-8.31 (1H, m, Ar-H), 7.99-7.88 (2H, m, Ar-H), 7.73-7.67 (1H, m, Ar-H), 7.59-7.50 (3H, m, Ar-H), 7.43 (1H, s, H_6), 6.59 (1H, s, Isoxazole-H), 6.19 (1H, t, 3J 7.2, H_1), 5.19-5.11 (1H, m, H_3), 4.71 (2H, m, OCH_2 -iso), 4.34-

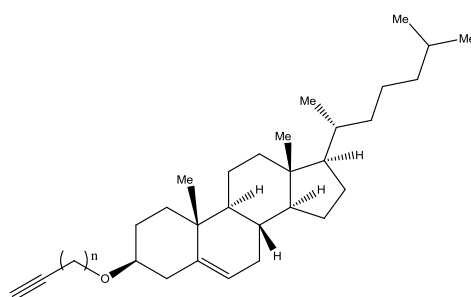
4.13 (5H, m, H₄, 2 x OCH₂), 3.88 (2H, br s, H₅), 3.67 (2H, t, ³J 6.0, OCH₂CH₂), 3.18 (1H, br s, OH), 2.77 (2H, t, ³J 6.0, CH₂CN), 2.58-2.40 (2H, m, H₂), 1.95-1.70 (7H, m, Me, CH₂CH₂CH₂CH₂).



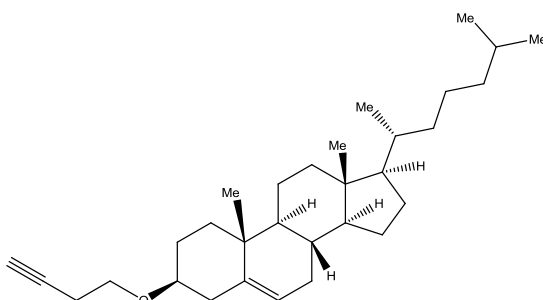
Propargyl cholesteryl ether **169**

This compound, prepared according to a literature procedure, was isolated as an off-white solid in 44% yield (483 mg). The data agreed with that reported.⁹⁰

¹H NMR: δ 5.37 (1H, br d, ²J 5.2, CH=C); 4.19 (2H, d, ³J 2.4 Hz, OCH₂), 3.47-3.31 (1H, m, OCH), 2.42-0.80 (47H, m), 0.68 (3H, s, Me).



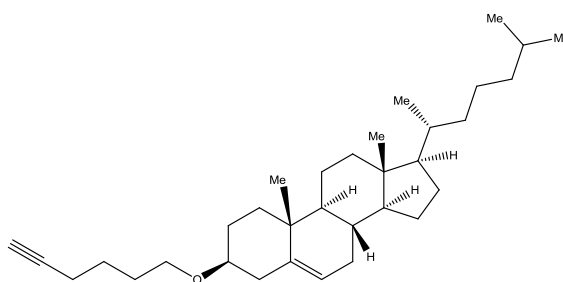
General etherification procedure: A mixture of cholesterol (500 mg, 1.29 mmol), alkyne alcohol (6.47 mmol, 5 eq), and MK-10 (1.00 g, activated at 120 °C overnight prior to use) in chloroform (5 mL), was heated to 90 °C for 8 h in a scientific MW (10 mL vessel, P_{max} = 300 W). After solvent removal under reduced pressure, hexane (20 mL) was added and the catalyst was removed by filtration and washed with hexane. Following the evaporation of the filtrate and washings, the residue was purified by flash column chromatography (SiO₂, hexane, AcOEt 0 to 5%) to give the title compound as a white solid (373 mg, 68% for **169** n = 1; 353 mg, 62% for **170** n = 2; 423 mg, 70% for **171** n = 4).



Butynyl cholesteryl ethers 170

The title compound was isolated as a white solid in 62% (353 mg). The data agreed with that reported in the literature.²²²

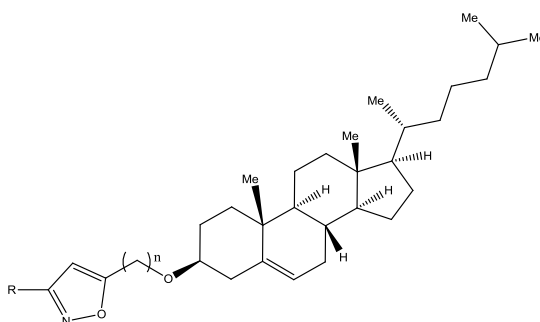
¹H NMR: δ 5.35 (1H, br d, ²J 5.2, CH=C), 3.60 (2H, t, ³J 7.1, OCH₂), 3.19-3.03 (1H, m, OCH), 2.45 (2H, t, ³J 2.6, 7.1, OCH₂CH₂), 1.97 (1H, t, ⁴J 2.6, CHCCH₂), 1.88-0.80 (40H, m), 0.68 (3H, s, Me).



Hexynyl cholesteryl ethers 171

The title compound was isolated as a white solid in 70% yield (423 mg).

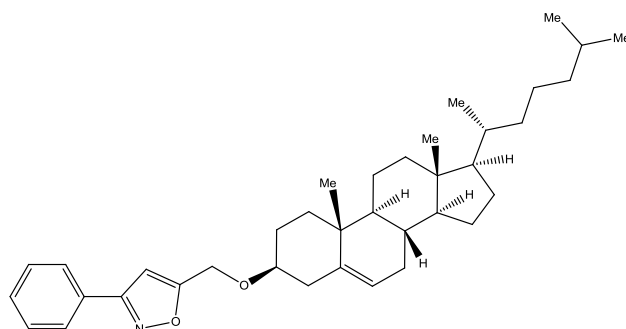
R_f : 0.80 (hexane, AcOEt, 9:1); Mp: 112-114 °C. ¹H NMR: δ 5.34 (1H, br d, ³J 5.2, CH=C), 3.47 (2H, t, ³J 7.1, OCH₂), 3.19-3.05 (1H, m, OCH), 2.45 (2H, t, ³J 7.1, OCH₂CH₂), 1.97 (1H, t, ⁴J 2.6, CHCCH₂), 1.88-0.80 (40H, m), 0.68 (3H, s, Me). ¹³C NMR: δ 141.1 (C=CH), 121.5 (C=CH), 84.4 (CH≡C), 79.0 (OCH), 68.3 (OCH₂), 67.4 (CH≡C), 56.8, 56.2, 50.2, 42.3, 39.8, 39.5, 39.2, 37.3, 36.9, 36.2, 35.8, 32.0, 31.9, 29.2, 28.5, 28.3, 28.0, 25.3, 24.3, 23.8, 22.8, 19.4, 18.8, 18.3, 11.9.



General procedure for the cycloaddition reaction to alkyne cholesterol ether:

To a round bottomed flask containing the oxime **118** or **119** (2 eq) and CAT (2.5 eq) in EtOH (1 mL per 0.1 mmol oxime) was added the alkyne **169**, **170** or **171** (1 eq). The mixture was stirred for 1 h at rt. After solvent removal, the residue was dissolved in chloroform and washed with H₂O. The organic layer was dried over anhydrous Na₂SO₄ and the solvent was

removed. The crude reaction product was purified by flash column chromatography (SiO₂, hexane, AcOEt 0 to 5%) to give the title compound as an off-white solid.

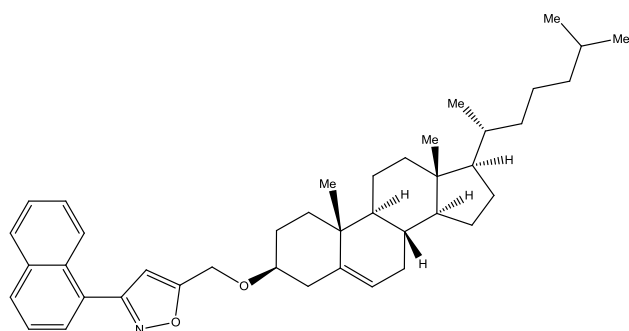


[3-Phenyl-isoxazole]methyl cholesteryl ether 172

Method 1 (general procedure): The title compound was isolated as a white solid in 19% yield (25 mg).

Method 2 (MW activation): To a 10 mL vessel containing the benzaldehyde oxime **118** (58 mg, 0.47 mmol, 2 eq) and CAT (134 mg, 0.59 mmol, 2.5 eq) in EtOH (3 mL) was added the cholesteryl propargyl ether **169** (100 mg, 0.24 mmol). The mixture was heated to 100 °C for 1 h in a scientific MW (Pmax = 300 W). After solvent removal, the residue was dissolved in chloroform and washed with H₂O. The organic layer was dried over anhydrous Na₂SO₄ and the solvent was removed under reduced pressure. The crude reaction product was purified by flash column chromatography (SiO₂, hexane, AcOEt 0 to 5%) to give the title compound as an off-white solid (103 mg, 78%).

R_f : 0.54 (hexane, AcOEt, 9:1); Mp: 123-125 °C. ¹H NMR: δ 7.85-7.76 (2H, m, Ar-H), 7.48-7.40 (3H, m, Ar-H), 6.56 (1H, s, Isoxazole-H), 5.37 (1H, br s, CH=C), 4.69 (2H, s, OCH₂), 3.42-3.27 (1H, m, OCH), 2.47-0.79 (40H, m), 0.68 (3H, s, Me). ¹³C NMR: δ 170.7 (C=N), 162.4 (isoxazole-CO), 140.4 (C=CH), 130.0, 129.1, 128.9, 126.8 (Ar-C + 5 x Ar-CH), 122.1 (C=CH), 100.7 (isoxazole-CH), 79.6 (OCH), 61.1 (OCH₂), 56.8, 56.2, 50.2, 42.3, 39.8, 39.5, 38.9, 37.1, 36.8, 36.2, 35.8, 32.0, 31.9, 28.3, 28.2, 28.0, 24.3, 23.8, 22.8, 22.6, 21.1, 19.4, 18.7, 11.9.

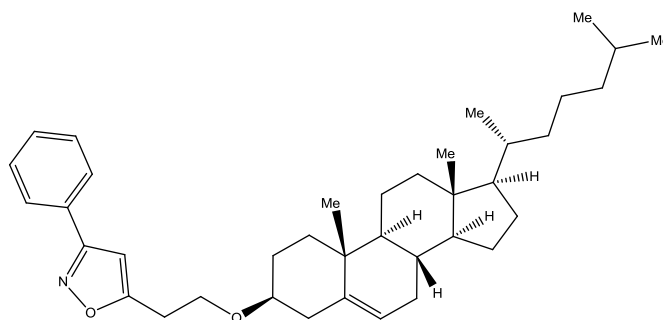


[3-(1-Naphtyl)isoxazole]methyl cholesteryl ether 173

Method 1 (general procedure): The title compound was isolated as a white solid in 43% yield (61 mg).

Method 2 (MW activation): To a 10 mL vessel containing the naphthalene oxime **119** (81 mg, 0.47 mmol, 2 eq) and CAT (134 mg, 0.59 mmol, 2.5 eq) in EtOH (3 mL) was added the cholesteryl propargyl ether **169** (100 mg, 0.24 mmol). The mixture was heated to 60 °C for 30 min in a scientific MW (Pmax = 300 W). After solvent removal, the residue was dissolved in chloroform and washed with H₂O. The organic layer was dried over anhydrous Na₂SO₄ and the solvent was removed under reduced pressure. The crude reaction product was purified by flash column chromatography (SiO₂, hexane, AcOEt 0 to 5%) to give the title compound as an off-white solid (138 mg, 96%).

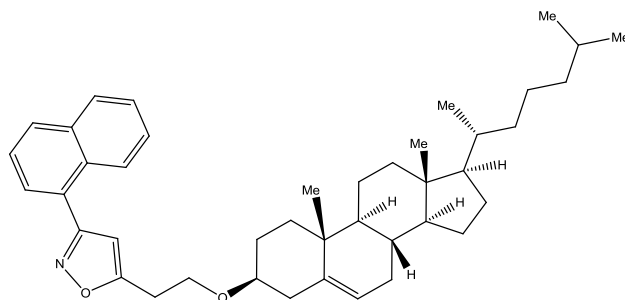
R_f : 0.62 (hexane, AcOEt, 9:1); Mp: 146-148 °C. ¹H NMR: δ 8.42-8.33 (1H, m, Ar-H), 7.98-7.85 (2H, m, Ar-H), 7.73-7.65 (1H, m, Ar-H), 7.53-7.47 (3H, m, Ar-H), 6.57 (1H, s, Isoxazole-H), 5.38 (1H, br s, CH=C), 4.76 (2H, s, OCH₂), 3.48-3.32 (1H, m, OCH), 2.53-2.24 (2H, m), 2.10-1.74 (6H, m), 1.66-0.80 (34H, m), 0.68 (3H, s, Me). ¹³C NMR: δ 170.0 (C=N), 162.5 (isoxazole-CO), 140.4 (C=CH), 133.9, 131.0, 130.2, 128.5, 127.8, 127.0, 126.9, 126.3, 125.7, 125.2 (3 x Ar-C + 7 x Ar-CH), 122.2 (C=CH), 104.1 (isoxazole-CH), 79.9 (OCH), 61.2 (OCH₂), 56.8, 56.2, 50.2, 42.3, 39.8, 39.6, 39.0, 37.2, 36.9, 36.2, 35.8, 32.0, 31.9, 28.3, 28.2, 28.0, 24.3, 23.8, 22.8, 22.6, 21.1, 19.4, 18.8, 11.9.



2-[3-Phenyl-5-isoxazolyl]-1-ethyl cholesteryl ether 174

The title compound was isolated as a white solid in 44% yield (57 mg).

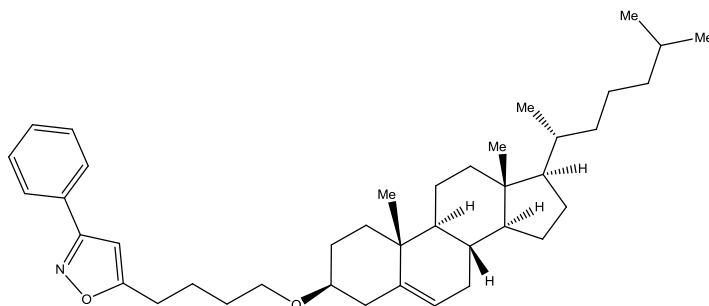
R_f : 0.60 (hexane, AcOEt, 9:1); Mp: 112-114 °C. ¹H NMR: δ 7.83-7.74 (2H, m, Ar-H), 7.49-7.42 (3H, m, Ar-H), 6.39 (1H, s, Isoxazole-H), 5.35 (1H, br s, CH=C), 3.86 (2H, t, ³J 6.6, OCH₂), 3.31-3.08 (1H, m, OCH), 3.11 (2H, t, ³J 6.6, isoxazole-CH₂), 2.45-0.80 (40H, m), 0.67 (3H, s, Me). ¹³C NMR: δ 170.6 (C=N), 162.2 (isoxazole-CO), 140.1 (C=CH), 130.0, 129.2, 128.8, 126.9 (Ar-C + 5 x Ar-CH), 122.0 (C=CH), 103.4 (isoxazole-CH), 79.6 (OCH), 65.0 (OCH₂), 56.8, 56.2, 50.2, 42.4, 39.8, 39.5, 39.2, 37.2, 36.9, 36.2, 35.8, 32.1, 31.9, 28.4, 28.2, 28.0, 24.3, 23.8, 22.8, 22.6, 21.1, 19.4, 18.8, 11.9.



2-[3-(1-Naphthyl)-5-isoxazolyl]-1-ethyl cholesteryl ether 175

The title compound was isolated as a white solid in 54% yield (76 mg).

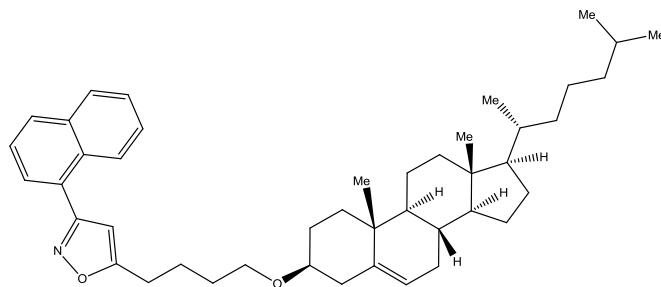
R_f : 0.65 (hexane, AcOEt, 9:1); Mp: 134-136 °C. ¹H NMR: δ 8.41-8.34 (1H, m, Ar-H), 7.99-7.87 (2H, m, Ar-H), 7.73-7.65 (1H, m, Ar-H), 7.57-7.46 (3H, m, Ar-H), 6.42 (1H, s, Isoxazole-H), 5.35 (1H, br s, CH=C), 3.87 (2H, t, ³J 6.6, OCH₂), 3.30-3.10 (1H, m, OCH), 3.14 (2H, t, ³J 6.6, isoxazole-CH₂), 2.45-2.14 (2H, m), 2.10-0.80 (38H, m), 0.67 (3H, s, Me). ¹³C NMR: δ 170.8 (C=N), 162.6 (isoxazole-CO), 140.7 (C=CH), 133.8, 131.1, 130.0, 128.4, 127.6, 127.3, 126.9, 126.2, 125.7, 125.2 (3 x Ar-C + 7 x Ar-CH), 121.9 (C=CH), 103.4 (isoxazole-CH), 79.5 (OCH), 65.1 (OCH₂), 56.8, 56.2, 50.2, 42.3, 39.8, 39.5, 39.1, 37.2, 36.9, 36.2, 35.8, 32.0, 31.9, 28.4, 28.2, 28.0, 24.3, 23.8, 22.8, 22.6, 21.1, 19.4, 18.7, 11.9.



4-[3-Phenyl-5-isoxazolyl]-1-butyl cholesteryl ether 176

The title compound was isolated as a white solid in 90% yield (115 mg).

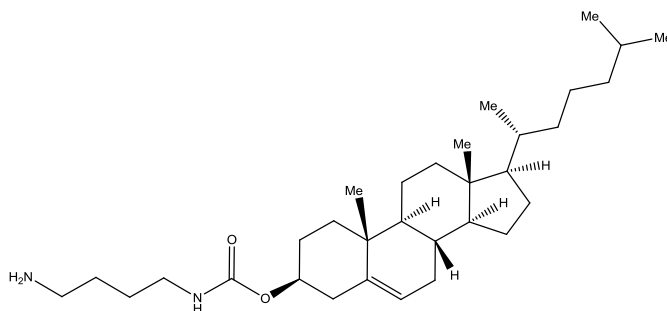
R_f : 0.60 (hexane, AcOEt, 9:1); Mp: 128-130 °C. ¹H NMR: δ 7.83-7.74 (2H, m, Ar-H), 7.49-7.42 (3H, m, Ar-H), 6.32 (1H, s, Isoxazole-H), 5.35 (1H, br s, CH=C), 3.53 (2H, t, ³J 6.3, OCH₂), 3.27-3.08 (1H, m, OCH), 2.90 (2H, t, ³J 6.3, isoxazole-CH₂), 2.44-0.80 (44H, m), 0.67 (3H, s, Me). ¹³C NMR: δ 174.0 (C=N), 162.4 (isoxazole-CO), 141.0 (C=CH), 129.9, 129.4, 128.9, 126.8 (Ar-C + 5 x Ar-CH), 121.6 (C=CH), 99.0 (isoxazole-CH), 79.1 (OCH), 67.3 (OCH₂), 56.8, 56.2, 50.2, 42.3, 39.8, 39.5, 39.2, 38.7, 37.3, 36.9, 36.2, 31.9, 31.0, 30.3, 29.6, 28.9, 28.5, 26.7, 24.4, 24.3, 23.8, 22.8, 22.6, 21.1, 18.8, 11.9.



4-[3-(1-Naphtyl)-5-isoxazolyl]-1-butyl cholesteryl ether 177

The title compound was isolated as a white solid in 90% yield (125 mg).

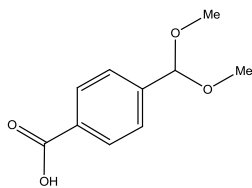
R_f : 0.69 (hexane, AcOEt, 9:1); Mp: 130-132 °C. ¹H NMR: δ 8.41-8.33 (1H, m, Ar-H), 7.98-7.87 (2H, m, Ar-H), 7.72-7.66 (1H, m, Ar-H), 7.59-7.49 (3H, m, Ar-H), 6.32 (1H, s, Isoxazole-H), 5.35 (1H, br s, CH=C), 3.53 (2H, t, ³J 6.3, OCH₂), 3.27-3.08 (1H, m, OCH), 2.90 (2H, t, ³J 6.3, isoxazole-CH₂), 2.44-0.80 (44H, m), 0.67 (3H, s, Me). ¹³C NMR: δ 172.2 (C=N), 161.4 (isoxazole-CO), 139.9 (C=CH), 132.7, 130.0, 129.0, 127.4, 126.6, 126.2, 125.9, 125.2, 124.7, 124.1 (3 x Ar-C + 7 x Ar-CH), 120.5 (C=CH), 101.4 (isoxazole-CH), 78.1 (OCH), 66.3 (OCH₂), 55.7, 55.1, 49.1, 41.3, 38.7, 38.5, 38.1, 36.2, 35.8, 35.2, 34.8, 30.9, 30.8, 28.6, 27.4, 27.2, 27.0, 25.6, 23.4, 23.3, 22.8, 21.5, 20.0, 18.4, 17.7, 10.8.



3β-Cholest-5-en-3-yl *N*-(3-aminobutyl)carbamate 180

This compound, prepared according to a literature procedure, was obtained as an off-white solid in 88% yield (mg). The data agreed with that reported.²²³

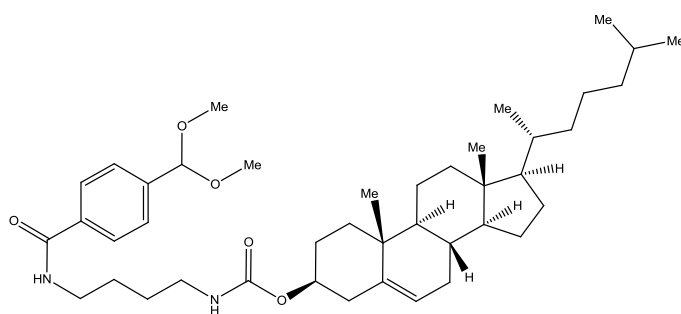
¹H NMR: δ 5.37 (1H, br s, CH=C), 4.77 (1H, br s, NH), 4.41-4.58 (1H, m, OCH), 3.25-3.12 (2H, m, NHCH₂), 2.66-2.2.80 (2H, m, NH₂CH₂), 2.21-0.96 (46H, m), 0.68 (3H, s, Me).



4-(Dimethoxymethyl)benzoic acid **181**

This compound prepared according to a literature procedure, was obtained as a colorless oil in 89% yield (620 mg). The data agreed with that reported.²²⁴

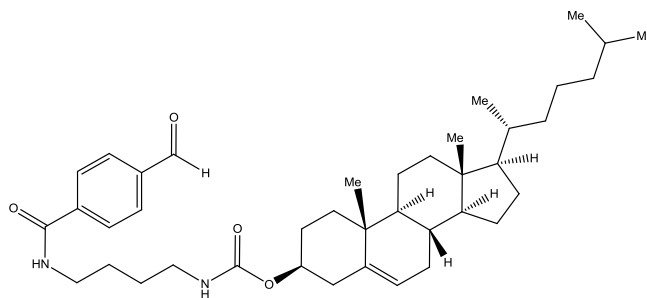
¹H NMR: δ 7.39 (2H, d, ³J 8.0, Ar-H), 7.32 (2H, d, ³J 8.0, Ar-H), 5.43 (1H, s, CH), 3.29 (6H, s, 2 x Me).



3 β -Cholest-5-en-3-yl *N*-{3-[(4-dimethoxylbenzoyl)amino]butyl}carbamate **182**

To a suspension of the amino-carbamate cholesterol **180** (200 mg, 0.40 mmol) and 4-(dimethoxymethyl)benzoic acid **181** (94 mg, 0.48 mmol, 1.2 eq) in dry DCM (5 mL) and dry toluene (5 mL) was added DCC (99 mg, 0.48 mmol, 1.2 eq) and DMAP (59 mg, 0.48 mmol, 1.2 eq) at 0 °C under argon. After stirring at room temperature for 17 h, the solvent was removed to afford the residue, which was purified by flash column chromatography (SiO₂, hexane, AcOEt 35%) to give the title compound as an off-white solid (144 mg, 53%).

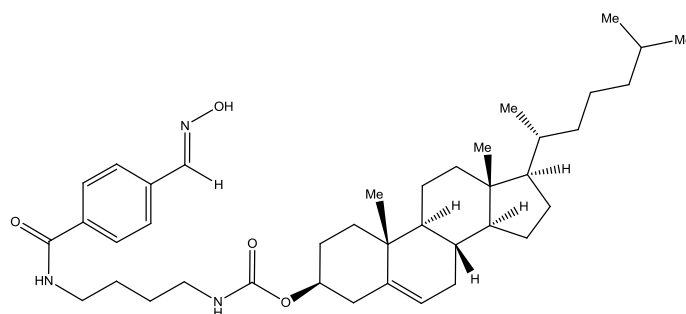
*R*_f : 0.79 (hexane, AcOEt, 7:3); Mp: 158-160 °C; ¹H NMR: δ 7.78 (2H, d, ³J 8.3, Ar-H), 7.52 (2H, d, ³J 8.3, Ar-H), 6.38 (1H, br s, NH), 5.52 (1H, s, CH(OMe)₂), 5.43 (1H, br s, CH=C), 4.70 (1H, br s, NH), 4.55-4.41 (1H, m, OCH), 3.55-3.45 (2H, m, CONHCH₂), 3.32 (3H, s, OMe), 3.31 (3H, s, OMe), 3.28-3.17 (2H, m, OCONHCH₂), 2.41-0.96 (44H, m), 0.68 (3H, s, Me). ¹³C NMR: δ 167.3 (CONH), 156.4 (OCONH), 141.4 (C=CH), 139.8, 134.7 (2 x Ar-C), 126.9, 126.9, 126.9, 126.8 (4 x Ar-CH), 122.5 (C=CH), 102.4 (CH(OMe)₂), 76.6 (OCH), 56.7, 56.2, 52.6, 50.0, 49.1, 42.3, 40.4, 39.8, 39.7, 39.5, 38.6, 37.0, 36.6, 36.2, 35.8, 34.0, 31.9, 28.2, 28.0, 27.7, 25.6, 25.2, 24.2, 23.8, 22.8, 22.6, 21.1, 19.4, 18.8, 11.9.



3β-Cholest-5-en-3-yl *N*-{3-[(4-formylbenzoyl)amino]butyl}carbamate **183**

To a solution of crude protected aldehyde **182** (512mg) in toluene (10 mL) was added a solution of 2N HCl (10 mL). After few minutes in a sonic bath, the emulsion was stirred for 2 h at rt. The reaction is carefully quenched with a sat. solution of NaHCO₃ until neutralization of the aqueous layer. The product is extracted with toluene, washed with water, dried over anhydrous Na₂SO₄ and the solvent was removed under reduced pressure to afford the residue which was purified by flash column chromatography (SiO₂, hexane, AcOEt 30 to 60%) to give the title compound as an off-white solid (from **181** to **183**, 50 mg, 10 %).

R_f : 0.58 (hexane, AcOEt, 8:2); Mp: 152-154 °C; ¹H NMR: δ 10.08 (1H, s, CHO), 7.96 (4H, s, Ar-H), 6.70 (1H, br s, NH), 5.37 (1H, br s, CH=C), 4.76 (1H, br s, NH), 4.56-4.42 (1H, m, OCH), 3.58-3.48 (2H, m, CONHCH₂), 3.28-3.17 (2H, m, OCONHCH₂), 2.41-0.81 (44H, m), 0.67 (3H, s, Me). ¹³C NMR: δ 191.6 (C=O), 167.8 (C=O), 157.4 (O=C), 139.8 (C=C), 138.1, 132.5 (2 x Ar-C), 130.9, 129.8, 128.8, 127.7 (4 x Ar-CH), 122.6 (C=C), 76.6 (OCH), 56.7, 56.2, 50.0, 42.3, 39.8, 39.6, 39.5, 38.7, 38.6, 37.0, 36.6, 36.2, 35.8, 31.9, 30.4, 28.9, 28.2, 28.0, 27.9, 24.3, 23.8, 23.0, 22.8, 22.6, 21.1, 19.3, 18.7, 11.0.



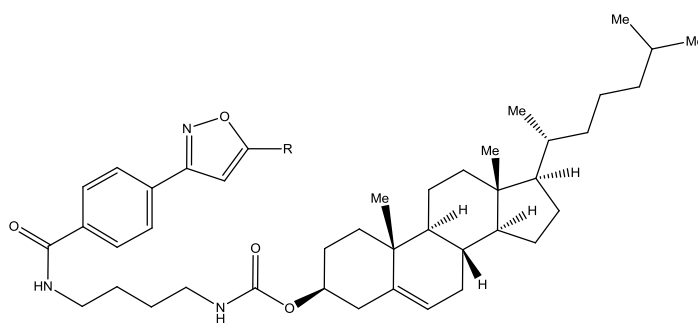
3β-Cholest-5-en-3-yl *N*-{3-[(4-hydroxyiminobenzoyl)amino]butyl}carbamate **178**

Method 1: A mixture of aldehyde **183** (80 mg, 0.13 mmol), hydroxylamine hydrochloride (14 mg, 0.19 mmol, 1.5 eq) and pyridine (15 mg, 0.19 mmol, 1.5 eq) in EtOH (3 mL) was heated to 125 °C for 1 h in MW (10 mL vessel, P_{max} = 300 W). After solvent

removal under reduced pressure, the residue was dissolved in chloroform, and washed with H₂O. The organic layer was dried over anhydrous Na₂SO₄, and the solvent was removed under reduced pressure to afford the pure oxime as a white-off solid (42 mg, 48%).

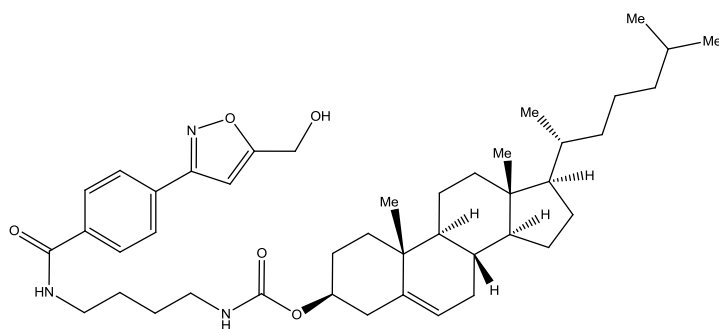
Method 2: A mixture of the protected aldehyde **182** (80 mg, 0.12 mmol), hydroxylamine hydrochloride (52 mg, 0.71 mmol, 6 eq) and pyridine (28 mg, 0.35 mmol, 3 eq) in EtOH (3 mL) was heated to 125 °C for 1 h in MW (10 mL vessel, P_{max} = 300 W). After solvent removal under reduced pressure, the residue was dissolved in chloroform, and washed with sat. sol. of NaHCO₃ and H₂O. The organic layer was dried over anhydrous Na₂SO₄, and the solvent was removed under reduced pressure to afford the pure oxime as a white-off solid (75 mg, 91%).

R_f : 0.60 (hexane, AcOEt, 8:2); Mp: 156-158 °C; ¹H NMR: δ 8.15 (1H, s, CHNOH), 7.80 (2H, d, ³J 8.1, Ar-H), 7.63 (2H, d, ³J 8.1, Ar-H), 6.47 (1H, br s, NH), 5.36 (1H, br s, CH=C), 4.73 (1H, br s, NH), 4.58-4.42 (1H, m, OCH), 3.56-3.45 (2H, m, CONHCH₂), 3.31-3.17 (2H, m, OCONHCH₂), 2.42-0.82 (44H, m), 0.68 (3H, s, Me). ¹³C NMR: δ 166.9 (C=O), 156.5 (OCONH), 149.9 (C=N), 139.8 (C=CH), 135.6, 135.0 (2 x Ar-C), 127.4, 127.4, 127.1, 127.1 (4 x Ar-CH), 122.5 (C=CH), 76.6 (OCH), 56.7, 56.2, 50.0, 42.3, 39.8, 39.5, 38.6, 37.0, 36.6, 36.2, 35.8, 31.9, 28.2, 28.2, 27.7, 26.5, 24.3, 23.8, 22.8, 22.6, 21.1, 19.3, 18.7, 11.9.



General Procedure for the cycloaddition:

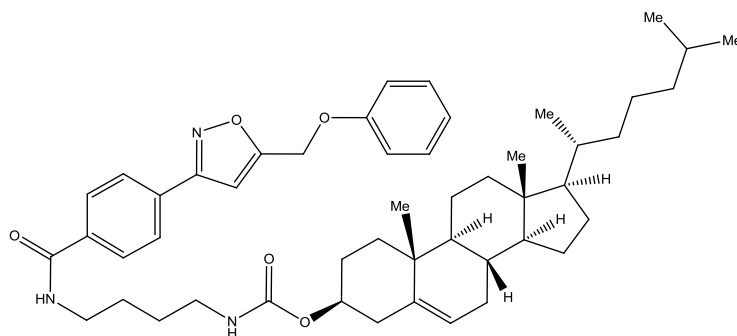
To a round bottomed flask containing the oxime **178** (2 eq) and CAT (2.5 eq) in EtOH (1 mL per 0.1 mmol oxime) was added the alkyne (1 eq). The mixture was stirred for 17 h at rt. The product was isolated following extraction with toluene, washed with H₂O. The organic layer was dried over anhydrous Na₂SO₄ and the solvent was removed under reduced pressure to afford the residue which was purified by flash column chromatography (SiO₂, hexane, AcOEt 0 to 15%) to give the title compound.



3β-Cholest-5-en-3-yl N-{3-[(4-[5-hydroxymethyl]-3-isoxazolyl)benzoyl]amino}butyl}carbamate 184

The title compound was isolated as a white-off solid in 21% yield (11 mg).

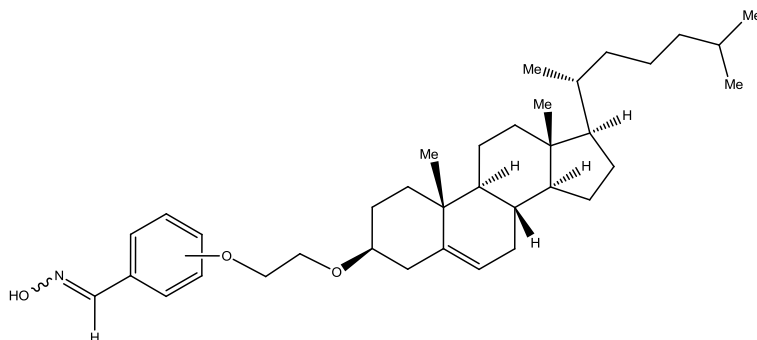
R_f : 0.26 (hexane, AcOEt, 8:2); Mp: 120-122 °C; ¹H NMR: 7.84 (2H, d, ³J 8.0, Ar-H), 7.26 (2H, d, ³J 8.0, Ar-H), 6.58 (1H, s, Isoxazole-H), 5.39 (1H, br s, CH=C), 4.81 (2H, s, HOCH₂), 4.74 (1H, br s, NH), 4.57-4.41 (1H, m, OCH), 3.63-3.55 (2H, m, CONHCH₂), 3.26-3.11 (2H, m, OCONHCH₂), 2.62-0.75 (45H, m), 0.67 (3H, s, Me). ¹³C NMR: δ 170.7 (C=N), 166.9 (C=O), 160.5 (isoxazole-CO), 156.5 (OCONH), 140.4 (C=CH), 134.6, 134.1 (2 x Ar-C), 129.7, 128.7, 128.7, 128.1 (4 x Ar-CH), 122.3 (C=CH), 99.8 (isoxazole-CH), 79.6 (OCH), 56.7, 56.2, 53.0, 50.1, 42.3, 39.8, 39.5, 38.6, 37.0, 36.6, 36.2, 35.9, 31.9, 28.2, 27.8, 26.5, 24.3, 23.8, 22.7, 22.6, 21.1, 19.3, 18.7, 11.9.



3β-Cholest-5-en-3-yl N-{3-[(4-[5-phenoxyethyl]-3-isoxazolyl)benzoyl]amino}butyl}carbamate 185

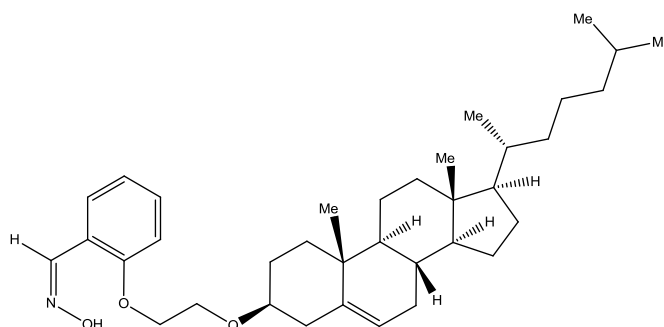
The title compound was isolated as a white-off solid in 37% yield (21 mg).

R_f : 0.45 (hexane, AcOEt, 8:2); Mp: 107-109 °C; ¹H NMR: 7.88-7.71 (4H, m, Ar-H), 7.50-7.41 (3H, m, Ar-H), 7.25 (2H, d, ³J 8.0, Ar-H), 6.56 (1H, s, Isoxazole-H), 5.37 (1H, br s, CH=C), 4.69 (OCH₂), 4.72 (br s, 1H, NH), 4.55-4.40 (1H, m, OCH), 3.65-3.55 (2H, m, CONHCH₂), 3.24-3.10 (2H, m, OCONHCH₂), 2.60-0.77 (45H, m), 0.68 (3H, s, Me). ¹³C NMR: δ 170.7 (C=N), 167.0 (C=O), 162.4 (isoxazole-CO), 156.5 (OCONH), 140.5 (C=CH), 134.6, 134.0, 130.0 (3 x Ar-C), 129.8, 129.7, 129.6, 129.6, 128.7, 128.2, 127.8 (9 x Ar-CH), 122.2 (C=CH), 100.7 (isoxazole-CH), 79.7 (OCH), 61.1 (OCH₂), 56.7, 56.3, 50.1, 42.3, 39.8, 39.6, 38.6, 37.1, 36.6, 36.3, 35.9, 31.9, 28.2, 27.8, 26.6, 24.3, 23.8, 22.8, 21.1, 19.3, 18.7, 11.9.



General procedure for oxime preparation:

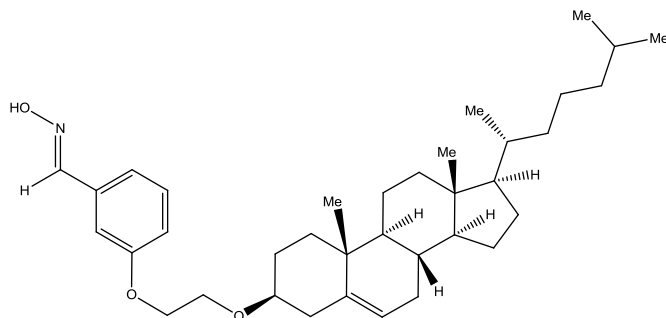
A mixture of aldehyde **187a-c** (500 mg, 0.94 mmol), hydroxylamine hydrochloride (97 mg, 1.40 mmol, 1.5 eq) and pyridine (110 mg, 1.40 mmol, 1.5 eq) in EtOH was heated to 125°C for 1 h in a scientific MW (10 mL vessel, $P_{\text{max}} = 300 \text{ W}$). After solvent removal under reduced pressure, the residue was dissolved in chloroform, and washed with H₂O. The organic layer was dried over anhydrous Na₂SO₄, and the solvent was removed under reduced pressure to afford the pure oximes as off-white solids in quantitative yields (**186a**, 511 mg; **186 b**, 512 mg; **186c**, 516 mg).



2-[2-(3β-Cholest-5-en-3-oxy)ethoxy]-3-benzaldehyde oxime **186a**

The title compound was isolated as a white-off solid with quantitative conversion (511 mg).

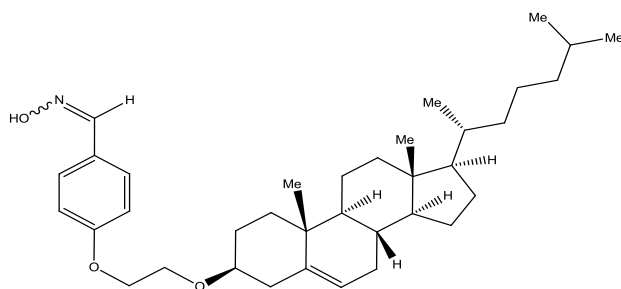
R_f : 0.57 (hexane, AcOEt, 8:2); Mp: 112-114 °C; ¹H NMR: δ 8.55 (1H, s, $\text{CH}=\text{NOH}$), 8.20 (1H, s, $\text{CH}=\text{NOH}$), 7.72 (1H, d, ³J 7.8, Ar-H), 7.36-7.27 (2H, m, Ar-H), 7.01-6.86 (1H, m, Ar-H), 5.40-5.25 (1H, m, CH=C), 4.15 (2H, t, ³J 5.1, OCH₂), 3.85 (2H, t, ³J 5.0, OCH₂), 3.35-3.20 (1H, m, OCH), 2.46-0.77 (40H, m), 0.68 (3H, s, Me). ¹³C NMR: δ 157.0 (Ar-C), 146.5 (C=N), 140.8 (C=CH), 131.1, 129.2 (2 x Ar-H), 123.4 (Ar-C), 121.8 (C=CH), 112.6 (2 x Ar-H), 79.8 (OCH), 76.6, 68.5, 66.3, 56.8, 56.2, 50.2, 42.3, 39.8, 39.5, 39.1, 37.2, 36.9, 36.2, 35.8, 32.0, 31.9, 28.4, 28.3, 28.0, 24.3, 23.9, 22.8, 22.6, 21.1, 19.4, 18.7, 11.9.



3-[2-(3β-Cholest-5-en-3-oxy)ethoxy]-3-benzaldehyde oxime 186b

The title compound was isolated as a white-off solid with quantitative conversion (512 mg).

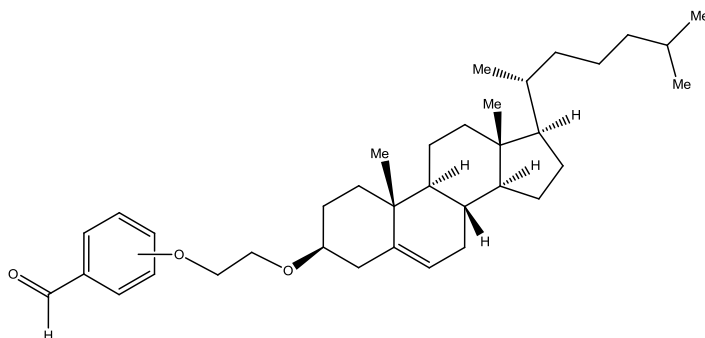
R_f : 0.59 (hexane, AcOEt, 8:2); Mp: 110-112 °C; ¹H NMR: δ 8.08 (1H, s, CH=NOH), 7.35-7.07 (4 H, m, Ar-H, CH=NOH), 7.03- 6.90 (1H, m, Ar-H), 5.40-5.25 (1H, m, CH=C), 4.13 (2H, t, ³J 5.1, OCH₂), 3.84 (2H, t, ³J 5.1, OCH₂), 3.35-3.20 (1H, m, OCH), 2.48-0.77 (40H, m), 0.68 (3H, s, Me). ¹³C NMR: δ 158.1 (Ar-C), 149.2 (C=N), 139.8 (C=CH), 132.4, 128.7 (2 x Ar-H), 124.8 (Ar-C), 120.7 (C=CH), 115.9 (2 x Ar-H), 78.8 (OCH), 75.6, 66.8, 65.4, 55.8, 55.1, 49.2, 41.3, 38.8, 38.5, 38.0, 36.2, 35.9, 35.2, 34.8, 30.9, 30.9, 27.2, 27.0, 23.3, 22.8, 21.8, 21.6, 20.1, 18.4, 17.7, 10.8.



4-[2-(3β-Cholest-5-en-3-oxy)ethoxy]-3-benzaldehyde oxime 186c

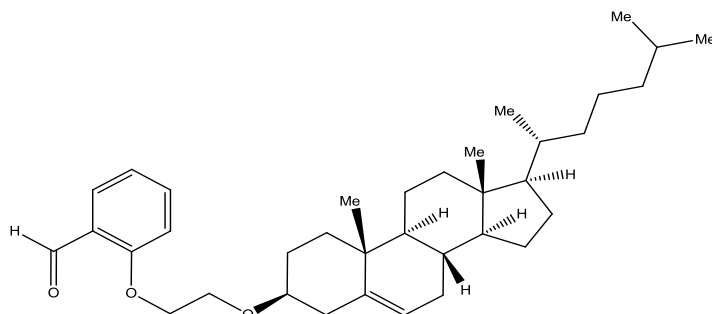
The title compound was isolated as a white-off solid with quantitative conversion (516 mg).

R_f : 0.60 (hexane, AcOEt, 8:2); Mp: 120-122 °C; ¹H NMR: δ 8.07 (1H, s, CH=NOH), 7.49 (2H, d, ³J 9.0, Ar-H), 7.35 (1H, br s, CH=NOH), 6.92 (2H, d, ³J 9.0, Ar-H), 5.42-5.29 (1H, m, CH=C), 4.13 (2H, t, ³J 5.1, OCH₂), 3.84 (2H, t, ³J 5.1, OCH₂), 3.35-3.19 (1H, m, OCH), 2.47-0.78 (40H, m), 0.68 (3H, s, Me). ¹³C NMR: δ 160.4 (Ar-C), 150.0 (C=N), 140.8 (C=CH), 128.4 (2 x Ar-H), 124.8 (Ar-C), 121.7 (C=CH), 115.4 (2 x Ar-H), 79.8 (OCH), 76.6, 67.8, 66.4, 56.8, 56.2, 50.2, 42.3, 39.8, 39.5, 39.1, 37.2, 36.9, 36.2, 35.8, 32.0, 31.9, 28.4, 28.2, 28.0, 24.3, 23.8, 22.8, 22.6, 21.1, 19.4, 18.7, 11.9.



General procedure for aldehyde preparation:

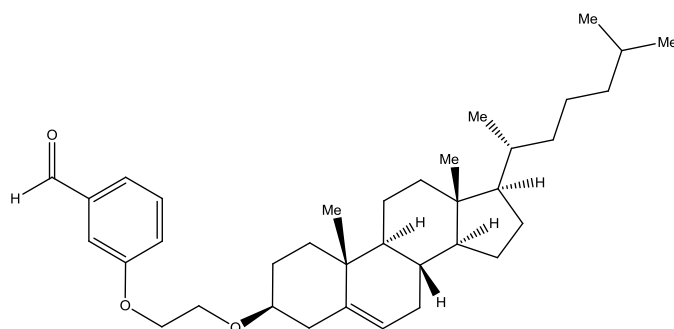
A mixture of cholesterol (1 g, 2.59 mmol), 2-, 3- or 4-(2-hydroxyethoxy)benzaldehyde (12.93 mmol, 5 eq, purchased from TCI), and MK-10 (2 g, activated at 120 °C overnight prior to use) in chloroform (5 mL), was heated to 90 °C for 8 h in a scientific MW (10 mL vessel, $P_{\max} = 300$ W). After solvent removal under reduced pressure, hexane (20 mL) was added, the catalyst was removed by filtration and washed with hexane. Following the evaporation of the solvent, the residue was purified by flash column chromatography (SiO_2 , hexane, AcOEt, 0 to 10%) to give the title compounds as white solid (485 mg, 35% for **187a**; 803 mg, 58% for **187 b**; 802 mg, 58% for **187c**).



2-[2-(3β-Cholest-5-en-3-oxy)ethoxy]-3-benzaldehyde **187a**

The title compound was isolated as a white-off solid in 35% yield (485 mg).

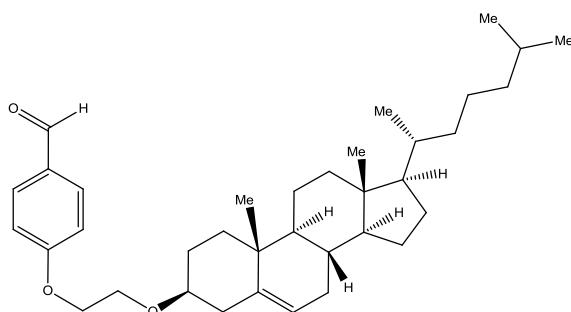
R_f : 0.62 (hexane, AcOEt, 8:2); Mp: 86-88 °C; ^1H NMR: δ 10.53 (1H, s, CHO), 7.88-7.80 (1H, m, Ar-H), 7.59-7.47 (1H, m, Ar-H), 7.11-6.95 (2H, m, Ar-H), 5.41-5.29 (1H, m, CH=C), 4.23 (2H, t, 3J 5.0, OCH_2), 3.89 (2H, t, 3J 5.0, OCH_2), 3.35-3.19 (1H, m, OCH), 2.46-0.77 (40H, m), 0.68 (3H, s, Me). ^{13}C NMR: δ 189.9 (C=O), 161.4 (Ar-C), 140.6 ($\text{C}=\text{CH}$), 135.8, 128.2 (2 x Ar-H), 125.1 (Ar-C), 121.9 ($\text{C}=\text{CH}$), 112.9 (2 x Ar-H), 79.9 (OCH), 76.6, 68.5, 65.9, 56.8, 56.2, 50.2, 42.3, 39.8, 39.5, 39.1, 37.2, 36.9, 36.2, 35.8, 31.9, 28.4, 28.2, 28.0, 24.3, 23.8, 22.8, 22.6, 21.1, 19.4, 18.7, 11.9.



3-[2-(3β-Cholest-5-en-3-oxy)ethoxy]-3-benzaldehyde 187b

The title compound was isolated as a white-off solid in 58% yield (803 mg).

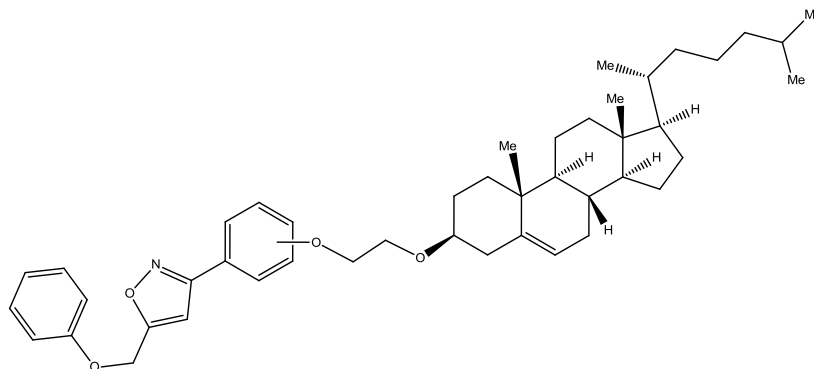
R_f : 0.62 (hexane, AcOEt, 8:2); Mp: 80-82 °C; ¹H NMR: δ 9.96 (1H, s, CHO), 7.64-7.38 (3H, m, Ar-H), 7.24-7.17 (1H, m, Ar-H), 5.49-5.32 (1H, m, CH=C), 4.17 (2H, t, ³J 4.8, OCH₂), 3.86 (2H, t, ³J 4.8, OCH₂), 3.35-3.19 (1H, m, OCH), 2.57-0.80 (40H, m), 0.68 (3H, s, Me). ¹³C NMR: δ 191.1 (C=O), 158.5 (Ar-C), 139.8 (C=CH), 136.7, 129.0 (2 x Ar-H), 122.5 (Ar-C), 120.7 (C=CH), 112.1 (2 x Ar-H), 78.8 (OCH), 75.6, 67.0, 65.3, 55.8, 55.2, 49.2, 41.3, 38.8, 38.5, 38.0, 36.2, 35.9, 35.2, 34.77, 30.94, 30.9, 27.4, 27.2, 27.0, 23.3, 22.8, 21.8, 21.6, 20.1, 18.4, 17.7, 10.9.



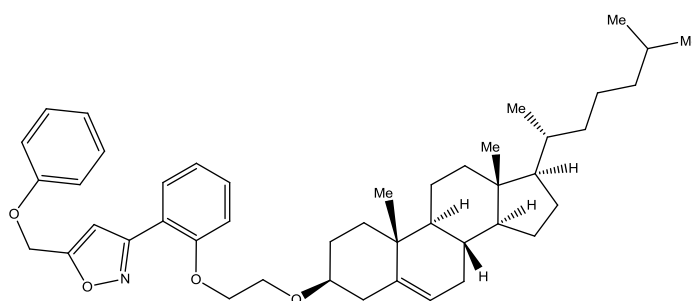
4-[2-(3β-Cholest-5-en-3-oxy)ethoxy]-3-benzaldehyde 187c

The title compound was isolated as a white-off solid in 58% yield (802 mg).

R_f : 0.60 (hexane, AcOEt, 8:2); Mp: 90-92 °C; ¹H NMR: δ 9.88 (1H, s, CHO), 7.84 (d, ³J 8.7, 2H, Ar-H), 7.03 (2H, d, ³J 8.7, Ar-H), 5.39-5.30 (1H, m, CH=C), 4.19 (2H, t, ³J 4.9, OCH₂), 3.86 (2H, t, ³J 4.9, OCH₂), 3.31-3.19 (1H, m, OCH), 2.45-0.75 (40H, m), 0.67 (3H, s, Me). ¹³C NMR: δ 190.8 (C=O), 164.0 (Ar-C), 140.7 (C=CH), 131.9, 130.0 (2 x Ar-H), 121.8 (Ar-C), 121.8 (C=CH), 114.9 (2 x Ar-H), 79.9 (OCH), 76.6, 68.1, 66.2, 65.9, 56.8, 56.2, 50.2, 42.3, 39.8, 39.5, 39.0, 37.2, 36.9, 36.2, 35.8, 32.0, 31.9, 31.6, 28.4, 24.3, 23.8, 22.8, 22.7, 22.6, 21.1, 19.4, 18.7, 11.9.



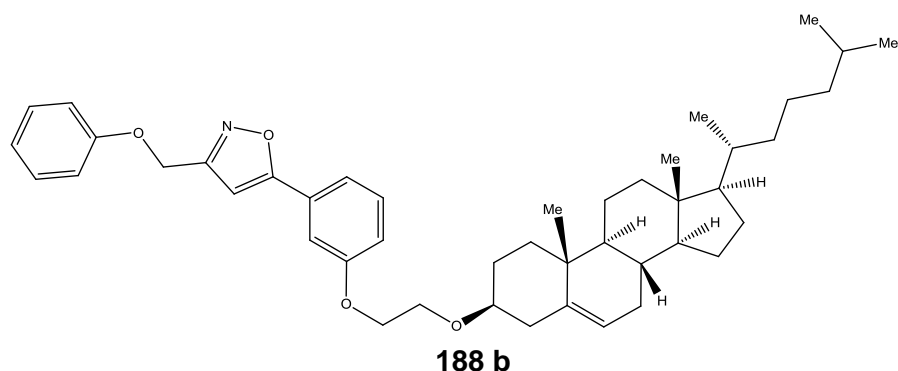
General procedure for the cycloaddition: To a round bottomed flask containing the (prop-2-yn-1-yloxy)benzene (16 mg, 0.12 mmol) was added the oxime **186c** (100 mg, 0.18 mmol, 1.5 eq) and CAT (54 mg, 0.24 mmol, 2 eq) in EtOH (1 mL per 0.1 mmol oxime). The mixture was stirred for 17 h at rt. After solvent removal under reduced pressure, the residue was dissolved in toluene, and washed with H₂O. The organic layer was dried over anhydrous Na₂SO₄, and the solvent was removed under reduced pressure to afford the crude reaction product which was purified by flash column chromatography (SiO₂, hexane, AcOEt 0 to 10%) to give the title compounds as off-white solids (20 mg, 25% for **188a**; 31 mg, 39% for **188 b**; 47 mg, 58% for **188c**).



188a

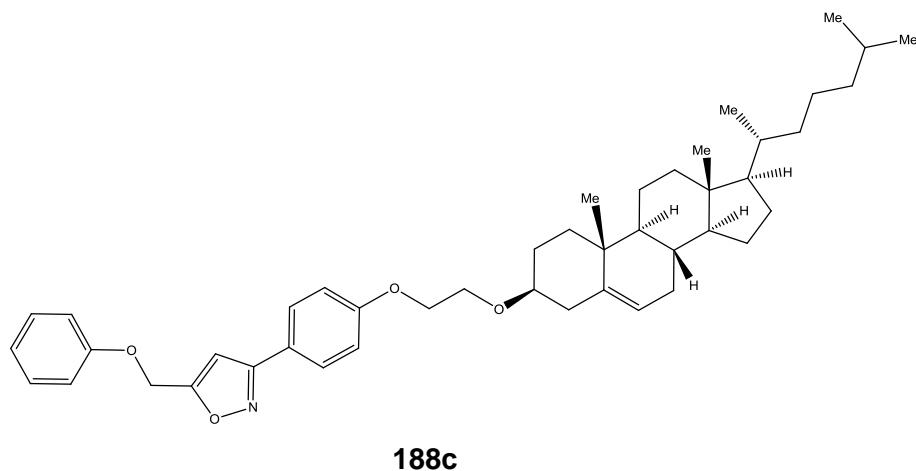
The title compound was isolated as a white-off solid in 25% yield (20 mg).

R_f : 0.40 (hexane, AcOEt, 8:2); ¹H NMR: δ 7.72 (1H, d, ³J 7.9, Ar-H), 7.38-7.20 (3H, m, Ar-H), 7.09-6.84 (5 H, m, Ar-H), 6.57 (1H, s, Isoxazole-H), 5.35 (1H, br s, CH=C), 5.18 (2H, s, OCH₂), 4.16 (2H, t, ³J 5.1, OCH₂), 3.85 (2H, t, ³J 4.9, OCH₂), 3.30-3.18 (1H, m, OCH), 2.50-0.79 (40H, m), 0.68 (3H, s, Me). ¹³C NMR: δ 164.2 (C=N), 162.0 (C=CH), 160.4 (Ar-C), 157.8 (Ar-C), 140.7 (isoxazole-CO), 134.8, 130.6, 130.6, 129.2, 126.8, 122.0, 121.8, 120.4, 116.0, 114.9, 114.8 (Ar-C + Ar-CH + C=CH), 101.2 (isoxazole-CH), 79.8 (OCH), 67.9 (OCH₂), 66.4 (OCH₂), 61.5 (CH₂OPh), 56.8, 56.2, 50.2, 42.2, 39.8, 39.5, 39.1, 37.2, 36.8, 36.2, 35.8, 32.0, 31.9, 28.4, 28.2, 28.0, 24.4, 23.8, 22.8, 22.6, 21.1, 19.4, 18.7, 11.9.



The title compound was isolated as a white-off solid in 39% yield (31 mg).

R_f : 0.44 (hexane, AcOEt, 8:2); ¹H NMR: δ 7.39-7.10 (5H, m, Ar-H), 7.09-6.84 (4 H, m, Ar-H), 6.57 (1H, s, Isoxazole-H), 5.34 (1H, br s, CH=C), 5.17 (2H, s, OCH₂), 4.15 (2H, t, ³J 5.1, OCH₂), 3.85 (2H, t, ³J 5.0, OCH₂), 3.32-3.19 (1H, m, OCH), 2.50-0.79 (40H, m), 0.68 (3H, s, Me). ¹³C NMR: δ 168.2 (C=N), 162.1 (C=CH), 159.8 (Ar-C), 159.6 (Ar-C), 140.7 (isoxazole-CO), 133.7, 130.5, 130.4, 129.7, 129.8, 122.1, 121.5, 118.9, 114.7, 114.6, 113.6 (Ar-C + Ar-CH + C=CH), 101.1 (isoxazole-CH), 79.8 (OCH), 67.9 (OCH₂), 66.4 (OCH₂), 61.6 (CH₂OPh), 56.8, 56.3, 50.2, 42.2, 39.8, 39.5, 39.0, 37.2, 36.8, 36.2, 35.8, 32.0, 31.9, 28.5, 28.2, 28.0, 24.4, 23.8, 22.8, 22.6, 21.1, 19.4, 18.7, 11.9.

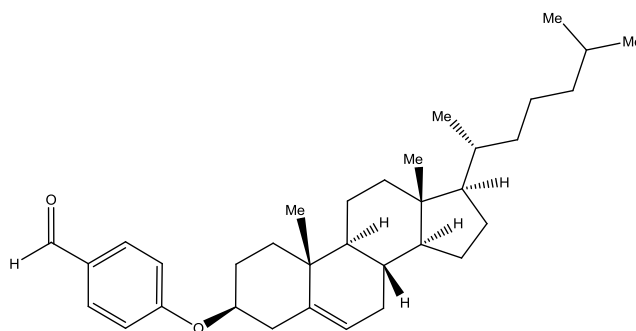


Method 1 (general procedure): The title compound was isolated as a white-off solid in 58% yield (47 mg).

Method 2 (multi-addition): To a round bottomed flask containing the (prop-2-yn-1-yloxy)benzene (16 mg, 0.12 mmol) was added the oxime **186c** (50 mg, 0.09 mmol, 0.75 eq) and CAT (27 mg, 0.12 mmol, 1 eq) in EtOH (1 mL per 0.1 mmol oxime). The mixture was stirred for 4 h at rt. The same dose of oxime/CAT was added again before stirring for another 17 h at rt. After solvent removal under reduced pressure, the residue was dissolved in toluene, and washed with H₂O. The organic layer was dried over anhydrous Na₂SO₄, and

the solvent was removed under reduced pressure to afford the crude reaction product which was purified by flash column chromatography (SiO₂, hexane, AcOEt 0 to 10%) to give the title compound as an off-white solid in 80% yield (65 mg).

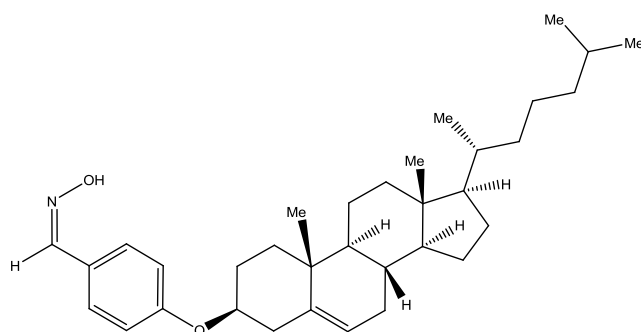
R_f : 0.45 (hexane, AcOEt, 8:2); ¹H NMR: δ 7.82-7.70 (2H, m, Ar-H), 7.37-7.22 (2H, m, Ar-H), 7.10-6.94 (5 H, m, Ar-H), 6.58 (1H, s, Isoxazole-H), 5.35 (1H, br s, CH=C), 5.19 (2H, s, OCH₂), 4.15 (2H, t, ³J 5.0, OCH₂), 3.85 (2H, t, ³J 4.8, OCH₂), 3.32-3.18 (1H, m, OCH), 2.50-0.78 (40H, m), 0.68 (3H, s, Me). ¹³C NMR: δ 168.3 (C=N), 162.1 (C=CH), 160.4 (Ar-C), 157.8 (Ar-C), 140.8 (isoxazole-CO), 133.9, 129.8, 129.7, 128.2, 127.9, 121.9, 121.7, 121.4, 115.4, 115.0, 114.8 (Ar-C + Ar-CH + C=CH), 101.1 (isoxazole-CH), 79.8 (OCH), 67.9 (OCH₂), 66.4 (OCH₂), 61.5 (CH₂OPh), 56.8, 56.2, 50.2, 42.3, 39.8, 39.5, 39.1, 37.2, 36.8, 36.2, 35.8, 32.0, 31.9, 28.4, 28.2, 28.0, 24.3, 23.8, 22.8, 22.6, 21.1, 19.4, 18.7, 11.9.



4-(3β-Cholest-5-en-3-oxy)-3-benzaldehyde 189

The title compound was isolated as a white-off solid in 62% yield (788 mg).

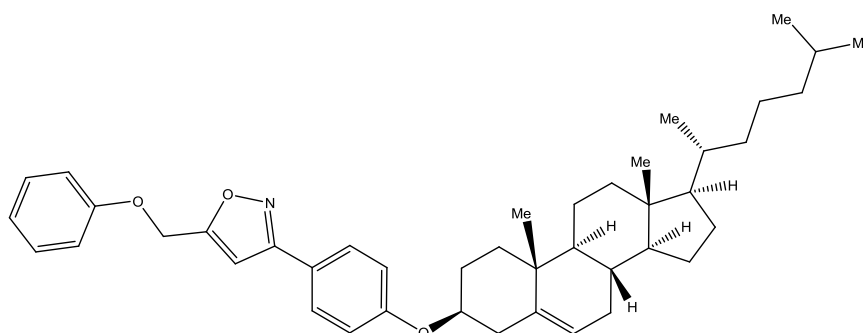
R_f : 0.71 (hexane, AcOEt, 8:2); ¹H NMR: δ 9.86 (1H, s, CHO), 7.81 (d, ³J 8.7, 2H, Ar-H), 6.97 (2H, d, ³J 8.7, Ar-H), 5.49-5.37 (1H, m, CH=C), 4.33-4.17 (1H, m, OCH), 2.56-0.77 (40H, m), 0.69 (3H, s, Me). ¹³C NMR: δ 189.7 (C=O), 163.1 (Ar-C), 139.8 (C=CH), 132.1, 129.6 (2 x Ar-H), 122.9 (Ar-C), 122.8 (C=CH), 115.6 (2 x Ar-H), 77.0 (OCH), 76.6, 56.8, 56.2, 50.2, 42.3, 39.8, 39.5, 38.4, 37.1, 36.8, 36.2, 35.8, 32.0, 31.9, 29.7, 28.2, 28.0, 24.3, 23.8, 22.8, 22.6, 21.1, 19.4, 18.7, 11.9.



4-(3β-Cholest-5-en-3-oxy)-3-benzaldehyde oxime 190

The title compound was isolated as a white-off solid with quantitative conversion (510 mg).

R_f : 0.69 (hexane, AcOEt, 8:2); ¹H NMR: δ 8.08 (1H, s, CH=NOH), 7.85 (1H, br s, CH=NOH), 7.48 (2H, d, ³J 8.7, Ar-H), 6.88 (2H, d, ³J 8.7, Ar-H), 5.48-5.33 (1H, m, CH=C), 4.25-4.06 (1H, m, OCH), 2.55-0.78 (40H, m), 0.69 (3H, s, Me). ¹³C NMR: δ 159.3 (Ar-C), 150.0 (C=N), 140.1 (C=CH), 128.5 (2 x Ar-H), 124.4 (Ar-C), 122.5 (C=CH), 115.9 (2 x Ar-H), 77.0 (OCH), 76.6, 56.8, 56.2, 50.2, 42.4, 39.8, 39.5, 38.6, 37.2, 36.8, 36.2, 35.8, 32.0, 31.9, 28.2, 28.2, 28.0, 24.3, 23.8, 22.8, 22.6, 21.1, 19.4, 18.7, 11.9.



191

The title compound was isolated as a white-off solid in 60% yield (46 mg).

R_f : 0.60 (hexane, AcOEt, 8:2); ¹H NMR: δ 7.80 (2H, d, ³J 8.4, Ar-H), 7.71 (d, ³J 8.4, 2H, Ar-H), 7.37-7.23 (2H, m, Ar-H), 7.05-6.91 (3H, m, Ar-H), 6.58 (1H, s, Isoxazole-H), 5.33-5.48 (1H, m, CH=C), 5.19 (2H, s, OCH₂), 4.25-4.08 (1H, m, OCH), 2.50-0.78 (40H, m), 0.69 (3H, s, Me). ¹³C NMR: δ 168.2 (C=N), 162.1 (C=CH), 159.7, 159.6 (2 x Ar-C), 140.6 (isoxazole-CH), 133.6, 130.5, 130.4, 129.8, 129.8, 122.1, 121.5, 118.9, 114.7, 114.6, 113.6 (Ar-C + 9 x Ar-CH + C=CH), 101.1 (isoxazole-CH), 79.8 (OCH), 61.5 (CH₂OPh), 56.8, 56.2, 50.2, 42.2, 39.8, 39.5, 39.0, 37.3, 36.8, 36.2, 35.8, 32.0, 31.9, 28.4, 28.2, 28.0, 24.4, 23.8, 22.8, 22.6, 21.1, 19.4, 18.7, 11.9.

General deprotection of DMT group procedure:

A solution of 3% DCA in DCM (homemade) (2 x 2 mL) was slowly passed through the column (1 μmol) containing the protected nucleic acid. Complete removal of the DMT group was judged by color. An intense orange color corresponded to formation of the trityl cation. The solid support was washed with CH₃CN (2 x 5 mL) and dried under high vacuum.

General cleavage/deprotection procedure:

The solid support bearing the oligonucleotide was deprotected and cleaved from the CPG by incubating the CPG-DNA/RNA in 40% aqueous MeNH₂ (500 μL) at 65 °C for 30 minutes or in 28% aqueous NH₄OH (500 μL) at rt for 17 h. The MeNH₂ or NH₄OH was evaporated using a concentrator. The CPG was washed with H₂O (5 x 200 μL), all solutions and washings were combined to afford an aqueous solution of DNA/RNA conjugates.

General procedure for the phosphitylation of [(5'-OH)DNA]-(CPG):

To manually couple the alkyne phosphoramidite **197** to the nucleotide/oligonucleotide 500 μL (100 mM in anhydrous CH₃CN) was added to the DNA-CPG (1 μmol) along with 500 μL of BMT in CH₃CN (0.3 M). The mixture was reacted for 15 min at rt with mixing between two syringes. This reaction was repeated with a second portion of each of a new solution of phosphoramidite **197** and BMT. The CPG was washed with CH₃CN (5 x 2 ml) before exposure to an iodine solution (0.1 M in THF: pyridine: water; 78:20:2; 0.7 mL for 2 min). The CPG was washed again with CH₃CN (2 x 5 mL) and dried in vacuo, yielding [(5'-alk)DNA]-(CPG). After cleavage of an analytical portion, the products were analyzed by reverse-phase HPLC (Method 1, p 151). Some structures have been confirmed by MALDI-TOF MS.

Table 6.1: Overview of the structures of the new DNA alkynes.

Product	DNA Sequences 5'-3'	HPLC analysis Rt (min)	Mass	
			Calcd	Found
/	(5'-alk)T	14.4	/	/
202	(5'-alk)dG	12.5	/	/
/	(5'-alk)TdGT	12.9	/	/
205	(5'-alk)TdCT	13.9	1025.8	1026.5*
206	(5'-alk)TdC^{Me}T	14.7	1039.8	1040.9*
/	(5'-alk)dC	13.4	/	/
211	(5'-alk)TdAT	14.8	/	/
212	(5'-alk)TdA^{Me}T	16.6	/	/
/	(5'-alk)dA	13.8	/	/
216	(5'-alk)TTTTT	15.4	1649.1	1725.9* [M+K] ⁺
224	(5'-alk)TTTTTTTTT	15.5	3168.7	3169.9*
220	(5'-alk)TdCdGdCdAdCdAdCdAdCdGdC	15.0	3813.7	3814.5

* MS recorded by Amersham Biosciences (England)

General procedure for the cycloaddition reaction between “small” ligands and [(5'-alk)DNA]-(CPG):

To solid supported DNA-alkyne (1 μ M) in an eppendorf tube was added the oxime RCHNOH (0.10 mmol, 100 eq, 12 mg for R = Ph; 17 mg for R = 2-NO₂-C₆H₄; 17 mg for R = 1-Naph; 22 mg for R = 9-Anth; 25 mg for R = 4-Pyr) and CAT (45 mg, 0.20 mmol, 200 eq) in EtOH (300 μ L) and H₂O (600 μ L). The mixture was agitated at rt for 30 min (or 3 h in the case of the anthracene-9-carbaldehyde oxime and pyrene-4-carbaldehyde oxime). Following settling, the supernatant liquid was removed by syringe and the CPG washed firstly with DMF (5 x 300 μ L, in the case of the anthracene 9-carbaldehyde oxime and pyrene 4-carbaldehyde oxime), CH₃CN (5 x 300 μ L) and then H₂O (5 x 300 μ L). Deprotection as described above using an aqueous solution of NH₄OH, afford the desire 5'-aryl isoxazole DNA conjugate, in quantitative yields, as evidenced by reverse-phase HPLC (Method 1, p 151). Some of the structures have been confirmed in MALDI-TOF MS.

Table 6.2: Overview of the structures of the new aryl-isoxazole DNA conjugates.

Product	Sequences 5'-3'	HPLC analysis Rt (min) ^a	Mass	
			Calcd	Found
196	(5'-(1-Naphtyl))T	28.3	/	/
198	(5'-Ph)T	23.7	/	/
199	(5'-(2'-NO ₂ -C ₆ H ₄))T	24.3	/	/
200	(5'-(9-Anth))T	30	/	/
201	(5'-(4-Pyr))T	32.7	/	/
203	(5'-(1-Naphtyl))dG	24.7	/	/
204	(5'-(1-Naphtyl))TdGT	23.2	1233.9	1235.0 ^b
207	(5'-(1-Naphtyl))TdCT	23.4	1194.9	1195.5 ^b
208	(5'-Ph)TdCT	19.7	1144.9	1146.1 ^b
209	(5'-(2'-NO ₂ -C ₆ H ₄))TdCT	20.6	1189.9	1190.8 ^b
210	(5'-(1-Naphtyl))dC	25.7	/	/
213	(5'-1Naphtyl)TdAT	24.5	1217.9	1218.8 ^b
214	(5'-Ph)TdAT	21.4	/	/
215	(5'-(1-Naphtyl))dA	26.0	/	/
217	(5'-(1-Naphtyl))TTTTT	22.4	1818.3	1819.4 ^b
218	(5'-Ph)TTTTT	17.3	1768.3	1769.5 ^b
219	(5'-(2'-NO ₂ -C ₆ H ₄))TTTTT	19.9	1813.3	1838.0 ^b [M+Na] ⁺
221	(5'-(1-Naphtyl))TdCdGdCdAdCdAdCdAdCdGdC	21.9	3984.2	3987.0
222	(5'-Ph)TdCdGdCdAdCdAdCdAdCdGdC	18.8	3934.2	3935.7

a. Method 1; b. MS recorded by Amersham Biosciences (England)

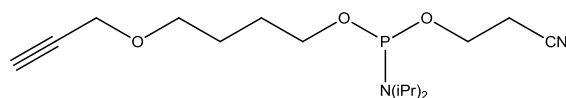
General procedure for the cycloaddition reaction between steroidal oxime **186c and [(5'-alk)DNA]-(CPG):**

To solid supported DNA-alkyne (1 μM) in an eppendorf tube was added the oxime **186c** (21 mg, 0.03 mmol, 30 eq) and CAT (14 mg, 0.06 mmol, 60 eq) in EtOH (1 mL). The mixture was agitated at rt for 6 h before addition of the same dose of **186c** and CAT and another stirring for 17 h at rt. Following settling, the supernatant liquid was removed by syringe and the CPG washed firstly with DCM (5 x 300 μL), EtOH (5 x 300 μL), CH_3CN (5 x 300 μL) and then H_2O (5 x 300 μL). Deprotection as described above afford the desire product (5'-Chol)DNA as evidenced by reverse-phase HPLC (Method 2, p 151). Some structures have been confirmed by MALDI-TOF MS.

Table 6.3: Overview of the structures of the new cholesterol DNA conjugates.

Product	DNA Sequences 5'-3'	Post-click conversion (%)	HPLC analysis Rt (min) ^a	Mass	
				Calcd	Found
225	(5'-Chol)T	b	c	d	d
226	(5'-Chol)TTTTT	53	39.3	2193.0	2195.3
227	(5'-Chol)TTTTTTTTTT	62	37.5	3710.0	3710.9
228	(5'-Chol)TdCdGdCdAdCdAdCdAdCdGdC	68	36.2	4298.0	4300.1

a. Method 2; b. Almost complete consumption of starting material; c. Monomers did not elute attractively on reverse-phase HPLC; d. Monomers did not respond to ESI MS or MALDI-TOF MS



4-(2-Propynyloxy)butan-1-yl-(2-cyanoethyl)-N,N-diisopropylphosphoramidite **197**

The title compound, prepared according to a literature procedure, was obtained as a yellow oil (89%). The data agreed with that reported.¹⁰¹

³¹P NMR (d6-DMSO) δ (ppm) 146.3.

General environment for RNA work – and in particular for the preparation of biological analysis samples:

RNA is highly susceptible to degradation by exogenous RNases introduced during handling. Therefore it is essential that all handling steps are conducted under sterile, RNase free conditions. RNA oligonucleotides should not be handled with ungloved hands.

The surfaces were cleaned with the spray cleaner, and wiped with paper towels. Eppendorf tubes were autoclaved (40 min, 121 °C) and kept in a screw top autoclave jar. RNase free water was bought from Sigma or autoclaved (having previously added diethylpyrocarbonate (DEPC) antimicrobial agent (100 µL in 1 L water) and allowed to stand 24 h). In general, RNase free reagents, barrier pipette tips (only commercial DNase/RNase free, pcr grade and autoclaved) were used. Dry RNA oligonucleotides were stored at -20 °C.

General procedure for the cycloaddition reaction between the steroidal oxime **186c and [RNA(2'-alk)]-(CPG) or [RNA(3'-alk)]-(CPG):**

To solid supported RNA-alkyne (1 µM) in an eppendorf tube was added the oxime **186c** and CAT in EtOH (1 mL).

- In the first method A, 50 eq of oxime **186c** (mg, 0.05 mmol, 50 eq) and 100 eq of CAT (23 mg, 0.10 mmol, 100 eq), were employed. The reaction was conducted for 17 h at rt.
- In the second method B, 30 eq of oxime **186c** (21 mg, 0.03 mmol, 30 eq) and 60 eq of CAT (14 mg, 0.06 mmol, 60 eq) were added at the beginning of the reaction, and the same dose 6 h later. The reaction was then stirred for another 17 h at rt.
- In a third method C, 30 eq of oxime **186c** (21 mg, 0.03 mmol, 30 eq) and 60 eq of CAT (14 mg, 0.06 mmol, 60 eq) were again employed, this time the reaction were left for 17 h at rt, the beads were washed free of any by-products before adding a fresh batch of oxime **186c**/CAT, 30 eq and 60 eq, respectively, and agitation of the reaction mixture for a further 17 h at rt.

Following settling, the supernatant liquid was removed by syringe and the CPG washed firstly with DCM (5 x 300 µL), EtOH (5 x 300 µL), CH₃CN (5 x 300 µL) and then H₂O (5 x 300 µL). Deprotection as described above afforded the desire products RNA(2'- or 3'-Chol) as evidenced by reverse-phase HPLC (Method 2, p 151). Some structures have been confirmed by MALDI-TOF MS.

Table 6.4: Overview of the structures of the new RNA conjugates.

Product	Sequences 5'-3'	HPLC analysis Rt (min)*	Mass	
			Calcd	Found
/	(5'-DMT)UUUUU(2'-alk)	29.7	/	/
/	UUUUU(2'-alk)	13.1	1563.0	1563.6
/	UUUUUUUUUU(2'-alk)	13.6	/	/
/	UUUUUG(2'-alk)	13.1	/	/
/	UUUUUUUUUG(2'-alk)	13.7	/	/
/	UUUUC(2'-alk)	12.7	3168.4	3169.3
/	UUUUUUUUUC(2'-alk)	13.3	/	/
/	UUUUUA(2'-alk)	13.1	/	/
/	(2'-alk)UUUUU	16.0	/	/
/	UUUUUU(2'-alk)UUUUU	18.0	/	/
/	UUUUU(3'-alk)	13.2	/	/
/	UUUUUUUUUU(3'-alk)	15.1	/	/
230	UUUUU(2'-Chol)	38.2	2110.0	2110.4
231	UUUUUUUUUU(2'-Chol)	36.5	3561.8	3563.0
232	UUUUUG(2'-Chol)	38.0	2150.0	2153.1
233	UUUUUUUUUG(2'-Chol)	36.0	3600.8	3601.2
234	UUUUC(2'-Chol)	38.1	2109.0	2110.5
235	UUUUUUUUUC(2'-Chol)	36.5	3560.8	3563.2
236	UUUUUA(2'-Chol)	38.3	2134.0	2135.8
237	UUUUUUUUUA(2'-Chol)	36.2	/	/
238	U(2'-Chol)UUUUU	41.3	2110.0	2111.7
239	UUUUUU(2'-Chol)UUUUU	39.8	3561.8	3562.9
240	UUUUU(3'-Chol)	38.2	2110.0	2111.1
241	UUUUUUUUUU(3'-Chol)	36.5	3561.8	3563.1
246	GGAGCAAACUACAGAGAUGTTU	29.6 ^b	6779.2	6780.4
247	GGAGCAAACUACAGAGAUGTTU(2'-Chol)	39.6	7937.2	7938.4
248	GGAGCAAACUACAGAGAUGTTU(3'-Chol)	39.7	7937.2	7941.2
249	U(2'-Chol)GGAGCAAACUACAGAGAUGTT	40	7937.2	7943.9
250	CAUCUCUGUAGUUUGCUCCTdG	29.8 ^b	6812.2	6815.4

a. Method 2; b. Method 1

General annealing procedure:²⁵⁰

RNA oligonucleotides were dissolved at a convenient concentration, e.g. 100 μ M, in RNase free water. The formula $C_1V_1 = C_2V_2$ was used to get the volume of each required to have equimolar amounts, the final volume was made up with annealing buffer. The mixture was incubated for 2 minutes at 95 °C (water bath) and cooled slowly to rt (over a period of 45 min). Annealed siRNA was safely stored frozen at -20 °C. It was not freeze-thawed more than 5 times.

Annealing buffer: 30 mM HEPES-KOH pH 7.4, 100 mM KCl, 2 mM MgCl₂, 50 mM NH₄Ac.

Luciferase reporter assay

Executed by collaboration with Dr. Mark Mellet and Dr. Paola Atzei, from the research group of Dr. Paul Moynagh (Immunology Institute, NUIM)

HEK293 cells were seeded (1.5×10^5 cells/mL) in 96-well plates (200 μ L/well) for 24 h. Cells were then transfected using Lipofectamine 2000 (Invitrogen) according to the manufacturer's instruction, with luciferase reporter construct (80 ng), constitutively expressed TK *Renilla*-luciferase reporter construct (phRL-TK) (20 ng) (Promega Biosciences) and varying amounts of expression constructs. Total DNA was kept constant (200 ng/well) using the appropriate empty vector. Post-transfection cells 24 h were stimulated with LPS (100 ng/ml) for 6 h. Cell extracts were generated using Reporter Lysis Buffer (Promega Biosciences) and extracts were assayed for firefly luciferase and *Renilla*-luciferase activity using the Luciferase Assay system (Promega Biosciences) and coelenterazine (0.1 μ g/mL Insight Biotechnology Ltd.), respectively. Luminescence was monitored with the Glomax microplate luminometer (Promega).

Knockdown of Sef increases LPS-induced NF- κ B activation:

HEK293 TLR4 cells were cotransfected with the NF- κ B luciferase reporter plasmid (80 ng), TK *Renilla* (40 ng) with Sef commercial siRNA or scrambled siRNA or the chemically modified siRNAs prepared by the author (si RNAs 1, 2, 3 and 4) (10 or 20 nM). Post-transfection cells 48 h were treated with or without LPS (100 ng/ml) for 6h. Cell extracts were assayed for firefly and *Renilla* luciferase activity.

Immunoblot analysis:

HEK293 cells were seeded (2×10^5 cells/mL) in 6-well plates and grown for 24 h. Cells were transfected, using Lipofectamine, with siRNA targeting IL-17RD (sense sequence: 5'- GGAGCAAACUACAGAGAUGTT -3') or with scrambled siRNA (sense

sequence: 5'- GGACAGAACACUAGAUGAGTT -3') (20 nM) (Ambion). Cells were washed in 1 mL of ice-cold PBS and lysed in 100 μ L of NP-40 lysis buffer (50 mM Tris-HCl, pH 7.5, containing 150 mM NaCl, 0.5% (w/v) igepal, 50 mM NaF, 1 mM Na₃VO₄, 1 mM dithiothreitol, 1 mM phenylmethylsulfonyl fluoride and complete protease inhibitor mixture (Roche)). The cell lysates were centrifuged at 12,000 g for 10 min, supernatants were collected and subjected to western blotting using the indicated antibodies. Immunoreactive bands were detected using the Odyssey Infrared Imaging System from LI-COR Bioscience, according to the instructions of the manufacturer.

The results of this assays are recorded and discussed in Chapter 5, section V.1, p 138.

siRNA Transfection into Cho-K1 cells for eGFP gene knockdown

Executed by collaboration with Dr. Luke O'Shaughnessy from the research group of Dr. Sean Doyle group (Biology department, NUIM)

Reagents:

1. Transfection reagent: Lipofectamine 2000.
2. siRNA Buffer: Opti-MEM I Reduced serum Medium
3. T25 Tissue culture plate
4. Serum free medium, (DMEM Hams F12, no antibiotics or serum)
5. Sterile Laminar Hood.
6. Sterile filter tips.
7. RNase ZAP.

Methodology:

1. One day before transfection, plate cells were in 2 mL of growth medium without antibiotics such that they will be 50-75% confluent at the time of transfection.
2. For each transfection sample, oligomer-Lipofectamine™ 2000 complexes were prepared as follows:
 - **A**, 0, 50, 100, 200, 300 or 400 picoM (final concentration) siRNAs were diluted in 250 μ L Opti-MEM® I Reduced Serum Medium and mixed gently.
 - **B**, Lipofectamine™ 2000 was gently mixed before use. It was then diluted, 8 μ L in 250 μ L Opti- MEM® I Reduced Serum Medium, mixed gently and incubated for 5 min at rt. **Note:** It was important to proceed to Step C within 25 minutes.

- **C**, after the 5-minute incubation, the diluted oligomers were combined with the diluted Lipofectamine™ 2000, mixed gently and incubated for 20 min at rt (the solution may appear cloudy).
3. The oligomer-Lipofectamine™ 2000 complexes were added to each well containing cell and medium, and mixed gently by rocking the plate back and forth. The cells were incubated at 37 °C in a CO₂ incubator for 4 h. The media was changed to complete media after the 4 h incubation period.
 4. The cells were incubated for 3 days in a CO₂ incubator at 37 °C.
 5. This cell were then harvested and washed twice with PBS to remove serum and allow accurate quantisation for SDS PAGE analysis.
 6. The cells were then lysed in HEPES lysis buffer pH 7.5 and sonicated to aid lysis.
 - 7 (for experiment 1). 25 µg of protein was loaded per tract on a 15% acrylamide gels (~4 x10⁵ cells).
 - 7 (for experiment 2). The supernatant was removed following centrifugation at 12,000 rpm.
 - 8 (for experiment 2). Duplicate 100 µL aliquots of this cell suspension were transferred to a black-walled, clear-bottom 96-well plate (Corning) for fluorescence reading.
 - 9 (for experiment 2). Mean fluorescence intensity was measured on a Fluorescence Plate Reader with the following settings: excitation 485 nm, emission 530 nm, and a bottom read with a sensitivity of 35.

The results of this assays are recorded and discussed in Chapter 5, section V.2, p 144.

APPENDIX

Detailed analysis of spectral data in support of compound 139, a representative member of the sugar derivatised compounds

In order to characterize the novel compound in this thesis various NMR spectral techniques were employed; ^1H , ^{13}C , DEPT (45, 90, 135), homonuclear and heteronuclear 2D-COSY. For all compounds, initially the ^1H NMR spectra were examined; resonance positions, multiplicity and relative integrations were recorded. Peaks were assigned based on resonance position and multiplicity. Homonuclear 2D-COSY highlighted coupling between the protons and ^{13}C were assigned with the help of DEPT (45, 90 and 135) spectra and heteronuclear 2D-COSY spectra.

NMR Spectral data of the protected maleimido sugar, 139

Included below are the NMR data obtained, which was used to characterize the protected maleimido-sugar **139**.

The signals of the six protons of the maleimide group appear as three distinct signals in the ^1H NMR spectrum (Figure 7.1), each of them being a singlet representing 2H 6.52 ppm (2H, s, 2 x CH=CH), 5.25 ppm (2H, s, 2 x OCH), and 2.83 ppm (2H, s, 2 x CH). Despite the appearance of a singlet resonance, upon examination of the homonuclear $^1\text{H}^1\text{H}$ 2D-COSY spectrum (Figure 7.2), minimal coupling is suggested between $\text{CH}=\text{CH}$ and OCH , and between the OCH and CH protons.

Typical resonance position for a glucofuranose shows H_1 to be the most downfield proton at 5.86 ppm, which appear as a doublet, coupling with H_2 (3J 3.6 Hz). The peak representative of H_2 is then found with the coupling in the $^1\text{H}^1\text{H}$ 2D-COSY spectrum. The signals for the other protons on the sugar are assigned the same way, with the coupling in the $^1\text{H}^1\text{H}$ 2D-COSY spectrum as represented by the coloured arrows. Couplings are observed between H_2 and H_3 , between H_3 and H_4 , between H_4 and H_5 , between H_5 and H_{6a} and between H_5 and H_{6b} . H_{6a} and H_{6b} are diastereotopic because C_5 is a chiral carbon.

The remaining multiplet signal, around 3.5 ppm, represents 4H and is assigned to the OCH₂ and the NCH₂. This signal is coupling with the busy multiplet, around 1.5 ppm, as it contains the internal CH₂ of the methylene bridge (OCH₂CH₂CH₂). In this same multiplet, four distinct singlets, with a relative integration of 3H each, represent the four methyl of the protected sugar moiety.

Rf: 0.77 (DCM, MeOH, 98:2); ¹H NMR: δ 6.52 (2H, s, 2 x CH=CH), 5.86 (1H, d, ³J 3.6, H₁), 5.25 (2H, s, 2 x OCH), 4.53 (1H, d, ³J 3.6, H₂), 4.32–4.23 (1H, m, H₅), 4.13-4.05 (2H, m, H_{6a}, H₄), 4.20-3.94 (1H, m, H_{6b}), 3.85 (1H, d, ³J 3.0, H₃), 3.64-3.44 (4H, m, OCH₂, NCH₂), 2.83 (2H, s, 2 x CH), 1.71-1.50 (4H, m, OCH₂CH₂CH₂), 1.49, 1.42, 1.34, 1.32 (3H each, s, 4 x Me).

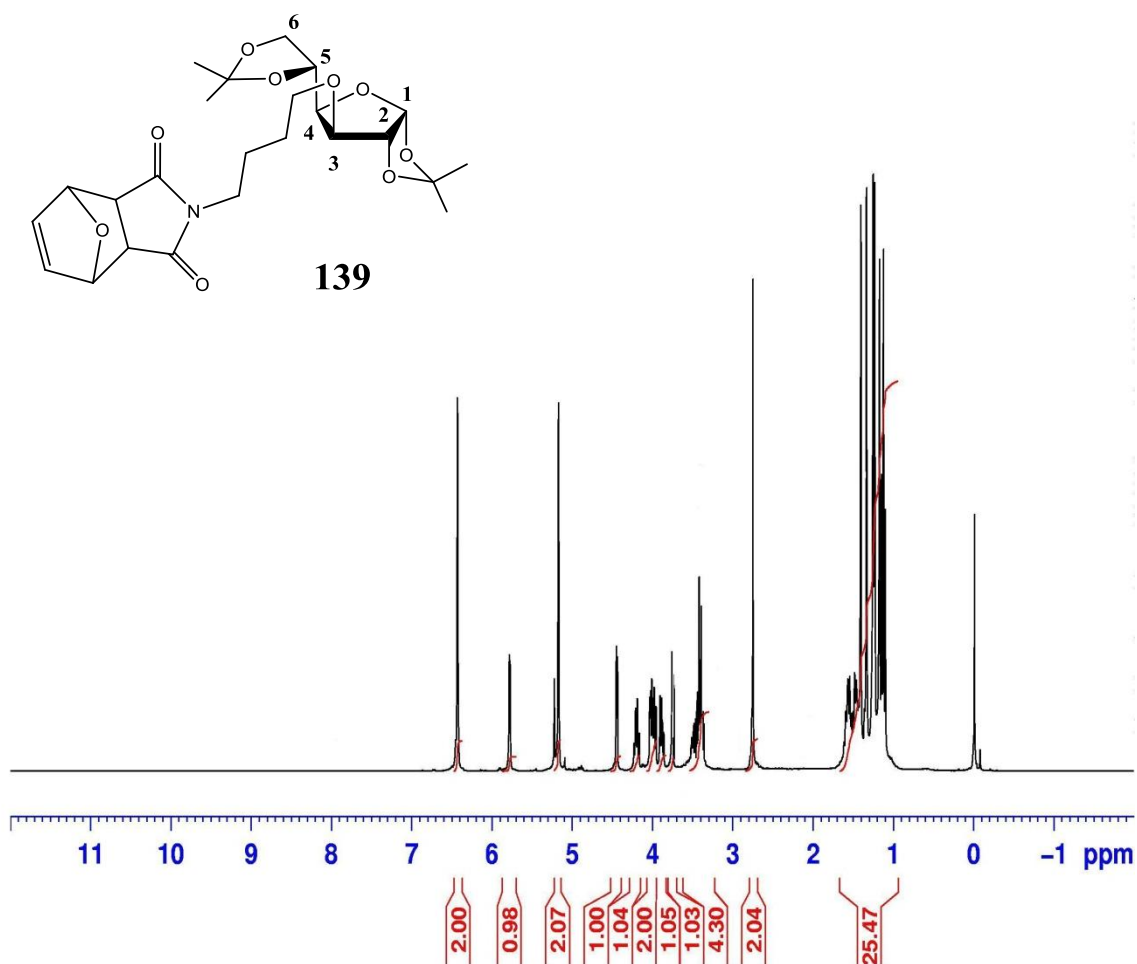


Figure 7.1: ¹H NMR spectrum of 139 (CDCl₃).

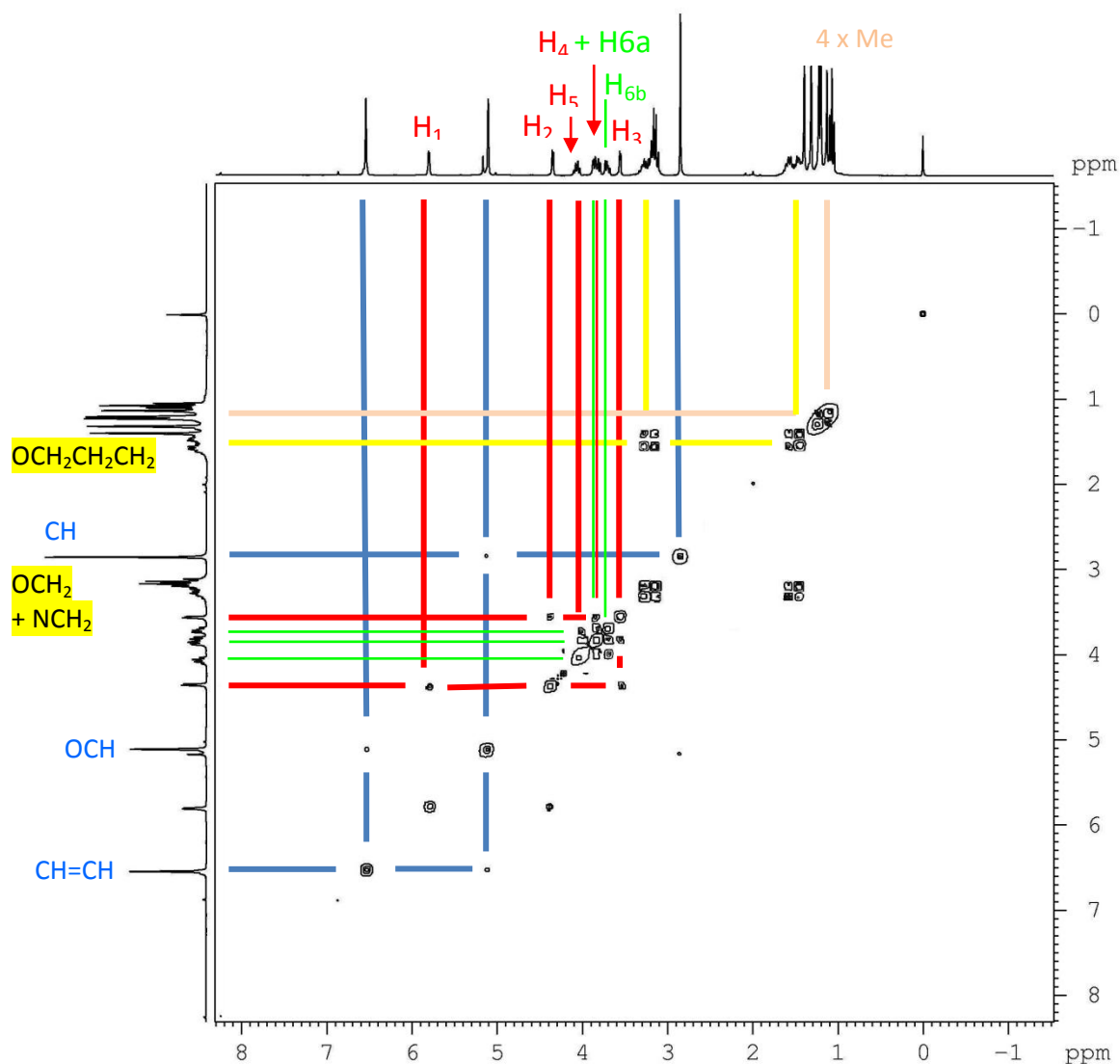


Figure 7.2: ^1H - ^1H 2D-COSY spectrum of 139 (CDCl_3).

The ^{13}C NMR spectrum can be assigned with the information from the heteronuclear $^1\text{H}^{13}\text{C}$ 2D-COSY (Figure 7.3), the DEPT 145 and the DEPT 45 spectra (Figure 7.4).

The most downfield peak at 177.8 ppm can be assigned to the carbonyl carbon. This is validated by the DEPT spectra where the quaternary carbon does not appear. The signals at 110.4 and 110.3 ppm are not showing up in DEPT either, they are assigned for the $2 \times \text{C}(\text{Me})_2$.

The second most downfield peak at 136.4 ppm, appears as a CH in the DEPT spectra and is assigned for $\text{CH}=\text{CH}$. The assignment of the sugar carbon atoms is

evidenced by the $^1\text{H}^{13}\text{C}$ COSY spectrum (Figure 7.4). Couplings are observed between H_1 and C_1 (104.5 ppm), between H_2 and C_2 (84.6 ppm), between H_3 and C_3 (79.9 ppm), between H_4 and C_4 (80.0 ppm), between H_5 and C_5 (73.2 ppm) and between H_{6a} , H_{6b} and C_6 (63.3 ppm).

The more upfield signals, four peaks representative of CH_3 (DEPT spectra) are assigned to the 4 x Me.

The remaining signals, not assigned, have negative intensities in DEPT 145 spectrum, therefore, they represent CH_2 . The two signals the more upfield at 29.4 and 28.5 ppm are assigned to the internal CH_2 in the methylene bridge. The more downfield carbon, at 68.4 ppm, is assigned to OCH_2 and the signal at 40.8 ppm to NCH_2 by using the $^1\text{H}^{13}\text{C}$ COSY spectrum.

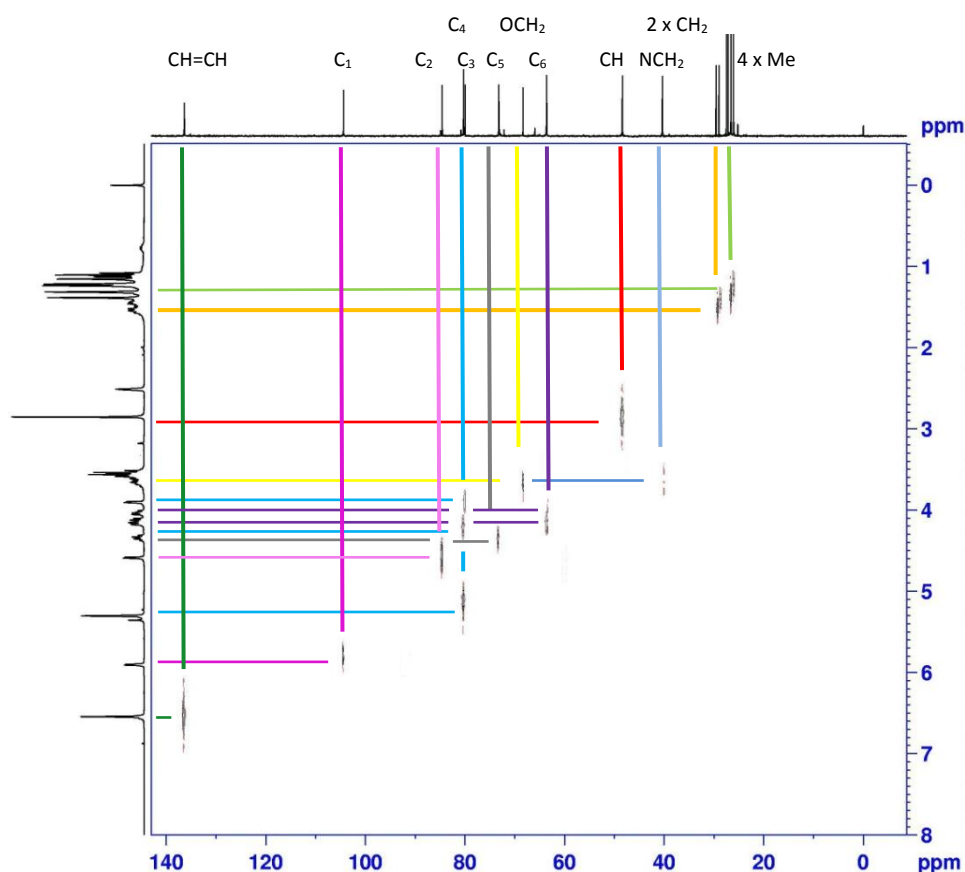


Figure 7.3: $^1\text{H}^{13}\text{C}$ 2D-COSY NMR spectrum of 139 (CDCl_3).

^{13}C NMR (DMSO- d_6): δ 177.8 (2 x C=O), 136.4 (CH=CH), 110.4 (C(CH $_3$) $_2$), 110.3 (C(CH $_3$) $_2$), 104.5 (C1), 84.6 (C2), 80.3 (2 x OCH), 80.0 (C4), 79.9 (C3), 73.2 (C5), 68.4 (OCH $_2$), 63.6 (C6), 48.4 (2 x CH), 40.8 (NCH $_2$), 29.4 (CH $_2$), 28.5 (CH $_2$), 26.8, 26.7, 26.2, 25.5 (4 x Me).

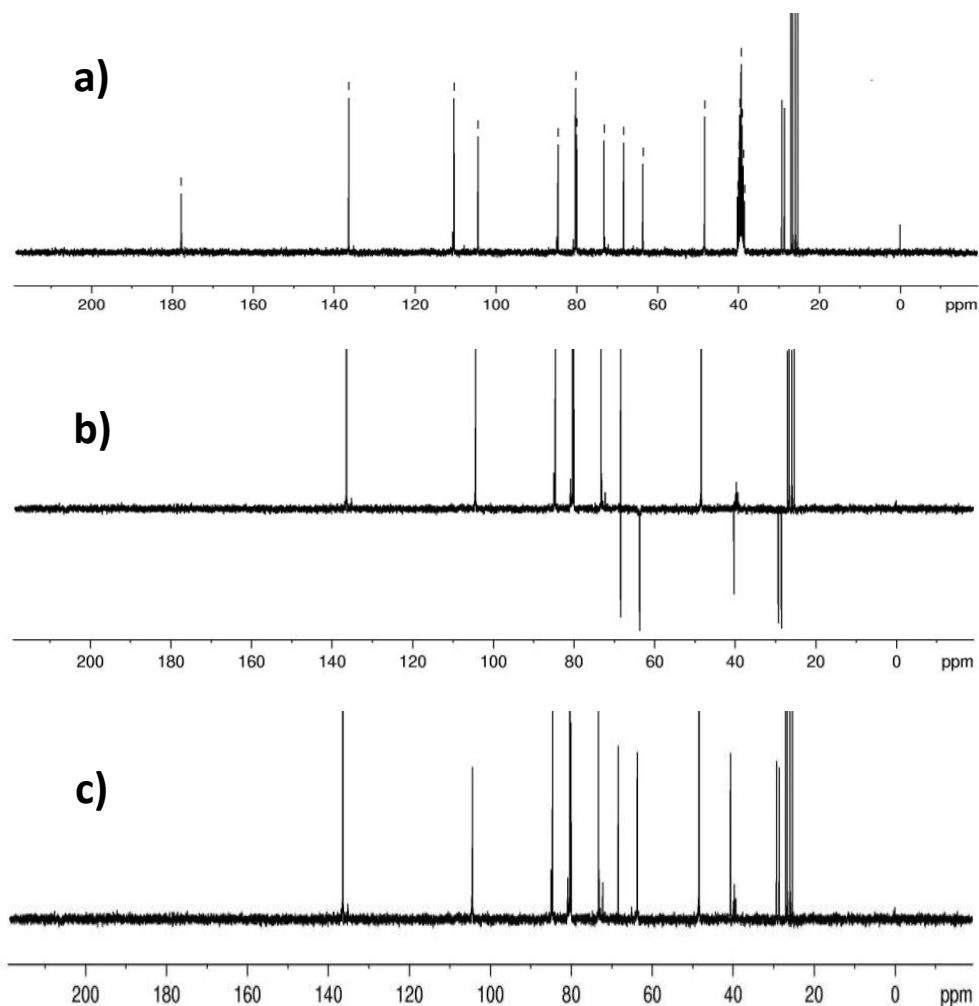


Figure 7.4: ^{13}C NMR (a), DEPT 145 (b), and DEPT 45 (c) spectra of 139 (CDCl_3).

Similar analyses were used to characterize all the compounds discussed in this thesis.

REFERENCES

- (1) Crick, F. H. C. *Nature (London)* **1970**, 227, 561-3.
- (2) <http://course1.winona.edu/sberg/241f08/Lec-note/Prot-Syn.htm> accessed January 2012.
- (3) Meares, C. F.; Yokoyama, M. *Acc. Chem. Res.* **2012**, 45, 959-960.
- (4) <http://www.atdbio.com/content/13/nucleic-acids-book> accessed May 2012.
- (5) Fox, M. A.; James, K. W. *Organic Chemistry*; Third ed.; Jones and Bartlett: Mississauga, 2004.
- (6) Bonn, D. *Lancet* **1996**, 347, 820.
- (7) Turner, C. *Clin Oncol (R Coll Radiol)* **1997**, 9, 54-8.
- (8) Narayanan, R.; Akhtar, S. *Curr Opin Oncol* **1996**, 8, 509-15.
- (9) https://www.softchalkcloud.com/lesson/files/ew6Z45XOmQVpGn/Module_11-2_X-Inactivation_print.html accessed May 2012.
- (10) Burrell, M. M. *Enzymes of Molecular Biology*; Human Press, 1993.
- (11) Winkler, J.; Stessl, M.; Amarty, J.; Noe, C. R. *ChemMedChem* **2010**, 5, 1344-1352.
- (12) Rozners, E. *Latv. Kim. Z.* **2006**, 28-40.
- (13) Maury, G.; el Alaoui, A.; Morvan, F.; Muller, B.; Imbach, J. L.; Goody, R. S. *Biochem Biophys Res Commun* **1992**, 186, 1249-56.
- (14) Iversen, P. *Anticancer Drug Des* **1991**, 6, 531-8.
- (15) MacKellar, C.; Graham, D.; Will, D. W.; Burgess, S.; Brown, T. *Nucleic Acids Res* **1992**, 20, 3411-7.
- (16) Zon, G.; Geiser, T. G. *Anticancer Drug Des* **1991**, 6, 539-68.
- (17) Ghisaidoobe, A. B. T.; de Koning, M. C.; Duynstee, H. I.; Ten Kortenaar, P. B. W.; Overkleeft, H. S.; Filippov, D. V.; van der Marel, G. A. *Tetrahedron Lett.* **2008**, 49, 3129-3132.
- (18) Wang, Z.; Olsen, P.; Ravikumar, V. T. *Nucleosides, Nucleotides Nucleic Acids* **2007**, 26, 259-269.
- (19) Wang, G.; Ramasamy, K.; Seifert, W.; (Icn Pharmaceuticals, U. S.). Application: WO WO, **1996**, p 81.
- (20) Morcos *Biochem Biophys Res Commun* **2007**, 358, 521-527.
- (21) U.S. Army Medical Research Institute of Infectious Diseases, Fort Detrick, Maryland. News Release: Gene-Specific Ebola Therapies Protect Nonhuman Primates from Lethal Disease. January 13, **2006**.
- (22) Lu, X.; Yu, Q.; Binder, G.; Chen, Z.; Slepishkina, T.; Rossi, J.; Dropulic, B. *J. Virol.* **2004**, 78, 7079-7088.
- (23) *University of Pennsylvania School of Medicine. "Phase II HIV Gene Therapy Trial Has Encouraging Results." ScienceDaily* 19 February, **2010**.
- (24) Ramrakha, P. *Exp. Ther.* **2003**, 195-210.
- (25) Walter, A.; Schutz, H.; Simon, H.; Birch-Hirschfeld, E. *J Mol Recognit* **2001**, 14, 122-39.
- (26) Mukherjee, A.; Vasquez, K. M. *Biochimie* **2011**, 93, 1197-1208.
- (27) Jenkins, T. C. *Curr Med Chem* **2000**, 7, 99-115.
- (28) Kamiya, M.; Shimizume, R.; Shindo, H.; Torigoe, H.; Sarai, A. *Nucleic Acids Symp Ser* **1995**, 57-8.
- (29) Lipps Hans, J.; Rhodes, D. *Trends Cell Biol* **2009**, 19, 414-22.
- (30) Li, W.; Miyoshi, D.; Nakano, S.-i.; Sugimoto, N. *Biochemistry* **2003**, 42, 11736-44.
- (31) Neidle, S.; Read, M. A. *Biopolymers* **2000**, 56, 195-208.
- (32) Gray Robert, D.; Chaires Jonathan, B. *Nucleic Acids Res* **2008**, 36, 4191-203.
- (33) Heidel, Jeremy David (**2005**) Targeted, systemic non-viral delivery of small interfering RNA in vivo. Dissertation (Ph.D.), California Institute of Technology.
- (34) Jorgensen, R. *Trends Biotechnol.* **1990**, 8, 340-4.
- (35) Romano, N.; Macino, G. *Mol. Microbiol.* **1992**, 6, 3343-53.

- (36) Ruiz, F.; Vayssie, L.; Klotz, C.; Sperling, L.; Madeddu, L. *Mol. Biol. Cell* **1998**, *9*, 931-943.
- (37) Guo, S.; Kempfues, K. J. *Cell (Cambridge, Mass.)* **1995**, *81*, 611-20.
- (38) Fire, A.; Xu, S.; Montgomery, M. K.; Kostas, S. A.; Driver, S. E.; Mello, C. C. *Nature (London)* **1998**, *391*, 806-811.
- (39) Tuschl, T.; Zamore, P. D.; Lehmann, R.; Bartel, D. P.; Sharp, P. A. *Genes Dev.* **1999**, *13*, 3191-3197.
- (40) Hammond, S. M.; Bernstein, E.; Beach, D.; Hannon, G. J. *Nature (London)* **2000**, *404*, 293-296.
- (41) Hamilton, A. J.; Baulcombe, D. C. *Science (Washington, D. C.)* **1999**, *286*, 950-952.
- (42) Zamore, P. D.; Tuschl, T.; Sharp, P. A.; Bartel, D. P. *Cell (Cambridge, Mass.)* **2000**, *101*, 25-33.
- (43) Bernstein, E.; Caudy, A. A.; Hammond, S. M.; Hannon, G. J. *Nature (London)* **2001**, *409*, 363-366.
- (44) Meister, G.; Tuschl, T. *Nature (London)* **2004**, *431*, 343-349.
- (45) Brummelkamp, T. R.; Bernards, R. *Nat. Rev. Cancer* **2003**, *3*, 781-789.
- (46) Dominska, M.; Dykxhoorn, D. M. *JCS* **2010**, *123*, 1183.
- (47) Koshkin, A. A.; Singh, S. K.; Nielsen, P.; Rajwanshi, V. K.; Kumar, R.; Meldgaard, M.; Olsen, C. E.; Wengel, J. *Tetrahedron* **1998**, *54*, 3607-3630.
- (48) Obika, S.; Nanbu, D.; Hari, Y.; Morio, K.-I.; In, Y.; Ishida, T.; Imanishi, T. *Tetrahedron Lett.* **1997**, *38*, 8735-8738.
- (49) Kaur, H.; Arora, A.; Wengel, J.; Maiti, S. *Biochemistry* **2006**, *45*, 7347-7355.
- (50) You, Y.; Moreira, B. G.; Behlke, M. A.; Owczarzy, R. *Nucleic Acids Res.* **2006**, *34*, e60/1-e60/11.
- (51) Adomas, A.; Heller, G.; Olson, A.; Osborne, J.; Karlsson, M.; Nahalkova, J.; Van Zyl, L.; Sederoff, R.; Stenlid, J.; Finlay, R.; Asiegbu, F. O. *Tree Physiol. (Victoria, BC, Can.)* **2008**, *28*, 885-897.
- (52) <http://www.ncbi.nlm.nih.gov/pmc/articles/PMC346675> accessed June 2012.
- (53) VanGuilder, H. D.; Vrana, K. E.; Freeman, W. M. *BioTechniques* **2008**, *44*, 619-626.
- (54) <http://www.ebiotrader.com/emqzf/spl1200604/16-17.pdf> accessed July 2012.
- (55) <http://www.hcvadvocate.org/hepatitis/hepC/HCVDrugs.html> accessed July 2012.
- (56) Nielsen, P. E.; Egholm, M.; Berg, R. H.; Buchardt, O. *Science (Washington, D. C.)* **1991**, *254*, 1497-500.
- (57) Egholm, M.; Buchardt, O.; Christensen, L.; Behrens, C.; Freier, S. M.; Driver, D. A.; Berg, R. H.; Kim, S. K.; Norden, B.; Nielsen, P. E. *Nature (London)* **1993**, *365*, 566-8.
- (58) Elbashir, S. M.; Harborth, J.; Lendeckel, W.; Yalcin, A.; Weber, K.; Tuschl, T. *Nature (London)* **2001**, *411*, 494-498.
- (59) Jeong, J. H.; Kim, S. W.; Park, T. G. *Prog. Polym. Sci.* **2007**, *32*, 1239-1274.
- (60) Guo, X.; Huang, L. *Acc. Chem. Res.* **2012**, *45*, 971-979.
- (61) Dorsett, Y.; Tuschl, T. *Nat. Rev. Drug Discovery* **2004**, *3*, 318-329.
- (62) Grimm, D.; Streetz, K. L.; Jopling, C. L.; Storm, T. A.; Pandey, K.; Davis, C. R.; Marion, P.; Salazar, F.; Kay, M. A. *Nature (London)* **2006**, *441*, 537-541.
- (63) Santel, A.; Aleku, M.; Keil, O.; Endruschat, J.; Esche, V.; Durieux, B.; Loeffler, K.; Fechtner, M.; Roehl, T.; Fisch, G.; Dames, S.; Arnold, W.; Giese, K.; Klippel, A.; Kaufmann, J. *Gene Ther.* **2006**, *13*, 1360-1370.
- (64) Yano, J.; Hirabayashi, K.; Nakagawa, S.-i.; Yamaguchi, T.; Nogawa, M.; Kashimori, I.; Naito, H.; Kitagawa, H.; Ishiyama, K.; Ohgi, T.; Irimura, T. *Clin. Cancer Res.* **2004**, *10*, 7721-7726.
- (65) Landen, C. N., Jr.; Chavez-Reyes, A.; Bucana, C.; Schmandt, R.; Deavers, M. T.; Lopez-Berestein, G.; Sood, A. K. *Cancer Res.* **2005**, *65*, 6910-6918.
- (66) Zimmermann, T. S.; Lee, A. C. H.; Akinc, A.; Bramlage, B.; Bumcrot, D.; Fedoruk, M. N.; Harborth, J.; Heyes, J. A.; Jeffs, L. B.; John, M.; Judge, A. D.; Lam, K.; McClintock, K.; Nechev, L. V.; Palmer, L. R.; Racie, T.; Roehl, I.; Seiffert, S.; Shanmugam, S.; Sood, V.; Soutschek, J.; Toudjarska, I.;

- Wheat, A. J.; Yaworski, E.; Zedalis, W.; Koteliensky, V.; Manoharan, M.; Vornlocher, H.-P.; MacLachlan, I. *Nature (London)* **2006**, *441*, 111-114.
- (67) Kim, S. H.; Mok, H.; Jeong, J. H.; Kim, S. W.; Park, T. G. *Bioconjugate Chem.* **2006**, *17*, 241-244.
- (68) Urban-Klein, B.; Werth, S.; Abuharbeid, S.; Czubayko, F.; Aigner, A. *Gene Ther.* **2005**, *12*, 461-466.
- (69) Mok, H.; Park, T. G. *Biopolymers* **2008**, *89*, 881-888.
- (70) Song, E.; Lee, S.-K.; Wang, J.; Ince, N.; Ouyang, N.; Min, J.; Chen, J.; Shankar, P.; Lieberman, J. *Nat. Med. (N. Y., NY, U. S.)* **2003**, *9*, 347-351.
- (71) Park, T. G.; Jeong, J. H.; Kim, S. W. *Adv. Drug Delivery Rev.* **2006**, *58*, 467-486.
- (72) Nishina, K.; Unno, T.; Uno, Y.; Kubodera, T.; Kanouchi, T.; Mizusawa, H.; Yokota, T. *Mol. Ther.* **2008**, *16*, 734-740.
- (73) Jeong, J. H.; Mok, H.; Oh, Y.-K.; Park, T. G. *Bioconjugate Chem.* **2009**, *20*, 5-14.
- (74) Pourceau, G.; Meyer, A.; Vasseur, J.-J.; Morvan, F. *J. Org. Chem.* **2009**, *74*, 6837-6842.
- (75) El-Sagheer, A. H.; Brown, T. *Chem. Soc. Rev.* **2010**, *39*, 1388-1405.
- (76) Lietard, J.; Meyer, A.; Vasseur, J.-J.; Morvan, F. *J. Org. Chem.* **2008**, *73*, 191-200.
- (77) Chittepu, P.; Sirivolu, V. R.; Seela, F. *Bioorg. Med. Chem.* **2008**, *16*, 8427-8439.
- (78) Gramlich, P. M. E.; Wirges, C. T.; Gierlich, J.; Carell, T. *Org. Lett.* **2008**, *10*, 249-251.
- (79) Lucas, R.; Zerrouki, R.; Granet, R.; Krausz, P.; Champavier, Y. *Tetrahedron* **2008**, *64*, 5467-5471.
- (80) Jawalekar, A. M.; Meeuwenoord, N.; Cremers, J. G. O.; Overkleeft, H. S.; van der Marel, G. A.; Rutjes, F. P. J. T.; van Delft, F. L. *J. Org. Chem.* **2008**, *73*, 287-290.
- (81) Andersen, N. K.; Chandak, N.; Brulikova, L.; Kumar, P.; Jensen, M. D.; Jensen, F.; Sharma, P. K.; Nielsen, P. *Bioorg. Med. Chem.* **2010**, *18*, 4702-4710.
- (82) Lonnberg, H. *Curr. Org. Synth.* **2009**, *6*, 400-425.
- (83) Zhang, J.; Pourceau, G.; Meyer, A.; Vidal, S.; Praly, J.-P.; Souteyrand, E.; Vasseur, J.-J.; Morvan, F.; Chevolut, Y. *Biosens. Bioelectron.* **2009**, *24*, 2515-2521.
- (84) Kiviniemi, A.; Virta, P.; Lonnberg, H. *Bioconjugate Chem.* **2010**, *21*, 1890-1901.
- (85) Seo, T. S.; Li, Z.; Ruparel, H.; Ju, J. *J. Org. Chem.* **2003**, *68*, 609-612.
- (86) Berndl, S.; Herzig, N.; Kele, P.; Lachmann, D.; Li, X.; Wolfbeis, O. S.; Wagenknecht, H.-A. *Bioconjugate Chem.* **2009**, *20*, 558-564.
- (87) Seela, F.; Ingale, S. A. *J. Org. Chem.* **2010**, *75*, 284-295.
- (88) Weisbrod, S. H.; Marx, A. *Chem. Commun. (Cambridge, U. K.)* **2008**, 5675-5685.
- (89) Gramlich, P. M. E.; Warncke, S.; Gierlich, J.; Carell, T. *Angew. Chem., Int. Ed.* **2008**, *47*, 3442-3444.
- (90) Godeau, G.; Staedel, C.; Barthelemy, P. *J. Med. Chem.* **2008**, *51*, 4374-4376.
- (91) Yamada, T.; Peng, C. G.; Matsuda, S.; Addepalli, H.; Jayaprakash, K. N.; Alam, M. R.; Mills, K.; Maier, M. A.; Charisse, K.; Sekine, M.; Manoharan, M.; Rajeev, K. G. *J. Org. Chem.* **2011**, *76*, 1198-1211.
- (92) Gogoi, K.; Mane, M. V.; Kunte, S. S.; Kumar, V. A. *Nucleic Acids Res.* **2007**, *35*, e139/1-e139/7.
- (93) Xu, Y.; Suzuki, Y.; Komiyama, M. *Angew. Chem., Int. Ed.* **2009**, *48*, 3281-3284, S3281/1-S3281/6.
- (94) Pourceau, G.; Meyer, A.; Chevolut, Y.; Souteyrand, E.; Vasseur, J.-J.; Morvan, F. *Bioconjugate Chem.* **2010**, *21*, 1520-1529.
- (95) Best, M. D. *Biochemistry* **2009**, *48*, 6571-6584.
- (96) Jewett, J. C.; Bertozzi, C. R. *Chem. Soc. Rev.* **2010**, *39*, 1272-1279.
- (97) Henriksson, A.; Friedbacher, G.; Hoffmann, H. *Langmuir* **2011**, *27*, 7345-7348.
- (98) Rostovtsev, V. V.; Green, L. G.; Fokin, V. V.; Sharpless, K. B. *Angew. Chem., Int. Ed.* **2002**, *41*, 2596-2599.

- (99) Salic, A.; Mitchison, T. J. *Proc. Natl. Acad. Sci. U. S.* **2008**, *105*, 2415-2420.
- (100) Laughlin, S. T.; Baskin, J. M.; Amacher, S. L.; Bertozzi, C. R. *Science (Washington, D. C.)* **2008**, *320*, 664-667.
- (101) Singh, I.; Vyle Joseph, S.; Heaney, F. *Chem Commun (Camb)* **2009**, 3276-8.
- (102) Singh, I.; Zarafshani, Z.; Lutz, J.-F.; Heaney, F. *Macromolecules (Washington, D. C.)* **2009**, *42*, 5411-5413.
- (103) Algay, V.; Singh, I.; Heaney, F. *Org. Biomol. Chem.* **2010**, *8*, 391-397.
- (104) Kang, Y. K.; Shin, K. J.; Yoo, K. H.; Seo, K. J.; Hong, C. Y.; Lee, C.-S.; Park, S. Y.; Kim, D. J.; Park, S. W. *Bioorg. Med. Chem. Lett.* **2000**, *10*, 95-99.
- (105) Xue, C.-B.; Roderick, J.; Mousa, S.; Olson, R. E.; DeGrado, W. F. *Bioorg. Med. Chem. Lett.* **1998**, *8*, 3499-3504.
- (106) Diana, G. D.; McKinlay, M. A.; Brisson, C. J.; Zalay, E. S.; Miralles, J. V.; Salvador, U. J. *J. Med. Chem.* **1985**, *28*, 748-52.
- (107) Lepage, F.; Tombret, F.; Cuvier, G.; Marivain, A.; Gillardin, J. M. *Eur. J. Med. Chem.* **1992**, *27*, 581-93.
- (108) Ryng, S.; Machon, Z.; Wieczorek, Z.; Zimecki, M.; Mokrosz, M. *Eur. J. Med. Chem.* **1998**, *33*, 831-836.
- (109) Badio, B.; Garraffo, H. M.; Plummer, C. V.; Padgett, W. L.; Daly, J. W. *Eur. J. Pharmacol.* **1997**, *321*, 189-194.
- (110) Carroll, F. I. *Bioorg. Med. Chem. Lett.* **2004**, *14*, 1889-1896.
- (111) http://en.wikipedia.org/wiki/Click_chemistry accessed September 2011.
- (112) Kolb, H. C.; Finn, M. G.; Sharpless, K. B. *Angew. Chem., Int. Ed.* **2001**, *40*, 2004-2021.
- (113) Woodward, R. B.; Hoffmann, R. In *Academic press* New York, **1970**.
- (114) Huisgen, R. In *Proceedings of the Chemical Society of London*, **1961**, p 357.
- (115) Huisgen, R. *J. Org. Chem.* **1976**, *41*, 403-19.
- (116) Sustmann, R. *Pure Appl. Chem.* **1974**, *40*, 569-93.
- (117) Sustmann, R.; Sicking, W.; Huisgen, R. *J. Am. Chem. Soc.* **1995**, *117*, 9679-85.
- (118) McKiernan, M. T. (**1996**) Dissertation (Ph.D.), NUI Galway.
- (119) Sustmann, R. *Tetrahedron Lett.* **1971**, 2717-20.
- (120) Bokach, N. A.; Kukushkin, V. Y. *Russ. Chem. Bull.* **2006**, *55*, 1869-1882.
- (121) Himo, F.; Lovell, T.; Hilgraf, R.; Rostovtsev, V. V.; Noodleman, L.; Sharpless, K. B.; Fokin, V. V. *J. Am. Chem. Soc.* **2005**, *127*, 210-216.
- (122) Tornøe, C. W.; Christensen, C.; Meldal, M. *J. Org. Chem.* **2002**, *67*, 3057-3064.
- (123) Duran Pachon, L.; van Maarseveen, J. H.; Rothenberg, G. *Adv. Synth. Catal.* **2005**, *347*, 811-815.
- (124) Molteni, G.; Bianchi, C. L.; Marinoni, G.; Santo, N.; Ponti, A. *New J. Chem.* **2006**, *30*, 1137-1139.
- (125) Rodionov, V. O.; Presolski, S. I.; Diaz Diaz, D.; Fokin, V. V.; Finn, M. G. *J. Am. Chem. Soc.* **2007**, *129*, 12705-12712.
- (126) Hein, J. E.; Fokin, V. V. *Chem. Soc. Rev.* **2010**, *39*, 1302-1315.
- (127) Ahlquist, M.; Fokin, V. V. *Organometallics* **2007**, *26*, 4389-4391.
- (128) Liang, L.; Astruc, D. *Coord. Chem. Rev.* **2011**, *255*, 2933-2945.
- (129) Boren, B. C.; Narayan, S.; Rasmussen, L. K.; Zhang, L.; Zhao, H.; Lin, Z.; Jia, G.; Fokin, V. V. *J. Am. Chem. Soc.* **2008**, *130*, 8923-8930.
- (130) Zhang, L.; Chen, X.; Xue, P.; Sun, H. H. Y.; Williams, I. D.; Sharpless, K. B.; Fokin, V. V.; Jia, G. *J. Am. Chem. Soc.* **2005**, *127*, 15998-15999.
- (131) Smith, L. I. *Chem. Rev.* **1938**, *23*, 193-285.
- (132) Parsons, P. J. *Synthetic Applications of 1,3-Dipolar Cycloaddition Chemistry toward Heterocycles and Natural Products* edited by Albert Padwa and William H. Pearson, **2004**; Vol. 8.
- (133) Beckmann, E. *Ber.* **1890**, *23*, 3319-31, and 3331-41.

- (134) Pfeiffer, P.; Braude, S.; Fritsch, R.; Halberstadt, W.; Kirchhoff, G.; Kleber, J.; Wittkop, P. *Justus Liebigs Ann. Chem.* **1916**, 411, 72-158.
- (135) Exner, O. *J. Phys. Org. Chem.* **1990**, 3, 190-4.
- (136) Komaromi, I.; Tronchet, J. M. J. *J. Mol. Struct.: THEOCHEM* **1996**, 366, 147-160.
- (137) Thirumalaikumar, M.; Sivasubramanian, S.; Ponnuswamy, A.; Mohan, P. *Eur. J. Med. Chem.* **1996**, 31, 905-908.
- (138) Burrell, A. J. M.; Coldham, I. *Curr. Org. Synth.* **2010**, 7, 312-331.
- (139) Goti, A.; Cardona, F.; Brandi, A.; Picasso, S.; Vogel, P. *Tetrahedron: Asymmetry* **1996**, 7, 1659-1674.
- (140) Larina, A. G.; Stepanov, A. V.; Boitsov, V. M.; Molchanov, A. P.; Gurzhiy, V. V.; Starova, G. L.; Lykholay, A. N. *Tetrahedron Lett.* **2011**, 52, 5777-5781.
- (141) Pinho e Melo, T. M. V. D. *Curr. Org. Chem.* **2009**, 13, 1406-1431.
- (142) Bakunova, S. M.; Kirilyuk, I. A.; Grigor'ev, I. A. *Russ. Chem. Bull.* **2001**, 50, 882-889.
- (143) van den Broek, L. A. G. M. *Tetrahedron* **1996**, 52, 4467-78.
- (144) Carmona, D.; Lamata, M. P.; Viguri, F.; Rodriguez, R.; Lahoz, F. J.; Fabra, M. J.; Oro, L. A. *Tetrahedron: Asymmetry* **2009**, 20, 1197-1205.
- (145) Huisgen, R.; Seidl, H. *Tetrahedron Lett.* **1963**, 2019-22.
- (146) Giera, H.; Huisgen, R. *Liebigs Ann./Recl.* **1997**, 1685-1689.
- (147) Karlsson, S.; Hogberg, H.-E. *Org. Prep. Proced. Int.* **2001**, 33, 103-172.
- (148) Howard, E. *Phil. Trans. Roy. Soc. London* **1800**, 204.
- (149) Gabriel, S.; Koppe, M. *Ber.* **2011**, 19, 1145-8.
- (150) Grundmann, C.; Datta, S. K. *J. Org. Chem.* **1969**, 34, 2016-18.
- (151) Pasinszki, T.; Hajgato, B.; Havasi, B.; Westwood, N. P. C. *Phys. Chem. Chem. Phys.* **2009**, 11, 5263-5272.
- (152) Rai, K. M. L.; Hassner, A. *Synth. Commun.* **1997**, 27, 467-472.
- (153) Beltrame, P.; Comotti, A.; Veglio, C. *Chem. Commun.* **1967**, 996-7.
- (154) Kim, J. N.; Ryu, E. K. *Synth. Commun.* **1990**, 20, 1373-7.
- (155) Hassner, A.; Rai, K. M. L. *Synthesis FIELD Full Journal Title:Synthesis* **1989**, 57-9.
- (156) Verner-Jeffreys, D. W.; Joiner, C. L.; Bagwell, N. J.; Reese, R. A.; Husby, A.; Dixon, P. F. *Aquaculture* **2009**, 286, 190-197.
- (157) Smail, D. A.; Grant, R.; Simpson, D.; Bain, N.; Hastings, T. S. *Aquaculture* **2004**, 240, 29-38.
- (158) Rolland, S. L.; Carrick, T. E.; Walls, A. W.; McCabe, J. F. *Dent. Mater.* **2007**, 23, 1468-1472.
- (159) Rai, K. M. L.; Hassner, A. *Indian J. Chem., Sect. B: Org. Chem. Incl. Med. Chem.* **1997**, 36B, 242-245.
- (160) Grundmann, C.; Kochs, P.; Boal, J. R. *Justus Liebigs Ann. Chem.* **1972**, 761, 162-81.
- (161) Shiraishi, S.; Shigemoto, T.; Miyahara, M.; Ogawa, S. *Bull. Chem. Soc. Jpn.* **1981**, 54, 3863-4.
- (162) Sicard, G.; Baceiredo, A.; Bertrand, G. *Angew. Chem.* **1988**, 100, 289-90.
- (163) Tsyganov, D. V.; Yakubov, A. P.; Belen'kii, L. I.; Krayushkin, M. M. *Izv. Akad. Nauk SSSR, Ser. Khim.* **1991**, 1398-403.
- (164) Smellie, I. A. S.; Moggach, S. A.; Paton, R. M. *Tetrahedron Lett.* **2011**, 52, 95-97.
- (165) Grundmann, C. *Synthesis* **1970**, 344-59.
- (166) Kozikowski, A. P. *Acc. Chem. Res.* **1984**, 17, 410-16.
- (167) Weygand, C.; Bauer, E.; Gunther, H.; Heynemann, W. *Justus Liebigs Ann. Chem.* **1927**, 459, 99-122.
- (168) Kozikowski, A. P.; Ghosh, A. K. *J. Org. Chem.* **1984**, 49, 2762-72.
- (169) Herrera, R.; Nagarajan, A.; Morales, M. A.; Mendez, F.; Jimenez-Vazquez, H. A.; Zepeda, L. G.; Tamariz, J. *J. Org. Chem.* **2001**, 66, 1252-1263.
- (170) Gucma, M.; Golebiewski, W. M. *J. Heterocycl. Chem.* **2008**, 45, 241-245.

- (171) Huisgen, R. *1,3 [One,Three]-Dipolar Cycloaddit. Chem.* **1984**, *1*, 1-176.
- (172) Rastelli, A.; Gandolfi, R.; Amade, M. S. *J. Org. Chem.* **1998**, *63*, 7425-7436.
- (173) Cossio, F. P.; Morao, I.; Jiao, H.; Schleyer, P. v. R. *J. Am. Chem. Soc.* **1999**, *121*, 6737-6746.
- (174) Weidner-Wells, M. A.; Fraga-Spano, S. A.; Turchi, I. J. *J. Org. Chem.* **1998**, *63*, 6319-6328.
- (175) Kim, J. N.; Chung, K. H.; Ryu, E. K. *Heterocycles* **1991**, *32*, 477-80.
- (176) Kaddar, H.; Hamelin, J.; Benhaoua, H. *J. Chem. Res., Synop.* **1999**, 718-719.
- (177) Kang, K. H.; Pae, A. N.; Choi, K. I.; Cho, Y. S.; Chung, B. Y.; Lee, J. E.; Jung, S. H.; Koh, H. Y.; Lee, H. Y. *Tetrahedron Lett.* **2001**, *42*, 1057-1060.
- (178) Shang, Y.-J.; Wang, Y.-G. *Tetrahedron Lett.* **2002**, *43*, 2247-2249.
- (179) Shang, Y.-J.; Wang, Y.-G. *Synthesis* **2002**, 1663-1668.
- (180) Slavica, A.; Dib, I.; Nidetzky, B. *Biotechnol Bioeng* **2007**, *96*, 9-17.
- (181) Lin, K.-F.; Lin, J.-S.; Cheng, C.-H. *Polymer* **1996**, *37*, 4729-4737.
- (182) Cava, M. P.; Deana, A. A.; Muth, K.; Mitchell, M. j. *Org. Synth.* **1961**, *41*, 93-5.
- (183) Schaerer, K.; Morgenthaler, M.; Paulini, R.; Obst-Sander, U.; Banner, D. W.; Schlatter, D.; Benz, J.; Stihle, M.; Diederich, F. *Angew. Chem., Int. Ed.* **2005**, *44*, 4400-4404.
- (184) Salonen, L. M.; Bucher, C.; Banner, D. W.; Haap, W.; Mary, J.-L.; Benz, J.; Kuster, O.; Seiler, P.; Schweizer, W. B.; Diederich, F. *Angew. Chem., Int. Ed.* **2009**, *48*, 811-814.
- (185) Muramatsu, S.; Kinbara, K.; Taguchi, H.; Ishii, N.; Aida, T. *J. Am. Chem. Soc.* **2006**, *128*, 3764-3769.
- (186) Gill, G. B.; James, G. D.; Oates, K. V.; Pattenden, G. *J. Chem. Soc., Perkin Trans. 1* **1993**, 2567-79.
- (187) Jones, R. C. F.; Martin, J. N.; Smith, P. *Synlett* **2000**, 967-970.
- (188) Dondas, H. A.; Grigg, R.; Hadjisoteriou, M.; Markandu, J.; Thomas, W. A.; Kennewell, P. *Tetrahedron* **2000**, *56*, 10087-10096.
- (189) Reimann, J. E.; Jencks, W. P. *J. Am. Chem. Soc.* **1966**, *88*, 3973-82.
- (190) Gedye, R.; Smith, F.; Westaway, K.; Ali, H.; Baldisera, L.; Laberge, L.; Rousell, J. *Tetrahedron Lett.* **1986**, *27*, 279-82.
- (191) Varma, R. S.; Dahiya, R.; Kumar, S. *Tetrahedron Lett.* **1997**, *38*, 2039-2042.
- (192) Caddick, S. *Tetrahedron* **1995**, *51*, 10403-32.
- (193) Valizadeh, H.; Heravi, M. M.; Amiri, M. *Mol. Diversity* **2010**, *14*, 575-579.
- (194) Heaney, F.; Rooney, O.; Cunningham, D.; McArde, P. *J. Chem. Soc., Perkin Trans. 2* **2001**, 373-378.
- (195) Drescher, M.; Hammerschmidt, F. *Monatsh. Chem.* **1997**, *128*, 713-723.
- (196) Gabriel, C.; Gabriel, S.; Grant, E. H.; Grant, E. H.; Halstead, B. S. J.; Mingos, D. M. P. *Chem. Soc. Rev.* **1998**, *27*, 213-224.
- (197) Pillai, U. R.; Sahle-Demessie, E.; Varma, R. S. *J. Mater. Chem.* **2002**, *12*, 3199-3207.
- (198) Wilson, N. S.; Sarko, C. R.; Roth, G. P. *Tetrahedron Lett.* **2001**, *42*, 8939-8941.
- (199) Rai, K. M. L.; Hassner, A. *Synth. Commun.* **1989**, *19*, 2799-807.
- (200) Pedatella, S.; Guaragna, A.; D'Alonzo, D.; De Nisco, M.; Palumbo, G. *Synthesis* **2006**, 305-308.
- (201) Bianchini, R.; Catelani, G.; Cecconi, R.; D'Andrea, F.; Guazzelli, L.; Isaad, J.; Rolla, M. *Eur. J. Org. Chem.* **2008**, 444-454.
- (202) Bezdushna, E.; Ritter, H. *Macromol. Rapid Commun.* **2005**, *26*, 1087-1092.
- (203) Bryce-Smith, D.; Gilbert, A.; McColl, I. S.; Drew, M. G. B.; Yianni, P. *J. Chem. Soc., Perkin Trans. 1* **1987**, 1147-51.
- (204) Zhu, J.; Kell, A. J.; Workentin, M. S. *Org. Lett.* **2006**, *8*, 4993-4996.
- (205) Zhu, J.; Lines, B. M.; Ganton, M. D.; Kerr, M. A.; Workentin, M. S. *J. Org. Chem.* **2008**, *73*, 1099-1105.
- (206) Coskun, N.; Mert, H.; Arikan, N. *Tetrahedron* **2006**, *62*, 1351-1359.

- (207) Ferreira, F.; Meyer, A.; Vasseur, J.-J.; Morvan, F. *J. Org. Chem.* **2005**, *70*, 9198-9206.
- (208) Singh, I.; Heaney, F. *Org. Biomol. Chem.* **2010**, *8*, 451-6.
- (209) Letsinger, R. L.; Caruthers, M. H.; Miller, P. S.; Ogilvie, K. K. *J. Amer. Chem. Soc.* **1967**, *89*, 7146-7.
- (210) Reddy, M. P.; Rampal, J. B.; Beaucage, S. L. *Tetrahedron Lett.* **1987**, *28*, 23-6.
- (211) Grecian, S.; Fokin, V. V. *Angew. Chem., Int. Ed.* **2008**, *47*, 8285-8287.
- (212) Reddy, K. S.; (Honeywell International Inc., U. S.). Application: US, **2006**, p 11.
- (213) Kühl, O. *Phosphorus-31 NMR Spectroscopy*, Springer, Berlin, **2008**.
- (214) Horner, L.; Hoffmann, H.; Ertel, H.; Klahre, G. *Tetrahedron Lett.* **1961**, 9-11.
- (215) Lucas, R.; Neto, V.; Hadj Bouazza, A.; Zerrouki, R.; Granet, R.; Krausz, P.; Champavier, Y. *Tetrahedron Lett. FIELD Full Journal Title: Tetrahedron Letters* **2008**, *49*, 1004-1007.
- (216) Lu, B.; Li, L.-J.; Li, T.-S.; Li, J.-T. *J. Chem. Res., Synop.* **1998**, 604-605.
- (217) Yadav, G. D.; Krishnan, M. S. *Ind. Eng. Chem. Res.* **1998**, *37*, 3358-3365.
- (218) Habibi, D.; Marvi, O. *ARKIVOC (Gainesville, FL, U. S.)* **2006**, 8-15.
- (219) Asakura, J.-i.; Robins, M. J.; Asaka, Y.; Kim, T. H. *J. Org. Chem.* **1996**, *61*, 9026-9027.
- (220) Zhang, Z.-H.; Li, T.-S.; Yang, F.; Fu, C.-G. *Synth. Commun.* **1998**, *28*, 3105-3114.
- (221) Loh, T.-P.; Li, X.-R. *Tetrahedron* **1999**, *55*, 10789-10802.
- (222) Rega, M.; Jimenez, C.; Rodriguez, J. *Steroids* **2007**, *72*, 729-735.
- (223) Ishi-i, T.; Iguchi, R.; Snip, E.; Ikeda, M.; Shinkai, S. *Langmuir* **2001**, *17*, 5825-5833.
- (224) Simpson, M. G.; Pittelkow, M.; Watson, S. P.; Sanders, J. K. M. *Org. Biomol. Chem.* **2009**, *8*, 1181-1187.
- (225) Beaucage, S. L.; Iyer, R. P. *Tetrahedron* **1992**, *48*, 2223-311.
- (226) Applied-Biosystems www.biosource.com accessed January 2012.
- (227) Pon, R. T. In *Protocols for Oligonucleotides and Analogs* Totowa, NJ, U. S. **1993**; Vol. 20, p 465-496.
- (228) Joyce, C. M.; Steitz, T. a. *J. Bacteriol.* **1995**, *177*, 6321-9.
- (229) Reddy, M. P.; Hanna, N. B.; Farooqui, F. *Tetrahedron Letters* **1994**, *35*, 4311-4314.
- (230) McBride, L. J.; Kierzek, R.; Beaucage, S. L.; Caruthers, M. H. *J. Am. Chem. Soc.* **1986**, *108*, 2040-8.
- (231) Margineanu, A.; De Feyter, S.; Melnikov, S.; Marchand, D.; van Aerschot, A.; Herdewijn, P.; Habuchi, S.; De Schryver, F. C.; Hofkens, J. *Biomacromolecules* **2007**, *8*, 3382-3392.
- (232) Chaltin, P.; Margineanu, A.; Marchand, D.; Van Aerschot, A.; Rozenski, J.; De Schryver, F.; Herrmann, A.; Muellen, K.; Juliano, R.; Fisher, M. H.; Kang, H.; De eyter, S.; Herdewijn, P. *Bioconjugate Chem.* **2005**, *16*, 827-836.
- (233) Krieg, A. M.; Tonkinson, J.; Matson, S.; Zhao, Q.; Saxon, M.; Zhang, L. M.; Bhanja, U.; Yakubov, L.; Stein, C. A. *Proc. Natl. Acad. Sci. U. S.* **1993**, *90*, 1048-52.
- (234) Chiu, Y.-L.; Rana, T. M. *RNA* **2003**, *9*, 1034-1048.
- (235) Khvorova, A.; Reynolds, A.; Jayasena, S. D. *Cell (Cambridge, MA, U. S.)* **2003**, *115*, 209-216.
- (236) Manoharan, M. *Biochim. Biophys. Acta, Gene Struct. Expression* **1999**, *1489*, 117-130.
- (237) Kim, S. H.; Jeong, J. H.; Cho, K. C.; Kim, S. W.; Park, T. G. *J. Controlled Release* **2005**, *104*, 223-232.
- (238) http://www.ambion.com/techlib/misc/oligo_calculator.html accessed September 2011.
- (239) Strapps, W. R.; Pickering, V.; Muiru, G. T.; Rice, J.; Orsborn, S.; Polisky, B. A.; Sachs, A.; Bartz, S. R. *Nucleic Acids Res.* **2010**, *38*, 4788-4797.
- (240) Ueno, Y.; Watanabe, Y.; Shibata, A.; Yoshikawa, K.; Takano, T.; Kohara, M.; Kitade, Y. *Bioorg. Med. Chem.* **2009**, *17*, 1974-1981.
- (241) Lee, H. S.; Lee, S. N.; Joo, C. H.; Lee, H.; Lee, H. S.; Yoon, S. Y.; Kim, Y. K.; Choe, H. *J. Mol. Graphics Modell.* **2007**, *25*, 784-793.

- (242) Elbashir, S. M.; Martinez, J.; Patkaniowska, A.; Lendeckel, W.; Tuschl, T. *EMBO J.* **2001**, *20*, 6877-6888.
- (243) Perrin, D. D.; Armarego, W. L. F. *Purification of Laboratory chemicals, third edition*; Pergamon Press.
- (244) Gray, D. M.; Hung, S.-H.; Johnson, K. H. *Methods Enzymol.* **1995**, *246*, 19-34.
- (245) Ben Hamadi, N.; Msaddek, M. *J. Soc. Chim. Tunis.* **2007**, *9*, 115-120.
- (246) Minakata, S.; Okumura, S.; Nagamachi, T.; Takeda, Y. *Org. Lett.* **2011**, *13*, 2966-2969.
- (247) Lim, J. E.; Shim, C. B.; Kim, J. M.; Lee, B. Y.; Yie, J. E. *Angew. Chem., Int. Ed.* **2004**, *43*, 3839-3842.
- (248) Gooden, D. M. *Molbank* **2009**, M638.
- (249) Struga, M.; Miroslaw, B.; Pakosinska-Parys, M.; Drzewiecka, A.; Borowski, P.; Kossakowski, J.; Koziol, A. E. *J. Mol. Struct.* **2010**, *965*, 23-30.
- (250) www.metabion.com accessed June 2010.